frontiers | Research Topics

Opportunistic pathogens: pathogenesis and multi-drug resistance mechanisms

Edited by
Shicheng Chen, Lisheng Liao and Mingxi Wang

Published in
Frontiers in Microbiology

ISSN 1664-8714
ISBN 978-2-8325-6246-8
DOI 10.3389/978-2-8325-6246-8

About Frontiers

Frontiers is more than just an open access publisher of scholarly articles: it is a pioneering approach to the world of academia, radically improving the way scholarly research is managed. The grand vision of Frontiers is a world where all people have an equal opportunity to seek, share and generate knowledge. Frontiers provides immediate and permanent online open access to all its publications, but this alone is not enough to realize our grand goals.

Frontiers journal series

The Frontiers journal series is a multi-tier and interdisciplinary set of open-access, online journals, promising a paradigm shift from the current review, selection and dissemination processes in academic publishing. All Frontiers journals are driven by researchers for researchers; therefore, they constitute a service to the scholarly community. At the same time, the *Frontiers journal series* operates on a revolutionary invention, the tiered publishing system, initially addressing specific communities of scholars, and gradually climbing up to broader public understanding, thus serving the interests of the lay society, too.

Dedication to quality

Each Frontiers article is a landmark of the highest quality, thanks to genuinely collaborative interactions between authors and review editors, who include some of the world's best academicians. Research must be certified by peers before entering a stream of knowledge that may eventually reach the public - and shape society; therefore, Frontiers only applies the most rigorous and unbiased reviews. Frontiers revolutionizes research publishing by freely delivering the most outstanding research, evaluated with no bias from both the academic and social point of view. By applying the most advanced information technologies, Frontiers is catapulting scholarly publishing into a new generation.

What are Frontiers Research Topics?

Frontiers Research Topics are very popular trademarks of the *Frontiers journals series*: they are collections of at least ten articles, all centered on a particular subject. With their unique mix of varied contributions from Original Research to Review Articles, Frontiers Research Topics unify the most influential researchers, the latest key findings and historical advances in a hot research area.

Find out more on how to host your own Frontiers Research Topic or contribute to one as an author by contacting the Frontiers editorial office: frontiersin.org/about/contact

Opportunistic pathogens: pathogenesis and multi-drug resistance mechanisms

Topic editors

Shicheng Chen — Northern Illinois University, United States

Lisheng Liao — South China Agricultural University, China

Mingxi Wang — Huaqiao University, China

Citation

Chen, S., Liao, L., Wang, M., eds. (2025). *Opportunistic pathogens: pathogenesis and multi-drug resistance mechanisms*. Lausanne: Frontiers Media SA.

doi: 10.3389/978-2-8325-6246-8

Table of contents

frontiers | Frontiers in Microbiology

TYPE Editorial
PUBLISHED 03 April 2025
DOI 10.3389/fmicb.2025.1597769

OPEN ACCESS

EDITED AND REVIEWED BY
Rustam Aminov,
University of Aberdeen, United Kingdom

*CORRESPONDENCE
Shicheng Chen
✉ schen1@niu.edu

RECEIVED 21 March 2025
ACCEPTED 24 March 2025
PUBLISHED 03 April 2025

CITATION
Chen S, Liao L and Wang M (2025) Editorial: Opportunistic pathogens: pathogenesis and multi-drug resistance mechanisms.
Front. Microbiol. 16:1597769.
doi: 10.3389/fmicb.2025.1597769

Editorial: Opportunistic pathogens: pathogenesis and multi-drug resistance mechanisms

Shicheng Chen[1]*, Lisheng Liao[2] and Mingxi Wang[3]

[1]Medical Laboratory Sciences Program, College of Health and Human Sciences, Northern Illinois University, DeKalb, IL, United States, [2]Guangdong Province Key Laboratory of Microbial Signals and Disease Control, Integrative Microbiology Research Centre, South China Agricultural University, Guangzhou, China, [3]Yun Leung Laboratory for Molecular Diagnostics, School of Medicine, Huaqiao University, Xiamen, Fujian, China

KEYWORDS

opportunistic pathogens, multi-drug resistant, resistance mechanisms, host defense, horizontal gene transfer, regulatory systems

Editorial on the Research Topic
Opportunistic pathogens: pathogenesis and multi-drug resistance mechanisms

Opportunistic infections have long been underestimated in clinical settings, as the responsible pathogens are often dismissed as normal flora or harmless environmental organisms. Opportunistic pathogens are caplable of causing severe infections in immunocompromised individuals, even leading to significant outbreaks in healthcare settings. The management of opportunistic infections remains particularly challenging due to the absence of standardized guidelines for antibiotic susceptibility testing and the rising prevalence of multidrug resistance. In this Research Topic, titled "*Opportunistic pathogens: pathogenesis and multi-drug resistance mechanisms*", we received 16 submissions and accepted nine manuscripts. Among these works, 8 original research explored pathogenesis and antimicrobial resistance mechanisms in *P. aeruginosa*, *Morganella morganii*, *Staphylococcus epidermidis* and *Klebsiella aerogenes*, *Mycobacterium tuberculosis*, and *Cryptococcus neoformans*. In addition, one manuscript reviewed roles of sterol metabolism in antifungal drug resistance.

The emerging carbapenem-resistant *Pseudomonas aeruginosa* (CRPA) poses a serious global health concern. Xie et al. analyzed 167 isolates in Fujian, China (2019–2021), revealing 58.7% antibiotic resistance and 70 CRPA cases. Molecular typing identified 46 sequence types, including two high-risk clones (ST1971 and ST357). Carbapenemase production was found in 22.9% of CRPA, mainly metallo-β-lactamases (MBLs), alongside *oprD* and *opdP* mutations. Increased biofilm formation and multidrug efflux pump gene expression were also observed. Zhao et al. screened and 143 clinical isolates of *P. aeruginosa* between 2021 and 2023 and found that at least 71 CRPA exhibiting a high carbapenem resistance. They further conducted genome analysis and predicted resistance genes in these CRPA isolates and identified a total of 54 resistance genes. They reported two novel metallo-β-lactamase genes (VIM-92 and blaVIM-24) discovered in this study. $bla_{\mathrm{VIM-92}}$ was embedded in class 1 integrons within the Tn1403 transposon and found on a plasmid. Saha et al. investigated the coexistence of multidrug resistance and virulence

factors in nosocomial *P. aeruginosa* strains. The isolates showed 70–75% susceptibility to aminoglycosides, 30–35% to quinolones, and lower rates for other antibiotics. Metallo-β-lactamase genes were found in 74.1% of strains. Additionally, 89% exhibited hemolysis, 80–90% produced pigments, and 46% formed strong biofilms. All displayed motility, and key virulence genes were detected in 60–80% of isolates.

Yang et al. studied the distribution of promoter types in class 1 integrons (intI1) in *Morganella morganii* clinical isolates and their role in regulating drug resistance gene expression. Among 97 isolates, 28.9% were positive for class 1 integrons, with 24.7% carrying gene cassettes that conferred resistance to aminoglycosides and trimethoprim. Three types of promoters (PcH1, PcS, and PcW) were identified, with P2 promoters found inactive. Stronger promoters led to increased expression of resistance genes, while a negative correlation between integrase (intI1) expression and promoter strength was observed, highlighting the regulatory role of these promoters in resistance.

Rodrigues et al. analyzed 10 *Klebsiella aerogenes* strains from ICU patients in a Brazilian hospital. Their results revealed that these strains exhibited the complete resistance to β-lactam antibiotics, including carbapenems, with varying resistance to aminoglycosides, quinolones, and tigecycline. Half of *K. aerogenes* strains were classified as multidrug-resistant, harboring β-lactamases genes such as *blaKPC-2* and *blaNDM-1*. A comprehensive genomic characterization of strain CRK317, which co-harbored *blaKPC-2* and *blaNDM-1*, identified numerous resistance determinants, including β-lactamases (*blaOXA-9, blaTEM-1, blaCTX-M-15*), aminoglycoside-modifying enzymes, and efflux pumps (*AcrA, tolC, mdtK*). Additionally, 22 genomic islands, insertion sequences, conjugative elements, and prophage regions were detected, suggesting their role in resistance gene dissemination. The presence of integrative and conjugative elements with a type IV secretion system further supports the horizontal transfer of resistance traits.

Lépine et al. investigated a linezolid-resistant *Staphylococcus epidermidis* (LRSE) outbreak at Tours University Hospital in France (2017–2021). Among 34 LRSE isolates, 20 were analyzed for antimicrobial susceptibility, genetic resistance mechanisms, and clonal relationships. All selected strains showed high-level linezolid resistance as well as multidrug resistance. G2576T mutation in the 23S rRNA may confer to the linezolid resistance, with no *cfr* gene detected. PFGE and MLST revealed 95% of strains belonged to ST2. Moreover, linezolid exposure was reported in 70% of patients, though no direct cross-transmission was found.

Singh and Dutta identified a virulence-associated small RNA (sRNA), MTS1338, that drove drug efflux in *Mycobacterium tuberculosis*. Rifampicin exposure increased MTS1338 expression over fourfold, enhancing bacterial growth under treatment. MTS1338 upregulated the efflux protein CydC by stabilizing its mRNA, reducing intracellular drug accumulation. Drug efflux assays confirmed that higher MTS1338 levels led to lower drug retention. These findings reveal a novel sRNA-driven regulatory mechanism contributing to drug resistance in *M. tuberculosis*, highlighting a potential target for developing more effective tuberculosis treatments.

Zheng et al. investigated genome plasticity as a mechanism of non-antifungal-induced antifungal resistance in *Cryptococcus neoformans*. This study further showed that tunicamycin, an ER stress inducer, affected aneuploidy formation in *Cryptococcus neoformans*. Both mild and severe ER stress induced aneuploid strains with diverse karyotypes, some showing resistance or cross-resistance to fluconazole and 5-flucytosine. These aneuploid strains also displayed genomic instability, losing extra chromosomes without stress. Tanwar et al. reviewed role of sterol metabolism in antifungal drug resistance. Sterols are crucial for eukaryotic cell membranes, affecting structure, function, and adaptability. Fungal sterol metabolism, including ergosterol, involves organelles like mitochondria and the ER, regulated by feedback mechanisms. Pathogenic fungi like *Candida*, *Aspergillus*, and *Cryptococcus* cause severe infections, especially in immunocompromised patients. Alterations in sterol metabolism and transport can contribute to antifungal resistance, emphasizing the challenges in treating these infections.

In summary, the nine articles included in this Research Topic cover multiple themes. For example, the rise of multidrug-resistant (MDR) pathogens, such as *Pseudomonas aeruginosa*, *Klebsiella aerogenes*, and *Staphylococcus epidermidis*, poses a significant global health threat. Moreover, studies in this Research Topic explored the pathogenesis, resistance mechanisms, and genetic factors behind these infections. Key findings include the identification of novel resistance genes, promoter types influencing gene expression in *Morganella morganii*, and the role of genome plasticity in antifungal resistance in *Cryptococcus neoformans*. Enhanced understanding of these mechanisms emphasizes the need for targeted treatments and antimicrobial stewardship.

Author contributions

SC: Writing – original draft, Writing – review & editing, Funding acquisition. LL: Writing – review & editing. MW: Writing – review & editing.

Acknowledgments

We sincerely appreciate the contributions to this Research Topic by all the authors, reviewers, and editors.

Conflict of interest

The authors declare that the research was conducted in the absence of any commercial or financial relationships that could be construed as a potential conflict of interest.

Publisher's note

frontiers | Frontiers in Microbiology

TYPE Original Research
PUBLISHED 14 February 2024
DOI 10.3389/fmicb.2024.1352851

OPEN ACCESS

EDITED BY
Mingxi Wang,
Huaqiao University, China

REVIEWED BY
Tahir Hussain,
Iowa State University, United States
Dhiviya Prabaa MS,
Christian Medical College and Hospital, India

*CORRESPONDENCE
Maria-Cristina da Silva Pranchevicius
✉ mcspranc@gmail.com

†These authors have contributed equally to this work

RECEIVED 09 December 2023
ACCEPTED 26 January 2024
PUBLISHED 14 February 2024

CITATION
Rodrigues SH, Nunes GD, Soares GG, Ferreira RL, Damas MSF, Laprega PM, Shilling RE, Campos LC, Costa AS, Malavazi I, Cunha AF and Pranchevicius M-CS (2024) First report of coexistence of blaKPC-2 and blaNDM-1 in carbapenem-resistant clinical isolates of *Klebsiella aerogenes* in Brazil. *Front. Microbiol.* 15:1352851. doi: 10.3389/fmicb.2024.1352851

First report of coexistence of blaKPC-2 and blaNDM-1 in carbapenem-resistant clinical isolates of *Klebsiella aerogenes* in Brazil

Saulo Henrique Rodrigues[1†], Gustavo Dantas Nunes[1†], Gabriela Guerrera Soares[1†], Roumayne Lopes Ferreira[1†], Marcelo Silva Folhas Damas[1†], Pedro Mendes Laprega[1†], Rebecca Elizabeth Shilling[1], Leslie Camelo Campos[2], Andrea Soares da Costa[1], Iran Malavazi[1], Anderson Ferreira da Cunha[1] and Maria-Cristina da Silva Pranchevicius[1*]

[1]Departamento de Genética e Evolução, Universidade Federal de São Carlos, São Carlos, São Paulo, Brazil, [2]Laboratório Central de Saúde Pública do Tocantins, Palmas, Tocantins, Brazil

Klebsiella aerogenes is an important opportunistic pathogen with the potential to develop resistance against last-line antibiotics, such as carbapenems, limiting the treatment options. Here, we investigated the antibiotic resistance profiles of 10 *K. aerogenes* strains isolated from patient samples in the intensive-care unit of a Brazilian tertiary hospital using conventional PCR and a comprehensive genomic characterization of a specific *K. aerogenes* strain (CRK317) carrying both the bla_{KPC-2} and bla_{NDM-1} genes simultaneously. All isolates were completely resistant to β-lactam antibiotics, including ertapenem, imipenem, and meropenem with differencing levels of resistance to aminoglycosides, quinolones, and tigecycline also observed. Half of the strains studied were classified as multidrug-resistant. The carbapenemase-producing isolates carried many genes of interest including: β-lactams (bla_{NDM-1}, bla_{KPC-2}, bla_{TEM-1}, $bla_{CTX-M-1}$ group, bla_{OXA-1} group and $bla_{SHVvariants}$ in 20-80% of the strains), aminoglycoside resistance genes [*aac(6')-Ib* and *aph(3')-VI*, 70 and 80%], a fluoroquinolone resistance gene (*qnrS*, 80%), a sulfonamide resistance gene (*sul-2*, 80%) and a multidrug efflux system transporter (*mdtK*, 70%) while all strains carried the efflux pumps *Acr* (subunit A) and *tolC*. Moreover, we performed a comprehensive genomic characterization of a specific *K. aerogenes* strain (CRK317) carrying both the bla_{KPC-2} and bla_{NDM-1} genes simultaneously. The draft genome assembly of the CRK317 had a total length of 5,462,831 bp and a GC content of 54.8%. The chromosome was found to contain many essential genes. *In silico* analysis identified many genes associated with resistance phenotypes, including β-lactamases (bla_{OXA-9}, bla_{TEM-1}, bla_{NDM-1}, $bla_{CTX-M-15}$, bla_{AmpC-1}, bla_{AmpC-2}), the bleomycin resistance gene (ble_{MBL}), an erythromycin resistance methylase (*ermC*), aminoglycoside-modifying enzymes [*aac(6')-Ib*, *aadA/ant(3")-Ia*, *aph(3')-VI*], a sulfonamide resistance enzyme (*sul-2*), a chloramphenicol acetyltransferase (*catA*-like), a plasmid-mediated quinolone resistance protein (*qnrS1*), a glutathione transferase (*fosA*), PEtN transferases (*eptA*, *eptB*) and a glycosyltransferase (*arnT*). We also detected 22 genomic islands, eight families of insertion sequences, two putative integrative and conjugative elements with a type IV secretion system, and eight prophage regions. This suggests the significant involvement of these genetic

structures in the dissemination of antibiotic resistance. The results of our study show that the emergence of carbapenemase-producing *K. aerogenes*, co-harboring bla_{KPC-2} and bla_{NDM-1}, is a worrying phenomenon which highlights the importance of developing strategies to detect, prevent, and control the spread of these microorganisms.

KEYWORDS

***Klebsiella aerogenes*, whole-genome sequencing, resistance genes, mobile genetic elements, metabolic features, intensive care unit**

Introduction

Klebsiella aerogenes, previously identified as *Enterobacter aerogenes*, is a Gram-negative bacterium belonging to the *Enterobacteriaceae* family. It can be found in various environments including water, soil, air, and the human digestive system as a commensal organism. However, this bacterium is also a significant opportunistic pathogen that has been associated with hospital-acquired diseases such as pneumonia, meningitis, skin, soft tissue and urinary tract infections (Chen et al., 2015).

β-lactam antibiotics are one of the most commonly prescribed drug classes with numerous clinical uses. These antibiotics are sub-classed as penicillins (these being the most commonly prescribed), cephalosporins, cephamycins, monobactams, and carbapenems (Sta Ana et al., 2021). *Klebsiella aerogenes* is intrinsically resistant to ampicillin, amoxicillin, first-generation cephalosporins, and cefoxitin due to the expression of a constitutive AmpC β-lactamase. AmpC type lactamases are also known as extended spectrum β-lactamases (ESBLs) and these provide resistance against the majority of β-lactam antibiotics, such as extended-spectrum cephalosporins and monobactams, with the exception of carbapenems and cephamycins (Davin-Regli and Pages, 2015; Castanheira et al., 2021).

The presence of ESBLs in *K. aerogenes* strains has been well-documented, leading to the use of carbapenems as a last-resort treatment for serious infections caused by these pathogens. However, previous studies have shown a high prevalence of antibiotic resistance to cephalosporins and carbapenems in clinically relevant *K. aerogenes* strains worldwide (Ma et al., 2020). These infections pose a significant public health challenge due to the limited treatment options available and their elevated mortality rates (Mulani et al., 2019; Denissen et al., 2022).

The main resistant mechanism of carbapenemase-producing *K. aerogenes* is the production of carbapenemases, although other mechanisms have been proposed, including overproduction of β-lactamases, efflux pumps, porin deficiency, and changes in penicillin-binding proteins (Pan et al., 2021). Carbapenem resistance in clinical isolates of Carbapenem Resistant Enterobacterales (CRE) is predominantly caused by the presence of these carbapenemases, especially *Klebsiella pneumoniae* Carbapenamase (KPC) and New Delhi Metallo-β-lactamase (NDM). bla_{KPC} is commonly found on various plasmids like IncF-, IncI-, IncA/C-, IncX-, and IncR-type plasmids, while bla_{NDM} is mostly associated with IncX3-type plasmids. These plasmids are easily transferable and can promote the dissemination of bla_{KPC} and bla_{NDM} through horizontal gene transfer among diverse bacterial populations spreading antibiotic resistance (Yuan et al., 2023).

Although carbapenemases such as KPC, NDM, and Imipenemase (IMP) have been detected in *K. aerogenes*, there are limited studies demonstrating the simultaneous presence of bla_{KPC} and bla_{NDM} genes. Here, we conducted an in-depth analysis of genes related to the antimicrobial resistance and mobile genetic elements in carbapenemase-producing *K. aerogenes*, found in Brazilian hospitals, to understand its genomic diversity. To the best of our knowledge, this paper is the first to report the simultaneous presence of both bla_{KPC} and bla_{NDM} in *K. aerogenes* isolated from clinical samples in Brazil.

Materials and methods

Bacterial isolates

A total of 10 *K. aerogenes* were isolated from clinical specimens and devices in the ICU and neonatal intensive care unit (NICU) at a tertiary care of a government hospital in Palmas, Tocantins, Brazil, between January 2017 and May 2020. The *K. aerogenes* strains were initially identified by the hospital's clinical microbiology laboratory before being forwarded to the Central Public Health Laboratory of the State of Tocantins (LACEN/TO) for species confirmation and drug susceptibility testing. LACEN is a healthcare facility under the Brazilian Ministry of Health that receives samples for antimicrobial resistance surveillance.

Detection of antibiotic resistance and carbapenemase productions

Bacterial identification and determination of antibiotic susceptibility were carried out using the VITEK2 compact automated system (bioMerieux, Hazelwood, MO, USA). The susceptibility of the *K. aerogenes* isolates were tested against a panel of 16 antibiotics, which included ampicillin/sulbactam (SAM), piperacillin/tazobactam (TZP), cefuroxime sodium (CXM-S), cefuroxime axetil (CXM-AX), cefoxitin (FOX), ceftazidime (CAZ), ceftriaxone (CRO), cefepime (FEP), ertapenem (ETP), imipenem (IPM), meropenem (MEM), amikacin (AMK), gentamicin (GEN), ciprofloxacin (CIP), tigecycline (TGC), and colistin (CST). The findings were interpreted in accordance with the guidelines set forth by Clinical and Laboratory Standards Institute (CLSI, 2023). Phenotypic detection of carbapenemase production in *K. aerogenes* was carried out by

modified Hodge test and ethylenediaminetetraacetic acid (EDTA) synergy tests under the CLSI guidelines (CLSI, 2023) as described elsewhere (Ferreira et al., 2019, 2020; Damas et al., 2022; Soares et al., 2023). *K. aerogenes* isolates were classified as multidrug-resistant (MDR) by non-susceptibility to at least one agent in three or more antimicrobial categories, as per the criteria established by Magiorakos et al. (2012). *K. aerogenes* are naturally resistant to ampicillin (AMP), amoxicillin/clavulanic acid (AMC), FOX, and cephalothin (CFL) due to the low production of the naturally induced cephalosporinase of Bush group 1 (class C) (Davin-Regli and Pages, 2015). Therefore, AMP and FOX were not included in the MDR classification (Magiorakos et al., 2012).

DNA isolation

Klebsiella aerogenes strains were subcultured on Brain Heart Infusion (BHI) broth (Oxoid, United Kingdom) and incubated for 24 h at 37°C. Genomic DNA extraction was performed from an overnight culture using the Cellco Genomic DNA purification kit (Cellco Biotech., São Carlos, Brazil), according to the manufacturer's instructions. The DNA was quantified using the NanoVue Plus instrument (GE Healthcare Life Sciences, Marlborough, MA, United States). The quality of the genomic DNA was examined through electrophoresis while the bacterial DNA concentration was determined using the Qubit® 3.0 fluorometer in combination with the Qubit® dsDNA Broad Range Assay Kit from Life Technologies (Carlsbad, CA, USA).

Detection of antibiotic resistant genes

Polymerase chain reaction (PCR) was performed for the detection of resistance-related genes, such as ESBL-encoding genes (bla_{TEM}, $bla_{SHV\ variants}$, $bla_{OXA-1,\ 4\ and\ 30}$, $bla_{CTX-M-1\ group}$, bla_{GES}, $bla_{PER-1\ and\ 3}$, $bla_{VEB-1\ to\ 6}$), carbapenemase genes (bla_{KPC}, bla_{OXA-48}, bla_{IMP-1}, bla_{VIM-2}, bla_{NDM}, bla_{SPM-1}, bla_{GIM-1}, bla_{SIM-1}), aminoglycosides [*armA*, *rmtB*, *aph(3′)*-VIa *(aphA6)*], tetracycline (*tetB*), sulfonamide (*sul-1*, *sul-2*), colistin resistance (*mcr-1*), plasmid mediated quinolone resistance (PMQR) gene [*aac(6′)-Ib-cr*, *qnrS1* and *qnrS2*], efflux pump (*acrAB*, *tol*C, and *mdtK*) genes. Amplicons were analyzed by gel electrophoresis in 1.0% agarose and visualized under ultraviolet (UV) light. Supplementary Table S1 provides information on amplicons length and PCR conditions.

One amplicon of each studied gene was purified using the Gel Band Purification Kit (Cellco Biotech., São Carlos, Brazil) and sequenced using the Sanger DNA sequencing method. The sequences were edited using Bioedit v7.0.5 (Hall, 1999), then compared with GenBank and Refseq sequences using BlastX tools: ACT53230.1 ($bla_{CTX-M-15}$), QXU68638.1 (bla_{TEM-1}), EKZ5222878.1 (bla_{NDM}), SCZ84112.1 (bla_{SHV-2}), WEA84669.1 (bla_{KPC}), WP_240093217.1 (bla_{OXA-1}), WP_047046709.1 (*tol*C), EFZ4507594.1 (*qnrS*), MCL7674773.1 (*acrA*), HBS1035150.1 (*aac-(6′)-Ib*), HEC1006964.1 (*aph(3′)*-VIa), QDB65114.1 (*sul-2*), and PLP19006.1 (*mdtK*). Subsequently, the nucleotide sequences of the genes were submitted to the GenBank database and assigned accession numbers: SRX22793090 (*sul-2*), SRX22793089 (*mdtK*), SRX22793063 (*qnrS*), SRX22793062 (*tolC*), SRX22793031 (*acrA*), SRX22789929 (*aph(3′)*-VIa), SRX22789927 (*aac-(6′)-Ib*), SRX22789878 (bla_{SHV-2}), SRX22789871 (bla_{OXA-1}), SRX22789802 (bla_{NDM}), SRX22789553 (bla_{KPC}), SRX22789857 (bla_{TEM-1}), and SRX22789858 ($bla_{CTX-M-15}$).

Genome sequencing

The *K. aerogenes* CRKA317 was selected for whole genome sequencing (WGS). The Nextera XT DNA Library Prep Kit (Illumina, San Diego, California, United States) was utilized to conduct the library preparation using 1 ng of DNA as our material to sequence. A limited cycle polymerase chain reaction (PCR) program was employed to amplify the libraries introducing Index 1 (i7) adapters, Index 2 (i5) adapters, and the requisite sequences for generating sequencing clusters. The amplified library was purified using 0.6 x Agencourt AMPure XP beads (Beckman Coulter, Brea, California, USA). The quality of the library and the size of fragmented DNA was evaluated on a 1.5% electrophoresis agarose gel and quantified using a fluorometric method involving the Qubit® 3.0 instrument and the Qubit® dsDNA Broad Range Assay Kit (Life Technologies, Carlsbad, California, United States). The resulting library concentrations were subsequently normalized to 4 nM using a standard dilution method. The libraries were then combined, denatured with 0.2 N sodium hydroxide (NaOH), and diluted to attain a final concentration of 1.8 pM. To ensure the run's accuracy and control, a PhiX control was added to achieve a final concentration of 1.5 pM. The sequencing run involved a paired-end run comprising 75 cycles for each read (2 × 75), plus up to eight cycles for two index reads.

Genome assembly, annotation and prediction of orthologous group

Initially, FastQC v.0.12.0[1] was used to check the raw reads quality. The raw reads were filtered by quality, length, and adapter regions using Trim Galore! v.0.6.10.[2] The genome assembly was made with SPAdes 3.2 (Bankevich et al., 2012) and SSPACE (Boetzer et al., 2011), using "careful" and "cov-cutoff auto" as settings. Contigs with less than 200 bp were discarded. PlasmidFinder 2.13[3] (Carattoli et al., 2014) and PlasmidSPAdes (Antipov et al., 2016) were used to plasmid detection and assembly attempts. QUAST v5.0.2 (Gurevich et al., 2013) were used to access the general statistics of assembled genome. The circular genome was built using Proksee[4] (Grant et al., 2023). For the annotations of genome, both Prokka v.1.14.5 (Seemann, 2014) and Rapid Annotation using Subsytems Technology (RAST)[5] (Aziz et al., 2008) servers were used. The completeness of the assembled genome was assessed using the BUSCO program (Simão et al., 2015).

The Clusters of Orthologous Group (COG) were annotated and distributed in categories using eggNOG-mapper v2[6] (Cantalapiedra et al., 2021). Kyoto Encyclopedia of Genes and Genomes

1 https://www.bioinformatics.babraham.ac.uk/projects/fastqc/
2 https://www.bioinformatics.babraham.ac.uk/projects/trim_galore/
3 https://cge.food.dtu.dk/services/PlasmidFinder/
4 https://proksee.ca/
5 https://rast.nmpdr.org/
6 http://eggnog-mapper.embl.de/

(KEGG) was used to determinate Gene Ontology (GO)[7] (Kanehisa et al., 2016).

Phylogenetic inferences using 16S rRNA gene sequences, ANI, dDDH, and TYGS

Our 16S rRNA gene sequence from our genome annotation was used in the analysis with another 36 16S rRNA reference sequences of *Klebsiella* genus obtained from the GenBank database (Supplementary Table S2). The 16S rRNA analysis was performed using *Escherichia coli* as its outgroup. Nucleotide sequences were aligned using the online software MAFFT[8] (Katoh and Standley, 2013). JModelTest v2.1.10 (Posada, 2008) was used to estimate the best-fitting nucleotide substitution model and PhyML v3.0 (Guindon et al., 2009) to construct a maximum likelihood (ML) phylogenetic tree. Branches was supported by bootstrap analysis of 1,000 replicates.

The OrthoANI v0.93.1 tool (Yoon et al., 2017) was used to calculate the Average Nucleotide Identity (ANI) between our genome and another 18 reference and uncharacterized complete *Klebsiella* genus genomes (Supplementary Table S3). For the *in silico* calculation of digital DNA–DNA Hybridization (dDDH), Genome to Genome Distance Calculator (GGDC 3.0)[9] (Meier-Kolthoff et al., 2013) was used with the same genomes. A heatmap with the results from OrthoANI and dDDH was constructed using CIMminer.[10] To reinforce our phylogenetic inference, the Type (Strain) Genome Server (TYGS)[11] was performed using all strains from the server database (Meier-Kolthoff et al., 2022).

Comparative pan-genome analysis of *Klebsiella aerogenes* strains

The online pipeline REALPHY[12] (Bertels et al., 2014) was used to build a whole-genome sequence-based phylogenetic tree, using the 26 complete genomes of clinical strains of *K. aerogenes* available in NCBI (Supplementary Table S4). The result showed the closest *Klebsiella* species to our strain. These species were used in Orthovenn2 web server[13] (Xu et al., 2019) to compare orthologous gene clusters using whole-genome sequence. Furthermore, Bacterial Pangenome Analysis Pipeline (BPGA) v.1.3 (Chaudhari et al., 2016) was performed against the Kyoto Encyclopedia Genomics and Genes Database (KEGG) to predict the core, accessory and unique genes as well as their functional distribution. REALPHY, Orthovenn2 and BPGA were used in default settings.

Characterization of resistance

The annotation of antibiotic resistance genes, efflux pumps and porins was made by CARD online[14] (Alcock et al., 2019), ResFinder 4.4.2[15] (Bortolaia et al., 2020), ABRicate[16] (Afgan et al., 2018), BlastKOALA[17] (Kanehisa et al., 2016) and CARD and ARG-ANNOT (Gupta et al., 2014) databases. The parameters used for databases were 1E-5 e-value, ≥ 70% of identity and ≥90% coverage cut-off.

Known mutations in *gyrA*, *gyrB*, and *parC*, that are responsible for quinolone resistance, were investigated using BLASTp comparison. Furthermore, even though *K. aerogenes* CRKA317 is not resistance to colistin, mutations in *phoP* and *phoQ* were also evaluated to investigate polymyxin resistance. For the alignment we used the following sequences: *gyrA* (*Klebsiella* [multispecies]: WP_004201688.1), *gyrB* (*Klebsiella* [multispecies]: WP_004173845.1), *parC* (*Klebsiella* [multispecies]: WP_004181324.1), *phoP* (*Klebsiella* [multispecies]: WP_025714403.1) and *phoQ* (*Klebsiella* [multispecies]: WP_045393745.1).

Genomic islands and mobile genetic elements

The presence of Genomic Islands (GIs) was investigated with IslandViewer 4 webserver[18] (Bertelli et al., 2017), using *K. aerogenes* isolate 57 as the reference strain. Integrons, transposons and insertion sequences were evaluated using Integron Finder (Afgan et al., 2018), TnCentral[19] (Ross et al., 2021) and ISfinder[20] (Siguier, 2006), respectively. MGEfinder[21] (Durrant et al., 2020) was used to understand the relation between resistance genes with mobile genetic elements. The webserver ICEfinder[22] (Liu et al., 2019) was used to identify Integrative and Conjugative Elements (ICE). Sequences of Clustered Regularly Interspaced Short Palindromic Repeats (CRISPR) were searched using CRISPRCas Finder[23] (Couvin et al., 2018). To identify and annotate prophage sequences in genome, the PHASTER webserver[24] (Arndt et al., 2016) was used. The Phigaro v.2.3.0 pipeline (Starikova et al., 2020) was used to indicate the possible phage family.

Genome accession number

Raw reads were submitted to Sequence Reads Archives,[25] with submission number JAXIVA000000000. The draft genome is available at GenBank BioProject accession PRJNA1047945.

7 https://www.kegg.jp/blastkoala/
8 https://www.ebi.ac.uk/Tools/msa/mafft/
9 https://ggdc.dsmz.de/ggdc.php
10 https://discover.nci.nih.gov/cimminer/oneMatrix.do
11 https://tygs.dsmz.de/
12 https://realphy.unibas.ch/realphy/
13 https://orthovenn2.bioinfotoolkits.net/task/create
14 https://card.mcmaster.ca/analyze/rgi
15 http://genepi.food.dtu.dk/resfinder
16 https://galaxy.pasteur.fr/
17 https://www.kegg.jp/blastkoala/
18 https://www.pathogenomics.sfu.ca/islandviewer/
19 https://tncentral.ncc.unesp.br/
20 https://www-is.biotoul.fr/index.php
21 https://cge.food.dtu.dk/services/MobileElementFinder/
22 https://bioinfo-mml.sjtu.edu.cn/ICEfinder/ICEfinder.html
23 https://crisprcas.i2bc.paris-saclay.fr/CrisprCasFinder/Index
24 https://phaster.ca/
25 https://www.ncbi.nlm.nih.gov/sra

Results

Antimicrobial susceptibility, detection of resistance-related genes

A total of 10 non-repetitive clinical isolates of *K. aerogenes* were isolated from rectal swabs, (40%, $n = 4$), urine (30%, $n = 3$), tracheal aspirate (10%, $n = 1$), blood (10%, $n = 1$) and catheter tips (10%, $n = 1$) from adult patients admitted to the intensive care unit (ICU) of a tertiary hospital located in Brazil. All isolates were resistant to the β-lactam antibiotics tested, including SAM, TZP, CXM-S, CXM-AX, FOX, CAZ, CRO, FEP, ETP, IPM, and MEM. MDR was observed in 50% ($n = 5$) of the strains, and the most common MDR profiles were related to β-lactam-aminoglycosides-quinolone (20%, $n = 2$), β-lactam-quinolone-glicylcycline (20%, $n = 2$), and β-lactam-aminoglycosides-quinolone-glicylcycline (10%, $n = 1$). On the other hand, 80% of the isolates were susceptible to GEN, 80% to AMK, 70% to TGC, 50% to CIP, and 100% to CST. General data and susceptibility profiles of all clinical carbapenem-resistant *K. aerogenes* (CRKA) isolates are showed in Table 1 and Supplementary Figure S1.

Of the 10 carbapenemase-producing *K. aerogenes* isolates, the $bla_{\text{NDM-1}}$ gene was detected in 8 isolates (80%), followed by $bla_{\text{KPC-2}}$ in 7 isolates (70%). Whereas the concomitant presence of $bla_{\text{KPC-2}}$ with $bla_{\text{NDM-1}}$ gene was detected in 5 isolates (50%). In addition, the $bla_{\text{TEM-1}}$ (80%, $n = 8$) was the most common ESBL-encoding gene among *K. aerogenes* investigated, followed by $bla_{\text{CTX-M1-group}}$ (50%, $n = 5$), $bla_{\text{OXA-1,4, and 30}}$ (40%, $n = 4$), and $bla_{\text{SHV variants}}$ (20%, $n = 2$) (Table 1 and Supplementary Figure S1).

Regarding the genes that provide resistance to aminoglycosides, 7 isolates (70%) carried the *aph(3′)-VI* (*aphA6*) and 8 strains (80%) carried the *aac(6′)-Ib* gene. Eight strains (80%) harbored *qnrS* (*qnrS1* and/or *qnrS2*), capable of causing resistance fluoroquinolones antibiotics. The sulfonamide resistance gene (*sul-2*) gene was present in 8 isolates (80%). All the CRKA isolates we investigated had genes related to efflux pumps *acrA* and *tolC*. The *mdtK* gene, which is a multidrug efflux system transporter, was present in 7 strains (70%) (Table 1 and Supplementary Figure S1). The genes related to antibiotic resistance $bla_{\text{OXA-48}}$; $bla_{\text{SPM-1;}}$ $bla_{\text{IMP-1}}$; $bla_{\text{VIM-2}}$; $bla_{\text{SIM-1}}$; $bla_{\text{GIM-1,}}$ $bla_{\text{GES-1, 9,11}}$; $bla_{\text{PER-1, 3}}$; $bla_{\text{VEB-1 to 6}}$, *mcr-1*, *sul-1*, *aac(6′)-Ib-cr*, *armA*, *rmtB* and *tetB* were not found in CRKA isolates.

Classes of antibiotics

β-lactams: SAM (ampicillin-sulbactam), TZP (piperacillin-tazobactam), CXM-S (cefuroxime sodium), CXM (cefuroxime axetil), FOX (cefoxitin), CAZ (ceftazidime), CRO (ceftriaxone), FEP (cefepime), ETP (ertapenem), IPM (imipenem), MEM (meropenem); aminoglycosides: GEN (gentamicin) and AMK (amikacin); quinolones: CIP. (ciprofloxacin); glycylcycline: TGC (tigecycline) and polymyxin: CST (colistin). MDR (multidrug-resistant) = resistance to at least one agent in three or more antibiotic categories. * Whole-genome sequencing was performed on CRKA317. +, the tested gene was detected by PCR and Sanger sequencing; –, the tested gene was not detected.

Genome and functional annotation

Given the existence of both the $bla_{\text{KPC-2}}$ and $bla_{\text{NDM-1}}$ genes in CRK317, as well as the strain's resistance to a broad spectrum of antibiotics (except for gentamicin and colistin), whole genome sequencing (WGS) was employed to obtain comprehensive genomic data from the *K. aerogenes* CRKA317. The draft genome of CRKA317 comprised one circular chromosome, which is 5,462,831 bp in size, with an average GC content of 54.8%. The annotation of the bacterial genome predicted a total of 51 contigs, 5,403 coding sequences and 5,374 genes that covered 88.88% of genome. Of the 65 RNA genes predicted, 5 were rRNAs, 59 were tRNAs and one was a transfer-messenger RNA (tmRNA) (Supplementary Table S5 and Figure 1A). The assembly of plasmids was unsuccessful, but fragments of IncFIB (pQil), IncC, and IncFII (K) plasmids were detected.

According to the RAST analysis, the genome of *K. aerogenes* CRKA317 is composed of 398 subsystems that can be categorized into 27 distinct categories (Figure 1B). The six most significant categories included "carbohydrates" with a total of 398 genes, followed by "amino acids and derivatives" (382 genes), "protein metabolism" (217 genes), "cofactors, vitamins, prosthetic groups, pigments" (177 genes), "membrane transport" (158 genes), and "respiration" (125 genes). In the specific category of "virulence, disease and defense," (52 genes) there were 32 genes related to resistance against antibiotics and toxic compounds; such as β-lactamase enzymes (one gene), fluoroquinolone resistance (two genes), fosfomycin resistance (one gene), copper homeostasis (11 genes), copper homeostasis: cooper tolerance (ten genes), cobalt-zinc-cadmium resistance (four genes), zinc resistance (two genes), adaptation to d-cysteine (one gene); Furthermore, we found 14 genes associated with invasion and intracellular resistance, four genes linked to adhesion, and two genes related to bacteriocins, ribosomally synthetized antibacterial peptides.

The analysis of protein-coding genes resulted in a total of 5,116 genes distributed across different functional categories within the Cluster of Orthologous Groups. The largest proportion of known protein coding genes was related to "transcription" (471; 9.21%), followed by categories such as "inorganic ion transport and metabolism" (431; 8.42%), "energy production and conversion" (384; 7.50%), "carbohydrate transport and metabolism" (368; 7.19%), and "amino acid transport and metabolism" (345; 6.74%). There were also gene associations with defense mechanisms (61; 1.19%) and a significant portion classified as having unknown functions (1,005; 19.64%) (Figure 1C).

Phylogenetic analysis and genome similarity among representative *Klebsiella* species

To gain insights into the evolutionary placement of *K. aerogenes* CRKA317, a phylogenetic tree was generated using 16S rRNA gene sequences from 36 reference sequences of *Klebsiella* species available at NCBI.[26] Our findings indicated that CRKA317 was not closely related to *K. aerogenes* (Figure 2A). The use of 16S rRNA gene for

26 https://www.ncbi.nlm.nih.gov/

TABLE 1 Antimicrobial resistance of *K. aerogenes* isolates and presence of genes coding for resistance, and efflux pumps.

Strains	Source of infection	Antibiotic resistance	MDR	Genes associated with drug resistance												
				β-lactams						Aminoglycosides		Quinolone	Sulfonamide	Multidrug efflux pump		
				bla_{KPC-2}	bla_{NDM-1}	bla_{TEM-1}	$bla_{oxa1, 4, 30}$	$bla_{SHV\ variants}$	$bla_{CTX-M-1\ group}$	*aac(6')-Ib*	*aph(3')*-VIa	*qnrS (qnrS1, S2)*	*sul-2*	*acrA*	*tolC*	*mdtK*
CRKA315	Rectal swab	SAM, TZP, CXM, CXM-S, FOX, CAZ, CRO, FEP, ETP, IPM, MEM	No	+	–	–	–	+	+	+	+	+	+	+	+	+
CRKA316	Rectal swab	SAM, TZP, CXM, CXM-S, FOX, CAZ, CRO, FEP, ETP, IPM, MEM	No	+	+	+	–	–	+	+	+	+	+	+	+	–
CRKA454	Rectal swab	SAM, TZP, CXM, CXM-S, FOX, CAZ, CRO, FEP, ETP, IPM, MEM, CIP, TGC	Yes	–	+	+	+	–	–	+	+	+	+	+	+	+
CRKA534	Rectal swab	SAM, TZP, CXM, CXM-S, FOX, CAZ, CRO, FEP, ETP, IPM, MEM, CIP, TGC	Yes	+	+	+	–	–	+	+	+	+	+	+	+	+
*CRKA317	Urine	SAM, TZP, CXM, CXM-S, FOX, CAZ, CRO, FEP, ETP, IPM, MEM, AMK, CIP, TGC	Yes	+	+	+	+	-	+	+	+	+	+	+	+	+
CRKA459	Urine	SAM, TZP, CXM, CXM-S, FOX, CAZ, CRO, FEP, ETP, IPM, MEM	No	+	+	–	–	–	–	–	+	+	+	+	+	–
CRKA538	Urine	SAM, TZP, CXM, CXM-S, FOX, CAZ, CRO, FEP, ETP, IPM, MEM, GEN, CIP	Yes	+	+	+	+	–	+	+	+	+	+	+	+	+
CRKA532	Tracheal aspirate	SAM, TZP, CXM, CXM-S, FOX, CAZ, CRO, FEP, ETP, IPM, MEM	No	–	+	+	+	–	–	+	–	–	–	+	+	+
CRKA211	Blood	SAM, TZP, CXM, CXM-S, FOX, CAZ, CRO, FEP, ETP, IPM, MEM, AMK, CIP	Yes	–	+	+	–	–	–	+	–	+	+	+	+	+
CRKA495	Catheter tip	SAM, TZP, CXM, CXM-S, FOX, CAZ, CRO, FEP, ETP, IPM, MEM	No	+	–	+	–	+	–	–	–	–	–	+	+	–
		Genes present (%)		**70**	**80**	**80**	**40**	**20**	**50**	**80**	**70**	**80**	**80**	**100**	**100**	**70**

10.3389/fmicb.2024.1352851

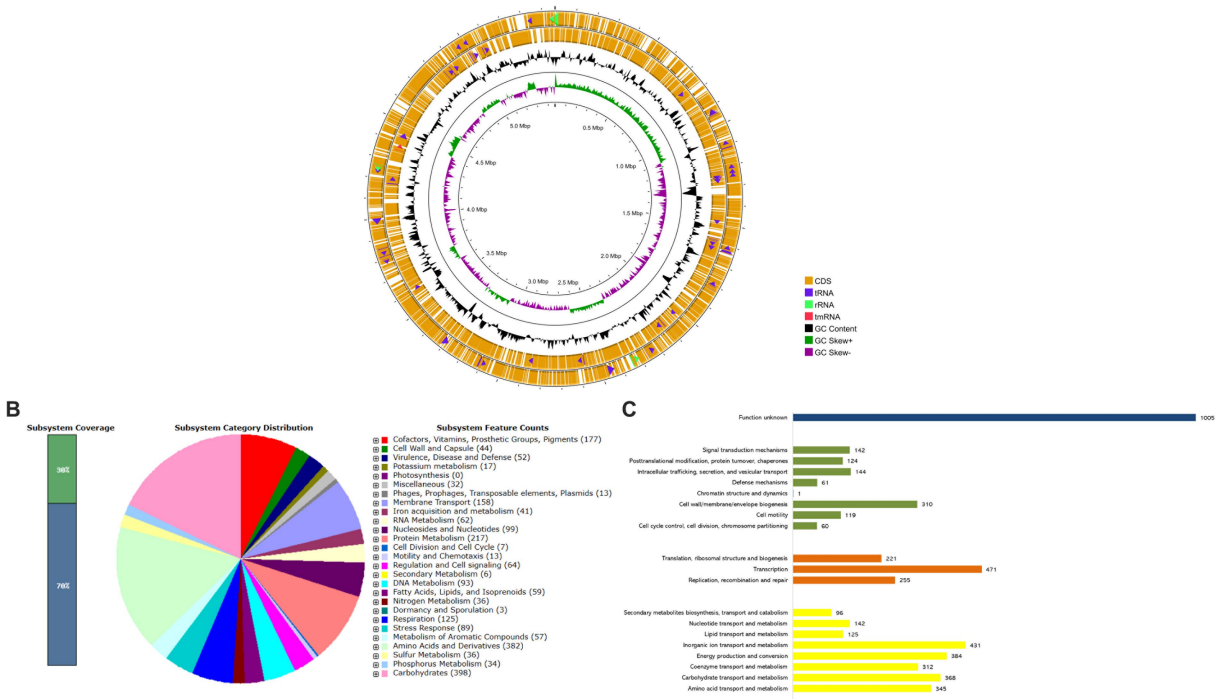

FIGURE 1
Whole-Genome Sequencing and functional annotations of *K. aerogenes* CRKA317. **(A)** The circular diagram consists of four circles, numbered from 1 (outer) to 4 (inner). The outer two orange circles represent the coding sequence (CDS), the transfer RNA (tRNA) is indicated by a purple arrowhead, the ribosomal RNA (rRNA) is shown with a green arrowhead, and the transfer-messenger RNA (tmRNA) is denoted by a red arrowhead. The third, black circle represents the GC content. The fourth circle displays the GC skew curve indicating a positive skew in green and negative skew in violet. **(B)** The bar indicates the percentage of subsystem coverage, with the green segment representing the proportion of proteins included. The pie chart presents an overview of the distribution of various categories within these subsystems. **(C)** COG classification in categories: metabolism (yellow bars), information processing and storage (orange bars), cellular processes and signaling (green bars), and unknown function (blue bar).

species identification presents significant challenges in interpretation because of its hypervariable domains (Koroiva and Santana, 2022). Nevertheless, this approach allowed for an assessment of its relationship in the broader context of the genus.

Next, species validation and genomic similarity were assessed through *in silico* ANI, DDH and TYGS analysis. Our next step was a comparative analysis of 13 reference sequences of *Klebsiella* species, including 5 clinical isolates of *Klebsiella* spp. and our *K. aerogenes* CRKA317. ANI analysis revealed high similarity between *K. aerogenes* CRKA317 and *K. aerogenes* (Ka37751; GCA_007632255.1), with a close match of approximately 98.52% (Figure 2B). The genetic relatedness between these two strains was also confirmed with a DDH value of 88.90% (Figure 2C). The TYGS-based results showed that *K. aerogenes* CRKA317 is most closely related to *K. aerogenes* KCTC 2190, with dDDH values of 89%, also positioning CKA317 as a *K. aerogenes* (Figure 2D).

Phylogenomic analysis of *Klebsiella aerogenes* strains

Next, we determined the genetic similarity between *K. aerogenes* CRKA317 and 26 genomes of *K. aerogenes* obtained from the NCBI database. Our findings indicated that our *K. aerogenes* CRKA317 strain is more closely related to *K. aerogenes* 57, *K. aerogenes* CAVI1320, and *K. aerogenes* EA46506, which are forming a monophyletic clade (Figure 3A). Although the isolation source for the closest strain (*K. aerogenes* 57) was not specified in the NCBI website, the other two strains were isolated from clinical samples (Figure 3B).

Comparative genomic analysis of four *Klebsiella aerogenes* strains

We also conducted a comparative analysis of the predicted gene numbers in three closely related strains of *K. aerogenes* with our *K. aerogenes* CRKA317. This allowed us to identify both common genes shared across these strains, as well as those that were unique to each individual strain. Our data showed the four *K. aerogenes* strains shared 4,242 genes, and *K. aerogenes* CRKA317 was found to contain 16 strain-specific gene clusters which were associated to metal ion transport including response to cadmium ion, and copper ion transport (Figure 4A). The *K. aerogenes* CRKA317 showed a higher number of singleton genes ($n = 574$) compared to other *K. aerogenes* strains (Figure 4B), including genes associated with resistance such as $bla_{\text{NDM-1}}$, *aadA*/*ant*(3")-Ia, *aph*(3')-VI, and *qnr*S1.

The analysis of KEGG functional distributions in the 4 strains (*K. aerogenes* 57, *K. aerogenes* CAVI1320, and *K. aerogenes* EA46506) showed that the majority of genes were associated with the core genomes (94.16%; $n = 2{,}950$), followed by unique genomes (3.16%;

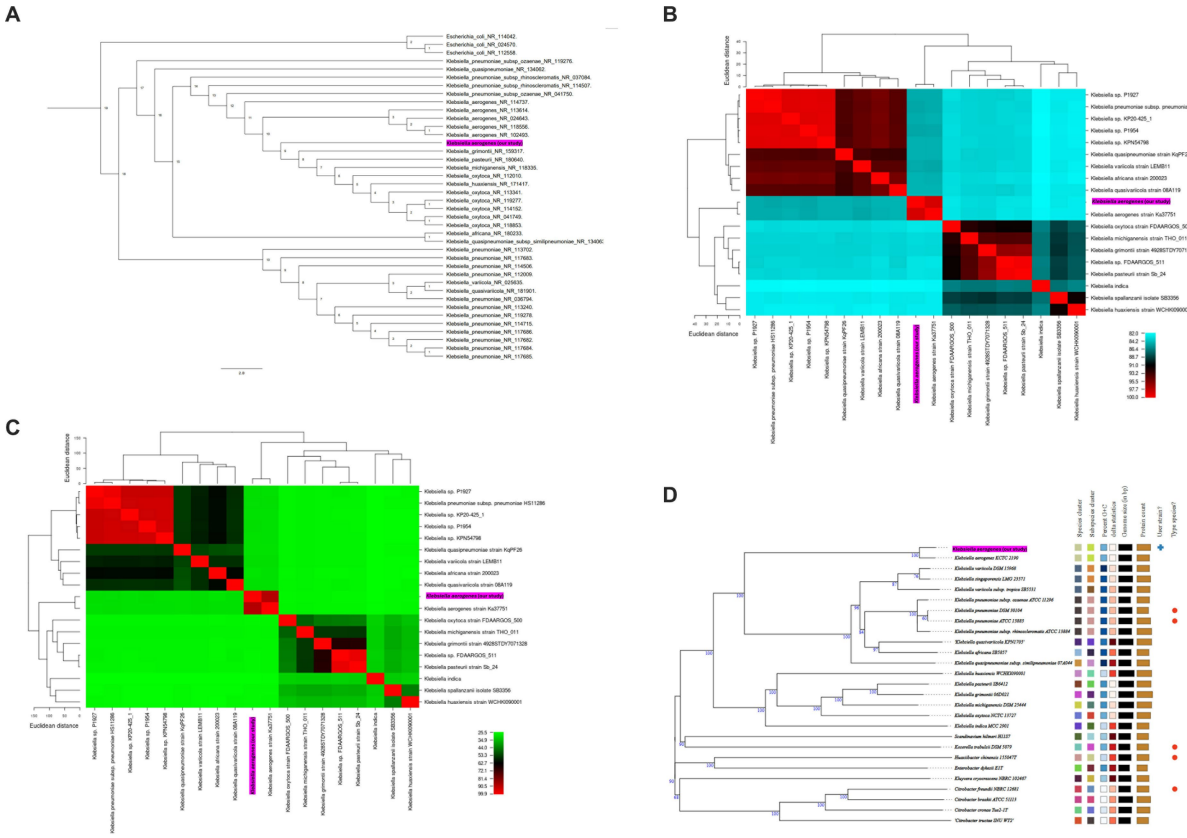

FIGURE 2
(A) Phylogenetic tree based on 16S rRNA gene sequences, which shows the relationship between *K. aerogenes* CRKA317 and other. The number next to the node represents the age value, and the scale bar indicates 2.0 substitutions per nucleotide position. **(B,C)** display heat maps of average nucleotide identity (ANI, **B**) and *in silico* DNA–DNA hybridization (DDH, **C**) respectively, which compare *K. aerogenes* CRKA317 to *Klebsiella* species. **(D)** Phylogenomic tree based on TYGS. The numbers above the branches represent GBDP pseudo-bootstrap support values >60% of 100 replications, with an average branch support of 86.2%. The tree was rooted at the midpoint. Our strain is highlighted in pink.

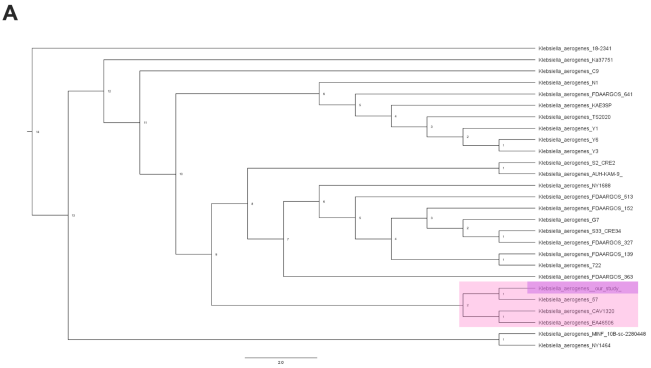

Bioproject	Host	Isolation source	Geographic location
PRJNA554399	*Homo sapiens*	-	South Korea: Seoul
PRJNA555744	*H. sapiens*	Sputum	China: Zhejiang
PRJNA550014	*H. sapiens*	Clinical sample	Australia: Sydney
PRJNA597473	*H. sapiens*	Feces	Ireland
PRJNA231221	*H. sapiens*	-	USA: KY
PRJNA757479	*H. sapiens*	Sputum	-
PRJNA855143	*H. sapiens*	Feces	China: Wuhan
PRJNA575100	*H. sapiens*	Blood	South Korea
PRJNA575100	*H. sapiens*	-	South Korea
PRJNA575100	*H. sapiens*	-	South Korea
PRJNA667445	*H. sapiens*	Bronchoalveolar lavage	USA: Durham, NC
PRJNA551102	*H. sapiens*	Urine	Lebanon
PRJNA817889	*H. sapiens*	Phlegm	China: Beijing
PRJNA231221	*H. sapiens*	Endotracheal aspirate	-
PRJNA231221	*H. sapiens*	Urine	USA: DC
PRJNA279469	*H. sapiens*	Bronchial aspiration	France
PRJNA667445	*H. sapiens*	Lt groin wound	USA: Durham, NC
PRJNA231221	*H. sapiens*	Skin swab	USA: DC
PRJNA231221	*H. sapiens*	Rectal swab	USA: DC
PRJNA836696	*H. sapiens*	Blood	USA: Houston
PRJNA231221	*H. sapiens*	Stool	USA: DC
PRJNA1047945	*H. sapiens*	Urine	Brazil: TO
PRJEB42440	*H. sapiens*	-	Spain
PRJNA246471	*H. sapiens*	Perirectal	USA: Virginia
PRJNA700516	*H. sapiens*	Rectal swab	Czech Republic
PRJNA646837	*H. sapiens*	Sputum	Australia
PRJNA818004	*H. sapiens*	Hydrothorax	China: Henan

FIGURE 3
Phylogenomic analysis of *K. aerogenes* strains. **(A)** Phylogenetic tree showing the similarity between CRKA317 and other 26 selected strains of *K. aerogenes*. **(B)** Genome Assembly and Annotation report of *K. aerogenes* strains. Our strain is highlighted in pink.

$n = 99$), and accessory genomes (2.7%; $n = 84$) (Figure 4C). The genes were associated mainly with "metabolism" and were highly abundant in the accessory genome (73.91%; $n = 62$), followed by the core (69.29%; $n = 2047$), and unique (59.59%, $n = 59$) genomes (Figure 4C). Out of the total number of genes linked to human diseases ($n = 158$), 12.3% were found in the unique gene clusters, while 7.14% were present in accessory gene clusters and 4.73% was assigned to core gene clusters (Figure 4C).

Analysis of the annotations for all core genes revealed that a majority were associated with "carbohydrate metabolism" (15.83%),

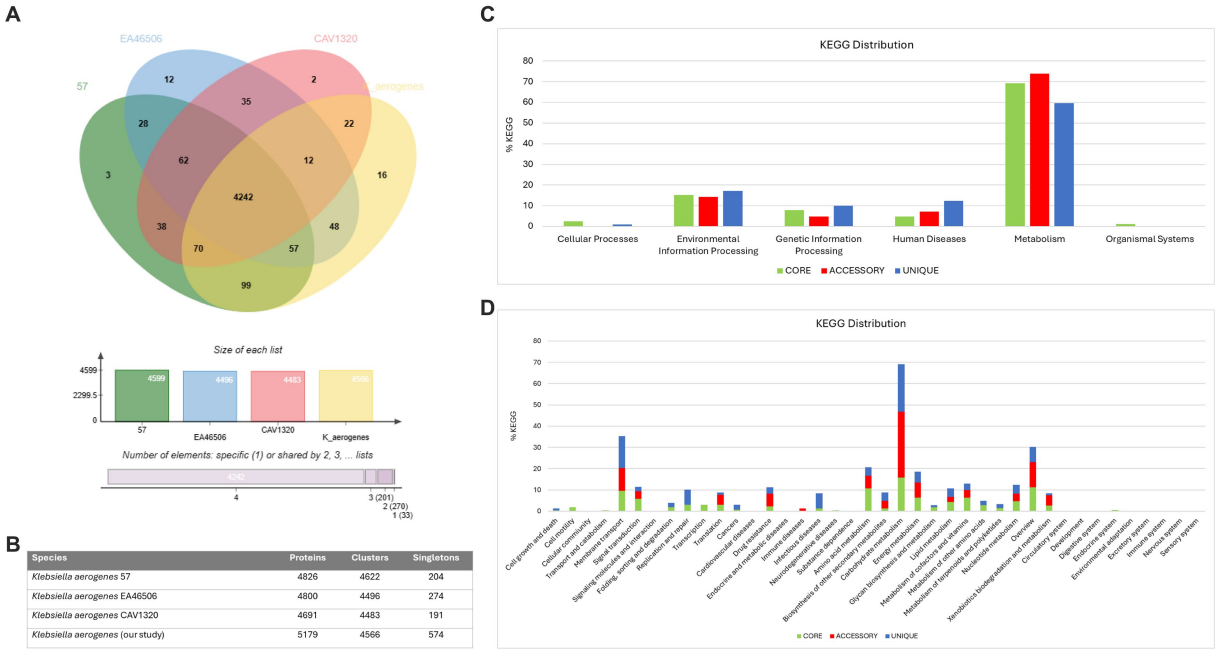

Species	Proteins	Clusters	Singletons
Klebsiella aerogenes 57	4826	4622	204
Klebsiella aerogenes EA46506	4800	4496	274
Klebsiella aerogenes CAV1320	4691	4483	191
Klebsiella aerogenes (our study)	5179	4566	574

FIGURE 4
Comparative genomic analysis. **(A)** Venn diagram and bar chart showing the numbers of unique and shared orthologous genes present in most closely related strains of *K. aerogenes*. **(B)** Number of proteins, clusters and singletons. **(C)** KEGG pathway classification in core, accessory and unique genomes. **(D)** Distribution of KEGG pathway classification.

"overview" (11.2%), and "amino acid metabolism" (10.68%). Within the unique genome, significant proportions of genes were identified as belonging to categories such as "carbohydrate metabolism" (22.22%), "membrane transport" (15.15%), and "overview," "infectious disease" and "replication and repair" with similar values (7.07%). In the accessory genome, most genes were categorized as "carbohydrate metabolism" (30.95%), "overview" (11.9%) and "membrane transport" (10.7%) (Figure 4D). Notably, we observed the presence of genes related to β-lactam resistance (0.61%, $n = 18$), vancomycin resistance (0.27%, $n = 8$), and cationic antimicrobial peptide resistance (1.35%, $n = 40$) within the core gene clusters specifically linked to drug resistance (Figure 4D).

Resistome of *Klebsiella aerogenes* CRKA317

Resistome analysis using WGS revealed that *K. aerogenes* CRKA317 harbored dozens of antibiotic resistance-associated genes, including genes coding for β-lactamases (bla_{OXA-9}, bla_{TEM-1}, bla_{NDM-1}, $bla_{CTX-M-15}$, bla_{AmpC-1}, bla_{AmpC-2}); aminoglycoside-modifying enzymes [*aac(6')-Ib*, *aadA/ant(3")-Ia*, *aph(3')-VI*], a chloramphenicol acetyltransferase (*catA-like* chloramphenicol resistance), an erythromycin resistance methylase (*ermC*), a plasmid-mediated quinolone resistance protein (*qnrS1*), a sulfonamide resistance enzyme (*sul-2*), a glutathione transferase (*fosA*: fosfomycin resistance), PEtN transferases (*eptA* and *eptB*: resistance to peptide antibiotic), a glycosyltransferase (*arnT*: resistance to peptide antibiotic) (Table 2). We also found the ble_{MBL} gene that encodes a bleomycin resistance protein (BRP). Although the majority of resistance genes identified through sequencing were consistent with those detected in whole genome sequencing (Table 1), bla_{KPC-2} was only detected through Polymerase Chain Reaction-based amplification and sequencing, but not predicted from incomplete genomic sequence of *K. aerogenes* CRKA317.

A rich repertoire of genes related to efflux-mediated resistance was found in the genome of *K. aerogenes* CRKA317 (Table 3), including an ATP-binding cassette (ABC) antibiotic efflux pumps (*tolC*), resistance-nodulation-cell division (RND)-type efflux pumps (*oqxA*, *oqxB*, *acrA*, *acrB, acrD, HAE1*, *EefA*, *EefB*, *mdtA, mdtB*), major facilitator superfamily membrane transport proteins (*mdtH, KdeA*, *MFS-MMR*-like), a multidrug and toxic compound extrusion transporter (MATE) (*mdtK*) and an outer membrane efflux protein (*oprM*). In addition, we have identified multiple MDR efflux pump acrAB transcriptional activators/regulators (*marR*, *ramA*, *soxS*), as well as genes that code for porin-associated proteins such as *oprD*, *ompA*, *ompX*, and *ompW*. The *ramA* and *soxS* genes were specifically associated with mobile genetic elements (Figure 5).

Klebsiella aerogenes CRKA317 presented amino acid substitutions in marR (Ser3Asn), which may play a role in the development of quinolone resistance (Maneewannakul and Levy, 1996). Additionally, we found more two novel mutations in marR (Val96Ile and Gly103Glu), and one novel mutation (Ala12Glu) in the transcription factor of the regulon, soxS (Supplementary Figure S2).

Genomic islands, mobile genetic elements, and prophage

We searched the *K. aerogenes* CRKA317 genome for the presence of GIs and Mobile Genetic Elements (MGEs). GIs are groups of genes within a bacterial genome that appear to have been obtained through horizontal gene transfer. We found 22 GIs in *K. aerogenes* CRKA317's

TABLE 2 Identification of the antibiotic resistance genes in the genome of *K. aerogenes* CRKA317.

Phenotypic antibiotic class	Phenotypic antibiotic resistance (Vitek 2)	Reference sequence (NCBI)	Putative resistance genes	Resistance gene/protein, mechanism function	Size (aa)	Coverage	aa identity (%)	Resistance gene characterization
β-lactam	Ampicillin-sulbactam, Piperacillin-tazobactam, Cefuroxime sodium Cefuroxime axetil, Cefoxitin, Ceftazidime, Ceftriaxone, Cefepime, Ertapenem, Imipenem, Meropenem	WP_282563773.1	bla_{OXA-9}	Class D β-lactamase OXA	284	100	100	CARD, ABRicate, ResFinder, Arg-Annot, KEGG, Prokka
		WP_000027057.1	bla_{TEM-1}	Class A broad-spectrum β-lactamase TEM	286	100	100	CARD, ABRicate, ResFinder, Arg-Annot, KEGG, Prokka
		WP_004201164.1	bla_{NDM-1}	Class B broad-spectrum β-lactamases NDM	270	100	100	CARD, ABRicate, ResFinder, Arg-Annot, KEGG, Prokka
		WP_000239590.1	$bla_{CTX-M-15}$	Class A extended-spectrum β-lactamases CTX-M	291	100	100	CARD, ABRicate, ResFinder, Arg-Annot, KEGG, Prokka
		KAA0468326.1	bla_{AmpC-1}	Class C β-lactamase	382	100	100	KEGG, Prokka, BLAST
		OUE80029.1	bla_{AmpC-2}	Class C β-lactamase	386	100	100	KEGG, Prokka, BLAST
Aminoglycosides	Amikacin	WP_004152783.1	*aac(6')-Ib*	Aminoglycoside 6' *N*-acetyltransferase	201	100	100	CARD, ABRicate, ResFinder, Arg-Annot, KEGG, Prokka
		WP_247187715.1	*aadA/ANT(3")-Ia*	Aminoglycoside nucleotidyltransferase	262	82.51	100	CARD, ABRicate, ResFinder, Arg-Annot, KEGG, Prokka
		WP_014386410.1	*aph(3')-VI*	Aminoglycoside 3'-*O* Phosphotransferase enzymes	259	100	100	CARD, ABRicate, ResFinder, Arg-Annot, KEGG, Prokka
Quinolones	Ciprofloxacin	WP_001516695.1	*qnrS1*	Plasmid-mediated quinolone resistance	218	100	100	CARD, ABRicate, ResFinder, Arg-Annot, KEGG, Prokka
Sulfonamide	NT	WP_011270145.1	*sul-2*	Sulfonamide resistant dihydropteroate synthase	283	100	100	CARD, ABRicate, ResFinder, Arg-Annot, KEGG, Prokka
Fosfomycin	NT	WP_015704268.1	*fosA*	Glutathione S-transferase	139	90.6	100	CARD, ABRicate, ResFinder, Arg-Annot, KEGG, Prokka
Macrolides	NT	WP_107318659.1	*ermC*	23S ribosomal RNA methyltransferase	289	100	100	KEGG, Prokka, BLAST
Phenicol	NT	WP_074165951.1	*catA-like*	Chloramphenicol acetyltransferase	221	100	100	KEGG, Prokka, BLAST
Bleomycin	NT	WP_004201167.1	*bleMBL*	Bleomycin binding protein	121	100	100	CARD, Prokka, BLAST
Peptide antibiotic	NT	WP_015704802.1	*eptA*	Phosphoethanolamine transferase	547	100	100	KEGG, Prokka, BLAST
		WP_047038023.1	*eptB*	Phosphoethanolamine transferase	563	91.16	98.08	KEGG, Prokka, BLAST
		WP_020077750.1	*arnT*	Phosphoethanolamine transferase	551	89.47	100	KEGG, Prokka, BLAST

NT (not tested), susceptibility testing was not performed. The DNA fragments verified by sequencing corresponded to the genes identified in whole genome sequencing.

genome, which contained both resistance genes and insertion sequences. It is noteworthy that these antimicrobial resistance genes (bla_{OXA-9}, bla_{TEM-1}, bla_{NDM-1}, ble_{MBL}, $bla_{CTX-M-15}$, *aac(6')-Ib*, *aadA/ant(3")-Ia*, *aph(3')-VI*, and *qnrS1*) were located within an island in the contigs of

TABLE 3 Identification of the genes encoding multidrug efflux, activators/regulators and outer membrane proteins genes in the genome of *K. aerogenes* CRKA317.

Type	Antibiotic resistance	Reference sequence (NCBI)	Putative resistance genes	Resistance gene/ protein, mechanism function	Size (aa)	Coverage (%)	aa identity (%)	Resistance gene characterization
Multidrug Efflux	Quinolones, Tigecycline	WP_015367128.1	*oqxA*	Multidrug efflux RND transporter periplasmic adaptor subunit A	391	100	84.35	CARD, ABRicate, ResFinder, Arg-Annot, KEGG, Prokka
		WP_047041493.1	*oqxB*	Multidrug efflux RND transporter periplasmic adaptor subunit B	1,050	99.30	88.25	CARD, ABRicate, ResFinder, Arg-Annot, KEGG, Prokka
	Tetracycline, Glycylcycline, Penam, Cephalosporin, Phenicol, Rifamycin, Fluoroquinolone, Tigecycline, Disinfecting Agents and Antiseptics	WP_047038885.1	*acrA*	Multidrug efflux pump subunit A	399	100	100	KEGG, Prokka, BLAST
		WP_015367916.1	*acrB*	Multidrug efflux pump subunit B	1,048	100	100	KEGG, Prokka, BLAST
		WP_032712139.1	*acrD*	Multidrug efflux pump subunit D	1,037	100	100	KEGG, Prokka, BLAST
	Not totally known	WP_047038579.1	*HAE1* Family Pump	Multidrug efflux RND transporter permease subunit	1,035	100	100	BLAST
	Chloramphenicol, Norfloxacin, Acriflavine	WP_015367543.1	*kdeA*	MdfA family multidrug efflux MFS transporter	410	100	100	BLAST
	Fluoroquinolone	WP_015367204.1	*mdtH*	Multidrug efflux MFS transporter	402	100	100	KEGG, Prokka, BLAST
	Aminocoumarin	WP_045367110.1	*mdtA*	MuxA family multidrug efflux RND transporter periplasmic adaptor subunit	414	100	100	KEGG, Prokka, BLAST
	Aminocoumarin	WP_270843647.1	*mdtB*	MuxB family multidrug efflux RND transporter periplasmic adaptor subunit	1,040	100	99.90	KEGG, Prokka, BLAST
	Fluoroquinolone	WP_015366890.1	*mdtK*	MdtK family multidrug efflux MATE transporter	457	100	100	KEGG, Prokka, BLAST
	Aminoglycosides, erythromycin	WP_063402362.1	*oprM*	Outer membrane efflux protein OprM	459	100	100	KEGG, Prokka, BLAST
	Methylenomycin	WP_047038952.1	*MFS-MMR-MDR-like*	Methylenomycin A resistance protein	475	100	100	Prokka, BLAST
	Chloramphenicol, Ciprofloxacin, Erythromycin, Tetracyclines	EIX9084829.1	*eefA*	Multidrug efflux RND transporter permease subunit A	374	99	99.73	BLAST
		WP_285197781.1	*eefB*	Multidrug efflux RND transporter permease subunit B	1,035	99	99.71	BLAST
Multidrug efflux activators and regulators	Tetracycline, Cephalosporin, Phenicol, Glycylcycline, Penam, Fluoroquinolone, Rifamycin, Monobactam, Cephamycin, Carbapenem	WP_015368734.1	*soxS*	Superoxide response transcriptional regulator	109	91	100	CARD, KEGG, Prokka, BLAST
	Cyprofloxacin, Tetracycline	WP_015366732.1	*marR**	Multiple antibiotic resistance transcriptional regulator	144	100	100	CARD, KEGG, Prokka, BLAST
Outer membrane proteins	Carbapenems	VAG14479.1	*oprD*	Outer membrane porin D	450	100	99.33	Prokka, BLAST
	Cephalosporin, Carbapenem, Penam, Monobactam, Cephamycin	WP_042894578.1	*ompC* (3 copies)	Outer membrane protein OprC	380	100	100	BLAST
	Peptide antibiotic/ β-lactam	WP_270843755.1	*ompA_C-like*	Peptidoglycan binding domains similar to the C-terminal domain of outer-membrane protein OmpA	560	100	100	BLAST
		WP_080473199.1	*ompA*	Outer membrane protein A	350	100	100	Prokka, BLAST
		WP_015367577.1	*ompX*	Outer membrane protein X	171	100	100	Prokka, BLAST
		WP_015705753.1	*ompW*	Outer membrane protein W	212	100	100	Prokka, BLAST

*Mutations found in genes may indicate the presence of antibiotic resistance.

the *K. aerogenes* CRKA317 genome that did not align with the reference strain *K. aerogenes* 57 isolate (Supplementary Figure S3). Furthermore, only one resistance gene (bla_{AmpC}) was identified in islands located within the aligned contigs with reference strain *K. aerogenes* 57.

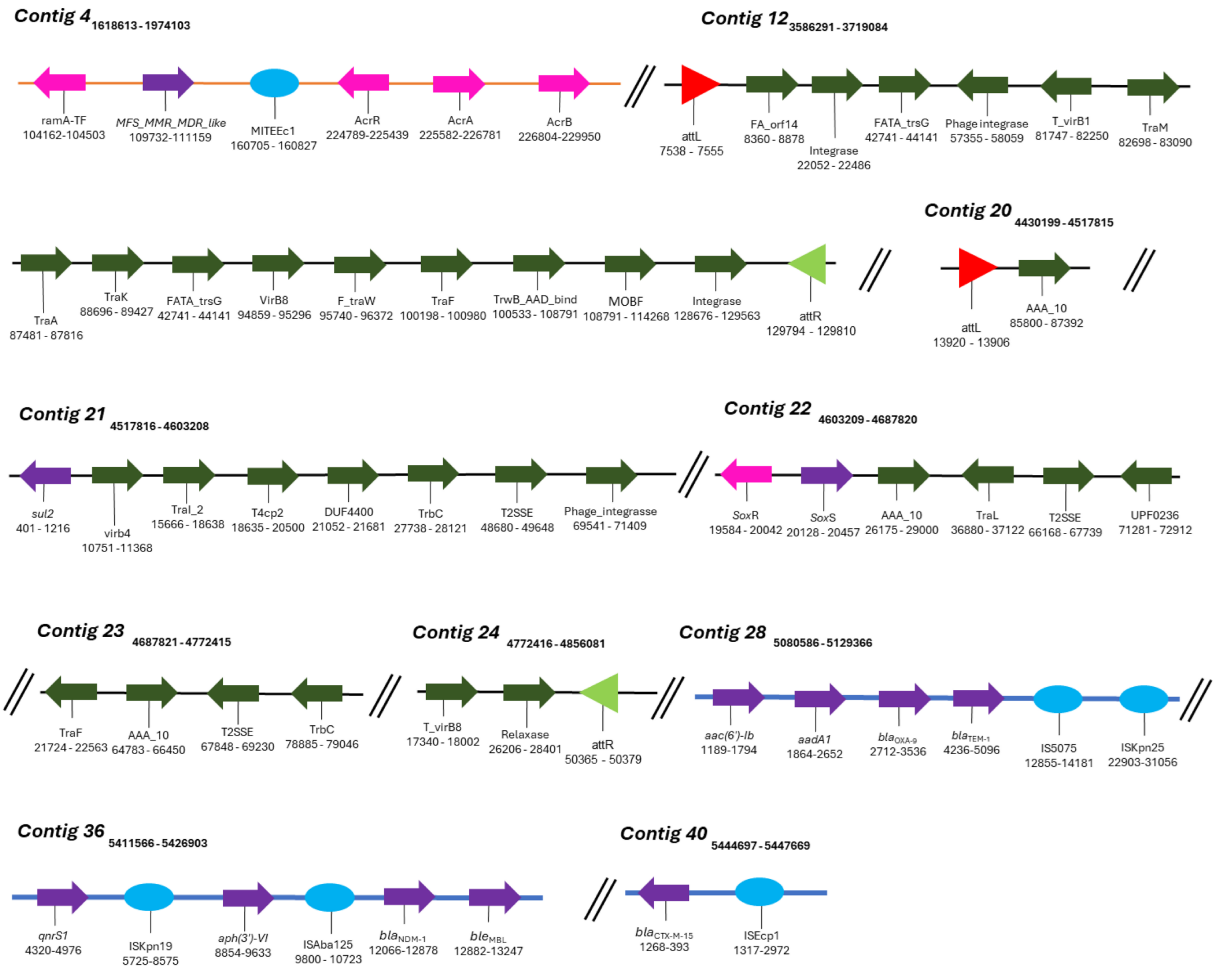

FIGURE 5
Mobile genetic elements (MGEs) identified in *K. aerogenes* CRKA317. Schematic representation of MGEs identified. The orange line represents the DNA strand (contig 4), blue lines represent GIs and black lines (contig 12 and contigs 20 to 24) represent the ICEs. The colored arrows represent the following genes: dark green - conjugation of the ICEs (e.g., contig 12), purple – resistance genes (e.g., contig 28), pink – efflux pumps and their respective activators/regulators (e.g., contig 4). The red (contig 20) and light green triangles (contig 24) represent *attL* and *attR* sequences, respectively. The light blue circles represent insertion sequences (e.g., contig 40).

MGEs consist of a broad array of genomic sequences, such as plasmids, prophages, pathogenicity islands, restriction and modification systems, transposons, and Insertion Sequences (ISs). Our analyses showed that the *K. aerogenes* CRKA317 genome contained eight families of ISs, two copies of putative integrative and conjugative elements (ICE) with type IV secretion system (T4SS), and eight prophage regions. ISs are mobile repetitive DNA sequences that have the capacity to replicate and relocate within a host genome, playing a role in genetic diversity and regulation of gene expression in prokaryotes (Tempel et al., 2022). Our CRK317 strain contained two copies of MITEEc1 from the IS630 family, albeit only one copy carried genes such as *MFS_MMR_MDR-like*, *acrR*, *acrA*, and *acrB* (contig 4). The IS110 family presented one copy of IS4321/IS5075 and one copy of ISKpn25 harboring the *aac(6')-Ib*, *aadA1*, $bla_{\text{OXA-9}}$, and $bla_{\text{TEM-1}}$ genes (contig 28). Contig 36 comprised the IS30 family harboring one copy of ISAba125, carrying $bla_{\text{NDM-1}}$ and ble_{MBL} genes and the ISKra4 family presenting one copy of ISKpn19, *aph(3')-VI* and *qnrS1* genes. The ISEcp1 member of the IS1380 family presented the $bla_{\text{CTX-M-15}}$ gene (contig 40) (Figure 5). The ISRaq1 member of the IS3 family, the ISR1 member of the IS1 family and the IS26 member of the IS6 family did not present any resistance genes.

ICEs are found in the bacterial host chromosome and play a significant role in spreading resistance genes which significantly contribute to the evolution of discrete bacterial strains (Bean et al., 2022). Among the two putative ICEs containing a type IV secretion system (T4SS), contig 12 exhibited elements features of the ICE backbone, including a 16-base pair direct repeat *attL* sequence (5'-AAGAAGGGGAGTCCTG-3'); various integrases such as virB(s), rve, and phage integrases; T4SSs; T4CP; relaxases; and another 16-base pair direct repeat *attrR* sequence (5'-AAGAAGGGGAGTCCTG-3'). Additionally, contigs 20-24 contained similar components with a slight variation in the length of its direct repeats, 15 base pairs for both *attL* and *attrR* (Table 4). We did not detect CRISPR or *Cas* genes in *K. aerogenes* CRKA317 genome.

Among the eight prophage regions identified in CRK317, two were completely intact, four were incomplete, and two were classified as uncertain. Similarly, two other phages were observed in the fully intact regions: the first region (43.2 kb in size with 50.3% CG content

TABLE 4 The genetic compositions of the MGEs predicted in *K. aerogenes* CKA317.

MGE type	Family	Contig	Position in contig	ID	Accession number	Program	Near resistance genes
Insertion sequences (ISs)	IS630	4	160705–160827	MITEEc1	U00096	TnCentral ISFinder	*ramA* *MFS_MMR_MDR*-like *acrR* *acrA* *acrB*
		16	75513–75586	MITEEc1	U00096	TnCentral ISFinder	–
	IS3	10	28955–30017	ISRaq1	AY528232	ISFinder	–
	IS110	28	12855–14181	IS4321/IS5075	AF457211	TnCentral MGEFinder	*aac(6')-Ib* *aadA1* bla_{OXA-9} bla_{TEM-1}
			22903–31056	ISKpn25	NC_009650	TnCentral MGEFinder	
	IS1	31	2536–3303	IS1R	J01730	TnCentral ISFinder	–
	ISKra4	36	5725–8575	ISKpn19	NC_010886	ISFinder MGEFinder	*qnrS1* *aph(3')-VI*
	IS30	36	9800–10723	ISAba125	AY751533	TnCentral	bla_{NDM-1} ble_{MBL}
	IS1380	40	1317–2972	ISEcp1	AJ242809	TnCentral ISFinder MGEFinder	$bla_{CTX-M-15}$
	IS6	48	1–820	IS26	X00011	TnCentral ISFinder MGEFinder	–
Integrative and conjugative elements (ICEs)	T4SS	12	*attL*: 3593829–3593844 *attR*: 3716086–3716101	Putative ICE with T4SS	–	ICEFinder	–
		20–24	*attL*: 4500895–4500909 *attR*: 4822781–4822795	Putative ICE with T4SS	–	ICEFinder	*sul-2* *soxS*

and 63 CDS) showed similarities to *Salmonella* phage SEN34 (NC_028699.1), while the second region (54.5 kb in size with 52.32% CG content and 54 CDS) exhibited similarities to *Escherichia* phage vB_EcoM_ECO1230-10 (NC_027995.1) (Supplementary Figure S4).

Discussion

Klebsiella aerogenes is known as an opportunistic pathogen of patients admitted to the intensive care unit and is frequently associated with multidrug resistance (MDR) (Azevedo et al., 2018). It has been detected in various hospital sources and is known for its ability to adapt to this setting. This study found that *K. aerogenes* was mainly detected in rectal swabs and urine samples, followed by tracheal aspirate, blood, and catheter tips. Previous studies have highlighted that *K. aerogenes* is commonly present in human specimens such as urinary, gastrointestinal, respiratory, blood, abscesses, and cutaneous samples (Davin-Regli et al., 2019). Additionally, rectal swabs are employed for active surveillance of asymptomatic carriers. These findings are also consistent with prior studies demonstrating the presence of *E. aerogenes* in surveillance rectal swabs (Vrioni et al., 2012). But the small number of *K. aerogenes* isolates is one of the major limitations of this study.

Our study found that all *K. aerogenes* isolates displayed some level of resistance to the β-lactams tested, including carbapenems, and 50% of *K. aerogenes* isolates exhibited a MDR profile (Table 1). Carbapenems have traditionally been a preferred treatment for infections caused by MDR Gram-negative strains (Bouza, 2021). Therefore, the emergence of carbapenem-resistant *K. aerogenes* strains present a new challenge in the treatment of these infections and pose a public health threat worldwide (Kamio and Espinoza, 2022).

The presence of resistance genes was verified using polymerase chain reactions. Out of the 10 isolates, we discovered that two only contained the bla_{KPC-2} gene and three only contained the bla_{NDM-1} gene while, interestingly, five strains carried both the bla_{KPC-2} and bla_{NDM-1} genes. Previous studies have reported the presence of bla_{KPC} or bla_{NDM}

genes in clinical *K. aerogenes* isolates from various countries (Pulcrano et al., 2016; Franolić et al., 2019; Ma et al., 2020), including Brazil (Bispo Beltrão et al., 2020; Soares et al., 2021). However, our literature review indicated that there has been only one study of *K. aerogenes* co-harboring both bla_{KPC} and bla_{NDM} genes, which was observed in China (Zhang et al., 2017). Therefore, to the best of our knowledge, this is the first report describing clinical samples of *K. aerogenes* isolated from Brazil with simultaneous carriage of bla_{KPC} and bla_{NDM} genes. It is noteworthy that we found a significant number of *K. aerogenes* isolates exhibiting a bla_{KPC-2} or bla_{NDM-1} carbapenemase in addition to ESBLs genes, including members of the $bla_{CTX-M-1}$; $bla_{OXA1, 4, 30}$; bla_{TEM}; and $bla_{SHVvariants}$. Our findings are in line with studies that reported the concomitant presence of carbapenemase and ESBLs genes in *K. aerogenes* strains (Ma et al., 2020; Pan et al., 2021).

Although most of the CRKA strains were susceptible to aminoglycosides (gentamicin and/or amikacin), a high percentage of the isolates were found to contain the *aph(3')-VI* gene, a plasmid-encoded aminoglycoside phosphotransferase that confers resistance to amikacin. Studies have shown that *Enterobacter aerogenes* can carry both *aph(3')-VI* and bla_{KPC} (Firmo et al., 2019), and also *aph(3')-VI* with bla_{NDM} (Chen et al., 2015). However, to the best of our knowledge, this is the first report of *Klebsiella aerogenes* concomitant harboring *aph(3')-VI*, bla_{KPC-2}, and bla_{NDM-1} genes, as can be seen in the CRKA315 strain. Most of the CRKA isolates also harbored the *aac(6')-Ib* gene, responsible for encoding an aminoglycoside 6'-N-acetyltransferase type Ib, which provides resistance to amikacin (Machuca et al., 2016). Interestingly, amikacin susceptible isolates harboring the *aac(6')-Ib* gene have been reported in *K. pneumoniae* strains (Almaghrabi et al., 2014; Haldorsen et al., 2014; Galani et al., 2019). Despite half of the CRKA strains being susceptible to ciprofloxacin, 80% of the isolates harbored the *qnrS* (*qnrS1* and/or *S2*) gene. The *qnrS* genes have been detected in a variety of microorganisms and environments, where they can be located in both the chromosome and in plasmids (Xu et al., 2023). Studies have indicated an association between *qnrS1* and a Tn3-like-blaTEM-1-containing transposon, leading to enhanced recombination and insertion effectiveness (Guan et al., 2013). The expression of the *qnrS1* gene is enhanced by quinolones, in contrast to certain other *qnr* genes (Monárrez et al., 2018). *QnrS2*, associated with quinolone resistance which demonstrates a 92% similarity in amino acid composition with *qnrS1*, is frequently identified in IncQ, IncU, and ColE-type plasmids as part of a mobile insertion cassette element bracketing inverted repeats but lacking a transposase (Picão et al., 2008; Han et al., 2012; Dobiasova et al., 2016; Wen et al., 2016). Notably, a newly identified surrounding genetic structure of *qnrS2* flanked by IS26 elements was observed in *E. coli* strains from China (Tao et al., 2020). This finding highlights the important role of IS26 in facilitating the horizontal spread of quinolone resistance genes. Therefore, our data suggests that the variance in results between phenotyping and genotyping may be linked to the presence of multiple concurrent resistance mechanisms (Galani et al., 2019). However, we should mention that the incomplete sequencing of *K. aerogenes* CRKA317 may undermine the confidence level of this speculation.

Efflux pumps are important membrane proteins that play a crucial role as defense mechanisms by actively exporting harmful substances, such as antibiotics, detergents, and heavy metals (Jang, 2023). In our study, all of the isolates studied harbored *acrA*, encoding a subunit that functions as an adapter protein linked to AcrB, and TolC outer membrane channel proteins. Although we did not identify *acrB* in our analysis, together these proteins form the AcrAB-TolC stable efflux complex, known to contribute to multidrug resistance in nosocomial pathogens (Chen et al., 2022). These genes have been identified in *K. aerogenes* clinical isolates and are responsible for expelling various compounds, including antimicrobial agents like quinolones, tetracyclines, and chloramphenicol (Pradel and Pagès, 2002; Masi et al., 2007; Chevalier et al., 2008). Although the expression levels of *acrAB* and *tolC* genes were not determined in our *K. aerogenes* isolates, it was observed that all strains carried both genes which might be involved in the development of MDR carbapenem-resistant profile of *K. aerogenes*. The *mdtK* gene encodes an efflux pump that has the ability to expel acriflavine, doxorubicin, norfloxacin, and dipeptides (Hayashi et al., 2010; Andersen et al., 2015). This gene was found in a majority of our CRKA strains. Previous studies have reported the presence of the *mdtK* gene in *K. aerogenes* isolated from river sediment (Iyer et al., 2017).

WGS is a valuable tool for identifying and characterizing disease-associated bacteria in clinical settings. Thus, we conducted a comprehensive analysis of the entire genome of *K. aerogenes* CRKA317 to gain deeper insights into its genomic diversity, and methods of resistance.

The draft genome of *K. aerogenes* CRKA317 comprised of a single circular chromosome with a length similar to most *K. aerogenes* genomes in NCBI GenBank and harbored various essential genes for bacterial cellular processes. Additionally, the results of the RAST and eggNOG analyses showed that our *K. aerogenes* CRKA317 carried genes linked to drug resistance.

Next, we explored the phylogenetic affiliation of *K. aerogenes* CRKA317. The16S rRNA gene sequence analysis showed that the *K. aerogenes* CRKA317 was not closely related to *K. aerogenes* as a specie. Although, 16S rRNA gene is used extensively in bacterial phylogenetics, the limitations of using 16S rRNA gene relatedness to classify bacteria have been extensively documented (Rossi-Tamisier et al., 2015; Thorell et al., 2019; Soares et al., 2023). Therefore, a combination of ANI, dDDH, and TYGS technologies were employed to determine the phylogenetic position of the *K. aerogenes* CRKA317, which predicted a close phylogenetic relationship with *K. aerogenes*.

In our investigation of the genetic relationship between *K. aerogenes* CRKA317 and another 26 *K. aerogenes* strains, we found three strains (*K. aerogenes* 57, *K. aerogenes* CAVI1320, and *K. aerogenes* EA46506) that were closely related to *K. aerogenes* CRKA317. When analyzing the distribution of shared gene families among four strains, we found that our *K. aerogenes* CRKA317 had the highest number of singleton genes compared to its closest three relatives. Some of these singleton genes were related to antibiotic resistance. Singleton genes are typically acquired through horizontal gene transfer (HGT) or mutations in pre-existing genes. These genes are often associated with specific metabolic pathways, virulence, antibiotic resistance mechanisms, or other environmental adaptations (Costa et al., 2020). Furthermore, the KEGG pathway analysis revealed that most of the genes were in the core genome and were related to metabolic pathways. As the analyses were based on small number of *K. aerogenes*, we cautiously speculated that *K. aerogenes* might have genomic plasticity, that may contribute to antibiotic resistance and environmental adaptation.

Our comprehensive analysis of the *K. aerogenes* CRKA317 using WGS confirmed the correlation between the genotype and the phenotype to its antimicrobial resistance. Furthermore, our analysis

found a large number of antibiotic resistance-associated genes such as porin and efflux pump-encoding genes giving resistance to both previously tested and untested antibiotics, suggesting a wide-ranging antibiotic resistance profile (Tables 2, 3). AmpC β-lactamases are usually encoded within the chromosome or found as *ampC* genes on a plasmid. Our *K. aerogenes* CRKA317 harbored two copies of bla_{AmpC} gene. Several Gram-negative organisms, including *E. aerogenes*, *Enterobacter cloacae*, *Serratia marcescens*, *Providencia stuartii*, *Pseudomonas aeruginosa*, *Hafnia alvei*, and *Morganella morganii*, have presented *AmpC* in their genomes (Jacoby, 2009; Ghanavati et al., 2018; Tamma et al., 2019). This enzyme provides resistance against aminopenicillins, cephalosporins, oxyimino-cephalosporins (e.g., ceftriaxone, cefotaxime, and ceftazidime), cephamycins (e.g., cefoxitin and cefotetan), and monobactams (aztreonam) (Jacoby, 2009). The gene *sul-2* implicated in sulphonamide resistance due to inducing high levels of dihydropteroate synthase was found in our strain (Teichmann et al., 2014). This gene has been widely studied and its association with sulfamethoxazole resistance has been demonstrated in numerous studies worldwide (Teichmann et al., 2014; Shin et al., 2015), including in an *E. aerogenes* from Brazil (Grazziotin et al., 2016). The *K. aerogenes* CRKA317 contained the *fosA* gene, which is commonly found in the genomes of *K. pneumoniae*, *K. oxytoca*, *E. cloacae*, *E. aerogenes*, *S. marcescens*, *M. morganii*, *P. stuartii*, and *P. aeruginosa*. All these species haboring *fosA* gene presented intrinsic resistance or reduced susceptibility to fosfomycin (Ito et al., 2017). The *ermC* gene, known for its role in conferring erythromycin resistance in *S. aureus* and other *Staphylococci* (Jamrozy et al., 2017) was also detected in the *K. aerogenes* CRKA317. The *K. aerogenes* CRKA317 also contained the *catA-like* gene, responsible for producing a chloramphenicol acetyltransferase that catalyzes chloramphenicol (Huang et al., 2017). This gene is commonly present on transposons and plasmids, and it is widespread among a range of organisms such as *Acinetobacter* spp., *Bacillus methylotrophicus* and *Chryseobacterium indologenes* (Obayiuwana and Ibekwe, 2020; Damas et al., 2022).

We also detected three alterations in amino acids in marA in our *K. aerogenes* CRKA317 (Ser3Asn, Val96Ile, Gly103Glu) and one in soxS (Ala2Glu). These findings partially corroborate the results of Maneewannakul and Levy (1996), where they identified three mutations in marA (Ser3Asn, Val96Glu, Gly103Ser) leading to resistance to fluoroquinolones in *E. coli*. Moreover, Aly et al. (2015) demonstrated that a mutation in soxS (Ala12Ser) contributed to resistance against ciprofloxacin, enrofloxacin, chloramphenicol, and doxycycline in *E. coli* strains. We suggest these same mechanisms gave rise to antimicrobial resistance in our *K. aerogenes* CRKA317 due to the similar mutations noted.

Additionally, our *K. aerogenes* CRKA317 presented several MGEs harboring resistance genes (Table 4). MGEs are important tools for acquiring resistance genes through horizontal gene transfer. ISs, for example, are transposable DNA segments that have been previously linked to resistance genes and can be transferred horizontally by plasmids or by bacteriophages (Siguier et al., 2014). The $bla_{\text{OXA-9}}$, $bla_{\text{TEM-1}}$ genes encoding for resistance to β-lactams, and *aac(6')-Ib*, *aadA1* encoding resistance aminoglycosides were related to an IS110 family transposase (IS4321/IS5075 and ISKpn25 insertion elements). These findings are partially supported by previous studies that have shown ESBL-encoding genes ($bla_{\text{TEM-1B}}$) and genes related to aminoglycoside resistance (*aph-Id*, *aph-Ib*) are located near to an IS5075 insert in *K. pneumoniae* (Pajand et al., 2023). The $bla_{\text{CTX-M-15}}$ gene was in close proximity to ISEcp1, which is a member of the IS1380 family (Poirel et al., 2008), and has been identified as one of several elements responsible for facilitating the transfer of $bla_{\text{CTX-M}}$ genes across various species of *Enterobacteriaceae* (Shawa et al., 2021; Wang et al., 2023). The $bla_{\text{NDM-1}}$ and ble_{MBL} genes (a class B3 β-lactamases with carbapenemase activity) were close to the insertion sequence *IS*Aba125 (*IS*30 family). Studies have proposed that the *IS*Aba125–ble_{NDM} combination occurred initially in *Acinetobacter* spp. and later transferred to other Gram-negative bacteria (Castanheira et al., 2023). Additionally, the *IS*Aba125–$bla_{\text{NDM-1}}$–ble_{MBL} combination has been found in a structure referred to as NDM-GE-U.S, first observed in a *K. pneumoniae* strain from the United States and subsequently detected in various strains worldwide (Hudson et al., 2014; Peirano et al., 2018).

The *qnrS1* the *aph(3")-VI* genes, were found in close proximity to the IS*K*pn19 insertion sequence of the *ISK*ra4 family in our isolate. Studies have shown that *qnrS1* gene, which confers resistance to ciprofloxacin, is related to *ISK*pn19 in various bacteria, such as *Leclercia adecarboxylata*, *Salmonella corvallis; K. pneumoniae*, *E. coli*, and *S. marcescens* (Xu et al., 2020; Chen et al., 2023; Sano et al., 2023; Zheng et al., 2024). The *aph(3")-VI* gene, responsible for amikacin modification, was not found to be flanked by the IS*K*pn19 insertion sequence in our literature review. It is worth noting that *K. aerogenes* CRKA317 presents a large number of singleton genes, including $bla_{\text{NDM-1}}$, *aadA/ant(3")-Ia*, *aph(3')-VI*, and *qnrS1* and its presence indicates the variability and diversity within the genome of our strain. It is possible that these genes were obtained from other lineages through horizontal gene transfer, leading to the development of new functions, such as resistance to antibiotics. This assumption can be reinforced by the presence of a genomic island that carries most of the resistance genes ($bla_{\text{OXA-9}}$, $bla_{\text{TEM-1}}$, $bla_{\text{NDM-1}}$, ble_{MBL}, $bla_{\text{CTX-M-15}}$, *aac(6')-Ib*, *aadA/ant(3")-Ia*, *aph(3')-VI*, and *qnrS1*) found in our genome. Genomic islands are distinct regions in the bacterial genome with genes related to each other and often associated with specific functions. These islands are often acquired through horizontal gene transfer events and are associated with the widespread distribution of antimicrobial resistance factors among bacteria (Juhas et al., 2009). The composition of genomic islands is conducive to the acquisition of new antibiotic resistance genes, as they include several MGEs, which facilitate the incorporation of new genes, but also their own transfer, for example, using tRNA genes as recombination sites into the chromosome (da Silva Filho et al., 2018).

Our *K. aerogenes* CRKA317 displayed many genes of interested linked to antibiotic resistance (Table 3). The *ramA*, *acrR*, *acrA* and *acrB* genes, and *MFS_MMR_MDR-like* gene were found to be associated with MITEEc. MITEEc belongs to the IS630 family and was found in an extensively drug-resistant (XDR) *Escherichia coli* isolate (Jain et al., 2021). *RamA* belongs to the AraC/XylS protein family and shows a close association with the marA and soxS proteins (Rosenblum et al., 2011). Elevated expression of *ramA* is associated with the activation of the acrAB efflux pump, which confers multidrug resistance in various bacterial species such as *E. aerogenes*, *K. pneumoniae*, and *E. cloacae* (Chollet et al., 2004; Keeney et al., 2007; Ruzin et al., 2008). The *acrR* gene regulates the multidrug efflux pump AcrAB-TolC (Subhadra et al., 2018). The *MFS_MMR_MDR-like* gene is linked to methylenomycin resistance, and the antibiotic Methylenomycin A is produced naturally by *Streptomyces coelicolor* A3, a model organism for streptomycetes (Bentley et al., 2002; Bowyer

et al., 2017). The *acrAB-tolC* system where the acrAB fusion protein, members of the RND-type efflux family, function with another antibiotic efflux pump, *tolC*, to pump out various compounds such as SDS, novobiocin, deoxycholate, aminoglycosides, and dianionic β-lactams including carbenicillin, oxacillin, nafcillin, and aztreonam (Guérin et al., 2023). We also found many other RND antibiotic efflux pumps, the first pair being *eefA* and *eefB* which are part of the *eefABC* locus known to encode a tripartite efflux pump that gives rise to resistance to erythromycin and other antibiotics in *E. aerogenes* (Pradel and Pagès, 2002; Masi et al., 2007). The *oqxA* and *oqxB* operon has also been described to increase antibiotic resistance in *E. aerogenes*, this time to quinolones as they combine to make the oqxAB efflux pump (Wong et al., 2015; Moosavian et al., 2021). The HAE1 family, also contained in our isolate, contains large number of identified RND transporters (Nikaido, 2018). These pumps are commonly found in Gram-negative bacteria, typically existing as trimers, and are involved in the transportation of drugs and other hydrophobic substances (Nikaido, 2018). In addition, we found members of the acrB/acrD/acrF family, specifically *acrD*, *mdtA* and *mdtB*. The *mdt*ABC operon is transcriptionally activated by *baeR* and leads to the formation of the mdtABC tripartite complex, which provides resistance to novobiocin and deoxycholate in *E. coli* (Nagakubo et al., 2002). Related to this complex, it was found *mdtH* and *mdtK* both of which give rise to proteins that function has multidrug efflux pumps that contribute to resistance against quinolone antibiotics such as norfloxacin and enoxacin in *E. coli* strains (Nishino and Yamaguchi, 2001; Yu et al., 2020). The final RND antibiotic efflux pump sequenced in our isolate is *oprM* which is part of MexX-MexY-OprM efflux systems that mediate intrinsic antibiotic resistance to aminoglycosides and erythromycin in bacteria such as *P. aeruginosa* (Wong et al., 2001), *Brevundimonas brasiliensis* sp. nov and *Burkholderia vietnamiensis* (Shinoy et al., 2013; Soares et al., 2023).

We also found putative ICE with T4SS just harboring *sul-2* gene, encoding for resistance to sulfonamide, and *sox* gene, a key component of a central regulatory system present in all *Enterobacteriaceae*, which detects and reacts to internal chemical stressors like antibiotics (Chubiz, 2023). ICEs are mobile elements integrated into the chromosomes that can be excised and transferred horizontally to other bacteria and, therefore, have been associated with antimicrobial resistance genes (Johnson and Grossman, 2015). Despite this, due to the finding of only one resistance gene in the ICEs studied here (*sul-2*), we can assume that this structure is not the main source of resistance gene acquisition in *K. aerogenes* CRKA317.

Genes associated with porins were the second category identified in our isolate (Table 3). Porins belong to a category of transmembrane proteins called omps, which form small channels in the membrane and facilitate the passive movement of hydrophilic compounds. They regulate cellular permeability and can either enhance or reduce resistance to antibiotics. In our strain, we specifically found the outer membrane protein encoding genes *oprD, ompC, ompA, ompX* and *ompW* which have been found to have clinical significance. For instance, a reduction or absence of OmpC in clinical *E. aerogenes* isolates has been linked to a slight increase in imipenem MIC (Lavigne et al., 2012). Meanwhile, overexpressing ompX in *E. aerogenes* results in elevated resistance to β-lactam antibiotics, possibly due to significant reduction in the Omp36 porin (Hejair et al., 2017). *Omp*W expression in *A. baumannii* isolates was found to increase when exposed to ciprofloxacin and decrease when exposed to imipenem (Gurpinar et al., 2022). Conversely, *A. baumannii* strains with mutations in ompA exhibited reduced permeability for cephalothin/cephaloridine and lower minimum inhibitory concentrations for a range of antibiotics including imipenem, colistin, meropenem, chloramphenicol, aztreonam, and nalidixic acid (Smani et al., 2014; Tsai et al., 2020). Finally, in *P. aeruginosa*, the porin oprD plays a significant role in the uptake of basic amino acids and carbapenems (Wong et al., 2001).

Other genes of interest included: a superoxide response transcriptional regulator (*soxS*), a multiple antibiotic resistance transcriptional regulator (*marA*), and a major facilitator superfamily member (*kdeA*),

Prophages play a role in the survival mechanisms of their hosts and contribute to the enhancement of genetic diversity within the host genome (Kondo et al., 2021). In our study, we found two intact regions which were associated with the presence of a prophage highly similar to the *Salmonella* phage SEN34 (National Center for Biotechnology Information reference sequence NC_028699.1), and *Escherichia* phage vB_EcoM_ECO1230-10 (NC_027995.1). Prophage regions of *Salmonella* phage SEN34 (NC_028699.1) has been identified in *Salmonella salamae* (Hounmanou et al., 2022), and *Salmonella enterica* serovar Paratyphi B (Castellanos et al., 2020) and have been linked to drug resistance.

There are limitations to our study that need to be acknowledged. We encountered difficulties in assembling complete plasmid sequences, primarily due to the short reads generated by high-throughput sequencer. This can result in antimicrobial resistance genes being located on incomplete contigs, leading to uncertainty about whether they are situated on a plasmid or within the chromosome (Orlek et al., 2017; Berbers et al., 2020). Nonetheless, it is important to highlight those studies conducted in China have shown that clinical isolates of carbapenem-resistant *K. aerogenes* carried $bla_{\text{NDM-1}}$ gene on plasmids of the IncFIIAs type. In another study, Shen et al. (2019) identified a plasmid (p1564) containing genes for plasmid replication (*Inc*A/C *rep*A), antibiotic resistance ($bla_{\text{NDM-1}}$, *rmtC*, *aacA4*, ble_{MBL}, $bla_{\text{CMY-6}}$ and *sul-1*), and conjugation (*tra* clusters). In *K. aerogenes*, there is still no consensus on the location of the $bla_{\text{KPC-2}}$ gene in the plasmid, the transposon variants capable of carrying this gene, and which incompatibility (Inc) groups carry the bla_{KPC} gene (Bispo Beltrão et al., 2020). However, a study conducted by Bispo Beltrão et al. (2020) in Brazil has described a non-Tn4401 element (NTEKPC-IId) that carries the $bla_{\text{KPC-2}}$ and *aph(3')-VII* genes in *Inc*Q1 plasmids in *K. aerogenes*. To date, the *Inc*Q1 $bla_{\text{KPC-2}}$-positive plasmids have been found in different strains such as *E. coli*, *K. pneumoniae* of CG258, *Klebsiella quasipneumoniae*, and *P. aeruginosa* (de Oliveira Santos et al., 2018).

Although *K. aerogens* has not been reported to carry the plasmids found in our sequencing study, it is important to note genes such as bla_{KPC} and bla_{NDM} are commonly associated with the plasmid fragments found in *K. aerogenes* CRKA317. Takei et al. (2022) found nine isolates of *K. pneumoniae* carrying $bla_{\text{NDM-1}}$ and $bla_{\text{CTX-M-15}}$ on the IncFIB (pQil) plasmid and another five isolates carrying $bla_{\text{NDM-1}}$ on the IncC plasmid. Similar data were also observed in the results of Zeng et al. (2022), who identified the $bla_{\text{NDM-1}}$ gene in IncC plasmids from 21 *K. pneumoniae* isolates. Finally, the fragmented INCFIIK plasmid observed in our genome has already been noted to carry genes such as $bla_{\text{KPC-2}}$, $bla_{\text{CTX-M-15}}$, $bla_{\text{TEM-1}}$ and, less commonly, $bla_{\text{NDM-1}}$ (Chen et al., 2013; Bi et al., 2018). This suggests an emerging mechanism, using Inc. groups, that plays a role in the dissemination of carbapenem resistance in clinically important bacteria.

In conclusion, our current research has uncovered a concerning scenario involving *K. aerogenes* demonstrating resistance to commonly utilized drugs for treating infections, including those considered as last-resort options for life-threatening infections in ICU patients. Moreover, the presence of mobile genetic elements highlights the alarming potential for the transmission of various resistance genes such as bla_{NDM-1} and bla_{KPC-2} within hospital settings to susceptible populations. This scenario poses significant challenges for managing infectious diseases and underscores the necessity of early detection of such genetic features or mutations.

Our study did not involve human genetic material or biological samples. The strains were obtained from the collection of the Central Laboratory of Public Health, a leading diagnostic center in Tocantins, Brazil. This was a retrospective study and epidemiological data were obtained from a database at LACEN-TO in accordance with Resolution 466/12 of the National Health Council (Conselho Nacional de Saúde/Ministério da Saúde, 2012). Informed consent was not required as per Resolution 466/12 regarding research involving humans by the National Health Council. The study received approval from the Committee of Ethics in Human Research at the Federal University of São Carlos (no. 1.088.936), and permissions to conduct it were obtained from the State Department of Health in Tocantins and LACEN/TO.

Data availability statement

The datasets presented in this study can be found in online repositories. The names of the repository/repositories and accession number(s) can be found in the article/Supplementary material.

Ethics statement

The studies involving humans were approved by Committee of Ethics in Human Research at the Federal University of São Carlos (no. 1.088.936). The studies were conducted in accordance with the local legislation and institutional requirements. Written informed consent for participation was not required from the participants or the participants' legal guardians/next of kin in accordance with the national legislation and institutional requirements.

Author contributions

SR: Formal analysis, Investigation, Methodology, Writing – review & editing. GN: Formal analysis, Investigation, Methodology, Writing – review & editing. GS: Formal analysis, Investigation, Methodology, Writing – review & editing. MD: Formal analysis, Investigation, Methodology, Writing – review & editing. RF: Formal analysis, Investigation, Methodology, Writing – review & editing. PL: Formal analysis, Investigation, Methodology, Writing – review & editing. RS: Formal analysis, Methodology, Writing – review & editing. LC: Methodology, Writing – review & editing. AC: Formal analysis, Writing – review & editing. IM: Visualization, Writing – review & editing. AC: Visualization, Writing – review & editing. M-CP: Conceptualization, Funding acquisition, Project administration, Supervision, Writing – original draft, Writing – review & editing.

Funding

The author(s) declare financial support was received for the research, authorship, and/or publication of this article. This study was supported by the Fundação de Amparo à Pesquisa do Estado de São Paulo-Brazil (FAPESP grant 2022/16872-6, 2020/11964-4, 2024/00886-3 to M-CP; and FAPESP grant 2022/01223-2, 2018/20697-0 to AC). This study was partially financed by the Fundação de Amparo à Pesquisa do Estado de São Paulo-Brazil (FAPESP) as a fellowship to SR. (FAPESP fellowship 2022/12429-0), GN (FAPESP fellowship 2023/08917-2), GS (FAPESP fellowship 2021/08423-4), MD (FAPESP fellowship 2018/24213-7), and PL (FAPESP fellowship 2021/00425-8).

Acknowledgments

The authors thank the Central Public Health Laboratory of the State of Tocantins (LACEN/TO) - Brazil for generously supplying the *K. aerogenes* strains and Tocantins State Health Department (SES/Tocantins) for enabling the progress of this project.

Conflict of interest

The authors declare that the research was conducted in the absence of any commercial or financial relationships that could be construed as a potential conflict of interest.

Publisher's note

Supplementary material

The Supplementary material for this article can be found online at: https://www.frontiersin.org/articles/10.3389/fmicb.2024.1352851/full#supplementary-material

References

Afgan, E., Baker, D., Batut, B., van den Beek, M., Bouvier, D., Čech, M., et al. (2018). The galaxy platform for accessible, reproducible and collaborative biomedical analyses: 2018 update. *Nucleic Acids Res.* 46, W537–W544. doi: 10.1093/nar/gky379

Alcock, B. P., Raphenya, A. R., Lau, T. T. Y., Tsang, K. K., Bouchard, M., Edalatmand, A., et al. (2019). CARD 2020: antibiotic resistome surveillance with the comprehensive antibiotic resistance database. *Nucleic Acids Res.* doi: 10.1093/nar/gkz935

Almaghrabi, R., Clancy, C. J., Doi, Y., Hao, B., Chen, L., Shields, R. K., et al. (2014). Carbapenem-resistant *Klebsiella pneumoniae* strains exhibit diversity in aminoglycoside-modifying enzymes, which exert differing effects on Plazomicin and other agents. *Antimicrob. Agents Chemother.* 58, 4443–4451. doi: 10.1128/AAC.00099-14

Aly, S. A., Boothe, D. M., and Suh, S.-J. (2015). A novel alanine to serine substitution mutation in sox S induces overexpression of efflux pumps and contributes to multidrug resistance in clinical *Escherichia coli* isolates. *J. Antimicrob. Chemother.* 70, 2228–2233. doi: 10.1093/jac/dkv105

Andersen, J., He, G.-X., Kakarla, P. K. C. R., Kumar, S., Lakra, W., et al. (2015). Multidrug efflux pumps from Enterobacteriaceae, Vibrio cholerae and *Staphylococcus aureus* bacterial food pathogens. *Int. J. Environ. Res. Public Health* 12, 1487–1547. doi: 10.3390/ijerph120201487

Antipov, D., Hartwick, N., Shen, M., Raiko, M., Lapidus, A., and Pevzner, P. A. (2016). Plasmid SPAdes: assembling plasmids from whole genome sequencing data. *Bioinformatics* 32, 3380–3387. doi: 10.1093/bioinformatics/btw493

Arndt, D., Grant, J. R., Marcu, A., Sajed, T., Pon, A., Liang, Y., et al. (2016). PHASTER: a better, faster version of the PHAST phage search tool. *Nucleic Acids Res.* 44, W16–W21. doi: 10.1093/nar/gkw387

Azevedo, P. A. A., Furlan, J. P. R., Oliveira-Silva, M., Nakamura-Silva, R., Gomes, C. N., Costa, K. R. C., et al. (2018). Detection of virulence and β-lactamase encoding genes in Enterobacter aerogenes and *Enterobacter cloacae* clinical isolates from Brazil. *Braz. J. Microbiol.* 49, 224–228. doi: 10.1016/j.bjm.2018.04.009

Aziz, R. K., Bartels, D., Best, A. A., DeJongh, M., Disz, T., Edwards, R. A., et al. (2008). The RAST server: rapid annotations using subsystems technology. *BMC Genomics* 9:75. doi: 10.1186/1471-2164-9-75

Bankevich, A., Nurk, S., Antipov, D., Gurevich, A. A., Dvorkin, M., Kulikov, A. S., et al. (2012). SPAdes: a new genome assembly algorithm and its applications to single-cell sequencing. *J. Comput. Biol.* 19, 455–477. doi: 10.1089/cmb.2012.0021

Bean, E. L., Herman, C., Anderson, M. E., and Grossman, A. D. (2022). Biology and engineering of integrative and conjugative elements: construction and analyses of hybrid ICEs reveal element functions that affect species-specific efficiencies. *PLoS Genet.* 18:e1009998. doi: 10.1371/journal.pgen.1009998

Bentley, S. D., Chater, K. F., Cerdeño-Tárraga, A.-M., Challis, G. L., Thomson, N. R., James, K. D., et al. (2002). Complete genome sequence of the model actinomycete *Streptomyces coelicolor* A3(2). *Nature* 417, 141–147. doi: 10.1038/417141a

Berbers, B., Ceyssens, P.-J., Bogaerts, P., Vanneste, K., Roosens, N. H. C., Marchal, K., et al. (2020). Development of an NGS-based workflow for improved monitoring of circulating plasmids in support of risk assessment of antimicrobial resistance gene dissemination. *Antibiotics* 9:503. doi: 10.3390/antibiotics9080503

Bertelli, C., Laird, M. R., Williams, K. P., Lau, B. Y., Hoad, G., Winsor, G. L., et al. (2017). Island viewer 4: expanded prediction of genomic islands for larger-scale datasets. *Nucleic Acids Res.* 45, W30–W35. doi: 10.1093/nar/gkx343

Bertels, F., Silander, O. K., Pachkov, M., Rainey, P. B., and van Nimwegen, E. (2014). Automated reconstruction of whole-genome phylogenies from short-sequence reads. *Mol. Biol. Evol.* 31, 1077–1088. doi: 10.1093/molbev/msu088

Bi, D., Zheng, J., Li, J.-J., Sheng, Z.-K., Zhu, X., Ou, H.-Y., et al. (2018). In silico typing and comparative genomic analysis of Inc FII K plasmids and insights into the evolution of replicons, plasmid backbones, and resistance determinant profiles. *Antimicrob. Agents Chemother.* 62. doi: 10.1128/AAC.00764-18

Bispo Beltrão, E. M., de Oliveira, É. M., dos Santos Vasconcelos, C. R., Cabral, A. B., Rezende, A. M., and Souza Lopes, A. C. (2020). Multidrug-resistant *Klebsiella aerogenes* clinical isolates from Brazil carrying Inc Q1 plasmids containing the Bla KPC-2 gene associated with non-Tn4401 elements (NTEKPC-IId). *J. Glob. Antimicrob. Resist.* 22, 43–44. doi: 10.1016/j.jgar.2020.05.001

Boetzer, M., Henkel, C. V., Jansen, H. J., Butler, D., and Pirovano, W. (2011). Scaffolding pre-assembled contigs using SSPACE. *Bioinformatics* 27, 578–579. doi: 10.1093/bioinformatics/btq683

Bortolaia, V., Kaas, R. S., Ruppe, E., Roberts, M. C., Schwarz, S., Cattoir, V., et al. (2020). Res finder 4.0 for predictions of phenotypes from genotypes. *J. Antimicrob. Chemother.* 75, 3491–3500. doi: 10.1093/jac/dkaa345

Bouza, E. (2021). The role of new carbapenem combinations in the treatment of multidrug-resistant gram-negative infections. *J. Antimicrob. Chemother.* 76, iv38–iv45. doi: 10.1093/jac/dkab353

Bowyer, J. E. L. C., De los Santos, E., Styles, K. M., Fullwood, A., Corre, C., and Bates, D. G. (2017). Modeling the architecture of the regulatory system controlling methylenomycin production in *Streptomyces coelicolor*. *J. Biol. Eng.* 11:30. doi: 10.1186/s13036-017-0071-6

Cantalapiedra, C. P., Hernández-Plaza, A., Letunic, I., Bork, P., and Huerta-Cepas, J. (2021). Egg NOG-mapper v2: functional annotation, Orthology assignments, and domain prediction at the metagenomic scale. *Mol. Biol. Evol.* 38, 5825–5829. doi: 10.1093/molbev/msab293

Carattoli, A., Zankari, E., García-Fernández, A., Voldby Larsen, M., Lund, O., Villa, L., et al. (2014). Detection and typing of plasmids using plasmid finder and plasmid multilocus sequence typing. *Antimicrob. Agents Chemother.* 58, 3895–3903. doi: 10.1128/AAC.02412-14

Castanheira, M., Mendes, R. E., and Gales, A. C. (2023). Global epidemiology and mechanisms of resistance of *Acinetobacter baumannii*-calcoaceticus complex. *Clin. Infect. Dis.* 76, S166–S178. doi: 10.1093/cid/ciad109

Castanheira, M., Simner, P. J., and Bradford, P. A. (2021). Extended-spectrum β-lactamases: an update on their characteristics, epidemiology and detection. *JAC Antimicrob Resist* 3. doi: 10.1093/jacamr/dlab092

Castellanos, L. R., van der Graaf-van Bloois, L., Donado-Godoy, P., Veldman, K., Duarte, F., Acuña, M. T., et al. (2020). Antimicrobial resistance in *Salmonella enterica* Serovar Paratyphi B variant Java in poultry from Europe and Latin America. *Emerg. Infect. Dis.* 26, 1164–1173. doi: 10.3201/eid2606.191121

Chaudhari, N. M., Gupta, V. K., and Dutta, C. (2016). BPGA- an ultra-fast pan-genome analysis pipeline. *Sci. Rep.* 6:24373. doi: 10.1038/srep24373

Chen, L., Chavda, K. D., Melano, R. G., Jacobs, M. R., Levi, M. H., Bonomo, R. A., et al. (2013). Complete sequence of a Bla KPC-2-harboring Inc FII K1 plasmid from a *Klebsiella pneumoniae* sequence type 258 strain. *Antimicrob. Agents Chemother.* 57, 1542–1545. doi: 10.1128/AAC.02332-12

Chen, Z., Li, H., Feng, J., Li, Y., Chen, X., Guo, X., et al. (2015). NDM-1 encoded by a pNDM-BJ01-like plasmid p3SP-NDM in clinical *Enterobacter aerogenes*. *Front. Microbiol.* 6:294. doi: 10.3389/fmicb.2015.00294

Chen, M., Shi, X., Yu, Z., Fan, G., Serysheva, I. I., Baker, M. L., et al. (2022). In situ structure of the Acr AB-Tol C efflux pump at subnanometer resolution. *Structure* 30, 107–113.e3. doi: 10.1016/j.str.2021.08.008

Chen, K., Xie, M., Wang, H., Chan, E. W.-C., and Chen, S. (2023). Intercontinental spread and clonal expansion of col RNA1 plasmid-bearing Salmonella Corvallis ST1541 strains: a genomic epidemiological study. *One Health Advances* 1:16. doi: 10.1186/s44280-023-00017-9

Chevalier, J., Mulfinger, C., Garnotel, E., Nicolas, P., Davin-Régli, A., and Pagès, J.-M. (2008). Identification and evolution of drug efflux pump in clinical *Enterobacter aerogenes* strains isolated in 1995 and 2003. *PLoS One* 3:e3203. doi: 10.1371/journal.pone.0003203

Chollet, R., Chevalier, J., Bollet, C., Pages, J.-M., and Davin-Regli, A. (2004). Ram a is an alternate activator of the multidrug resistance Cascade in *Enterobacter aerogenes*. *Antimicrob. Agents Chemother.* 48, 2518–2523. doi: 10.1128/AAC.48.7.2518-2523.2004

Chubiz, L. M. (2023). The mar, sox, and rob Systems. *Eco Sal Plus* 11. doi: 10.1128/ecosalplus.esp-0010-2022

CLSI. (2023). Performance Standards for Antimicrobial Susceptibility Testing. 33rd ed.Wayne PA: CLSI supplement M100.

Conselho Nacional de Saúde/Ministério da Saúde. (2012). *Resolução Nº 466*.

Costa, S. S., Guimarães, L. C., Silva, A., Soares, S. C., and Baraúna, R. A. (2020). First steps in the analysis of prokaryotic Pan-genomes. *Bioinform Biol Insights* 14:117793222093806. doi: 10.1177/1177932220938064

Couvin, D., Bernheim, A., Toffano-Nioche, C., Touchon, M., Michalik, J., Néron, B., et al. (2018). CRISPRCasFinder, an update of CRISRFinder, includes a portable version, enhanced performance and integrates search for Cas proteins. *Nucleic Acids Res.* 46, W246–W251. doi: 10.1093/nar/gky425

da Silva Filho, A. C., Raittz, R. T., Guizelini, D., De Pierri, C. R., Augusto, D. W., dos Santos-Weiss, I. C. R., et al. (2018). Comparative analysis of Genomic Island prediction tools. *Front. Genet.* 9:619. doi: 10.3389/fgene.2018.00619

Damas, M. S. F., Ferreira, R. L., Campanini, E. B., Soares, G. G., Campos, L. C., Laprega, P. M., et al. (2022). Whole genome sequencing of the multidrug-resistant *Chryseobacterium indologenes* isolated from a patient in Brazil. *Front. Med (Lausanne)* 9:931379. doi: 10.3389/fmed.2022.931379

Davin-Regli, A., Lavigne, J.-P., and Pagès, J.-M. (2019). Enterobacter spp.: update on taxonomy, clinical aspects, and emerging antimicrobial resistance. *Clin. Microbiol. Rev.* 32. doi: 10.1128/CMR.00002-19

Davin-Regli, A., and Pages, J.-M. (2015). Enterobacter aerogenes and *Enterobacter cloacae*; versatile bacterial pathogens confronting antibiotic treatment. *Front. Microbiol.* 6:392. doi: 10.3389/fmicb.2015.00392

de Oliveira Santos, I. C., Albano, R. M., Asensi, M. D., and D'Alincourt Carvalho-Assef, A. P. (2018). Draft genome sequence of KPC-2-producing *Pseudomonas aeruginosa* recovered from a bloodstream infection sample in Brazil. *J. Glob. Antimicrob. Resist.* 15, 99–100. doi: 10.1016/j.jgar.2018.08.021

Denissen, J., Reyneke, B., Waso-Reyneke, M., Havenga, B., Barnard, T., Khan, S., et al. (2022). Prevalence of ESKAPE pathogens in the environment: antibiotic resistance status, community-acquired infection and risk to human health. *Int. J. Hyg. Environ. Health* 244:114006. doi: 10.1016/j.ijheh.2022.114006

Dobiasova, H., Videnska, P., and Dolejska, M. (2016). Complete Sequences of IncU Plasmids Harboring Quinolone Resistance Genes qnrS2 and aac(6\u0027)-Ib-cr in Aeromonas spp. from Ornamental Fish. *Antimicrob Agents Chemother* 60, 653–657. doi: 10.1128/AAC.01773-15

Durrant, M. G., Li, M. M., Siranosian, B. A., Montgomery, S. B., and Bhatt, A. S. (2020). A Bioinformatic analysis of integrative Mobile genetic elements highlights their role in bacterial adaptation. *Cell Host Microbe* 27, 140–153.e9. doi: 10.1016/j.chom.2019.10.022

Ferreira, R. L., da Silva, B. C. M., Rezende, G. S., Nakamura-Silva, R., Pitondo-Silva, A., Campanini, E. B., et al. (2019). High prevalence of multidrug-resistant *Klebsiella pneumoniae* harboring several virulence and β-lactamase encoding genes in a Brazilian intensive care unit. *Front. Microbiol.* 9:3198. doi: 10.3389/fmicb.2018.03198

Ferreira, R. L., Rezende, G. S., Damas, M. S. F., Oliveira-Silva, M., Pitondo-Silva, A., Brito, M. C. A., et al. (2020). Characterization of KPC-producing *Serratia marcescens* in an intensive care unit of a Brazilian tertiary hospital. *Front. Microbiol.* 11:956. doi: 10.3389/fmicb.2020.00956

Firmo, E. F., Cabral, A. B., De Oliveira, É. M., and Lopes, A. C. S. (2019). Emergence of aph(3')-VI and accumulation of aminoglycoside modifying enzyme genes in KPC-2-possessing *Enterobacter aerogenes* isolates from infections and colonization in patients from Recife-PE, Brazil. *Rev. Soc. Bras. Med. Trop.* 52. doi: 10.1590/0037-8682-0460-2018

Franolić, I., Bedenić, B., Beader, N., Lukić-Grlić, A., Mihaljević, S., Bielen, L., et al. (2019). NDM-1-producing *Enterobacter aerogenes* isolated from a patient with a JJ ureteric stent in situ. *CEN Case Rep.* 8, 38–41. doi: 10.1007/s13730-018-0360-z

Galani, I., Nafplioti, K., Adamou, P., Karaiskos, I., Giamarellou, H., and Souli, M. (2019). Nationwide epidemiology of carbapenem resistant *Klebsiella pneumoniae* isolates from Greek hospitals, with regards to plazomicin and aminoglycoside resistance. *BMC Infect. Dis.* 19:167. doi: 10.1186/s12879-019-3801-1

Ghanavati, R., Emaneini, M., Kalantar-Neyestanaki, D., Maraji, A. S., Dalvand, M., Beigverdi, R., et al. (2018). Clonal relation and antimicrobial resistance pattern of extended-spectrum β-lactamase- and amp C β-lactamase-producing Enterobacter spp. isolated from different clinical samples in Tehran, Iran. *Rev. Soc. Bras. Med. Trop.* 51, 88–93. doi: 10.1590/0037-8682-0227-2017

Grant, J. R., Enns, E., Marinier, E., Mandal, A., Herman, E. K., Chen, C., et al. (2023). Proksee: in-depth characterization and visualization of bacterial genomes. *Nucleic Acids Res.* 51, W484–W492. doi: 10.1093/nar/gkad326

Grazziotin, A. L., Vidal, N. M., Palmeiro, J. K., Dalla-Costa, L. M., and Venancio, T. M. (2016). Genome sequencing of four multidrug-resistant *Enterobacter aerogenes* isolates from hospitalized patients in Brazil. *Front. Microbiol.* 7:1649. doi: 10.3389/fmicb.2016.01649

Guan, X., Xue, X., Liu, Y., Wang, J., Wang, Y., Wang, J., et al. (2013). Plasmid-mediated quinolone resistance – current knowledge and future perspectives. *J. Int. Med. Res.* 41, 20–30. doi: 10.1177/0300060513475965

Guérin, F., Gravey, F., Reissier, S., Penven, M., Michaux, C., Le Hello, S., et al. (2023). Temocillin resistance in the *Enterobacter cloacae* Complex is conferred by a single point mutation in bae S, leading to overexpression of the Acr D efflux pump. *Antimicrob. Agents Chemother.* 67. doi: 10.1128/aac.00358-23

Guindon, S., Delsuc, F., Dufayard, J.-F., and Gascuel, O. (2009). *Estimating maximum likelihood phylogenies with Phy ML*, 113–137.

Gupta, S. K., Padmanabhan, B. R., Diene, S. M., Lopez-Rojas, R., Kempf, M., Landraud, L., et al. (2014). ARG-ANNOT, a new Bioinformatic tool to discover antibiotic resistance genes in bacterial genomes. *Antimicrob. Agents Chemother.* 58, 212–220. doi: 10.1128/AAC.01310-13

Gurevich, A., Saveliev, V., Vyahhi, N., and Tesler, G. (2013). QUAST: quality assessment tool for genome assemblies. *Bioinformatics* 29, 1072–1075. doi: 10.1093/bioinformatics/btt086

Gurpinar, S. S., Kart, D., and Eryilmaz, M. (2022). The effects of antidepressants fluoxetine, sertraline, and amitriptyline on the development of antibiotic resistance in *Acinetobacter baumannii*. *Arch. Microbiol.* 204:230. doi: 10.1007/s00203-022-02853-6

Haldorsen, B. C., Simonsen, G. S., Sundsfjord, A., and Samuelsen, Ø. (2014). Increased prevalence of aminoglycoside resistance in clinical isolates of Escherichia coli and Klebsiella spp. in Norway is associated with the acquisition of AAC (3)-II and AAC (6′)-Ib. *Diagn. Microbiol. Infect. Dis.* 78, 66–69. doi: 10.1016/j.diagmicrobio.2013.10.001

Hall, T. A. (1999). Bio edit: a user-friendly biological sequence alignment editor and analysis program for windows 95/98/NT. *Nucleic Acids Symp. Ser.* 41, 95–98.

Han, J. E., Kim, J. H., Choresca, C. H., Shin, S. P., Jun, J. W., Chai, J. Y., et al. (2012). First description of ColE-type plasmid in Aeromonas spp. carrying quinolone resistance (qnrS2) gene. *Lett Appl Microbiol* 55, 290–294. doi: 10.1111/j.1472-765X.2012.03293.x

Hayashi, M., Tabata, K., Yagasaki, M., and Yonetani, Y. (2010). Effect of multidrug-efflux transporter genes on dipeptide resistance and overproduction in *Escherichia coli*. *FEMS Microbiol. Lett.* 304, 12–19. doi: 10.1111/j.1574-6968.2009.01879.x

Hejair, H. M. A., Zhu, Y., Ma, J., Zhang, Y., Pan, Z., Zhang, W., et al. (2017). Functional role of omp F and omp C porins in pathogenesis of avian pathogenic *Escherichia coli*. *Microb. Pathog.* 107, 29–37. doi: 10.1016/j.micpath.2017.02.033

Hounmanou, Y. M. G., Baniga, Z., García, V., and Dalsgaard, A. (2022). Salmonella Salamae and S. Waycross isolated from Nile perch in Lake Victoria show limited human pathogenic potential. *Sci. Rep.* 12:4229. doi: 10.1038/s41598-022-08200-5

Huang, L., Yuan, H., Liu, M.-F., Zhao, X.-X., Wang, M.-S., Jia, R.-Y., et al. (2017). Type B chloramphenicol acetyltransferases are responsible for chloramphenicol resistance in *Riemerella anatipestifer*, China. *Front. Microbiol.* 8. doi: 10.3389/fmicb.2017.00297

Hudson, C. M., Bent, Z. W., Meagher, R. J., and Williams, K. P. (2014). Resistance determinants and Mobile genetic elements of an NDM-1-encoding *Klebsiella pneumoniae* strain. *PLoS One* 9:e99209. doi: 10.1371/journal.pone.0099209

Ito, R., Mustapha, M. M., Tomich, A. D., Callaghan, J. D., McElheny, C. L., Mettus, R. T., et al. (2017). Widespread Fosfomycin resistance in gram-negative Bacteria attributable to the chromosomal fos a gene. *MBio*:8. doi: 10.1128/mBio.00749-17

Iyer, R., Iken, B., and Damania, A. (2017). Whole genome of *Klebsiella aerogenes* PX01 isolated from San Jacinto River sediment west of Baytown, Texas reveals the presence of multiple antibiotic resistance determinants and mobile genetic elements. *Genom Data* 14, 7–9. doi: 10.1016/j.gdata.2017.07.012

Jacoby, G. A. (2009). Amp C β-Lactamases. *Clin. Microbiol. Rev.* 22, 161–182. doi: 10.1128/CMR.00036-08

Jain, P., Bepari, A. K., Sen, P. K., Rafe, T., Imtiaz, R., Hossain, M., et al. (2021). High prevalence of multiple antibiotic resistance in clinical *E. coli* isolates from Bangladesh and prediction of molecular resistance determinants using WGS of an XDR isolate. *Sci. Rep.* 11:22859. doi: 10.1038/s41598-021-02251-w

Jamrozy, D., Coll, F., Mather, A. E., Harris, S. R., Harrison, E. M., Mac Gowan, A., et al. (2017). Evolution of mobile genetic element composition in an epidemic methicillin-resistant *Staphylococcus aureus*: temporal changes correlated with frequent loss and gain events. *BMC Genomics* 18:684. doi: 10.1186/s12864-017-4065-z

Jang, S. (2023). Acr AB-Tol C, a major efflux pump in gram negative bacteria: toward understanding its operation mechanism. *BMB Rep.* 56, 326–334. doi: 10.5483/BMBRep.2023-0070

Johnson, C. M., and Grossman, A. D. (2015). Integrative and conjugative elements (ICEs): what they do and how they work. *Annu. Rev. Genet.* 49, 577–601. doi: 10.1146/annurev-genet-112414-055018

Juhas, M., van der Meer, J. R., Gaillard, M., Harding, R. M., Hood, D. W., and Crook, D. W. (2009). Genomic islands: tools of bacterial horizontal gene transfer and evolution. *FEMS Microbiol. Rev.* 33, 376–393. doi: 10.1111/j.1574-6976.2008.00136.x

Kamio, K., and Espinoza, J. L. (2022). The predominance of *Klebsiella aerogenes* among Carbapenem-resistant Enterobacteriaceae infections in Japan. *Pathogens* 11:722. doi: 10.3390/pathogens11070722

Kanehisa, M., Sato, Y., and Morishima, K. (2016). Blast KOALA and ghost KOALA: KEGG tools for functional characterization of genome and metagenome sequences. *J. Mol. Biol.* 428, 726–731. doi: 10.1016/j.jmb.2015.11.006

Katoh, K., and Standley, D. M. (2013). MAFFT multiple sequence alignment software version 7: improvements in performance and usability. *Mol. Biol. Evol.* 30, 772–780. doi: 10.1093/molbev/mst010

Keeney, D., Ruzin, A., and Bradford, P. A. (2007). Ram a, a transcriptional regulator, and Acr AB, an RND-type efflux pump, are associated with decreased susceptibility to Tigecycline in *Enterobacter cloacae*. *Microb. Drug Resist.* 13, 1–6. doi: 10.1089/mdr.2006.9990

Kondo, K., Kawano, M., and Sugai, M. (2021). Distribution of antimicrobial resistance and virulence genes within the prophage-associated regions in nosocomial pathogens. *mSphere*:6. doi: 10.1128/mSphere.00452-21

Koroiva, R., and Santana, D. J. (2022). Evaluation of partial 12S rRNA, 16S rRNA, COI and Cytb gene sequence datasets for potential single DNA barcode for hylids (Anura: Hylidae). *An. Acad. Bras. Cienc.* 94. doi: 10.1590/0001-3765202220200825

Lavigne, J.-P., Sotto, A., Nicolas-Chanoine, M.-H., Bouziges, N., Bourg, G., Davin-Regli, A., et al. (2012). Membrane permeability, a pivotal function involved in antibiotic resistance and virulence in *Enterobacter aerogenes* clinical isolates. *Clin. Microbiol. Infect.* 18, 539–545. doi: 10.1111/j.1469-0691.2011.03607.x

Liu, M., Li, X., Xie, Y., Bi, D., Sun, J., Li, J., et al. (2019). ICEberg 2.0: an updated database of bacterial integrative and conjugative elements. *Nucleic Acids Res.* 47, D660–D665. doi: 10.1093/nar/gky1123

Ma, D.-Y., Huang, H.-Y., Zou, H., Wu, M.-L., Lin, Q.-X., Liu, B., et al. (2020). Carbapenem-resistant *Klebsiella aerogenes* clinical isolates from a teaching Hospital in Southwestern China: detailed molecular epidemiology, resistance determinants, risk factors and clinical outcomes. *Infect. Drug Resist.* 13, 577–585. doi: 10.2147/IDR.S235975

Machuca, J., Ortiz, M., Recacha, E., Díaz-De-Alba, P., Docobo-Perez, F., Rodríguez-Martínez, J.-M., et al. (2016). Impact of AAC (6′)-Ib-cr in combination with chromosomal-mediated mechanisms on clinical quinolone resistance in *Escherichia coli*. *J. Antimicrob. Chemother.* 71, 3066–3071. doi: 10.1093/jac/dkw258

Magiorakos, A.-P., Srinivasan, A., Carey, R. B., Carmeli, Y., Falagas, M. E., Giske, C. G., et al. (2012). Multidrug-resistant, extensively drug-resistant and pandrug-resistant bacteria: an international expert proposal for interim standard definitions for acquired resistance. *Clin. Microbiol. Infect.* 18, 268–281. doi: 10.1111/j.1469-0691.2011.03570.x

Maneewannakul, K., and Levy, S. B. (1996). Identification for mar mutants among quinolone-resistant clinical isolates of *Escherichia coli*. *Antimicrob. Agents Chemother.* 40, 1695–1698. doi: 10.1128/AAC.40.7.1695

Masi, M., Saint, N., Molle, G., and Pagès, J.-M. (2007). The *Enterobacter aerogenes* outer membrane efflux proteins Tol C and Eef C have different channel properties. *Biochim. Biophys. Acta Biomembr.* 1768, 2559–2567. doi: 10.1016/j.bbamem.2007.06.008

Meier-Kolthoff, J. P., Auch, A. F., Klenk, H.-P., and Göker, M. (2013). Genome sequence-based species delimitation with confidence intervals and improved distance functions. *BMC Bioinformatics* 14:60. doi: 10.1186/1471-2105-14-60

Meier-Kolthoff, J. P., Carbasse, J. S., Peinado-Olarte, R. L., and Göker, M. (2022). TYGS and LPSN: a database tandem for fast and reliable genome-based classification

and nomenclature of prokaryotes. *Nucleic Acids Res.* 50, D801–D807. doi: 10.1093/nar/gkab902

Monárrez, R., Wang, Y., Fu, Y., Liao, C.-H., Okumura, R., Braun, M. R., et al. (2018). Genes and proteins involved in *qnr S1* induction. *Antimicrob. Agents Chemother.* 62. doi: 10.1128/AAC.00806-18

Moosavian, M., Khoshkholgh Sima, M., Ahmad Khosravi, N., and Abbasi Montazeri, E. (2021). Detection of Oqx AB efflux pumps, a multidrug-resistant agent in bacterial infection in patients referring to teaching hospitals in Ahvaz, southwest of Iran. *Int. J. Microbiol.* 2021, 1–5. doi: 10.1155/2021/2145176

Mulani, M. S., Kamble, E. E., Kumkar, S. N., Tawre, M. S., and Pardesi, K. R. (2019). Emerging strategies to combat ESKAPE pathogens in the era of antimicrobial resistance: a review. *Front. Microbiol.* 10:539. doi: 10.3389/fmicb.2019.00539

Nagakubo, S., Nishino, K., Hirata, T., and Yamaguchi, A. (2002). The putative response regulator bae R stimulates multidrug resistance of *Escherichia coli* via a novel multidrug exporter system, Mdt ABC. *J. Bacteriol.* 184, 4161–4167. doi: 10.1128/JB.184.15.4161-4167.2002

Nikaido, H. (2018). RND transporters in the living world. *Res. Microbiol.* 169, 363–371. doi: 10.1016/j.resmic.2018.03.001

Nishino, K., and Yamaguchi, A. (2001). Analysis of a complete library of putative drug transporter genes in *Escherichia coli*. *J. Bacteriol.* 183, 5803–5812. doi: 10.1128/JB.183.20.5803-5812.2001

Obayiuwana, A., and Ibekwe, A. M. (2020). Antibiotic resistance genes occurrence in wastewaters from selected pharmaceutical facilities in Nigeria. *Water (Basel)* 12:1897. doi: 10.3390/w12071897

Orlek, A., Stoesser, N., Anjum, M. F., Doumith, M., Ellington, M. J., Peto, T., et al. (2017). Plasmid classification in an era of whole-genome sequencing: application in studies of antibiotic resistance epidemiology. *Front. Microbiol.* 8:182. doi: 10.3389/fmicb.2017.00182

Pajand, O., Rahimi, H., Badmasti, F., Gholami, F., Alipour, T., Darabi, N., et al. (2023). Various arrangements of mobile genetic elements among CC147 subpopulations of *Klebsiella pneumoniae* harboring Bla NDM-1: a comparative genomic analysis of carbapenem resistant strains. *J. Biomed. Sci.* 30:73. doi: 10.1186/s12929-023-00960-0

Pan, F., Xu, Q., and Zhang, H. (2021). Emergence of NDM-5 producing Carbapenem-resistant *Klebsiella aerogenes* in a pediatric Hospital in Shanghai, China. *Front. Public Health* 9:621527. doi: 10.3389/fpubh.2021.621527

Peirano, G., Matsumura, Y., Adams, M. D., Bradford, P., Motyl, M., Chen, L., et al. (2018). Genomic epidemiology of global Carbapenemase-producing Enterobacter spp., 2008–2014. *Emerg. Infect. Dis.* 24, 1010–1019. doi: 10.3201/eid2406.171648

Picão, R. C., Poirel, L., Demarta, A., Silva, C. S. F., Corvaglia, A. R., Petrini, O., et al. (2008). Plasmid-mediated quinolone resistance in *Aeromonas allosaccharophila* recovered from a Swiss lake. *J. Antimicrob. Chemother.* 62, 948–950. doi: 10.1093/jac/dkn341

Poirel, L., Naas, T., and Nordmann, P. (2008). Genetic support of extended-spectrum β-lactamases. *Clin. Microbiol. Infect.* 14, 75–81. doi: 10.1111/j.1469-0691.2007.01865.x

Posada, D. (2008). jModelTest: Phylogenetic Model Averaging. *Mol. Biol. Evol.* 25, 1253–1256. doi: 10.1093/molbev/msn083

Pradel, E., and Pagès, J.-M. (2002). The Acr AB-Tol C efflux pump contributes to multidrug resistance in the nosocomial pathogen *Enterobacter aerogenes*. *Antimicrob. Agents Chemother.* 46, 2640–2643. doi: 10.1128/AAC.46.8.2640-2643.2002

Pulcrano, G., Pignanelli, S., Vollaro, A., Esposito, M., Iula, V. D., Roscetto, E., et al. (2016). Isolation of *Enterobacter aerogenes* carrying bla TEM-1 and Bla KPC-3 genes recovered from a hospital intensive care unit. *APMIS* 124, 516–521. doi: 10.1111/apm.12528

Rosenblum, R., Khan, E., Gonzalez, G., Hasan, R., and Schneiders, T. (2011). Genetic regulation of the ram a locus and its expression in clinical isolates of *Klebsiella pneumoniae*. *Int. J. Antimicrob. Agents* 38, 39–45. doi: 10.1016/j.ijantimicag.2011.02.012

Ross, K., Varani, A. M., Snesrud, E., Huang, H., Alvarenga, D. O., Zhang, J., et al. (2021). TnCentral: a prokaryotic transposable element database and web portal for transposon analysis. *mBio*:12. doi: 10.1128/mBio.02060-21

Rossi-Tamisier, M., Benamar, S., Raoult, D., and Fournier, P.-E. (2015). Cautionary tale of using 16S rRNA gene sequence similarity values in identification of human-associated bacterial species. *Int. J. Syst. Evol. Microbiol.* 65, 1929–1934. doi: 10.1099/ijs.0.000161

Ruzin, A., Immermann, F. W., and Bradford, P. A. (2008). Real-time PCR and statistical analyses of acr AB and ram a expression in clinical isolates of *Klebsiella pneumoniae*. *Antimicrob. Agents Chemother.* 52, 3430–3432. doi: 10.1128/AAC.00591-08

Sano, E., Fontana, H., Esposito, F., Cardoso, B., Fuga, B., Costa, G. C. V., et al. (2023). Genomic analysis of fluoroquinolone-resistant *Leclercia adecarboxylata* carrying the ISKpn19-orf-qnr S1-ΔIS3-Bla LAP-2 module in a synanthropic pigeon, Brazil. *J. Glob. Antimicrob. Resist.* 33, 256–259. doi: 10.1016/j.jgar.2023.04.013

Seemann, T. (2014). Prokka: rapid prokaryotic genome annotation. *Bioinformatics* 30, 2068–2069. doi: 10.1093/bioinformatics/btu153

Shawa, M., Furuta, Y., Mulenga, G., Mubanga, M., Mulenga, E., Zorigt, T., et al. (2021). Novel chromosomal insertions of ISEcp1-Bla CTX-M-15 and diverse antimicrobial resistance genes in Zambian clinical isolates of Enterobacter cloacae and *Escherichia coli*. *Antimicrob. Resist. Infect. Control* 10:79. doi: 10.1186/s13756-021-00941-8

Shen, X., Liu, L., Yu, J., Cao, X., Zhan, Q., Guo, Y., et al. (2019). Coexistence of bla_{NDM-1} and rmt C on a transferrable plasmid of a novel ST192 *Klebsiella aerogenes* clinical isolate. *Infect. Drug Resist.* 12, 3883–3891. doi: 10.2147/IDR.S228130

Shin, H. W., Lim, J., Kim, S., Kim, J., Kwon, G. C., and Koo, S. H. (2015). Characterization of trimethoprim-sulfamethoxazole resistance genes and their relatedness to class 1 Integron and insertion sequence common region in gram-negative Bacilli. *J. Microbiol. Biotechnol.* 25, 137–142. doi: 10.4014/jmb.1409.09041

Shinoy, M., Dennehy, R., Coleman, L., Carberry, S., Schaffer, K., Callaghan, M., et al. (2013). Immunoproteomic analysis of proteins expressed by two related pathogens, Burkholderia multivorans and *Burkholderia cenocepacia*, during human infection. *PLoS One* 8:e80796. doi: 10.1371/journal.pone.0080796

Siguier, P. (2006). ISfinder: the reference Centre for bacterial insertion sequences. *Nucleic Acids Res.* 34, D32–D36. doi: 10.1093/nar/gkj014

Siguier, P., Gourbeyre, E., and Chandler, M. (2014). Bacterial insertion sequences: their genomic impact and diversity. *FEMS Microbiol. Rev.* 38, 865–891. doi: 10.1111/1574-6976.12067

Simão, F. A., Waterhouse, R. M., Ioannidis, P., Kriventseva, E. V., and Zdobnov, E. M. (2015). BUSCO: assessing genome assembly and annotation completeness with single-copy orthologs. *Bioinformatics* 31, 3210–3212. doi: 10.1093/bioinformatics/btv351

Smani, Y., Fàbrega, A., Roca, I., Sánchez-Encinales, V., Vila, J., and Pachón, J. (2014). Role of Omp a in the multidrug resistance phenotype of *Acinetobacter baumannii*. *Antimicrob. Agents Chemother.* 58, 1806–1808. doi: 10.1128/AAC.02101-13

Soares, G. G., Campanini, E. B., Ferreira, R. L., Damas, M. S. F., Rodrigues, S. H., Campos, L. C., et al. (2023). Brevundimonas brasiliensis sp. nov.: a new multidrug-resistant species isolated from a patient in Brazil. *Microbiol. Spectr.* 11. doi: 10.1128/spectrum.04415-22

Soares, C. R. P., Oliveira-Júnior, J. B., and Firmo, E. F. (2021). First report of a Bla NDM-resistant gene in a *Klebsiella aerogenes* clinical isolate from Brazil. *Rev. Soc. Bras. Med. Trop.* 54. doi: 10.1590/0037-8682-0262-2020

Sta Ana, K. M., Madriaga, J., and Espino, M. P. (2021). β-Lactam antibiotics and antibiotic resistance in Asian lakes and rivers: an overview of contamination, sources and detection methods. *Environ. Pollut.* 275:116624. doi: 10.1016/j.envpol.2021.116624

Starikova, E. V., Tikhonova, P. O., Prianichnikov, N. A., Rands, C. M., Zdobnov, E. M., Ilina, E. N., et al. (2020). Phigaro: high-throughput prophage sequence annotation. *Bioinformatics* 36, 3882–3884. doi: 10.1093/bioinformatics/btaa250

Subhadra, B., Kim, J., Kim, D. H., Woo, K., Oh, M. H., and Choi, C. H. (2018). Local repressor Acr R regulates Acr AB efflux pump required for biofilm formation and virulence in *Acinetobacter nosocomialis*. *Front. Cell. Infect. Microbiol.* 8:270. doi: 10.3389/fcimb.2018.00270

Takei, S., Lu, Y. J., Tohya, M., Watanabe, S., Misawa, S., Tabe, Y., et al. (2022). Spread of Carbapenem-resistant *Klebsiella pneumoniae* clinical isolates producing NDM-type Metallo-β-lactamase in Myanmar. *Microbiol. Spectr.* 10. doi: 10.1128/spectrum.00673-22

Tamma, P. D., Doi, Y., Bonomo, R. A., Johnson, J. K., Simner, P. J., Tamma, P. D., et al. (2019). A primer on amp C β-lactamases: necessary knowledge for an increasingly multidrug-resistant world. *Clin. Infect. Dis.* 69, 1446–1455. doi: 10.1093/cid/ciz173

Tao, Y., Zhou, K., Xie, L., Xu, Y., Han, L., Ni, Y., et al. (2020). Emerging coexistence of three PMQR genes on a multiple resistance plasmid with a new surrounding genetic structure of qnr S2 in *E. coli* in China. *Antimicrob. Resist. Infect. Control* 9:52. doi: 10.1186/s13756-020-00711-y

Teichmann, A., Agra, H. N. D. C., Nunes, L. D. S., Da Rocha, M. P., Renner, J. D. P., Possuelo, L. G., et al. (2014). Antibiotic resistance and detection of the sul 2 gene in urinary isolates of *Escherichia coli* in patients from Brazil. *J. Infect. Develop. Countries* 8, 039–043. doi: 10.3855/jidc.3380

Tempel, S., Bedo, J., and Talla, E. (2022). From a large-scale genomic analysis of insertion sequences to insights into their regulatory roles in prokaryotes. *BMC Genomics* 23:451. doi: 10.1186/s12864-022-08678-3

Thorell, K., Meier-Kolthoff, J. P., Sjöling, Å., and Martín-Rodríguez, A. J. (2019). Whole-genome sequencing redefines Shewanella taxonomy. *Front. Microbiol.* 10:1861. doi: 10.3389/fmicb.2019.01861

Tsai, Y.-K., Liou, C.-H., Lin, J.-C., Fung, C.-P., Chang, F.-Y., and Siu, L. K. (2020). Effects of different resistance mechanisms on antimicrobial resistance in *Acinetobacter baumannii*: a strategic system for screening and activity testing of new antibiotics. *Int. J. Antimicrob. Agents* 55:105918. doi: 10.1016/j.ijantimicag.2020.105918

Vrioni, G., Daniil, I., Voulgari, E., Ranellou, K., Koumaki, V., Ghirardi, S., et al. (2012). Comparative evaluation of a prototype chromogenic medium (Chrom ID CARBA) for detecting carbapenemase-producing enterobacteriaceae in surveillance rectal swabs. *J. Clin. Microbiol.* 50, 1841–1846. doi: 10.1128/JCM.06848-11

Wang, W., Wei, X., Arbab, S., Wu, L., Lu, N., Zhu, Q., et al. (2023). Multidrug-resistant *Escherichia coli* isolate of Chinese bovine origin carrying the Bla CTX-M-55 gene located in IS26-mediated composite Translocatable units. *Microorganisms* 11:2795. doi: 10.3390/microorganisms11112795

Wen, Y., Pu, X., Zheng, W., and Hu, G. (2016). High Prevalence of Plasmid-Mediated Quinolone Resistance and IncQ Plasmids Carrying qnrS2 Gene in Bacteria from Rivers

near Hospitals and Aquaculture in China. *PLoS One* 11:e0159418. doi: 10.1371/journal.pone.0159418

Wong, K. K. Y., Brinkman, F. S. L., Benz, R. S., and Hancock, R. E. W. (2001). Evaluation of a structural model of *Pseudomonas aeruginosa* outer membrane protein Opr M, an efflux component involved in intrinsic antibiotic resistance. *J. Bacteriol.* 183, 367–374. doi: 10.1128/JB.183.1.367-374.2001

Wong, M. H. Y., Chan, E. W. C., and Chen, S. (2015). Evolution and dissemination of Oqx AB-like efflux pumps, an emerging quinolone resistance determinant among members of Enterobacteriaceae. *Antimicrob. Agents Chemother.* 59, 3290–3297. doi: 10.1128/AAC.00310-15

Xu, L., Dong, Z., Fang, L., Luo, Y., Wei, Z., Guo, H., et al. (2019). Ortho Venn 2: a web server for whole-genome comparison and annotation of orthologous clusters across multiple species. *Nucleic Acids Res.* 47, W52–W58. doi: 10.1093/nar/gkz333

Xu, Q., Fu, Y., Zhao, F., Jiang, Y., and Yu, Y. (2020). Molecular characterization of Carbapenem-resistant *Serratia marcescens* clinical isolates in a tertiary Hospital in Hangzhou, China. *Infect. Drug Resist.* 13, 999–1008. doi: 10.2147/IDR.S243197

Xu, Y., Zheng, Z., Ye, L., Chan, E. W.-C., and Chen, S. (2023). Identification and genetic characterization of conjugative plasmids encoding Coresistance to ciprofloxacin and cephalosporin in foodborne *Vibrio* spp. *Microbiol Spectr.* 11. doi: 10.1128/spectrum.01032-23

Yoon, S.-H., Ha, S.-M., Kwon, S., Lim, J., Kim, Y., Seo, H., et al. (2017). Introducing EzBioCloud: a taxonomically united database of 16S rRNA gene sequences and whole-genome assemblies. *Int. J. Syst. Evol. Microbiol.* 67, 1613–1617. doi: 10.1099/ijsem.0.001755

Yu, L., Li, W., Li, Q., Chen, X., Ni, J., Shang, F., et al. (2020). Role of Lsr R in the regulation of antibiotic sensitivity in avian pathogenic *Escherichia coli*. *Poult. Sci.* 99, 3675–3687. doi: 10.1016/j.psj.2020.03.064

Yuan, Q., Xia, P., Xiong, L., Xie, L., Lv, S., Sun, F., et al. (2023). First report of coexistence of Bla KPC-2-, Bla NDM-1- and mcr-9-carrying plasmids in a clinical carbapenem-resistant *Enterobacter hormaechei* isolate. *Front. Microbiol.* 14:1153366. doi: 10.3389/fmicb.2023.1153366

Zeng, Z., Lei, L., Li, L., Hua, S., Li, W., Zhang, L., et al. (2022). In silico characterization of Bla NDM-harboring plasmids in *Klebsiella pneumoniae*. *Front. Microbiol.* 13:1008905. doi: 10.3389/fmicb.2022.1008905

Zhang, R., Liu, L., Zhou, H., Chan, E. W., Li, J., Fang, Y., et al. (2017). Nationwide surveillance of clinical Carbapenem-resistant Enterobacteriaceae (CRE) strains in China. *EBioMedicine* 19, 98–106. doi: 10.1016/j.ebiom.2017.04.032

Zheng, X., Xu, D., Yan, J., Qian, M., Wang, P., Zaeim, D., et al. (2024). Mobile genetic elements facilitate the transmission of antibiotic resistance genes in multidrug-resistant Enterobacteriaceae from duck farms. *Food Sci. Human Wellness* 13, 729–735. doi: 10.26599/FSHW.2022.9250062

frontiers | Frontiers in Microbiology

TYPE Original Research
PUBLISHED 05 September 2024
DOI 10.3389/fmicb.2024.1431154

OPEN ACCESS

EDITED BY
Mingxi Wang,
Huaqiao University, China

REVIEWED BY
Fabrice Compain,
L'Institut Mutualiste Montsouris, France
Justin R. Lenhard,
California Northstate University, United States

*CORRESPONDENCE
Xueqin Xie
✉ cherryxie36@163.com
Gangsen Zheng
✉ aronsen@163.com

RECEIVED 11 May 2024
ACCEPTED 05 August 2024
PUBLISHED 05 September 2024

CITATION
Xie X, Liu Z, Huang J, Wang X, Tian Y, Xu P and Zheng G (2024) Molecular epidemiology and carbapenem resistance mechanisms of *Pseudomonas aeruginosa* isolated from a hospital in Fujian, China.
Front. Microbiol. 15:1431154.
doi: 10.3389/fmicb.2024.1431154

Molecular epidemiology and carbapenem resistance mechanisms of *Pseudomonas aeruginosa* isolated from a hospital in Fujian, China

Xueqin Xie[1,2,3]*, Zhou Liu[1,2,3], Jingyan Huang[1], Xueting Wang[1], Yuting Tian[1], Pinying Xu[1] and Gangsen Zheng[4]*

[1]Department of Basic Medical Science, Xiamen Medical College, Xiamen, China, [2]Provincial Key Laboratory of Functional and Clinical Translational Medicine of Universities in Fujian, Xiamen Medical College, Xiamen, China, [3]Institute of Respiratory Disease, Xiamen Medical College, Xiamen, China, [4]Xiamen Key Laboratory of Genetic Testing, Department of Laboratory Medicine, The First Affiliated Hospital of Xiamen University, School of Medicine, Xiamen University, Xiamen, China

The worldwide spread of *Pseudomonas aeruginosa*, especially carbapenem-resistant *P. aeruginosa* (CRPA), poses a serious threat to global public health. In this research, we collected and studied the clinical prevalence, molecular epidemiology, and resistance mechanisms of CRPA in Fujian, China. Among 167 non-duplicated *P. aeruginosa* isolates collected during 2019–2021, strains from respiratory specimens and wound secretions of older males in the intensive care unit dominated. Ninety-eight isolates (58.7 %) were resistant to at least one tested antibiotic, among which 70 strains were carbapenem-resistant. Moleclar typing of the CRPA isolates revealed they were highly divergent, belonging to 46 different sequence types. It is noteworthy that two previously reported high risk clones, ST1971 specific to China and the globally prevalent ST357, were found. Several carbapenem resistance-related characteristics were also explored in 70 CRPA isolates. Firstly, carbapenemase was phenotypically positive in 22.9 % of CRPA, genetically predominant by metallo-β-lactamase (MBL) and co-carrige of different carbapenemase genes. Then, mutations of the carbapenem-specific porins oprD and opdP were commonly observed, with frequencies of 97.1% and 100.0%, respectively. Furthermore, the biofilm formation and relative transcription levels of 8 multidrug efflux pump genes were also found to be increased in 48.6 % and 72.9 % of CRPA isolates compared to the reference strain PAO1. These findings will help fill the data gaps in molecular characteristics of CRPA on the southeastern coast of China and emphasize the urgent need for data-based specific stewardship for antipseudomonal practices to prevent the dissemination of CRPA.

KEYWORDS

***Pseudomonas aeruginosa*, multilocus sequence typing, carbapenemase, porins mutation, biofilm, multidrug efflux pump genes**

Introduction

Pseudomonas aeruginosa (PA) is widely distributed and is considered as one of the most common opportunistic pathogens responsible for hospital-acquired infections (HAIs) (Qin et al., 2022). In recent years, the emerging and worldwide spread of multidrug-resistant (MDR)/extensively drug-resistant (XDR) 'high-risk clones', especially carbapenem-resistant *P. aeruginosa* (CRPA), have further worsened patient outcomes for nosocomial infections of this pathogen (Karruli et al., 2023).

CRPA has been ranked by the World Health Organization (WHO) as a pathogen of highest priority in the "critical" category, urgently requiring novel antibiotics in clinical settings [World Health Organization (WHO) (2017)]. The global increase in CRPA incidence is particularly concerning due to the lack of effective treatment alternative. Various mechanisms, alone or combined, including mutation leading to an impermeable outer membrane (Atrissi et al., 2021), production of carbapenemase (Tenover et al., 2022), overexpression of efflux systems (Kao et al., 2016), and formation of biofilm (Ma et al., 2023), have been reported to be commonly found in CRPA. Among them, the carbapenemase-mediated mechanism is an increasing contributor of significant concern worldwide (Wang et al., 2021; Tenover et al., 2022). Firstly, the emergence of carbapenemase greatly weakens the efficacy of both commonly used antipseudomonal agents and newly introduced β-lactam/β-lactamase inhibitor combinations (Canton et al., 2022; Tenover et al., 2022). Furthermore, the carbapenem-resistant determinants in these organisms are usually carried by mobile genetic elements and frequently harbor additional resistance determinants (Yoon and Jeong, 2021). Thus, they not only greatly limit the choice of anti-infective strategies but also enhance the dissemination risk of resistant clones.

However, the carbapenemase enzymogram present in *P. aeruginosa* varies widely by region, including the Ambler Class A β-lactamases, metallo-β-lactamases (MBL), and the Class D enzymes (Hammoudi Halat and Ayoub Moubareck, 2022). Rapid confirmation and differentiation among the various classes of carbapenemases are crucial for initiating early and effective therapy. Local surveillance and prompt profiling of the predominant carbapenemase phenotype and genotype will facilitate data-driven precise therapeutic decisions and thus positive outcomes. In this paper, we analyze the clinical prevalence, molecular epidemiology and carbapenem resistance-ralated characteristics of clinical *P. aeruginosa*, particularly CRPA isolates, collected over three consecutive years in a representative hospital in Xiamen, Fujian, in southeast China. This study aims to enhance our understanding of their prevalence and thus facilitate developing effective control strategies.

Materials and methods

Bacterial isolates

A total of 167 non-duplicate (one strain maximum per patient) clinical isolates of *P. aeruginosa* were collected at the First Affiliated Hospital of Xiamen University from April 2019 to June 2021. Strains were isolated from various clinical specimens and identified using MALDI-TOF MS (Bruker Daltonics, Germany). *P. aeruginosa* PAO1 (Grace et al., 2022) was used as a reference strain in porin mutation analysis, quantification of biofilm production and relative transcription of efflux pump genes.

Antimicrobial susceptibility test of all collected isolates

The minimum inhibitory concentrations (MICs) of 167 clinical PA isolates against 13 antibacterial drugs from 7 different categories were determined using the broth microdilution method following the guidelines of the Clinical and Laboratory Standards Institute (CLSI), with *P. aeruginosa* ATCC 27853 as the quality control strain [Clinical and Laboratory Standards Institute (CLSI), 2022]. The antimicrobials tested included aminoglycosides (amikacin/AMK, gentamicin/GEN, and tobramycin/TOB), cephalosporins (ceftazidime/CAZ and cefepime/FEP), carbapenems (imipenem/IMP and meropenem/MEM), quinolones (ciprofloxacin/CIP and levofloxacin/LVX), β-lactams/β-lactamase inhibitors (piperacillin/tazobactam/TZP and ticarcillin/clavulanic acid/TCC), monobactam (aztreonam/ATM), and penicillin (piperacillin/PIP). MDR isolates were defined as those resistant to at least one agent in three or more antimicrobial categories (Magiorakos et al., 2012). The CRPA isolates were defined as strains resistant to either imipenem or meropenem, or both, with a MIC value of $\geq$8 μg/mL.

Multilocus sequence typing (MLST) of CRPA

MLST analysis of 70 CRPA isolates was performed as described in the PubMLST database of *P. aeruginosa* (Jolley et al., 2018) through polymerase chain reaction (PCR) amplification and sequencing of seven housekeeping genes (*acsA*, *aroE*, *guaA*, *mutL*, *nuoD*, *ppsA*, and *trpE*). Gene sequences were then submitted to query the PubMLST database (http://pubmlst.org/paeruginosa/) to determine the allelic numbers and sequence types (STs). The types that could not match any known types were submitted to obtain new STs. A minimum spanning tree (MST) was inferred using the goeBURST algorithm (http://www.phyloviz.net/) (Ribeiro-Gonçalves et al., 2016) based on the MLST allelic profiles. A clonal complex (CC) is defined as containing at least two STs sharing any six out of the seven alleles.

Carbapenem resistance mechanisms of CRPA

Phenotypic and genotypic carbapenemase testing of CRPA

Testing and interpreting of phenotypic carbapenemase in 70 CRPA isolates were performed by modified carbapenem inactivation method (mCIM) per CLSI standard [Clinical and Laboratory Standards Institute (CLSI), 2022]. Routine quality control was conducted with each mCIM run with carbapenemase-positive *Klebsiella pneumoniae* ATCC BAA-1705

TABLE 1 Primers used in this study.

Aims	Genes	Primers (5′-3′)	Amplicon (bp)	References
Carbapenemase genotyping by PCR	bla_{KPC}	KPC-F/R: TGTCACTGTATCGCCGTC/ TCAGTGCTCTACAGAAAACC	1111	Khan et al. (2017)
	bla_{GES}	GES-F/R: ATGCGCTTCATTCACGCAC/ CTATTTGTCCGTGCTCAGG	864	Poirel et al. (2000)
	bla_{IMP}	IMP-F/R: GGAATAGAGTGGCTTAAYTCTC/ GGTTTAAYAAAACAACCACC	232	Poirel et al. (2011)
	bla_{NDM}	NDM-F/R: TGGAATTGCCCAATATTATGC/ TCAGCGCAGCTTGTCGGCCATGCG	813	Nordmann et al. (2012)
	bla_{VIM}	VIM-F/R: GATGGTGTTTGGTCGCATA/ CGAATGCGCAGCACCAG	400	This study
	$bla_{OXA-23-like}$	OXA-23-F/R: GATCGGATTGGAGAACCAGA/ ATTTCTGACCGCATTTCCAT	501	Woodford et al. (2006)
	$bla_{OXA-24-like}$	OXA-24-F/R: GGTTAGTTGGCCCCCTTAAA/ AGTTGAGCGAAAAGGGGATT	249	Woodford et al. (2006)
	$bla_{OXA-48-like}$	OXA-48-F/R: GCGTGGTTAAGGATGAACAC/ CATCAAGTTCAACCCAACCG	438	Poirel et al. (2011)
	$bla_{OXA-58-like}$	OXA-58-F/R:AAGTATTGGGGCTTGTGCTG/ CCCCTCTGCGCTCTACATAC	599	Woodford et al. (2006)
Porin mutation analysis by PCR	*oprD*	OprD-F/R: CGCCGACAAGAAGAACTAGC/ CGGTACCTACGCCCTTCCTT	1496	Yin et al. (2018)
	opdP	OpdP-F/R: CCGGCGCAGGCGAAACCGGCGC/ CAGGTGTCGGAGCAACGGATGG	1604	This study
Quantitative real-time PCR (qRT-PCR) of multidrug efflux pump genes	*MexA*	MexA-RT-F/R: AGCCATGCGTGTACTGGTTC/ CTCGGTATTCAGGGTCACCG	145	This study
	MexB	MexB-RT-F/R: CTGTCGATCCTCAGTCTGCC/ TCGATCCCGTTCATCTGCTG	146	This study
	MexC	MexC-RT-F/R: TACCGGCGTCATGCAGGGTTC/ TTACTGTTGCGGCGCAGGTGACT	164	This study
	MexD	MexD-RT-F/R: AAGCGTGCTCGAGCTATACG/ CCCTCTTCCCATTTCACGCT	84	This study
	MexE	MexE-RT-F/R: CTGAGCTTCACCCGGATCAC/ CGTCGAAGTAGGCGTAGACC	139	This study
	MexF	MexF-RT-F/R: GCTTCGGCCGTACCTATCAG/ AGGTGTCGCTGACCTTGATG	141	This study
	MexX	MexX-RT-F/R: GAAGGCCAGGTGAAGGGTG/ CCAGGTCGGAGAACAGCAG	106	This study
	MexY	MexY-RT-F/R: TCGCCGTGATGTACCTGTTC/ ACGTTGATCGAGAAGCCCAG	121	This study
	RspL	rspL-140-F/R: CACAACCTGCAAGAGCACAG/ CCGTACTTCGAACGACCCTG	140	This study

and carbapenemase-negative *K. pneumoniae* ATCC BAA-1706. Additionally, meropenem disks incubated in tryptic soy broth (TSB) with no microbial inocula for 4 h at 37°C were also applied to the *Escherichia coli* ATCC 25922 lawn. Zones were evaluated after overnight incubation to ensure they fell within CLSI quality control ranges.

All mCIM positive isolates were then assessed for the presence of carbapenemase genes through PCR. Nine carbapenemase genes, including bla_{KPC}, bla_{GES}, bla_{IMP}, bla_{NDM}, bla_{VIM}, $bla_{OXA-23-like}$, $bla_{OXA-24-like}$, $bla_{OXA-48-like}$ and $bla_{OXA-58-like}$, were amplified using the primers presented in Table 1. The positive amplification products were sequenced and compared with those available in the GenBank database (www.ncbi.nil.gov/BLAST) to identify specific variant.

Analysis of oprD and opdP mutations in CRPA

The full-length *oprD* and *opdP* genes from each CRPA isolate were amplified and sequenced using the primers listed in Table 1. DNA sequences and protein transcripts were compared with the corresponding sequences from the reference strain PAO1 (accession number NC_002516) using MEGA11 to dentify mutations (Tamura et al., 2021).

qRT-PCR assay for transcriptional levels of multidrug efflux pump genes in CRPA

To evaluate the correlation of multidrug efflux system with carbapenem resistance, the relative transcriptional levels of 8 Mex transporter genes (Table 1) in all 70 CRPA isolates were determined against PAO1 using qRT-PCR. Total RNA of these strains was extracted and purified using the RNAsimple Total RNA Kit (Tiangen Biotech, Beijing, China) according to the manufacturer's instructions. The cDNA was synthesized using the Hifair® V one-step RT-gDNA digestion SuperMix for qPCR (Yeasen, Shanghai, China). qRT-PCR was performed on the QuantStudio 5 real-time PCR system (Applied Biosystems) with SYBR Green Master Mix (Yeasen, Shanghai, China). The housekeeping gene *rspL* was used for normalization of the expression levels of the target genes. Each test was performed in triplicates and the results were analyzed by the QuantStudio Design & Analysis Software 2.6.0.

Assay for biofilm formation of CRPA

The biofilm formed by 70 CRPA isolates was quantified using microtiter plate assay (Haney et al., 2021). Briefly, the isolates were grown overnight in LB at 37°C and then adjusted to an OD_{600} = 0.1. Twenty microliters of each culture were inoculated to 180 μL LB in 96-well plates, and incubated at 37°C in a static incubator for 24h. Eight replicates were tested for each isolates and negative control wells contained LB only. After measuring the OD_{600} to evaluate planktonic growth, the bacteria were discarded and each well was washed three times with 250 μL PBS, dried for 30 min at room temperature, and then stained with 250 μL of 0.1 % crystal violet for 40 min. After rinsing off excess stains by washing three times with PBS, the plate was dried for another 30 min. The biofilm was resuspended with 260 μL of 95 % ethanol and quantified at 590 nm using a SpectraMax_i3X microplate spectrophotometer (Molecular Devices, Austria).

Statistical analysis

Data were analyzed with the GraphPad Prism analysis package. The antimicrobial rates of PA in different groups was compared using Pearson's chi-square test. One-way ANOVA (Analysis of Variance) analysis with Holm-Sidak comparison test was used to determine statistical differences of biofilm formation and relative transcription level of efflux genes between groups. A Spearman correlation test was performed to analyze the association of carbapenem resistance (indicated with MIC values) with possible mechanisms (i.e., carbapenemase production, porin mutation, relative transcription of multidrug pump genes and biofilm yield). $P < 0.05$ was considered statistically significant.

Moreover, an overall flowchart of the research (Supplementary Figure S1) was presented.

TABLE 2 The prevalent characteristics of clinical *Pseudomonas aeruginosa* (PA) isolates.

Prevalent characteristics of clinical PA isolates	Means ± SD (range) or *n* (%)
Isolation sources	
ICU	38 (22.8 %)
Geriatric medicine department	23 (13.8 %)
Orthopedics	11 (6.6 %)
Hepatobiliary and pancreatic vascular surgery	10 (6.0 %)
Hematology	10 (6.0 %)
Others (21 different departments)	75 (44.9 %)
Specimen types	
Respiratory samples	43 (25.7 %)
Wound secretions	43 (25.7 %)
Puncture fluids[a]	30 (18.0 %)
Blood	23 (13.8 %)
Urine	11 (6.6 %)
Gastrointestinal tract samples	7 (4.2 %)
Others (6 different specimen types)	10 (6.0 %)
Demographics of patients	
Age, years	61 ± 22 (1–94)
Gender	
Female	45 (26.9 %)
Male	122 (73.1 %)

[a]The puncture fluids there included cerebral spinal fluid, bile, pleural effusion, ascites and synovial fluid.

10.3389/fmicb.2024.1431154

TABLE 3 Number of resistant isolates within clinical *P. aeruginosa* isolates.

Antibiotics	By year			*P*	By carbapenem resistance			Total ($n = 167$)
	2019 ($n = 52$)	2020 ($n = 59$)	2021 ($n = 56$)		CRPA[a] ($n = 70$)	CNPA[a] ($n = 97$)	*P*	
Penicillin								
Piperacillin (PIP)	6	18	11	0.0475	28	7	<0.0001	35
Cephalosporin								
Ceftazidime (CAZ)	2	10	9	0.0723	17	4	0.0002	21
Cefepime (FEP)	4	12	5	0.0805	16	5	0.0008	21
Monolactam								
Aztreonam (ATM)	14	22	9	0.0374	32	13	<0.0001	45
Carbapenem								
Imipenem (IMP)	19	32	13	0.0027	64	0	<0.0001	64
Meropenem (MEM)	15	29	13	0.0085	57	0	<0.0001	57
β-Lactam/ β-Lactamase inhibitor								
Ticarcillin/ clavulanic acid (TCC)	21	28	21	0.5372	47	23	<0.0001	70
Piperacillin/ tazobactam (TZP)	3	4	4	0.5969	8	3	0.0718	11
Aminoglycoside								
Amikacin (AMK)	0	3	2	0.2784	5	0	0.0119	5
Gentamicin (GEN)	3	10	4	0.0989	15	2	<0.0001	17
Tobramycin (TOB)	1	4	2	0.0910	5	2	0.1313	7
Quinolone								
Ciprofloxacin (CIP)	8	18	7	0.0336	21	12	0.0059	33
Levofloxacin (LVX)	20	28	11	0.0066	43	16	<0.0001	59
P	<0.0001	<0.0001	<0.0001	-	<0.0001	<0.0001	-	<0.0001

[a]CRPA (carbapenem-resistant *P. aeruginosa*) denoted isolates resistant to IMP or MEM or both; CNPA (carbapenem-nonresistant *P. aeruginosa*) denoted isolates other than CRPA.

Results

Clinical prevalence of all collected *P. aeruginosa* isolates

Isolation sources, specimen types, and demographics of patients

A total of 167 non-duplicate PA isolates were collected from samples across 26 different clinical departments (Table 2). They were most commonly isolated from the intensive care unit (ICU) followed by the geriatric medicine department. Varying numbers (n = 1–11) of PA strains were also isolated in departments such as orthopedics, hepatobiliary and pancreatic vascular surgery, hematology, and so on.

The respiratory samples and wound secretions represented as the most common specimen. Puncture fluids and blood were also frequently encountered, with more than 20 isolates collected each. The remaining 28 PA strains were isolated from various sources such as urine, gastrointestinal tract samples, etc., varying from 0.6 % to 6.6 %.

These strains were recovered from patients aged 1 to 94 years old. The median age of the patients was 82 years, with patients over 60 years old accounting for 59.9 % ($n = 100$). As for patient gender, male was overwhelmingly higher than female (Table 2).

Antimicrobial susceptibility of all collected PA isolates

Overall, 58.7 % ($n = 98$) of the 167 clinical PA isolates were resistant to at least one tested drug. The resistant ratio of PA to the 13 tested antibiotics differed significantly from each other ($P < 0.01$), regardless of within a specific year or totally (Table 3). Among them, the highest resistant rates were found for PA against the TCC, IMP, LVX and MEM, reaching 41.9 %, 38.3 %, 35.3 % and 34.1 %, respectively. Tested PA strains were most sensitive to AMK and TOB, with fewer than 10 out of 167 strains found to be resistant.

10.3389/fmicb.2024.1431154

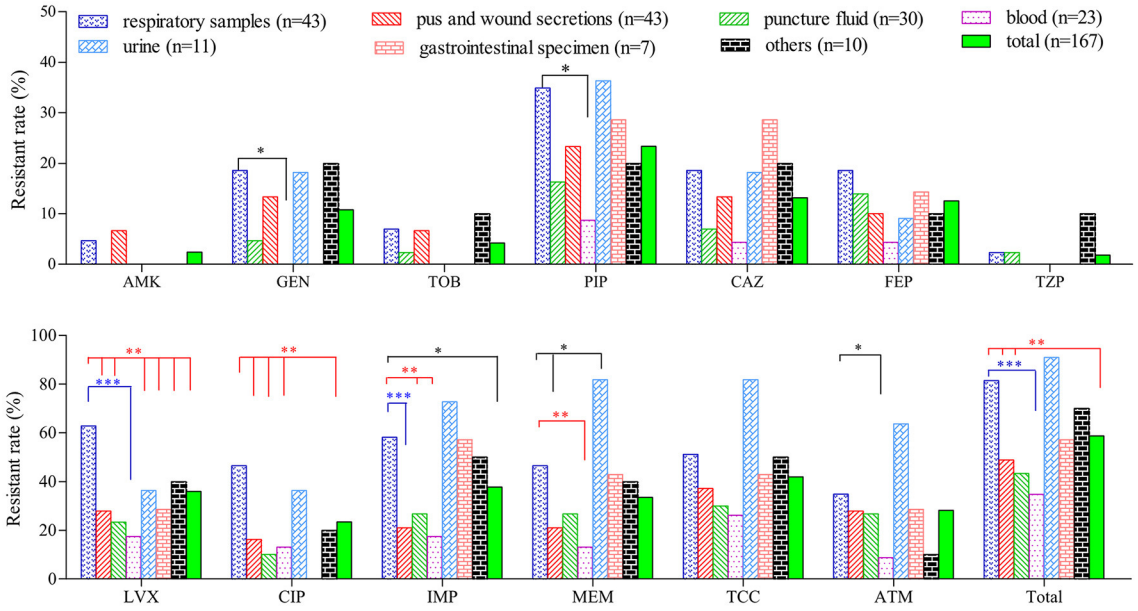

FIGURE 1
Comparison of resistant rates of *P. aeruginosa* isolated from different clinical specimens. $^{*}(P < 0.05)$, $^{**}(P < 0.01)$ and $^{***}(P < 0.001)$ denoted statistical difference of resistant rate between PA strains of respiratory sources and those from other sources determined by chi-square test.

For antibacterial drugs other than the 6 types mentioned above, the resistant rate of PA strains ranged from 6.6 % to 26.9 %. The resistant rates of PA to PIP, ATM, IMP, MEM, CIP, and LVX varied significantly from year to year, whereas the resistant rates to the other 7 antibiotics remained relatively stable. However, there was no overall trend of change over the years, but a relatively high drug resistant rate was found in 2020. More isolates and longer duration of collection are needed for further confirmation of such trend.

It was particularly noteworthy that PA had developed a high level of resistance against carbapenems, one of the last resorts for effective treating of MDR gram-negative bacteria. Totally, 70 isolates were found to be resistant to imipenem and/or meropenem, accounting for 41.9 % of the tested strains. Among them, 51 were resistant to both carbapenems while 13 and 6 exhibited resistance against only IMP or MEM. Furthermore, compared to carbapenem-nonresistant PA (CNPA), the resistant rates to antibiotics other than TZP and TOB were significantly higher ($P < 0.05$) in CRPA (Table 3).

The combined use of β-lactamase inhibitor tazobactam, with PIP significantly enhanced its inhibitory effect against PA, leading to a decrease in the overall resistant rate from 21.0 % to 6.6 %. In contrast, another tested complex TCC with clavulanic acid as an inhibitor has no such effect. Seventy out of 167 isolates were found to be resistant to TCC. The proportion of strains with a MIC value over 128 μg/mL to ticarcillin (β-Lactam in TCC complex) was 46.7 % ($n = 78$), which was not significantly higher than that of TCC-resistant PA (with MIC value ≥128/2 μg/mL).

Compared with isolates collected from other clinical specimens, PA isolates from the respiratory tract ($n = 43$) and urine ($n = 11$) exhibited a higher resistant rate to the majority of the tested antibiotics (Figure 1). The proportion of resistant strains in these two sample types exceeded 80.0 %, which is significantly higher than strains from wound secretions, puncture fluids and blood. On contrary, strains collected from blood are highly sensitive to most tested drugs. Twenty-three blood isolates were fully sensitive to AMK, GEN, TOB and TZP while their resistant rates to the remaining 9 drugs were all below 20.0 %, except for TCC (26.1 %).

Ninety-eight resistant strains were distributed among 44 different resistotypes (Supplementary Table S1). Among them, 13 isolates were resistant to antimicrobial in one category, with 9 being carbapenem-resistant. Within the 23 isolates resistant to two types of antibiotic, there were 7 different resistotypes. The most common combinations were co-resistance to carbapenem with TCC or quinolone, and quinolone with TCC. An overwhelming majority (62 out of 98) of the resistant isolates were MDR. They were dispersed diversely into 34 different resistotypes, with co-resistance to quinolone-carbapenem- β-Lactam/β-Lactamase inhibitor-monolactam being the most common ($n = 10$). One isolate recovered from ascites of an 85 year old male patient in geriatric medicine department was found to resist against all 7 tested antimicrobial categories.

Molecular epidemiology and phylogenetic relationship of CRPA isolates

High clonal diversity was revealed among 70 CRPA isolates, with 34 known sequence types (STs) identified among 56 isolates, while 12 new STs were found for 14 other isolates. ST553 was the most common ST with 6 strains identified. There are three strains in each of the five types: ST162, ST485, ST1437, ST2330, and ST3306. Out of the remaining 40 ST types, 9 types contain two strains, and 31 types only contain one isolate. The dominant

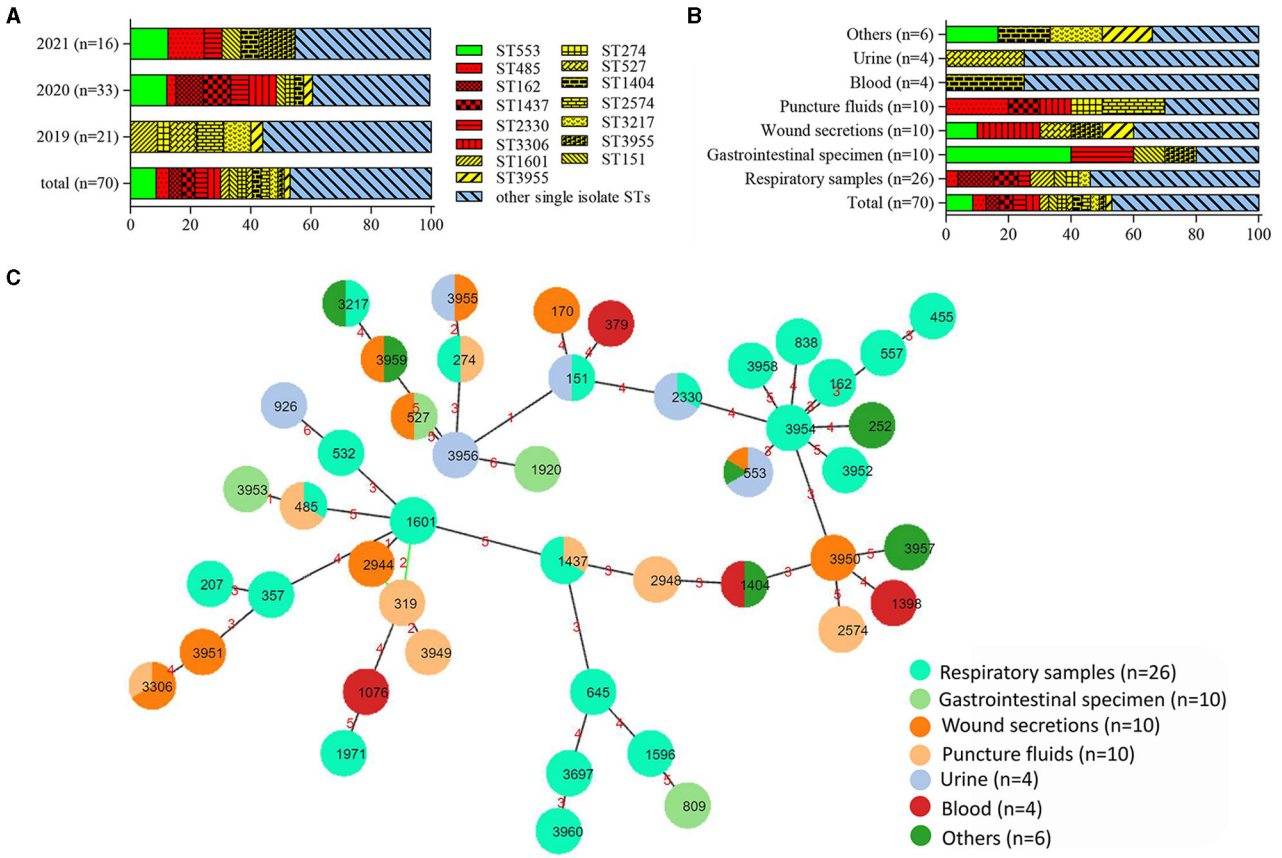

FIGURE 2
Distribution and relationship analysis of sequence types (STs) of 70 CRPA isolates. **(A)** Distribution of STs over different years. **(B)** Distribution of STs within various samples. Green, red, yellow and blue in **(A, B)** denoted STs with 6, 3, 2 and 1 isolates, respectively. **(C)** Minimum spanning tree created by PHYLOViZ Online (https://online.phyloviz.net/index). Each solid circle represented one ST and colors were assigned to nodes per sample sources. The circle size was related to the number of strains within this ST. The numbers on the lines connecting each node indicated the genetic distance between the two adjacent ST types.

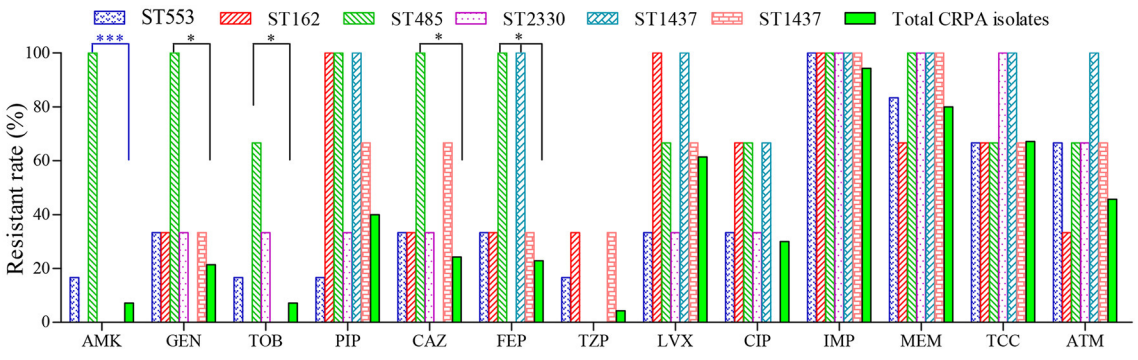

FIGURE 3
Antimicrobial susceptibility of CRPA strains belonging to the top six sequence types (STs). $^{*}(P < 0.05)$ and $^{***}(P < 0.001)$ indicated statistical differences determined by chi-square test.

ST types varied depending on the year of collection and sample types. Compared to the following 2 years, the isolates collected in 2019 were relatively diverse (Figure 2A). Among various sample sources, the PA isolates from respiratory samples exhibited the highest diversity in STs harboring more than 2 strains (Figure 2B). This result indicated that *P. aeruginosa* isolated from samples such as sputum and bronchoalveolar lavage fluid (BALF) were more diverse than those isolated from other samples. It was noteworthy that two previously reported high-risk STs, the regionally specific ST1971 (Zhao et al., 2023c) and the globally prevalent ST357 (Del Barrio-Tofiño et al., 2020), were found. They each only have one isolate collected from sputum and BALF, respectively.

The BURST analysis (https://pubmlst.org) revealed 4 CCs within the tested CRPA isolates. While the largest CC contained only 4 STs (ST1601, ST319, ST2944, and ST3949) with 5 strains, the remaining 3 CCs included only 2 STs. Out of a total of 46 ST types, thirty-six were found to be singletons. As showed in the MLST-based MST, four main groups were clustered, with most isolates from the respiratory specimen grouped in the center with a new ST (ST3954) (Figure 2C). Other CRPA isolates were relatively sporadically distributed and had distant genetic relationships.

Furthermore, no specific ST type was found to be associated with any particular resistance profile. Compared to other CRPA isolates, strains of ST485 were found to be more resistant against cephalosporins and aminoglycosides (Figure 3). However, it contained only 3 isolates in this study. Further investigation with more clinical isolates is needed to confirm this correlation.

Carbapenem resistance mechanisms of CRPA isolates

Carbapenemase production by CRPA isolates

Using the mCIM, a total of 16 carbapenemase-positive isolates were identified from 70 CRPA strains, accounting for 22.9 %. As presented in Table 4, the specimen types and genetic distribution of such isolates were highly diverse. No correlation of carbapenem production with specific specimen type or ST could be found.

Six out of the 16 strains exhibited strong enzyme activity comparable to that of the positive control strain *K. pneumoniae* ATCC BAA-1705. The meropenem disc treated with these CRPA strains showed little to no inhibitory effect against the carbapenem-susceptible indicator *E. coli* ATCC 25922 (Table 4). The enzyme activity of the remaining 10 strains was relatively weak, as indicated by an inhibitory diameter ranging from 11.3 to 14.7 mm. From the perspective of drug resistance spectrum, 13 out of 16 carbapenemase-producing CRPA (CP-CRPA) strains were resistant to both tested carbapenems, accounting for 81.3 %.

Through PCR screening, 16 CP-CRPA isolates were revealed to carry diverse carbapenemase genes (Table 4). MBL-encoding genes were the most widespread, with bla_{IMP} and bla_{VIM} detected in 12 (75.0 %) and 10 (62.5 %) isolates, respectively. However, bla_{NDM} is far less prevalent, being positive in only 3 out of 16 isolates. As for A-type carbapenemases, bla_{KPC} was detected in 6 isolates, while no bla_{GES} was amplified. D-type carbapenemases were the least common, with only 1 isolate carrying the $bla_{\mathrm{OXA-23}}$ gene. Overall, 9 different carbapenemase gene profiles were found. Except for 5 isolates harboring a single bla_{IMP} ($n = 4$) or bla_{VIM} ($n = 1$) gene, most strains (68.8 %) were found to simultaneously carry two or more different carbapenemase genes. It was noteworthy that 6 isolates co-harbored MBLs along with class A (KPC-2) and/or class D (OXA-23-like) carbapenemases. Sequence analysis revealed that each identified gene encoded a distinct carbapenemase variant, such as IMP-9, NDM-1, VIM-2, and KPC-2.

Spearman correlation test revealed no significant ($P > 0.05$) association of carbapenemase activity (indicated by inhibitory zone diameter) with carbapenem resistance levels (indicated by MIC values of IMP or MEM) of CP-CRPA isolates. This may be due to the fact that different mechanisms interplayed with each, but not worked singularly, to determine the antibiotic phenotypes. For example, when $bla_{\mathrm{IMP-9}}$ was first described, it seemed that MEM was consistently more active than IMP against $bla_{\mathrm{IMP-9}}$-harboring strains (Xiong et al., 2006). However, the $bla_{\mathrm{IMP-9}}$-carring isolate No. 6 in this study was found to be more resistant to MEM rather than IMP (Table 4). Other resistance mechanisms such as efflux overexpression by nearly 5 folds or OprD and OpdP mutation might also work there.

Mutation of carbapenem-specific porins OprD and OpdP in CRPA isolates

Sixty-eight out of 70 CRPA isolates showed at least one change in oprD. Forty-three isolates (61.4 %) were found to harbor truncated OprD proteins varying in length from 5 amino acids (aa) to 435aa instead of the intact 443aa. Among them, a frameshift mutation caused by the deletion or insertion of 1∼26 bp nucleotides were most commonly found (n = 26). Premature stop codons created by point mutations were detected in 13 other isolates, with G831A leading to a truncated 276aa protein being most common (n = 7). Furthermore, the other 4 isolates simultaneously contained both forms of the mutation. For the remaining 27 isolates, 24 contained amino acid substitutions, 2 remained intact, and 1 was tested negative by PCR amplification, possibly due to a more severe mutation or complete deletion. Amino acid substitutions of T103S and F170L, located in loop 2 (L2) and loop 3 (L3) of the OprD topology, were most frequently found (8 out of 24). L2 and L3 in the OprD protein have been revealed to contain entrance and/or binding sites for imipenem (Ochs et al., 2000). Therefore, any mutations within these two regions could cause conformational changes and thus carbapenem resistance.

In contrast to OprD, the inactivated premature mutation in OpdP was less frequently encountered. Only 7 out of 70 CRPA strains contained premature OpdP due to the insertion or deletion of 1-2 nucleotides, resulting in truncated OprP with only 6aa or 336aa rather than 484aa. All other CRPA-sourced OpdP proteins were found to contain 15-21aa substitutions or a completely different sequence after amino acid 307. Among them, 11 kinds of amino acid mutations (N4Y, S9G, L17M, A19S, S20A, N31T, A34T, E42Q, A50E, T60S, and V63F) located within the first 63 amino acids were identified in the OpdP of all 63 isolates.

TABLE 4 Characteristics of 16 carbapenemase-positive CRPA isolates.

No.	Sources	ST	MIC (μg/mL)		Inhibitory zone diameter (mm)[a]	Carbapenemase genes	Relative transcription of Mex pumps	Biofilm	Mutation of porins[b]	
			IMP	MEM					OprD	OpdP
1	BALF	1601	16.0	4.0	7.3 ± 1.2	bla_{IMP-9}, bla_{NDM-1}, bla_{VIM-2}	5.3 ± 0.5	1.5 ± 0.2	Td(93)	S(15)
2	Blood	1076	16.0	8.0	6.3 ± 0.6	bla_{IMP-9}, bla_{VIM-2}	1.1 ± 0.2	2.6 ± 0.4	Tp(276)	S(15)
3	Live tissue sections	553	128.0	64.0	6.7 ± 1.2	bla_{KPC-2}, bla_{IMP-9}, bla_{VIM-2}	4.9 ± 0.5	1.7 ± 0.2	S(28)	S(16)
4	Wound	3951	64.0	64.0	6.0 ± 0.0	bla_{NDM-1}, bla_{VIM-2}	0.7 ± 0.08	3.9 ± 0.1	S(9)	S(15)
5	Sputum	485	32.0	16.0	6.0 ± 0.0	bla_{IMP-9}, bla_{VIM-2}	3.5 ± 0.5	1.4 ± 0.1	Tp(276)	S(16)
6	Purulent ear discharge	3957	2.0	16.0	6.0 ± 0.0	bla_{IMP-9}	4.9 ± 0.07	0.73 ± 0.1	N	Ti(336)
7	Gastric juice	1920	16.0	16.0	14.7 ± 1.2	bla_{IMP-9}	0.9 ± 0.05	0.22 ± 0.02	Td(134)	S(16)
8	Hydrothorax	3949	16.0	16.0	12.3 ± 1.5	bla_{VIM-2}	2.9 ± 0.2	3.8 ± 0.3	Td(68)	Td(6)
9	Blood	1398	64.0	32.0	11.3 ± 0.6	bla_{IMP-9}, bla_{VIM-2}	26.1 ± 0.9	1.3 ± 0.1	S(4)	S(16)
10	Wound	1404	64.0	32.0	11.7 ± 1.2	bla_{IMP-9}	4.1 ± 0.6	3.6 ± 0.4	Td(258)	Ti(336)
11	Sputum	1596	16.0	4.0	12.0 ± 1.0	bla_{IMP-9}	4.2 ± 0.4	1.4 ± 0.1	Tp(276)	Ti(336)
12	Wound	3306	32.0	32.0	14.7 ± 0.6	bla_{KPC-2}, bla_{IMP-9}	6.1 ± 0.9	2.7 ± 0.2	Ti(95)	S(16)
13	Wound	3306	64.0	16.0	14.7 ± 0.6	bla_{KPC-2}, bla_{NDM-1}, bla_{VIM-2}, bla_{OXA-23}	5.9 ± 0.6	2.2 ± 0.2	Ti(95)	S(16)
14	Ascites	3306	64.0	16.0	14.3 ± 1.2	bla_{KPC-2}, bla_{VIM-2}	2.2 ± 0.3	1.9 ± 0.2	Ti(95)	S(16)
15	Ascites	485	16.0	64.0	14.3 ± 0.6	bla_{KPC-2}, bla_{IMP-9}	0.8 ± 0.06	1.0 ± 0.1	Tp(276)	S(16)
16	Ascites	485	32.0	128.0	11.3 ± 1.2	bla_{KPC-2}, bla_{IMP-9}, bla_{VIM-2}	2.1 ± 0.3	1.9 ± 0.3	Tp(276)	S(16)

[a]Bactrial isolates with zone diameter of 6–15 mm or presence of pinpoint colonies within a 16–18 mm zone were defined as carbapenemase positive. [b]T (number)-Truncated (length of the mutated porins) because of nucleotide insertion (Ti) or deletion (Td)-caused frameshift or nucleotide mutation-caused premature stop codon (Tp); S(number)-Substitution (number of substituted amino acids); N-No amplification.

10.3389/fmicb.2024.1431154

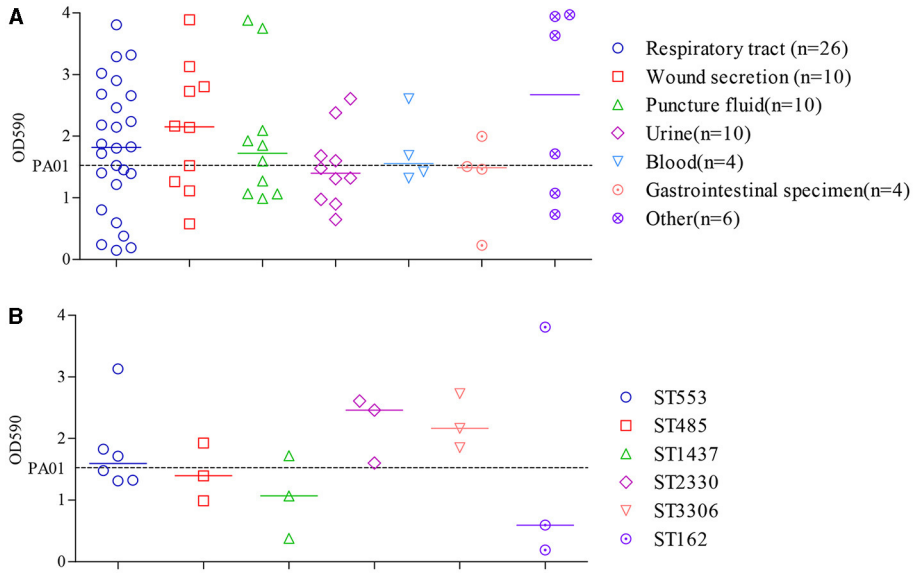

FIGURE 4
Comparison of biofilm formation by clinical CRPA isolates collected from various anatomical sites **(A)** or belonging to different MLST types **(B)**. Data points represented the average biofilm biomass of individual isolates as determined by the microtiter plate assay. Line bar represented the median biofilm biomass for each group. Only ST types with more than three individual strains were used for the comparison. One-way ANOVA analysis with the Holm-Sidak comparison test was used to determine statistical differences between groups. A dashed line represents the biofilm biomass formed by PAO1.

Biofilm formation by CRPA isolates

By conducting a one-way ANOVA, it was found that the biofilm developed by individual isolates significantly differed from each other ($P < 0.0001$). Among the 70 clinical CRPA strains assessed, 34 (48.6 %) and 14 (20.0 %) were found to exhibit significantly higher or statistically equivalent biofilm-forming capabilities compared to PAO1 (Figure 4A).

The median biofilm biomass (indicated by OD_{590}) of *P. aeruginosa* strains from seven specimen types varied from 1.4 to 2.7. Except for isolates from urine and gastrointestinal specimens, which showed lower biofilm formation compared to PAO1, those from the other five sources exhibited a higher median level of biofilm formation. However, there were no statistically significant differences in biofilm formation ability among strains from different sources ($P > 0.05$).

ST types with more than three isolates were further assessed to determine the relationship between biofilm formation and specific ST. As shown in Figure 4B, clinical isolates from ST2330 and ST3306 exhibited a slightly higher, yet statistically insignificant, capacity for biofilm formation compared to the other four STs, as indicated by the median OD590 levels after crystal violet staining of the biofilms. Moreover, correlation analysis showed that the different ST types also did not have a significant impact on bacterial biofilm formation ability ($P > 0.05$).

Relative efflux pump gene transcript levels of CRPA isolates

Compared to PAO1, 72.9 % of CRPA isolates (51 out of 70) had higher general *Mex* (*MexA*~*MexY*) transcription levels, with median relative transcription level ranging from 1.1 to 149.2. For the other 19 isolates with lower *Mex* levels, the relative transcription level was 0.1~1.0 of that from PAO1. Therefore, most of the clinical CRPA isolates exhibited higher transcript levels of efflux pump genes compared to the control strain. One-way ANOVA analysis revealed that the total transcription level of the 8 tested *Mex* genes varied significantly among different isolates. However, no significant correlation ($P < 0.05$) was found between their overall transcriptional level and the sources of isolation.

Among strains from various isolation sources, significant differences in relative transcription levels of specific *Mex* gene were observed only among the respiratory, urine, and blood samples of the *MexA* gene compared to the "others" group. In contrast, the transcription levels of the other seven genes were not significantly associated with the sample sources (Figure 5). Among them, only the median relative transcriptional levels of the *MexA* gene of PA isolates in all specimen types exceeded that of PAO1, while those of the *MexD* gene are lower than PAO1 in all types of samples except for those from urine. Regarding the overall transcriptional levels of each gene in 70 CRPA strains, apart from *MexD*, the transcriptional levels of all other genes were increased to varying degrees (1.1 to 2.9-fold) compared to PAO1.

Relationship of carbapenem resistance levels with the resistance-related mechanisms tested

No significant ($P > 0.05$) associations was found between carbapenem resistance levels (MIC values of CRPA against IMP or MEM) with any singular factor tested (i.e. carbapenemase activity

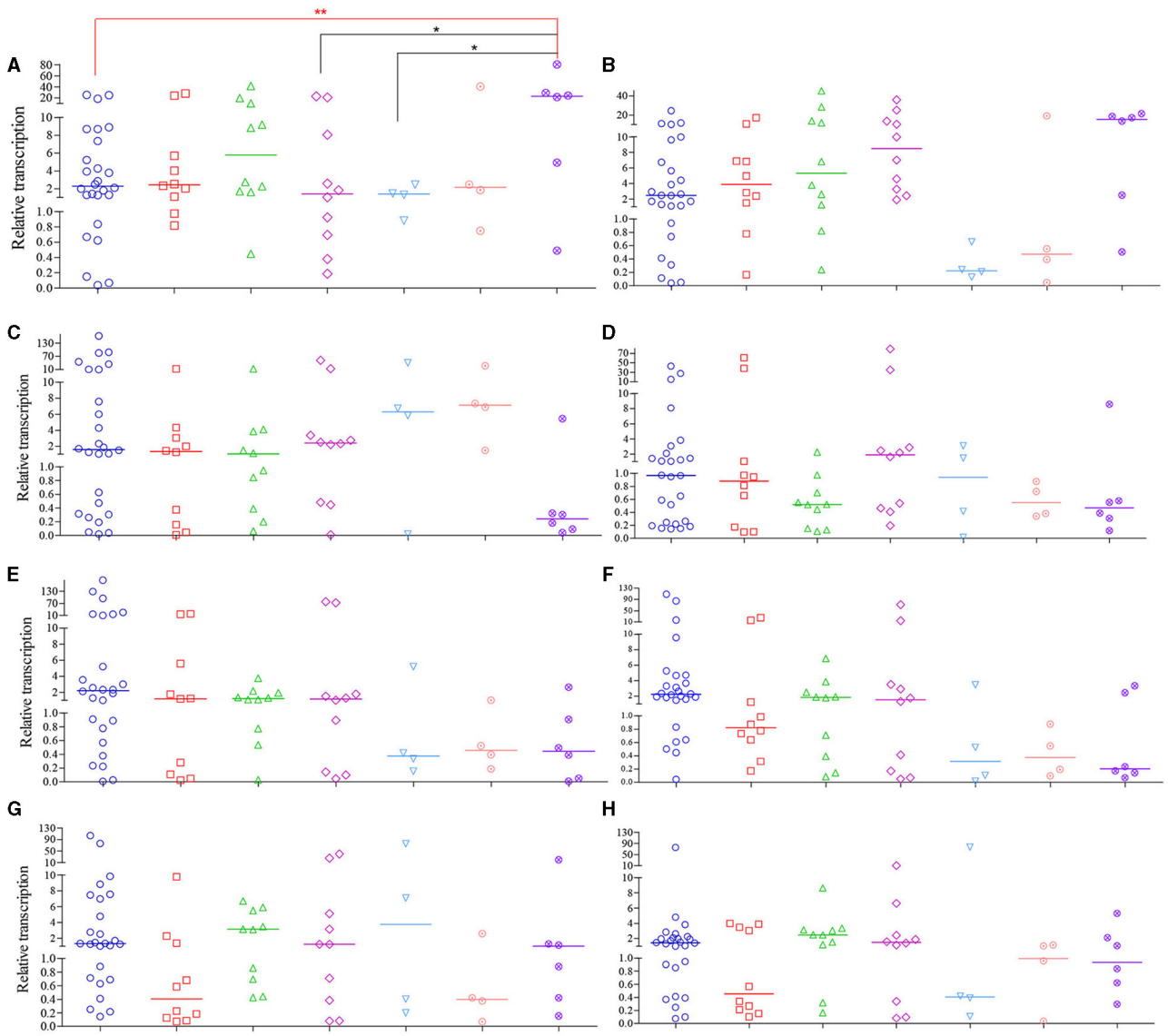

FIGURE 5
Relative transcription levels of *MexA*~*MexY* of CRPA isolates compared to PAO1. **(A–H)** *MexA*, *MexB*, *MexC*, *MexD*, *MexE*, *MexF*, *MexX* and *MexY*, respectively. The figure legends were the same as those of **(A)**. Data points represented the average transcription level of each gene from individual isolate compared to PAO1. Line bar represented the median transcription level for each group. One-way ANOVA analysis with Holm-Sidak comparison test was used to determine statistical differences between groups. $^{*}(P < 0.05)$ and $^{**}(P < 0.01)$ inidcated significant differences between the two groups as determined by chi-square test.

or genotype, OprD or OpdP mutations, relative transcription of *mex* genes and biofilm production).

Discussion

P. aeruginosa is one of the most common opportunistic pathogens in nosocomial infections, posing a significant threat to immunocompromised and ICU patients, with very high morbidity and mortality rates (Botelho et al., 2019; Behzadi et al., 2022a). In this study, we analyzed the clinical prevalence, epidemiology and carbapenem resistance mechanisms of 167 *P. aeruginosa* isolates collected from a tertiary hospital in southeast China between 2019 and 2021. It was found that respiratory and wound secretion samples were the primary specimen of isolation, while elderly male patients in the ICU and geriatric health units were the most common hosts. Nearly 60 % of the strains showed resistance to at least one antibiotic commonly used for treating *P. aeruginosa*, with 44 different resistotypes. The carbapenem-resistant isolates accounted for an alarmingly high rate of 41.9 % and were dispersed among 46 sequence types. A high proportion of porin mutation, together with elevated multidrug efflux pump gene transcription and biofilm production were found in CRPA isolates, while 22.9 % ($n = 16$) of them were carbapenemase-positive.

In this study, respiratory specimens were the most common sample where clinical PA isolates, especially CRPA, were recovered.

Similar results were obtained not only from global cohort studies (Gill et al., 2022; Reyes et al., 2023), but also from specific national or regional research (Del Barrio-Tofiño et al., 2019; Folic et al., 2021; Zhao et al., 2023b; Bai et al., 2024). These facts showed that the respiratory system was the most common site of *P. aeruginosa* infection, making it a serious threat for hospital-acquired pneumonia. In terms of the demographics of the patients, elderly males in ICU or geriatric health units were found to be significantly more prevalent than other populations. The same epidemiological characteristics were also identified in other studies from Japan (Kainuma et al., 2018), the USA (Dunphy et al., 2021), China (Fan et al., 2016; Bai et al., 2024), and multi-center, multinational data (Gill et al., 2021; Reyes et al., 2023). The high incidence rate of male patients may be associated with the underlying lung diseases caused by their higher smoking rates compared to women.

The clinical PA isolates we collected exhibited a high resistant rate to various anti-pseudomonal drugs. The top 5 drugs with the highest resistant rates were TCC, IMP, LVX, MEM and ATM. The trend was consistent with the latest data reported by the China National Monitoring Network (CHINET) (available at http://www.chinets.com/Data/AntibioticDrugFast). The relatively higher resistant ratio of *P. aeruginosa* from respiratory specimen found in this work had also been documented in a nationwide study in Spain (Del Barrio-Tofiño et al., 2019) and a multidimensional surveillance in the USA (Dunphy et al., 2021). Through the collection of the 10 most commonly prescribed antimicrobials prior to PA isolation from each source, a strong association was found between specific antimicrobial resistance and the history of prescribing antipseudomonal medications in the latter study.

The CRPA ratio identified in this study was comparable to previous findings from a burn center in southwestern China (Yin et al., 2018) and a general hospital in Zhejiang (Hu et al., 2021), but twice of that from a hospital in southeastern Shanxi (Bai et al., 2024). However, the counterpart was reported to be alarmingly high (over 90 %) for 212 PA strains collected from Guangdong (Zhao et al., 2023a). Differences in carbapenem resistance were also notable within European Union (EU) member states, ranging from 2.4 % to 59.3 % in different countries (European Centre for Disease Prevention Control, 2023). Such differences may be attributed to variations in antimicrobial treatment strategies and methods for evaluating *in vitro* drug sensitivity among hospitals in different regions. Nationally, a resistant rate of 23.0 % (Zeng et al., 2023) was reported in China, equivalent to that reported in EU (European Centre for Disease Prevention Control, 2023) and United States (Tenover et al., 2022). Furthermore, we also found the CRPA isolates had a significantly higher resistant rate against various other antibiotics compared to the CNPA in this study. This may be due to the fact that carbapenem-resistant gram-negative bacteria usually carry resistance determinants to other drugs, thus limiting treatment options for their infections (Jean et al., 2022).

MLST is a crucial epidemiological typing method based on the sequences of seven different housekeeping genes. It has been widely utilized in studies on the evolution and population diversity of *P. aeruginosa* isolates (Castañeda-Montes et al., 2018). The high genetic heterogeneity of CRPA strains found in this research had also been reported in multiple regional (Hu et al., 2021; Zhao et al., 2023a,b; Bai et al., 2024) and national (Fan et al., 2016) studies in China. In addition, a similar phenomenon was found in an international collaborative study that involved strains from multiple countries (Reyes et al., 2023; Zhao et al., 2023c). The high genetic diversity and varied resistance patterns revealed among *P. aeruginosa* isolates collected in this study indicate that the clonal dissemination of this bacterium is low in this region. Contrastly, a nationwide survey in Spain reported a convergent relationship within1445 clinical PA isolates, with over 50 % of the strains being attributed to the top two most prevalent types (Del Barrio-Tofiño et al., 2019). Moreover, among the 46 STs revealed for 70 CRPA isolates in this study, two previously reported high-risk clones (HiRiCs), the global prevalent ST357 (Del Barrio-Tofiño et al., 2020) and China-specific ST1971 (Zhao et al., 2023b), were found. ST357 is an exoU+ T3SS genotype that appears to be particularly common in Asia, but has also been reported in Europe and South America (Kainuma et al., 2018). The multidrug-resistant and highly virulent clone ST1971 has only been identified in China and defined as a regional epidemic risk type for nosocomial healthcare (Zhao et al., 2023c). This is the first report of ST1971 in Fujian, which is geographically close to previously reported collection locations Guangxi and Guangdong.

Carbapenem-resistant *P. aeruginosa* poses a serious threat to public health due to the limited alternatives for antimicrobial therapy and high mortality rates (Mancuso et al., 2023). Carbapenemase production is thought to be a relatively uncommon but increasingly significant cause of carbapenem resistance in *P. aeruginosa* (Wang et al., 2021; Tenover et al., 2022). It had been revealed that the prevalence and carbapenemase enzymogram carried by CRPA varied widely across geographical regions. In our study, 22.9 % CRPA isolates were found to produce carbapenemase, genetically dominated by MBL. The proportion is higher than those reported from other researches in China. The carbapenemase gene-positive ratio in CRPA strains collected in Guangdong is 12.7 % (54/416), with $bla_{\mathrm{IMP-45}}$ and $bla_{\mathrm{CARB-3}}$ being the most prevalent (Zhao et al., 2023b). Only two out of the 57 CRPA collected in Shanxi, China carried the acquired carbapenemase genes, being $bla_{\mathrm{IMP-1}}$- or $bla_{\mathrm{IMP-10-}}$ and $bla_{\mathrm{OXA-10}}$-positive, respectively (Bai et al., 2024). A national surveillance in China found 9.8 % of 182 IMP-insusceptible PA isolates carried KPC or IMP carbapenemases (Zhu et al., 2023). This was comparable to the data reported by Fan et al. (2016), in which 19 out of 254 (8.2 %) CRPA isolates collected nationally carried acquired carbapenemase genes. Similarly to our finding, IMP-9 was found to be most prevalent in this study, followed by VIM-2, IMP-1, IPM-10 and KPC-2. However, a high ratio of 32% (54 out of 171) were identified as CP-CRPA genetically for PA isolates collected from Zhejiang, Beijing, Shanghai, and Sichuan of China in a global cohort study (Reyes et al., 2023). KPC-2 (74.1 %) and VIM-2 (11.1 %) were most commonly found there. Globally, carbapenemase genes were detected in 22 % of 972 CRPA isolates, with 19% having a single carbapenemase gene and 3 % having two (Reyes et al., 2023). The prevalence of carbapenemase-positive CRPA (CP-CRPA) was lowest in the USA (2 %) and varied from 30 % to 69 % in other regions. According to another study on the global collection of

CRPA with no Chinese isolates included, 33 % of the strains tested were positive for carbapenemase production, with rates varying by region from 11 % to 68 % (Gill et al., 2021). Among them, 86 % were genetically positive, with the most common being VIM followed by GES.

In contrast to the predominance of single enzymology reported in other studies (Gill et al., 2021, 2022; Reyes et al., 2023), we found that the majority (11 out of 16, 68.8 %) of CP-CRPA strains collected in this study co-harbored two or more carbapenemase genes. The coexistence of multiple enzymes further restricted treatment options. It has been proven that KPC-producing organisms are resistant to the anti-pseudomonal drug ceftolozane-tazobactam, while VIM carbapenemases cannot be inhibited by avibactam and relebactam, making them resistant to both ceftazidime-avibactam and imipenem-relebactam (Bail et al., 2022). On the other hand, the detection of carbapenemases, especially MBLs (Behzadi et al., 2020), will indicate the need to consider cefiderocol (Timsit et al., 2022; Gill et al., 2024) or combination therapy including aztreonam (Losito et al., 2022). Thus, the increased resistance of CP-CRPA contributed to the higher mortality reported among patients infected with these organisms compared to non-carbapenemase-producing CRPA (Reyes et al., 2023).

Except for carbapenemase, some other mechanisms have also been found to be critically responsible for carbapenem resistance in CRPA. In China, the inactivation of the oprD gene was commonly found in CRPA. Zhao et al. (2023b) showed oprD in an overwhelming proportion of 96.2 % of CRPA isolates were mutated. However, no correlation was explore between specific mutation forms with IMP or MEM resistant level. Overexpression of MexAB-oprM caused by mutations in regulatory genes *MexR* and *nalD* might also drive the development of CRPA. Similar results were also reported in a study covering 196 PA isolates collected in a burn center in southeast China (Yin et al., 2018). Mutational inactivation of oprD (88.65 %), accompanied by overexpression of AmpC (68.09 %), were both popular in CRPA. AmpC has been well characterized to related to resistance against penicillin, cephalosporins, β-lactamase inhibitors in *P. aeruginosa* (Berrazeg et al., 2015; Slater et al., 2020). The high proportion of elevated *AmpC* transcription revealed there may due to high resistant rate against AmpC-targeted drugs in CRPA isolates. Extended spectrum cephalosporinase-related carbapenem resistance was previously described in PA (Rodríguez-Martínez et al., 2009), but it is commonly considered as a rare carbapenem-resistance mechanism which was not explored in the present study. Furthermore, we also found a high mutation frequency of porins, being 97.1 % and 100 % for oprD and opdP, respectively. The outer membrane porins OprD and OpdP serve as important entry ports for carbapenems (Ude et al., 2021). The oprD mutations were also commonly found in a global collection of CRPA isolates. Reyes et al. (2023) found that 69 % of 972 CRPA isolates collected from 44 hospitals in 10 countries were identified to harbor oprD mutations. A high ratio of oprD mutations was also found in XDR PA isolates collected nationwide in Spain (Del Barrio-Tofiño et al., 2019). Regretfully, similar to Zhao et al. (2023b), we also cannot found a significant correlation of IMP or MEM MIC values with porin mutations. Moreover, the connection of antimicrobial resistance with biofilm production in CRPA isolates was also explored in this study, but again with negative results produced. Similar results were obtained by Gajdács et al. (2021) and Behzadi et al. (2022b) with clinical and environmental PA isolates, respectively. However, using MIC_{90} or MIC_{50} as indicator, Cho et al. (2018) revealed significantly higher resistance in aminoglycoside (AMK, GEN and TOB) and cephalosporins (CAZ and FEP), but not carbapenems (IMP and MEM) and quinolone (LVX) in biofilmproducer (n = 76) compared to non-producer (n = 6) within CRPA isolates. Likewise, a significantly elevated biofilm formation for XDR clinical PA group compared to nonXDR ones was reported by Kaiser et al. (2017). The difference may attribute to lacking of universal and robust association of these two factors among different PA isolates.

In conclusion, a high carbapenem resistance rate was found among clinical PA isolates collected from a specific hospital in southeast China. CRPA isolates there were most commonly recovered from respiratory specimens and were characterized with high genetic diversity. The emergence of high-risk clones (ST 357 and ST 1971) and prevalence of co-carriage of more than one carbapenemase genes in CRPA indicated an urgent need for specific antimicrobial therapy stewardship in this region. To the best of our knowledge, this is the first molecular epidemiological study on the clinical isolates of PA in this region. These findings highlighted the importance of regular monitoring and accurate establishing clinical diagnosis-based antibiotic prescriptions to improve the effectiveness of anti-infection measures and prevent the spread of CRPA. Unfortunately, though carbapenemase production, elevated biofilm production and multidrug efflux pump gene transcription, together with high proportion of carbapenem-related porin mutations were commonly found in CRPA isolates in this work, we failed to explore their significant association with the carbapenem resistance levels. This may be due to the following reasons: the carbapenem resistance of PA isolates was developed through mixed and complicated mechanisms and differed by strains. Multiple mechanisms interplayed with each other to finally produce the antimicrobial phenotype. So it may be hard to find a significant and robust association of the carbapenem MIC with singular and limited resistance-related mechanisms tested in this work. Furthermore, CRPA isolates is different from each other not only in varied carbapenem resistance levels, but also resistance to other antibiotics and maybe virulence levels and other phenotypes connecting to the tested mechanisms. Thereafter, we will seek coupled clinical isolates with similar genetic background but different carbapenem resistance and apply them for exploring the possible mechanisms underlying the carbapenem resistance development. More resistance-related mechanisms through next generation whole genomic sequencing, transcriptome and proteomics should be included for full exploration.

Data availability statement

The original contributions presented in the study are included in the article/Supplementary material, further inquiries can be directed to the corresponding authors.

Author contributions

XX: Conceptualization, Data curation, Funding acquisition, Investigation, Methodology, Project administration, Supervision, Writing – original draft, Writing – review & editing. ZL: Data curation, Investigation, Software, Supervision, Writing – original draft. JH: Investigation, Validation, Writing – original draft. XW: Investigation, Methodology, Writing – original draft. YT: Investigation, Validation, Writing – original draft. PX: Investigation, Validation, Writing – original draft. GZ: Investigation, Resources, Writing – review & editing.

Funding

The author(s) declare financial support was received for the research, authorship, and/or publication of this article. This work was supported by the grants from the Natural Science Foundation of Fujian Province (2021J01347, 2022J011406), Medical and Health Guidance Project of Xiamen Science and Technology Bureau (3502Z202142D1329), and Xiamen Medical College Science and Technology Plan Project (K2022-02).

Conflict of interest

The authors declare that the research was conducted in the absence of any commercial or financial relationships that could be construed as a potential conflict of interest.

Publisher's note

All claims expressed in this article are solely those of the authors and do not necessarily represent those of their affiliated organizations, or those of the publisher, the editors and the reviewers. Any product that may be evaluated in this article, or claim that may be made by its manufacturer, is not guaranteed or endorsed by the publisher.

Supplementary material

The Supplementary Material for this article can be found online at: https://www.frontiersin.org/articles/10.3389/fmicb.2024.1431154/full#supplementary-material

References

Atrissi, J., Milan, A., Bressan, R., Lucafò, M., Petix, V., Busetti, M., et al. (2021). Interplay of OpdP porin and chromosomal carbapenemases in the determination of carbapenem resistance/susceptibility in *Pseudomonas aeruginosa*. *Microbiol. Spect.* 9:e0118621. doi: 10.1128/Spectrum.01186-21

Bai, Y., Gong, Y. E., Shen, F., Li, H., Cheng, Y., Guo, J., et al. (2024). Molecular epidemiological characteristics of carbapenem-resistant *Pseudomonas aeruginosa* clinical isolates in southeast Shanxi, China. *J. Global Antimicrob. Resist.* 36, 301–306. doi: 10.1016/j.jgar.2023.12.029

Bail, L., Sanches Ito, C. A., Stangler Arend, L. N. V., da Silva Nogueira, K., and Tuon, F. F. (2022). Activity of imipenem-relebactam and ceftolozanetazobactam against carbapenem-resistant *Pseudomonas aeruginosa* and KPC-producing *Enterobacterales*. *Diagn. Microbiol. Infect. Dis.* 102:115568. doi: 10.1016/j.diagmicrobio.2021.115568

Behzadi, P., Ambrosi, C., Scribano, D., Zanetti, S., Sarshar, M., Gajdács, M., et al. (2022a). Editorial: Current perspectives on *Pseudomonas aeruginosa*: epidemiology, virulence and contemporary strategies to combat multidrug-resistant (MDR) pathogens. *Front Microbiol.*, 13:975616. doi: 10.3389/fmicb.2022.975616

Behzadi, P., Gajdács, M., Pallós, P., Ónodi, B., Stájer A, Matusovits, D., Kárpáti, K., et al. (2022b). Relationship between biofilm-formation, phenotypic virulence factors and antibiotic resistance in environmental *Pseudomonas aeruginosa*. *Pathogens* 11:1015. doi: 10.3390/pathogens11091015

Behzadi, P., García-Perdomo, H. A., Karpiński, T. M., and Issakhanian, L. (2020). Metallo-ß-lactamases: a review. *Mol. Biol. Rep.* 47, 6281–6294. doi: 10.1007/s11033-020-05651-9

Berrazeg, M., Jeannot, K., Ntsogo Enguén,é V. Y., Broutin, I., Loeffert, S., Fournier, D., et al. (2015). Mutations in β-lactamase ampc increase resistance of *Pseudomonas aeruginosa* isolates to antipseudomonal cephalosporins. *Antimicrob. Agents Chemother.* 59, 6248–6255. doi: 10.1128/AAC.00825-15

Botelho, J., Grosso, F., and Peixe, L. (2019). Antibiotic resistance in *Pseudomonas aeruginosa*-mechanisms, epidemiology and evolution. *Drug Resist. Updat.* 44:100640. doi: 10.1016/j.drup.2019.07.002

Canton, R., Doi, Y., and Simner, P. J. (2022). Treatment of carbapenem-resistant *Pseudomonas aeruginosa* infections: a case for cefiderocol. *Expert Rev. Anti Infect. Ther.* 20, 1077–1094. doi: 10.1080/14787210.2022.2071701

Castañeda-Montes, F. J., Avitia, M., Sepúlveda-Robles, O., Cruz-Sánchez, V., Kameyama, L., Guarneros, G., et al. (2018). Population structure of *Pseudomonas aeruginosa* through a MLST approach and antibiotic resistance profiling of a Mexican clinical collection. *Infect. Genet. Evol.* 65, 43–54. doi: 10.1016/j.meegid.2018.06.009

Cho, H. H., Kwon, K. C., Kim, S., Park, Y., and Koo, S. H. (2018). Association between biofilm formation and antimicrobial resistance in carbapenem-resistant *Pseudomonas aeruginosa*. *Ann. Clin. Lab. Sci.* 48, 363−368.

Clinical and Laboratory Standards Institute (CLSI) (2022). *Performance Standards for Antimicrobial Susceptibility Testing; 32nd ed.* Wayne, PA: Clinical and Laboratory Standards Institute.

Del Barrio-Tofiño, E., López-Causapé C., and Oliver, A. (2020). *Pseudomonas aeruginosa* epidemic high-risk clones and their association with horizontally-acquired β-lactamases: 2020 update. *Int. J. Antimicrob. Agents* 56:106196. doi: 10.1016/j.ijantimicag.2020.106196

Del Barrio-Tofiño, E., Zamorano, L., Cortes-Lara, S., López-Causapé C., Sánchez-Diener, I., Cabot, G., et al. (2019). Spanish nationwide survey on *Pseudomonas aeruginosa* antimicrobial resistance mechanisms and epidemiology. *J. Antimicrob. Chemother.* 74, 1825–1835.

Dunphy, L. J., Kolling, G. L., Jenior, M. L., Carroll, J., Attai, A. E., Farnoud, F., et al. (2021). Multidimensional clinical surveillance of *Pseudomonas aeruginosa* reveals complex relationships between isolate source, morphology, and antimicrobial resistance. *mSphere* 6:e0039321. doi: 10.1128/mSphere.00393-21

European Centre for Disease Prevention and Control (2023). *Antimicrobial Resistance in the EU/EEA (EARS-Net) - Annual Epidemiological Report 2022.* Stockholm: ECDC.

Fan, X., Wu, Y., Xiao, M., Xu, Z. P., Kudinha, T., Bazaj, A., et al. (2016). Diverse genetic background of multidrug-resistant *Pseudomonas aeruginosa* from mainland China, and emergence of an extensively drug-resistant ST292 clone in Kunming. *Sci. Rep.* 6:26522. doi: 10.1038/srep26522

Folic, M. M., Djordjevic, Z., Folic, N., Radojevic, M. Z., and Jankovic, S. M. (2021). Epidemiology and risk factors for healthcare-associated infections caused by *Pseudomonas aeruginosa*. *J. Chemother.* 33, 294–301. doi: 10.1080/1120009X.2020.1823679

Gajdács, M., Baráth, Z., Kárpáti, K., Szabó, D., Usai, D., Zanetti, S., Donadu, M. G. (2021). No correlation between biofilm formation, virulence factors, and antibiotic resistance in *Pseudomonas aeruginosa*: results from a laboratory-based *in vitro* study. *Antibiotics*. 10:E1134. doi: 10.3390/antibiotics10091134

Gill, C. M., Aktaþ E., Alfouzan, W., Bourassa, L., Brink, A., Burnham, C. D., et al. (2021). The ERACE-PA global surveillance program: ceftolozane/tazobactam and ceftazidime/avibactam *in vitro* activity against a global collection of carbapenem-resistant *Pseudomonas aeruginosa*. *Eur. J. Clin. Microbiol.* 40, 2533–2541. doi: 10.1007/s10096-021-04308-0

Gill, C. M., Nicolau, D. P., and RACE-PA Global Study Group (2022). Carbapenem-resistant *Pseudomonas aeruginosa*: an assessment of frequency of isolation from ICU versus non-ICU, phenotypic and genotypic profiles in a multinational population of hospitalized patients. *Antimicrob. Resist. Infect. Control* 11:146. doi: 10.1186/s13756-022-01187-8

Gill, C. M., Santini, D., Nicolau, D. P., and RACE-PA Global Study Group (2024). *In vitro* activity of cefiderocol against a global collection of carbapenem-resistant *Pseudomonas aeruginosa* with a high level of carbapenemase diversity. *J. Antimicrob. Chemother.* 79, 412–416. doi: 10.1093/jac/dkad396

Grace, A., Sahu, R., Owen, D. R., and Dennis, V. A. (2022). *Pseudomonas aeruginosa* reference strains PAO1 and PA14: a genomic, phenotypic, and therapeutic review. *Front. Microbiol.* 13:1023523. doi: 10.3389/fmicb.2022.1023523

Hammoudi Halat, D., and Ayoub Moubareck, C. (2022). The intriguing carbapenemases of *Pseudomonas aeruginosa*: current status, genetic profile, and global epidemiology. *Yale J. Biol. Med.* 95, 507–515.

Haney, E. F., Trimble, M. J., and Hancock, R. E. W. (2021). Microtiter plate assays to assess antibiofilm activity against bacteria. *Nat. Protoc.* 16, 2615–2632. doi: 10.1038/s41596-021-00515-3

Hu, Y., Peng, W., Wu, Y., Li, H., Wang, Q., Yi, H., et al. (2021). A potential high-risk clone of *Pseudomonas aeruginosa* ST463. *Front. Microbiol.* 12:670202. doi: 10.3389/fmicb.2021.670202

Jean, S. S., Harnod, D., and Hsueh, P. R. (2022). Global threat of carbapenem-resistant gram-negative bacteria. *Front. Cell. Infect. Microbiol.* 12:823684. doi: 10.3389/fcimb.2022.823684

Jolley, K. A., Bray, J. E., and Maiden, M. C. J. (2018). Open-access bacterial population genomics: BIGSdb software, the PubMLST.org website and their applications. *Wellcome Open Res.* 3:124. doi: 10.12688/wellcomeopenres.14826.1

Kainuma, A., Momiyama, K., Kimura, T., Akiyama, K., Inoue, K., Naito, Y., et al. (2018). An outbreak of fluoroquinolone-resistant *Pseudomonas aeruginosa* ST357 harboring the exoU gene. *J. Infect. Chemother.* 24, 615–622. doi: 10.1016/j.jiac.2018.03.008

Kaiser, S. J., Mutters, N. T., DeRosa, A., Ewers, C., Frank, U., and Günther, F. (2017). Determinants for persistence of *Pseudomonas aeruginosa* in hospitals: interplay between resistance, virulence and biofilm formation. *Eur. J. Clin. Microbiol. Infect. Dis.* 36, 243–253. doi: 10.1007/s10096-016-2792-8

Kao, C. Y., Chen, S. S., Hung, K. H., Wu, H. M., Hsueh, P. R., Yan, J. J., et al. (2016). Overproduction of active efflux pump and variations of OprD dominate in imipenem resistant *Pseudomonas aeruginosa* isolated from patients with bloodstream infections in Taiwan. *BMC Microbiol.* 16:107. doi: 10.1186/s12866-016-0719-2

Karruli, A., Catalini, C., D'Amore, C., Foglia, F., Mari, F., Harxhi, A., et al. (2023). Evidence-based treatment of *Pseudomonas aeruginosa* infections: a critical reappraisal. *Antibiotics* 12:399. doi: 10.3390/antibiotics12020399

Khan, A. U., Maryam, L., and Zarrilli, R. (2017). Structure, genetics and worldwide spread of New Delhi Metallo-β-lactamase (NDM): a threat to public health. *BMC Microbiol.* 17:101. doi: 10.1186/s12866-017-1012-8

Losito, A. R., Raffaelli, F., Del Giacomo, P., and Tumbarello, M. (2022). New drugs for the treatment of *Pseudomonas aeruginosa* infections with limited treatment options: a narrative review. *Antibiotics* 11:579. doi: 10.3390/antibiotics11050579

Ma, Y., Aung, T. T., Lakshminarayanan, R., and Chua, S. L. (2023). Biofilm formation and virulence potential of carbapenem-resistant *Pseudomonas aeruginosa*. *Lancet Microbe* 4:e489. doi: 10.1016/S2666-5247(23)00097-6

Magiorakos, A. P., Srinivasan, A., Carey, R. B., Carmeli, Y., Falagas, M. E., Giske, C. G., et al. (2012). Multidrug-resistant, extensively drug-resistant and pandrug-resistant bacteria: an international expert proposal for interim standard definitions for acquired resistance. *Clini. Microbiol. Infect.* 18, 268–281. doi: 10.1111/j.1469-0691.2011.03570.x

Mancuso, G., De Gaetano, S., Midiri, A., Zummo, S., and Biondo, C. (2023). The challenge of overcoming antibiotic resistance in carbapenem-resistant gram-negative bacteria: "attack on titan". *Microorganisms* 11:1912. doi: 10.3390/microorganisms11081912

Nordmann, P., Boulanger, A. E., and Poirel, L. (2012). NDM-,4 metallo-β-lactamase with increased carbapenemase activity from *Escherichia coli*. *Antimicrob. Agents Chemother.* 56, 2184–2186. doi: 10.1128/AAC.05961-11

Ochs, M. M., Bains, M., and Hancock, R. E. (2000). Role of putative loops 2 and 3 in imipenem passage through the specific porin OprD of *Pseudomonas aeruginosa*. *Antimicrob. Agents Chemother.* 44, 1983–1985. doi: 10.1128/AAC.44.7.1983-1985.2000

Poirel, L., Le Thomas, I., Naas, T., Karim, A., and Nordmann, P. (2000). Biochemical sequence analyses of GES-1, a novel class A extended-spectrum beta-lactamase, and the class 1 integron In52 from *Klebsiella pneumoniae*. *Antimicrob. Agents Chemother.* 44, 622–632. doi: 10.1128/AAC.44.3.622-632.2000

Poirel, L., Walsh, T. R., Cuvillier, V., and Nordmann, P. (2011). Multiplex PCR for detection of acquired carbapenemase genes. *Diagn. Microbiol. Infect Dis.* 70, 119–123. doi: 10.1016/j.diagmicrobio.2010.12.002

Qin, S., Xiao, W., Zhou, C., Pu, Q., Deng, X., Lan, L., et al. (2022). *Pseudomonas aeruginosa*: pathogenesis, virulence factors, antibiotic resistance, interaction with host, technology advances and emerging therapeutics. *Signal Transduc. Targ. Ther.* 7:199. doi: 10.1038/s41392-022-01056-1

Reyes, J., Komarow, L., Chen, L., Ge, L., Hanson, B. M., Cober, E., et al. (2023). Global epidemiology and clinical outcomes of carbapenem-resistant *Pseudomonas aeruginosa* and associated carbapenemases (POP): a prospective cohort study. *Lancet Microbe* 4, e159–e170. doi: 10.1016/S2666-5247(22)00329-9

Ribeiro-Gonçalves, B., Francisco, A. P., Vaz, C., Ramirez, M., and Carriço, J. A. (2016). PHYLOViZ Online: web-based tool for visualization, phylogenetic inference, analysis and sharing of minimum spanning trees. *Nucleic Acids Res.* 44, W246–W251. doi: 10.1093/nar/gkw359

Rodríguez-Martínez, J. M., Poirel, L., and Nordmann, P. (2009). Extended-spectrum cephalosporinases in *Pseudomonas aeruginosa*. *Antimicrob. Agents Chemother.* 53, 1766–1771. doi: 10.1128/AAC.01410-08

Slater, C. L., Winogrodzki, J., Fraile-Ribot, P. A., Oliver, A., Khajehpour, M., and Mark, B. L. (2020). Adding insult to injury: mechanistic basis for how ampc mutations allow *Pseudomonas aeruginosa* to accelerate cephalosporin hydrolysis and evade avibactam. *Antimicrob. Agents Chemother.* 64, e00894–e00820. doi: 10.1128/AAC.00894-20

Tamura, K., Stecher, G., and Kumar, S. (2021). MEGA11: molecular evolutionary genetics analysis version 11. *Mol. Biol. Evol.* 38, 3022–3027. doi: 10.1093/molbev/msab120

Tenover, F. C., Nicolau, D. P., and Gill, C. M. (2022). Carbapenemase-producing *Pseudomonas aeruginosa* -an emerging challenge. *Emerg. Microbes Infect.*11, 811–814. doi: 10.1080/22221751.2022.2048972

Timsit, J.-F., Wicky, P.-H., and de Montmollin, E. (2022). Treatment of severe infections due to metallo-betalactamases *Enterobacterales* in critically ill patients. *Antibiotics* 11:144. doi: 10.3390/antibiotics11020144

Ude, J., Tripathi, V., Buyck, J. M., Söderholm, S., Cunrath, O., Fanous, J., et al. (2021). Outer membrane permeability: antimicrobials and diverse nutrients bypass porins in *Pseudomonas aeruginosa*. *Proc. Natl. Acad. Sci. USA.* 118:e2107644118. doi: 10.1073/pnas.2107644118

Wang, M. G., Liu, Z. Y., Liao, X. P., Sun, R. Y., Li, R. B., Liu, Y., et al. (2021). Retrospective data insight into the global distribution of carbapenemase-producing *Pseudomonas aeruginosa*. *Antibiotics* 10:548. doi: 10.3390/antibiotics10050548

Woodford, N., Ellington, M. J., Coelho, J. M., Turton, J. F., Ward, M. E., Brown, S., et al. (2006). Multiplex PCR for genes encoding prevalent OXA carbapenemases in *Acinetobacter* spp. *Int. J. Antimicrob. Agents.,* 27, 351–353. doi: 10.1016/j.ijantimicag.2006.01.004

World Health Organization (WHO) (2017). *Global Priority List of Antibiotic-Resistant Bacteria to Guide Research, Discovery, and Development of New Antibiotics*. Available at: https://www.who.int/news/item/27-02-2017-who-publishes-list-of-bacteria-for-which-new-antibiotics-are-urgently-needed (accessed April 20, 2024).

Xiong, J., Hynes, M. F., Ye, H., Chen, H., Yang, Y., M'zali, F., and Hawkey, P. M. (2006). bla(IMP-9) and its association with large plasmids carried by Pseudomonas aeruginosa isolates from the People's Republic of China. *Antimicrob. Agents Chemother.* 50, 355–358. doi: 10.1128/AAC.50.1.355-358.2006

Yin, S., Chen, P., You, B., Zhang, Y., Jiang, B., Huang, G., et al. (2018). Molecular typing and carbapenem resistance mechanisms of *Pseudomonas aeruginosa* isolated from a Chinese burn center from 2011 to 2016. *Front. Microbiol.* 9:1135. doi: 10.3389/fmicb.2018.01135

Yoon, E. J., and Jeong, S. H. (2021). Mobile carbapenemase genes in *Pseudomonas aeruginosa*. *Front. Microbiol.* 12:614058. doi: 10.3389/fmicb.2021.614058

Zeng, M., Xia, J., Zong, Z., Shi, Y., Ni, Y., Hu, F., et al. (2023). Guidelines for the diagnosis, treatment, prevention and control of infections caused by carbapenem-resistant gram-negative bacilli. *J. Microbiol. Immunol. Infect.* 56, 653–671. doi: 10.1016/j.jmii.2023.01.017

Zhao, Y., Chen, D., Chen, K., Xie, M., Guo, J., Chan, E. W. C., et al. (2023b). Epidemiological and genetic characteristics of clinical carbapenem-resistant *Pseudomonas aeruginosa* strains in Guangdong province, China. *Microbiol. Spect.* 11:e0426122. doi: 10.1128/spectrum.04261-22

Zhao, Y., Chen, D., Ji, B., Zhang, X., Anbo, M., and Jelsbak, L. (2023a). Whole-genome sequencing reveals high-risk clones of *Pseudomonas aeruginosa* in Guangdong, China. *Front. Microbiol.* 14:1117017. doi: 10.3389/fmicb.2023.1117017

Zhao, Y., Xie, L., Wang, C., Zhou, Q., and Jelsbak, L. (2023c). Comparative whole-genome analysis of China and global epidemic *Pseudomonas aeruginosa* high-risk clones. *J. Global Antimicrob. Resist.* 35, 149–158. doi: 10.1016/j.jgar.2023.08.020

Zhu, Y., Jia, P., Yu, W., Chu, X., Liu, X., and Yang, Q. (2023). The epidemiology and virulence of carbapenem-resistant *Pseudomonas aeruginosa* in China. *Lancet Microbe* 4:e665. doi: 10.1016/S2666-5247(23)00113-1

frontiers | Frontiers in Microbiology

TYPE Original Research
PUBLISHED 11 September 2024
DOI 10.3389/fmicb.2024.1455945

OPEN ACCESS

EDITED BY
Mingxi Wang,
Huaqiao University, China

REVIEWED BY
Marina Rosa Pulido,
University of Seville, Spain
Dexi Li,
Henan Agricultural University, China

*CORRESPONDENCE
Nadège Lépine
✉ nadege.lepine@etu.univ-tours.fr
Marie-Frédérique Lartigue
✉ lartigue@univ-tours.fr

RECEIVED 27 June 2024
ACCEPTED 19 August 2024
PUBLISHED 11 September 2024

CITATION
Lépine N, Bras-Cachinho J, Couratin E, Lemaire C, Chaufour L, Junchat A and Lartigue M-F (2024) Investigation of a linezolid-resistant *Staphylococcus epidermidis* outbreak in a French hospital: phenotypic, genotypic, and clinical characterization.
Front. Microbiol. 15:1455945.
doi: 10.3389/fmicb.2024.1455945

Investigation of a linezolid-resistant *Staphylococcus epidermidis* outbreak in a French hospital: phenotypic, genotypic, and clinical characterization

Nadège Lépine[1,2]*, José Bras-Cachinho[1], Eva Couratin[3], Coralie Lemaire[1,2], Laura Chaufour[1], Armelle Junchat[3] and Marie-Frédérique Lartigue[1,2]*

[1]Service de Bactériologie-Virologie-Hygiène, Centre Hospitalier Universitaire de Tours, Tours, France, [2]ISP, UMR1282, Université de Tours, INRAe, Tours, France, [3]Equipe Opérationnelle d'Hygiène, Centre Hospitalier Universitaire de Tours, Tours, France

Purpose: We aimed to retrospectively investigate an outbreak of linezolid-resistant *Staphylococcus epidermidis* (LRSE), at Tours University Hospital between 2017 and 2021.

Methods: Twenty of the 34 LRSE isolates were included in the study. Antimicrobial susceptibility testing was performed using the disk diffusion method and MICs of last-resort antibiotics were determined using broth microdilution or Etest®. Seventeen of the 20 resistant strains were sent to the French National Reference Centre for *Staphylococci* to determine the mechanism of resistance to linezolid. The clonal relationship between LRSE strains was assessed by PFGE and the sequence type determined by MLST. We retrospectively evaluated a new typing tool, IR-Biotyper®, and compared its results to PFGE to evaluate its relevance for *S. epidermidis* typing. Medical records were reviewed, and antibiotic consumption was determined. Search for a cross transmission was performed.

Results: All LRSE strains showed high levels of resistance to linezolid (MICs ≥ 256 mg/L) and were multi-drug resistant. Linezolid resistance was associated with the 23S rRNA G2576T mutation and none of the 17 strains analyzed carried the *cfr* gene. Ninety-five percent of the 20 LRSE studied strains were genetically related and belonged to sequence-type ST2. The dendrogram obtained from IR-Biotyper® showed 87% congruence with the PFGE analysis. Prior to isolation of the LRSE strain, 70% of patients received linezolid. No patients stayed successively in the same room.

Conclusion: Linezolid exposure may promote the survival and spread of LRSE strains. At Tours University Hospital, acquisition of the resistant clone may also have been triggered by hand-to-hand transmission by healthcare workers. In addition, IR-Biotyper® is a promising typing tool for the study of clonal outbreaks due to its low cost and short turnaround time, although further studies are needed to assess the optimal analytical parameters for routine use.

10.3389/fmicb.2024.1455945

KEYWORDS

Staphylococcus epidermidis, linezolid, multi-drug resistance, genotyping, sequence type ST2, IR-Biotyper®

1 Introduction

Coagulase-negative *Staphylococci* (CoNS), including *Staphylococcus epidermidis*, are opportunistic pathogens that are frequently implicated in human disease, particularly in the context of healthcare-associated infections such as catheter-associated bloodstream or prosthetic joint infections (PJI) in immunocompromised patients. Linezolid is one of the most widely used antibiotics against Gram-positive cocci. Linezolid resistance is mediated by different mechanisms, often co-expressed. Mutations in 23S rRNA at linezolid binding sites (the G2576U substitution being the most frequent) and mutations in ribosomal proteins L3 and L4 located on the surface of the 50S RNA subunit are the most prevalent. Acquisition of plasmid-mediated multidrug resistance genes, either *cfr* encoding an RNA-methyltransferase, or *optrA* or *poxtA* encoding ABC transporters, confers transferable resistance to oxazolidinones (Brenciani et al., 2022; Long and Vester, 2012). Global surveillance studies report that only 0.75% of CoNS are resistant to linezolid (Flamm et al., 2016). Nevertheless, the spread of LRSE is an emerging public health concern because methicillin and linezolid resistance are often combined, leaving very few therapeutic options.

Numerous previous studies have already reported hospital outbreaks of linezolid-resistant *S. epidermidis* (LRSE) from countries around the world (Bouiller et al., 2020; Dortet et al., 2018; Kelly et al., 2008; Liakopoulos et al., 2010). Coustillères et al. described highly linezolid-resistant *S. epidermidis* strains isolated from patients with PJI since the introduction of protocolized postoperative linezolid in six French referral centers, including Tours University Hospital. They noted that LRSE carriage appeared to be directly related to linezolid use (Coustillères et al., 2023).

An increase in the incidence of LRSE has however been reported despite a decrease in linezolid use in some institutions (Huber et al., 2021). Linezolid resistance has also been observed in patients with no history of linezolid administration (Huber et al., 2021; Kelly et al., 2008; Liakopoulos et al., 2010; Seral et al., 2011), suggesting that clonal cross-transmission may lead to the emergence of LRSE outbreaks in addition to the selection of resistant strains under linezolid antibiotic treatment (Mihaila et al., 2012).

In this study, we report an outbreak of LRSE mainly in the orthopedic surgery department and the surgical intensive care unit (ICU) of the Tours University Hospital between 2017 and 2021. The strains were phenotypically and genotypically characterized to demonstrate their clonal relationship. These results were linked with the patients' clinical characteristics in order to analyze potential risk factors for the acquisition of clonal LRSE strains. Furthermore, the ability of IR-Biotyper® (IRBT) as a *S. epidermidis* typing method was evaluated and these results were compared to those of pulsed-field gel electrophoresis (PFGE), given the lack of bibliographic data on *S. epidermidis* IRBT typing.

2 Materials and methods

2.1 Bacterial strains

Thirty-four LRSE strains were isolated from clinical diagnostic samples between 2017 and 2021 at the Tours University Hospital. However, only 20 isolates were included as the other 14 were not preserved due to the retrospective nature of the study. In addition, linezolid-susceptible *S. epidermidis* (LSSE) strains had been isolated from three patients before their LRSE infection. These three isolates were also included in the study.

In accordance with standard hospital laboratory methods, strains were previously identified to species level by matrix-assisted laser desorption/ionization time-of-flight mass spectrometry (MALDI-TOF MS, Bruker Daltonik, Bremen, Germany) using the Biotyper reference library. Linezolid resistance was detected by the disk diffusion method (30 µg) and/or E-test®. The isolates were then stored appropriately at −80°C. All subsequent analyses were carried out on fresh strains after 18 to 24 h of aerobic incubation on Columbia blood agar plates at 35 ± 2°C.

A random isolate of *S. epidermidis* was used as an unrelated PFGE control strain. It was susceptible to methicillin and linezolid.

2.2 Susceptibility testing

In vitro phenotypic antimicrobial susceptibility testing was performed using the disk diffusion method according to CASFM-EUCAST 2021 recommendations for penicillin G, kanamycin, tobramycin, gentamicin, ofloxacin, tetracycline, rifampicin, and trimethoprim-sulfamethoxazole. Methicillin-resistance was detected with cefoxitin disks (30 µg). The following MICs were determined using the E-test method: ceftaroline, ceftobiprole, linezolid, tedizolid, daptomycin, dalbavancin, tigecycline, and delafloxacin. Susceptibility to vancomycin and teicoplanin was determined by the broth microdilution method. The results were interpreted using the CASFM-EUCAST 2021 *Staphylococcus aureus* breakpoints.

Seventeen of the 20 LRSE strains were sent to the French National Reference Centre for *Staphylococci*: genetic determinants of resistance were evaluated by whole genome sequencing. The acquired *mecA* gene, the acquired *cfr, optrA* and *poxtA* resistance genes, as well as point mutations in 23S rRNA were investigated by *in silico* analysis (Côrtes et al., 2022).

2.3 Patient characteristics

Medical record review was used to retrospectively collect demographic and clinical data. Search for a cross transmission was

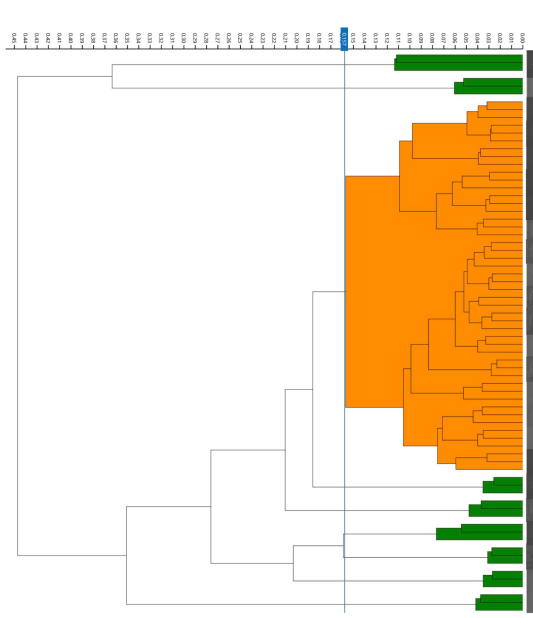

Patient	Linezolid susceptibility	PFGE pulsotype	IR-type	ST
Patient 1	R	A	f	2
Patient 14	S	C	c	87
Patient 18	R	A	a	2
Patient 19	R	A	a	2
Patient 4	R	A	a	2
Patient 5	R	A	a	2
Patient 13	R	A	a	2
Patient 12	R	A	a	2
Patient 10	R	A	a	2
Patient 7	R	A	a	2
Patient 16	R	A	a	2
Patient 8	R	A	a	2
Patient 15	R	A	a	2
Patient 9	R	A	a	2
Patient 14	R	A	a	2
Patient 3	R	A	a	2
Patient 17	R	A	a	2
Patient 2	R	A	a	2
Patient 1	R	A	g	2
Patient 6	R	A	h	2
Patient 11	R	B	b	57
PFGE Control	S	F	j	ND
Patient 3	S	D	d	470
Patient 17	S	E	e	21

FIGURE 1
Dendrogram of 24 *Staphylococcus epidermidis* isolates (including one unrelated control strain) based on IR-Biotyper® spectra. In the dendrogram, isolates that were clustered using the IR-Biotyper® are shown in orange, while those that were not clustered are shown in green. ND, No Data.

performed. Written information about the study was posted in each center and the non-opposition of each patient was sought before inclusion. Ethic approval was not required.

2.4 Linezolid usage data

Annual data on linezolid use were examined in the surgical ICU and orthopedic surgery from 2017 to 2021. Linezolid use was measured in Defined Daily Doses (DDDs) per 100 patient-days. Doses of 1,200 mg/day were considered as 1 DDD. These data were compared with the number of LRSE strains in these two units. The aim was to identify whether there was a trend in the use of linezolid and whether this might be linked to the emergence of linezolid resistance in *S. epidermidis* at Tours University Hospital.

2.5 PFGE and MLST typing

To search for clonality, strains were genotyped by pulsed-field gel electrophoresis (PFGE) of *Sma*I-digested total DNA for molecular typing, as previously described (Neoh et al., 2019), allowing bacterial isolates to be clustered into pulsotypes. We further characterized our strains using multilocus sequence typing (MLST) (Thomas et al., 2007) using primers listed in Supplementary Table S1. We assigned sequence types (STs) to each allelic profile using an MLST website.[1]

1 https://pubmlst.org/organisms/staphylococcus-epidermidis

2.6 FTIR spectroscopic analysis

Further phenotyping studies were performed using a new typing method, the IR-Biotyper® (IRBT) (Bruker Daltonik, Bremen, Germany), a Fourier transform infrared (FTIR) spectroscopy system that provides cost-effective results within 4 h (Hong et al., 2022).

Here, we retrospectively tested 22 of the 23 isolates from our study after they had been genotyped by PFGE. Each sample was analyzed in triplicate in a single experiment (Figure 1). Ethanol/water suspensions were prepared from blood agar cultures according to the manufacturer's recommendations. We applied each bacterial suspension in triplicate to the FTIR silicon plate along with the two quality control spots provided in the kit. Dendrograms were automatically generated after spectra acquisition. The IRBT software automatically calculates a cut-off value that defines the distance at which spectra are considered to belong to the same cluster.

3 Results

3.1 Patient characteristics

In this study, 20 patients were retrospectively included with at least one LRSE isolate. Fourteen were male and six were female patients, with a mean age of 65 ± 16 years. These patients were hospitalized in three clinical departments: orthopedic surgery (12 patients), surgical ICU (6 patients), and gastrointestinal and liver surgery (2 patients). The clinical characteristics of the patients are shown in Table 1. The majority had at least one comorbidity, including type 2 diabetes (30%), hypertension (45%), or obesity (35%).

Fourteen of 20 patients were exposed to linezolid in the 3 months prior to the onset of LRSE, with exposure ranging from five to 16 days

TABLE 1 Clinical characteristics of patients.

Patient	Ward of occurrence	Period of hospitalization (days)	Age	M/F	Initial BMI	Cause of admission	Date of culture	Culture site	No of LRSE positive samples	Prior LSSE isolation	Prior exposure to linezolid within 3 months Y/N (days)	Other antimicrobial treatment prior LRSE isolation	LRSE triggered antibiotic therapy (Y/N, molecule)	Infection, colonization, or contamination
1	Digestive and liver surgery	06/08/2017 to 16/10/2017 (71)	64	M	25.3	Liver transplant	19/08/2017	Peritoneal fluid	1/2	N	ND	ND	ND	ND
2	Digestive and liver surgery	11/07/2018 to 09/11/2018 (121)	61	F	23.7	Liver transplant	28/09/2018	Ascites	1/3	N	Y (14)	Ertapenem Ceftriaxone Ofloxacin PTZ Ceftazidime-avibactam	N	Colonization or contamination
3	Orthopedic surgery	04/11/2018 to 13/11/2018 (9)	61	M	26.5	Two-stage shoulder prosthesis exchange	05/11/2018	Right shoulder biopsy	3/5	Y: 1/5 MSSE (06/08/2018)	N	Levofloxacin Rifampicin	Y: doxycycline	Infection
4	Surgical ICU	06/01/2019 to 24/04/2019 (108)	50	M	25	Acute pancreatitis	30/01/2019	Peritoneal fluid	3/3 (Enriched broth culture only)	N	N	Ceftriaxone Metronidazole Amikacin Ciprofloxacin Ceftazidime PTZ Meropenem Vancomycin Cefepime	Y: vancomycin	Infection
5	Surgical ICU	28/02/2019 to 19/03/2019 (19)	74	M	31.5	Liver abscess, peritonitis, septic shock	28/02/2019 04/03/2019 10/03/2019	BAL Hepatectomy Blood	1 (10^6LRSE) 2/5 1/4 bottle	N	Y (5)	PTZ Vancomycin Ceftriaxone Metronidazole Cefepime Ciprofloxacin	Y: vancomycin	Colonization
6	Orthopedic surgery	24/06/2019 to 05/07/2019 (11)	73	M	34.8	Two-stage hip prosthesis exchange	27/06/2019	Left hip biopsy	1/5	N	Y (11)	Levofloxacin	N	Colonization or contamination
7	Orthopedic surgery	08/08/2019 to 29/08/2019 (21)	90	F	27	Knee prosthesis infection	19/08/2019	Right knee biopsy	5/5	N	Y (10)	Amoxicillin PTZ Levofloxacin Rifampicin	Y: doxycycline	Infection
8	Orthopedic surgery	17/03/2020 to 31/03/2020 (14)	62	M	29.4	Intercostal chondrosarcoma	24/03/2020	Coastal biopsy	5/5	N	N	N	Y: dalbavancin	Infection
9	Orthopedic surgery	27/02/2020 to 07/04/2020 (40)	59	F	23.4	Hip prosthesis infection early recurrence	15/04/2020	Right hip biopsy	1/5	N	Y (7)	PTZ TMP-SMX	Y: doxycycline	Colonization or contamination
10	Orthopedic surgery	10/05/2020 to 28/05/2020 (18)	45	M	20.6	3 months post-sacrotomy urinary sepsis	25/05/2020	Perineal abscess drainage	1/2 (Enriched broth culture only)	N	Y (2 + 7)	AMC PTZ Gentamicin Meropenem Cefotaxime Ciprofloxacin	N	Colonization or contamination
11	Surgical ICU	01/06/2020 to 04/07/2020 (33)	50	F	62.7	Mediastinitis and septic shock	11/06/2020	Mediastinal and pre-sternal drainage	4/4	N	N	AMC Ceftriaxone Metronidazole Gentamicin	Y: vancomycin	Infection

(Continued)

10.3389/fmicb.2024.1455945

TABLE 1 (Continued)

Patient	Ward of occurrence	Period of hospitalization (days)	Age	M/F	Initial BMI	Cause of admission	Date of culture	Culture site	No of LRSE positive samples	Prior LSSE isolation	Prior exposure to linezolid within 3 months Y/N (days)	Other antimicrobial treatment prior LRSE isolation	LRSE triggered antibiotic therapy (Y/N, molecule)	Infection, colonization, or contamination
12	Orthopedic surgery	28/07/2020 to 02/09/2020 (36)	64	M	23.3	Ankle fracture	15/08/2020	Synovial fluid	1/3	N	Y (11)	AMC Gentamicin PTZ Levofloxacin Moxifloxacin	N	Colonization or contamination
13	Surgical ICU	19/09/2020 to 13/11/2020 (55)	73	M	35	Liver transplant	23/09/2020	Blood	1/6 bottle	N	Y (5)	PTZ Tobramycin Cloxacillin Vancomycin Gentamycin	Y: vancomycin	Contamination
14	Orthopedic surgery	16/09/2020 to 24/09/2020 (8)	70	M	32.7	Acute sepsis, one-stage knee prosthesis exchange	17/09/2020	Biopsy	4/5	Y: 1/5 MRSE (15/12/2019)	Y (4)	TMP-SMX Ciprofloxacin PTZ	Y: dalbavancin then doxycycline	Infection
15	Orthopedic surgery	02/10/2020 to 03/11/2020 (32)	73	F	26	Two-stage hip prosthesis exchange	16/10/2020	Right hip biopsy	5/5	N	Y (5)	PTZ Ciprofloxacin	Y: vancomycin then dalbavancin	Infection
16	Orthopedic surgery	16/12/2020 to 02/02/2021 (48)	19	M	34.6	Femoral fracture	22/01/2021	Hip biopsy	1/3	N	Y (5)	PTZ Cefepime Moxifloxacin Meropenem Levofloxacin	Y: teicoplanin then doxycycline	Colonization or contamination
17	Orthopedic surgery	08/12/2020 to 19/02/21 (73)	82	F	33.8	One-stage knee prosthesis exchange	28/01/2021	Right hip biopsy	3/5	Y: 4/5 MRSE (21/12/2020)	Y (14) Tedizolid (4)	PTZ	Y: Daptomycin and doxycycline	Infection
18	Surgical ICU	01/02/2021 to 12/02/2021 (12)	68	M	34.4	Cardiogenic refractory shock	05/02/2021	Blood	1/4 bottle	N	Y (9)	AMC Daptomycin PTZ	Y: vancomycin	Contamination
19	Orthopedic surgery	09/07/2021 to 13/08/2021 (35)	88	M	28	Hip prosthesis removal	04/08/2021	Left hip biopsy	3/4	N	Y (6 + 10)	PTZ Cefepime Rifampicin ciprofloxacin	N (palliative care)	Infection
20	Surgical ICU	08/10/2021 to 18/11/2021 (41)	68	M	27.9	Liver transplant	16/10/2021	Peritoneal fluid	1/4	N	N	PTZ Meropenem Vancomycin	Y: vancomycin	Infection or colonization

AMC, amoxicillin-clavulanic acid; PTZ, piperacillin-tazobactam; TMP-SMX, trimethoprim-sulfamethoxazole; MSSE, Methicillin-susceptible *S. epidermidis*; MRSE, Methicillin-resistant *S. epidermidis*; ND, No Data.

10.3389/fmicb.2024.1455945

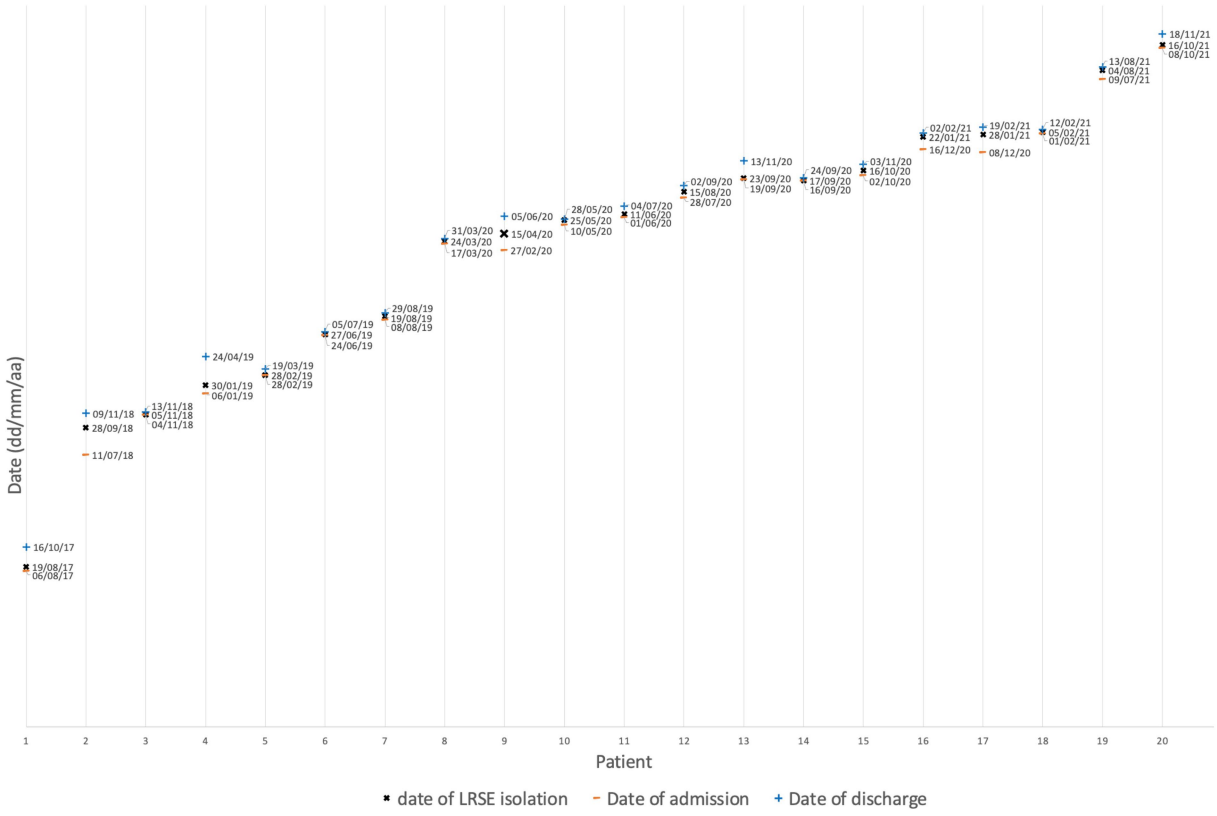

FIGURE 2
Dates of patient hospitalization and isolation of LRSE strains.

(Table 1). The patients' hospitalization date and LRSE isolation date are shown in Figure 2. No patients were found to have shared a double room or stayed successively in the same room within a department.

3.2 Linezolid usage data

We reviewed linezolid consumption in surgical ICU and orthopedic surgery (Figure 3). In relation to hospital-wide linezolid use at our institution, the surgical ICU and orthopedic surgery accounted for 1.5 and 16.7% of the total number of linezolid dosage units dispensed in 2017, 2.8 and 15.6% in 2018, 0.63 and 30.7% in 2019, 1.2 and 30.0% in 2020, and 1.7 and 28.7% in 2021, respectively.

3.3 Clonality of LRSE isolates: PFGE and MLST analysis

Twenty LRSE isolates were genotyped and shared the same PFGE pulsotype (A), with the exception of one (called pulsotype B) obtained from patient 11 (Figure 1). The three LSSE were not genetically related to each other or to the LRSE clone, demonstrating the genomic diversity among susceptible strains (Figure 1). The PFGE results were confirmed by MLST typing, which showed that all LRSE isolates with pulsotype A belonged to ST2. The pulsotype B strain belonged to ST57. The LSSE strains were ST21, ST87, and ST470 (Figure 1).

3.4 Correlation between IR-Biotyper® dendrogram and PFGE

The ability of the IRBT to assess the degree of genomic relatedness between isolates using a dendrogram generated by the instrument was evaluated and compared to PFGE, considered the gold standard in this study. IRBT clustering showed a clonal distribution of the population similar to that obtained by PFGE (Figure 1). Due to colony dissociation, one strain was tested twice. The PFGE profiles of both isolates were identical, whereas IRBT surprisingly identified two different spectra. Eight IR-spectra were identified among the isolates: IRBT detected clonality of 16 of the 19 ST2 LRSE strains of pulsotype A and distinguished the non-ST2 LRSE strain of pulsotype B and the three LSSE strains from the clonal strain. However, the IRBT assigned different IR-spectra to the Pulsotype A LRSE strains of Patient 1 and Patient 6 (Figure 1). The discriminatory power of IRBT was calculated using Simpson's index of diversity. It assesses the reliability of IRBT in distinguishing between unrelated strains (Hunter and Gaston, 1988). The concordance of clusters of related strains identified by PFGE and IRBT was determined by calculating the adjusted Wallace coefficient (Severiano et al., 2020). These results are presented in Table 2, together with the sensitivity, specificity, positive predictive value and negative predictive value of IRBT.

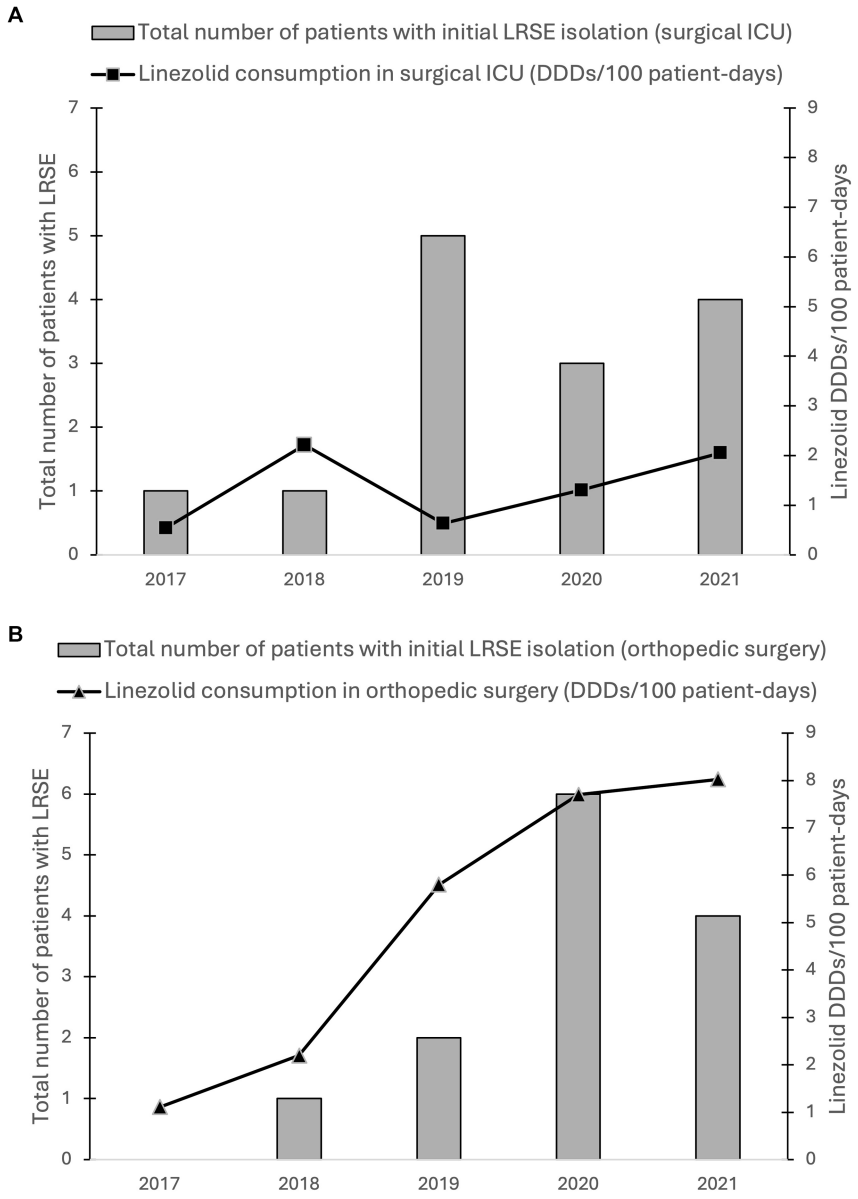

FIGURE 3
Annual linezolid consumption data from **(A)** the surgical ICU and **(B)** the orthopedic surgery from 2017 to 2021 versus the total number of LRSE isolates, including those that were not preserved. Linezolid use was calculated in DDDs/100 patient-days. Doses of 1,200 mg/day were considered as 1 DDD. Bars indicate the number of patients with initial detection of LRSE in the respective year in the unit.

TABLE 2 **Discriminatory power, concordance between IRBT and PFGE and performance of IRBT.**

Simpson's index of diversity (95% CI)	Adjusted Wallace coefficient (95% CI)	Sensitivity	Specificity	Positive predictive value	Negative predictive value
0.565 (0.325–0.806)	0.472 (0.002–0.943)	0.842	1.00	1.00	0.714

CI, confidence interval.

3.5 Antimicrobial susceptibility and determinants of methicillin and linezolid resistance

LRSE isolates were resistant to methicillin, gentamicin, ofloxacin, erythromycin, clindamycin, rifampicin, and cotrimoxazole. No resistance to vancomycin or teicoplanin was observed. LRSE showed a high level of resistance to linezolid, with MICs ≥ 256 mg/L, and to tedizolid (MICs > 32 mg/L), except for the pulsotype B LRSE strain. Surprisingly, this latter was susceptible to tedizolid (MIC = 0.19 mg/L) (Table 3). Most LRSE isolates were susceptible to delafloxacin (18/20), but resistant to ceftaroline (13/20), and ceftobiprole (19/20). Methicillin resistance was due to the presence of the *mecA* gene. Analysis of the 23S rRNA fragment

10.3389/fmicb.2024.1455945

TABLE 3 Antimicrobial susceptibility results of 20 LRSE and three LSSE strains, and characterization of the resistance determinants.

		MICs (mg/L)											Mutation
Patient	Strain	Methi-R (Y/N)	VAN	TEC	TIG	DLF	DLB	LNZ	TDZ	DPT	CFT	CTB	23S rRNA
1	LRSE	Y	2	2	0.25	0.032	0.060	>256	>32	0.50	0.50	3	G2576T
2	LRSE	Y	1	1	0.25	0.032	0.064	>256	>32	0.50	0.50	2	ND
3	LRSE	Y	1	2	0.50	0.094	0.094	>256	>32	0.50	0.75	4	G2576T
	LSSE	N	1	0.25	0.094	0.004	0.016	0.75	0.025	0.50	0.094	0.5	WT
4	LRSE	Y	1	1	0.094	0.032	0.047	>256	>32	0.38	0.75	3	G2576T
5	LRSE	Y	1	1	0.19	0.064	0.064	>256	>32	0.75	2	4	G2576T
6	LRSE	Y	1	1	0.50	0.38	0.94	>256	16	0.75	0.75	4	ND
7	LRSE	Y	1	0.50	0.50	0.032	0.094	>256	>32	0.75	2	4	G2576T
8	LRSE	Y	1	0.50	0.38	0.047	0.060	>256	>32	0.50	2	4	G2576T
9	LRSE	Y	1	0.50	0.19	0.19	0.064	>256	>32	0.25	2	4	G2576T
10	LRSE	Y	1	0.50	0.064	0.032	0.064	>256	>32	0.38	1.5	4	G2576T
11	LRSE	Y	0.50	0.50	0.094	0.047	0.047	256	0.19	0.19	0.38	1	G2576T
12	LRSE	Y	1	0.50	0.38	0.064	0.064	>256	>32	0.38	1.5	4	G2576T
13	LRSE	Y	2	2	0.25	0.032	0.094	>256	>32	0.38	2	4	G2576T
14	LRSE	Y	1	2	0.25	0.094	0.094	>256	>32	0.25	0.75	4	G2576T
	LSSE	Y	0.50	0.50	0.047	0.023	0.016	1	0.008	0.125	0.094	0.075	WT
15	LRSE	Y	1	0.50	0.38	0.064	0.064	>256	>32	0.50	1.5	4	G2576T
16	LRSE	Y	1	0.50	0.25	0.023	0.064	>256	>32	0.25	2	4	ND
17	LRSE	Y	1	0.50	0.38	0.064	0.094	>256	>32	0.75	1.5	3	G2576T
	LSSE	Y	2	2	0.047	0.064	0.032	0.75	0.094	0.25	0.5	0.5	WT
18	LRSE	Y	1	0.50	0.38	0.032	0.064	>256	>32	0.75	2	4	G2576T
19	LRSE	Y	1	0.50	0.38	0.094	0.060	>256	>32	0.50	2	4	G2576T
20	LRSE	Y	1	0.50	0.25	0.032	0.060	>256	>32	0.50	2	4	G2576T

Methi-R, methicillin-resistant; VAN, vancomycin; TEC, teicoplanin; TIG, tigecycline; DLF, delafloxacin; DLB, dalbavancin; LNZ, linezolid; TDZ, tedizolid; DPT, daptomycin; CFT, ceftaroline; CTB, ceftobiprole; ND, No Data; WT, Wild-Type.

performed on 17 of the 20 LRSE strains showed the G2576T mutation (regardless of pulsotype), as previously described in clinical isolates of LRSE (Bouiller et al., 2020; Coustillères et al., 2023; Treviño et al., 2009). No transferable oxazolidinone resistance genes, including the *cfr*, *optrA* and *poxtA* genes, were acquired by any of these 17 strains.

4 Discussion

In our study, we phenotypically and genotypically characterized the LRSE strains involved in an outbreak at the Tours University Hospital between 2017 and 2021. All LRSE strains, even the non-clonal one, showed high levels of resistance to linezolid, with MICs ≥ 256 mg/L. All 17 LRSE strains analyzed had the G2576T mutation in domain V of the 23S rRNA gene, which appears to be most common in clinical settings (Pillai et al., 2002). None of the 17 strains analyzed carried the *cfr* gene, limiting concerns about plasmid-mediated resistance spreading to more pathogenic *Staphylococcus* species such as *S. aureus*.

PFGE showed that all but one of the LRSE strains tested were genetically related. They belonged to the ST2 according to MLST, which appears consistent with previous studies reporting LRSE clonal occurrence of ST2 (Bouiller et al., 2020; Coustillères et al., 2023; Kosecka-Strojek et al., 2020). However, ST2 appears to be a common lineage in *S. epidermidis*, regardless of linezolid susceptibility (Martínez-Santos et al., 2022). Although PFGE is still a routinely used tool in nosocomial outbreak investigations, it would have been interesting for this study to perform whole genome sequencing (WGS), which provides greater resolution than any other microbial strain typing method.

We used IRBT to analyze the outbreak after PFGE typing. It was mostly congruent with the PFGE results: IRBT showed 87% congruence with PFGE analysis. One limitation of our study, however, is that because IRBT was performed retrospectively, it could have introduced a bias into our analysis. Also, IRBT discriminated two deposits of the same strain as two different IR-types. Because our IRBT experiment was only performed once, we assumed this could have been caused by technical factors. Random error or a contamination could also not be excluded. Moreover, our study included only a small number and low diversity of strains tested, so further studies are needed to assess the optimal analytical parameters to validate the technique for routine epidemiological use. Rakovitsky et al. showed that performing a dozen replicates in a single run, instead of three or four, can optimize the generated cut-off value, thus limiting the under- or over-sensitivity of the IRBT analysis (Rakovitsky et al., 2020). To date, our study is the first one to evaluate IRBT for *S. epidermidis*, but previous studies have shown promising results for the typing of other microorganisms, including for clinical outbreak investigation purposes (Hong et al., 2022; Hu et al., 2020; Pascale et al., 2022; Rakovitsky et al.,

2020). IRBT is less expensive than PFGE, with a cost of 20 Euros per sample analyzed in triplicate, although it requires the purchase of an automated system. In comparison, PFGE costs 50 Euros per sample. IRBT is technically easy to use, and a sample can be prepared in about 20 min, compared to 4–5 h for PFGE, which requires skilled technicians. Thus, due to its short turnaround time, IRBT appears to be a promising tool for outbreak investigation. Results can be obtained in a matter of hours (compared to several days for PFGE), allowing infection control measures to be implemented quickly to contain the outbreak.

Regarding the emergence of the LRSE epidemic clone, three patients (3, 14, 17) harbored linezolid-susceptible *S. epidermidis* (LSSE) strains a few months before isolation of the clone, with, respectively, 1/5, 1/5, and 4/5 positive osteoarticular intraoperative specimens. As the LSSE strains belonged to a different clone from the LRSE strain, this may argue against the selection of linezolid resistance mutations in pre-existing LSSE strains.

Most patients (at least 14 out of 20) had prior exposure to linezolid in the 3 months prior to isolation of the LRSE clone. The orthopedic surgery department and the surgical ICU were at the center of the outbreak. Orthopedic surgery was the biggest user of linezolid, with consumption accounting for almost a third of the total doses dispensed by Tours University Hospital in 2019, 2020, and 2021. Previous studies have mainly highlighted the direct link with the consumption of linezolid in healthcare establishments. In fact, selective antimicrobial pressure may promote the survival and spread of LRSE strains by suppressing patients' susceptible microbiota, allowing resistant strains to predominate (Huber et al., 2021; Weßels et al., 2018). Thus, limiting the prescription of oxazolidinones could help to limit this incidence (Dortet et al., 2018).

However, an Austrian institution reported an increase in the isolation of LRSE strains, with a peak of 84 isolates in 2018, despite the reduction in linezolid consumption compared with 2012 and 2013 (Huber et al., 2021). The authors reported that 47 of the 347 patients had no history of linezolid administration in the year prior to isolation of LRSE strains.

The development of linezolid resistance does not appear to be triggered solely by the use of linezolid. Indeed, the number of LRSE isolates appears to be associated with linezolid use data in orthopedic surgery, but not in the surgical ICU. The total number of LRSE strains was similar in both departments, whereas linezolid consumption was lower in the surgical ICU.

In our study, 5 out of 20 patients did not receive linezolid prior to isolation of the LRSE strain, suggesting the hypothesis of a reservoir and hand transmission of the clone by healthcare workers.

In addition, more than 40% of LRSE clonal strains were considered colonization or contamination. Indeed, the clinical histories of two patients (13 and 18) showed that the LRSE strain isolated in their blood cultures was a contaminant, suggesting (i) skin colonization of the patients with this strain and/or (ii) hand-carriage of this strain by healthcare workers. These two patients were hospitalized in the same department, but never shared the same room. A year and a half separated the two stays. Given that carriage of the strain by healthcare staff would probably be more transient, we cannot rule out the possibility that contaminated surfaces, such as computer keyboards, acted as a reservoir for the LRSE strain.

The retrospective nature of the study did not allow us to screen patients and healthcare providers in these units for carriage, nor to sample the environment, thus limiting exploration of the chain of transmission. It is likely that infection with the resistant strain was linked to surface contamination, followed by hand-transmission by healthcare workers, leading to colonization of patients' skin. Since most of the patients in our study had previously received linezolid, this antibiotic may have suppressed the susceptible skin microbiota, allowing the LRSE clone to take advantage of this niche.

Kelly et al. (2008) reported an outbreak of a LRSE clonal strain in 16 ICU patients: the epidemic clonal strain was found in the ICU environment and surfaces and may therefore be a reservoir. None of the 58 ICU healthcare workers screened for nasal carriage were carriers of the epidemic strain, but transient skin carriage may have occurred during the early stages of the outbreak. Other studies have reported transmission of *S. epidermidis* by healthcare workers through hand contact (Christensen et al., 1982; Kotilainen et al., 1990; Simpson et al., 1986). Although 6 of 16 patients did not receive linezolid, the authors reported a significant increase in linezolid use prior to the LRSE clonal outbreak. Restriction of linezolid use and reinforcement of contact precautions eradicated the outbreak (Kelly et al., 2008). A Spanish study also reported an outbreak of linezolid resistant *S. aureus*. Again, none of the healthcare providers carried the epidemic clone, but it was recovered from environmental surfaces (Sánchez García et al., 2010).

To maintain the efficacy of linezolid, it is important to carefully manage its use. The increase in linezolid resistance in *S. epidermidis* should temper its probabilistic use in infections commonly caused by *Staphylococci*, such as catheter-associated bloodstream infections.

The multidrug-resistant ST2 LRSE clone was able to persist and spread within the same hospital for 4 years and, to our knowledge, may continue to spread today. This is why the emergence of resistant clones should be detected at an early stage so that appropriate measures may be taken to control their spread, especially since CoNS are known to be a reservoir of resistance genes (Côrtes et al., 2022).

Data availability statement

The raw data supporting the conclusions of this article will be made available by the authors, without undue reservation.

Author contributions

NL: Conceptualization, Investigation, Writing – original draft. JB-C: Investigation, Writing – review & editing. EC: Investigation, Writing – review & editing. CL: Writing – review & editing. LC: Writing – review & editing. AJ: Supervision, Writing – review & editing. M-FL: Conceptualization, Methodology, Supervision, Writing – review & editing.

Funding

The author(s) declare that no financial support was received for the research, authorship, and/or publication of this article.

Acknowledgments

We thank Dr. Lucie Noël, Dr. Maryam Abid and the technicians of our department for their contribution to this study. Many thanks to Dr. Vianney Tuloup for providing us with the

linezolid usage data. We also thank the technicians, engineers, and biologists of the French National Reference Centre for *Staphylococci* for their help. We thank Bruker for providing us with the IR-Biotyper®. Many thanks to Prof. Philippe Lanotte, Dr. Adrien Lemaignen, Dr. Anne-Charlotte Tellier and to the reviewers for their proofreading and critical feedback.

Conflict of interest

The authors declare that the research was conducted in the absence of any commercial or financial relationships that could be construed as a potential conflict of interest.

Publisher's note

Supplementary material

The Supplementary material for this article can be found online at: https://www.frontiersin.org/articles/10.3389/fmicb.2024.1455945/full#supplementary-material

References

Bouiller, K., Ilic, D., Wicky, P. H., Cholley, P., Chirouze, C., and Bertrand, X. (2020). Spread of clonal linezolid-resistant *Staphylococcus epidermidis* in an intensive care unit associated with linezolid exposure. *Eur. J. Clin. Microbiol. Infect. Dis.* 39, 1271–1277. doi: 10.1007/s10096-020-03842-7

Brenciani, A., Morroni, G., Schwarz, S., and Giovanetti, E. (2022). Oxazolidinones: mechanisms of resistance and mobile genetic elements involved. *J. Antimicrob. Chemother.* 77, 2596–2621. doi: 10.1093/jac/dkac263

Christensen, G. D., Bisno, A. L., Parisi, J. T., McLaughlin, B., Hester, M. G., and Luther, R. W. (1982). Nosocomial septicemia due to multiply antibiotic-resistant *Staphylococcus epidermidis*. *Ann. Intern. Med.* 96, 1–10. doi: 10.7326/0003-4819-96-1-1

Côrtes, M. F., André, C., Martins Simões, P., Corvec, S., Caillon, J., Tristan, A., et al. (2022). Persistence of a multidrug-resistant worldwide-disseminated methicillin-resistant *Staphylococcus epidermidis* clone harbouring the *cfr* linezolid resistance gene in a French hospital with evidence of interspecies transfer to several *Staphylococcus aureus* lineages. *J. Antimicrob. Chemother.* 77, 1838–1846. doi: 10.1093/jac/dkac119

Coustillères, F., Renault, V., Corvec, S., Dupieux, C., Simões, P. M., Lartigue, M. F., et al. (2023). Clinical, bacteriological, and genetic characterization of bone and joint infections involving linezolid-resistant *Staphylococcus epidermidis*: a retrospective multicenter study in French reference centers. *Microbiol. Spectr.* 11:e0419022. doi: 10.1128/spectrum.04190-22

Dortet, L., Glaser, P., Kassis-Chikhani, N., Girlich, D., Ichai, P., Boudon, M., et al. (2018). Long-lasting successful dissemination of resistance to oxazolidinones in MDR *Staphylococcus epidermidis* clinical isolates in a tertiary care hospital in France. *J. Antimicrob. Chemother.* 73, 41–51. doi: 10.1093/jac/dkx370

Flamm, R. K., Mendes, R. E., Hogan, P. A., Streit, J. M., Ross, J. E., and Jones, R. N. (2016). Linezolid surveillance results for the United States (LEADER surveillance program 2014). *Antimicrob. Agents Chemother.* 60, 2273–2280. doi: 10.1128/AAC.02803-15

Hong, J. S., Kim, D., and Jeong, S. H. (2022). Performance evaluation of the IR Biotyper® system for clinical microbiology: application for detection of *Staphylococcus aureus* sequence type 8 strains. *Antibiotics* 11:909. doi: 10.3390/antibiotics11070909

Hu, Y., Zhou, H., Lu, J., Sun, Q., Liu, C., Zeng, Y., et al. (2020). Evaluation of the IR Biotyper for *Klebsiella pneumoniae* typing and its potentials in hospital hygiene management. *Microb. Biotechnol.* 14, 1343–1352. doi: 10.1111/1751-7915.13709

Huber, S., Knoll, M. A., Berktold, M., Würzner, R., Brindlmayer, A., Weber, V., et al. (2021). Genomic and phenotypic analysis of linezolid-resistant *Staphylococcus epidermidis* in a tertiary Hospital in Innsbruck, Austria. *Microorganisms* 9:1023. doi: 10.3390/microorganisms9051023

Hunter, P. R., and Gaston, M. A. (1988). Numerical index of the discriminatory ability of typing systems: an application of Simpson's index of diversity. *J. Clin. Microbiol.* 26, 2465–2466. doi: 10.1128/jcm.26.11.2465-2466.1988

Kelly, S., Collins, J., Maguire, M., Gowing, C., Flanagan, M., Donnelly, M., et al. (2008). An outbreak of colonization with linezolid-resistant *Staphylococcus epidermidis* in an intensive therapy unit. *J. Antimicrob. Chemother.* 61, 901–907. doi: 10.1093/jac/dkn043

Kosecka-Strojek, M., Sadowy, E., Gawryszewska, I., Klepacka, J., Tomasik, T., Michalik, M., et al. (2020). Emergence of linezolid-resistant *Staphylococcus epidermidis* in the tertiary children's hospital in Cracow, Poland. *Eur. J. Clin. Microbiol. Infect. Dis.* 39, 1717–1725. doi: 10.1007/s10096-020-03893-w

Kotilainen, P., Nikoskelainen, J., and Huovinen, P. (1990). Emergence of ciprofloxacin-resistant coagulase-negative staphylococcal skin flora in immunocompromised patients receiving ciprofloxacin. *J. Infect. Dis.* 161, 41–44. doi: 10.1093/infdis/161.1.41

Liakopoulos, A., Spiliopoulou, I., Damani, A., Kanellopoulou, M., Schoina, S., Papafragas, E., et al. (2010). Dissemination of two international linezolid-resistant *Staphylococcus epidermidis* clones in Greek hospitals. *J. Antimicrob. Chemother.* 65, 1070–1071. doi: 10.1093/jac/dkq065

Long, K. S., and Vester, B. (2012). Resistance to linezolid caused by modifications at its binding site on the ribosome. *Antimicrob. Agents Chemother.* 56, 603–612. doi: 10.1128/AAC.05702-11

Martínez-Santos, V. I., Torres-Añorve, D. A., Echániz-Aviles, G., Parra-Rojas, I., Ramírez-Peralta, A., and Castro-Alarcón, N. (2022). Characterization of *Staphylococcus epidermidis* clinical isolates from hospitalized patients with bloodstream infection obtained in two time periods. *Peer J* 10:e14030. doi: 10.7717/peerj.14030

Mihaila, L., Defrance, G., Levesque, E., Ichai, P., Garnier, F., Derouin, V., et al. (2012). A dual outbreak of bloodstream infections with linezolid-resistant Staphylococcus epidermidis and *Staphylococcus pettenkoferi* in a liver intensive care unit. *Int. J. Antimicrob. Agents* 40, 472–474. doi: 10.1016/j.ijantimicag.2012.06.014

Neoh, H., Tan, X.-E., Sapri, H. F., and Tan, T. L. (2019). Pulsed-field gel electrophoresis (PFGE): a review of the "gold standard" for bacteria typing and current alternatives. *Infect. Genet. Evol.* 74:103935. doi: 10.1016/j.meegid.2019.103935

Pascale, M. R., Bisognin, F., Mazzotta, M., Girolamini, L., Marino, F., Dal Monte, P., et al. (2022). Use of Fourier-transform infrared spectroscopy with IR Biotyper® system for *Legionella pneumophila* serogroups identification. *Front. Microbiol.* 13:866426. doi: 10.3389/fmicb.2022.866426

Pillai, S. K., Sakoulas, G., Wennersten, C., Eliopoulos, G. M., Moellering, R. C., Ferraro, M. J., et al. (2002). Linezolid resistance in *Staphylococcus aureus*: characterization and stability of resistant phenotype. *J. Infect. Dis.* 186, 1603–1607. doi: 10.1086/345368

Rakovitsky, N., Frenk, S., Kon, H., Schwartz, D., Temkin, E., Solter, E., et al. (2020). Fourier transform infrared spectroscopy is a new option for outbreak investigation: a retrospective analysis of an extended-Spectrum-Beta-lactamase-producing *Klebsiella pneumoniae* outbreak in a neonatal intensive care unit. *J. Clin. Microbiol.* 58, e00098–e00020. doi: 10.1128/JCM.00098-20

Sánchez García, M., De la Torre, M. A., Morales, G., Peláez, B., Tolón, M. J., Domingo, S., et al. (2010). Clinical outbreak of linezolid-resistant *Staphylococcus aureus* in an intensive care unit. *JAMA* 303, 2260–2264. doi: 10.1001/jama.2010.757

Seral, C., Sáenz, Y., Algarate, S., Duran, E., Luque, P., Torres, C., et al. (2011). Nosocomial outbreak of methicillin- and linezolid-resistant *Staphylococcus epidermidis* associated with catheter-related infections in intensive care unit patients. *Int. J. Med. Microbiol.* 301, 354–358. doi: 10.1016/j.ijmm.2010.11.001

Severiano, A., Pinto, F. R., Ramirez, M., and Carriço, J. A. (2020). Adjusted Wallace coefficient as a measure of congruence between typing methods. *J. Clin. Microbiol.* 49, 3997–4000. doi: 10.1128/jcm.00624-11

Simpson, R. A., Spencer, A. F., Speller, D. C., and Marples, R. R. (1986). Colonization by gentamicin-resistant *Staphylococcus epidermidis* in a special care baby unit. *J. Hosp. Infect.* 7, 108–120. doi: 10.1016/0195-6701(86)90053-8

Thomas, J. C., Vargas, M. R., Miragaia, M., Peacock, S. J., Archer, G. L., and Enright, M. C. (2007). Improved multilocus sequence typing scheme for *Staphylococcus epidermidis*. *J. Clin. Microbiol.* 45, 616–619. doi: 10.1128/JCM.01934-06

Treviño, M., Martínez-Lamas, L., Romero-Jung, P. A., Giráldez, J. M., Alvarez-Escudero, J., and Regueiro, B. J. (2009). Endemic linezolid-resistant *Staphylococcus epidermidis* in a critical care unit. *Eur. J. Clin. Microbiol. Infect. Dis.* 28, 527–533. doi: 10.1007/s10096-008-0657-5

Weßels, C., Strommenger, B., Klare, I., Bender, J., Messler, S., Mattner, F., et al. (2018). Emergence and control of linezolid-resistant *Staphylococcus epidermidis* in an ICU of a German hospital. *J. Antimicrob. Chemother.* 73, 1185–1193. doi: 10.1093/jac/dky010

frontiers | Frontiers in Microbiology

TYPE Original Research
PUBLISHED 19 September 2024
DOI 10.3389/fmicb.2024.1469280

OPEN ACCESS

EDITED BY
Shicheng Chen,
Northern Illinois University, United States

REVIEWED BY
Runhua Han,
University of Manitoba, Canada
Dexi Li,
Henan Agricultural University, China

*CORRESPONDENCE:
Tanmay Dutta
✉ dtanmay@chemistry.iitd.ac.in

RECEIVED 23 July 2024
ACCEPTED 03 September 2024
PUBLISHED 19 September 2024

CITATION
Singh S and Dutta T (2024) A virulence-associated small RNA MTS1338 activates an ABC transporter CydC for rifampicin efflux in *Mycobacterium tuberculosis*.
Front. Microbiol. 15:1469280.
doi: 10.3389/fmicb.2024.1469280

A virulence-associated small RNA MTS1338 activates an ABC transporter CydC for rifampicin efflux in *Mycobacterium tuberculosis*

Saumya Singh and Tanmay Dutta*

RNA Biology Laboratory, Department of Chemistry, Indian Institute of Technology Delhi, New Delhi, India

The efficacy of the tuberculosis treatment is restricted by innate drug resistance of *Mycobacterial tuberculosis* and its ability to acquire resistance to all anti-tuberculosis drugs in clinical use. A profound understanding of bacterial ploys that decrease the effectiveness of drugs would identify new mechanisms for drug resistance, which would subsequently lead to the development of more potent TB therapies. In the current study, we identified a virulence-associated small RNA (sRNA) MTS1338-driven drug efflux mechanism in *M. tuberculosis*. The treatment of a frontline antitubercular drug rifampicin upregulated MTS1338 by >4-fold. Higher intrabacterial abundance of MTS1338 increased the growth rate of cells in rifampicin-treated conditions. This fact was attributed by the upregulation of an efflux protein CydC by MTS1338. Gel-shift assay identified a stable interaction of MTS1338 with the coding region of *cydC* mRNA thereby potentially stabilizing it at the posttranscriptional level. The drug efflux measurement assays revealed that cells with higher MTS1338 abundance accumulate less drug in the cells. This study identified a new regulatory mechanism of drug efflux controlled by an infection-induced sRNA in *M. tuberculosis*.

KEYWORDS

small RNAs, gene regulation, antimicrobial resistance, efflux protein, drug efflux

1 Introduction

Persistence of *Mycobacterial tuberculosis*, the aetiological agent of tuberculosis (TB), in the hostile environment of host macrophages relies on fast and precise reprogramming of transcriptional profile in response to external stimuli (Miotto et al., 2022; Arnvig and Young, 2012; Dutta and Srivastava, 2018; Taneja and Dutta, 2019). An array of complex regulatory networks controlled by transcriptional modulators, two-component systems, sigma factors, riboswitches, and small RNAs (sRNAs) fine-tune the mycobacterial gene expression for adaptation to external challenges in real-time (Miotto et al., 2022; Taneja and Dutta, 2019; Smith et al., 2013; Petchiappan and Chatterji, 2017), which render them notoriously difficult to eliminate from infected patients. Consequently, prolonged treatment with frequent administration of multiple antibiotics is required to treat TB (Ginsberg and Spigelman, 2007; Dhar and McKinney, 2010; van den Boogaard et al., 2009). *M. tuberculosis* exploits a plethora of intrinsic mechanisms to combat anti-TB drug therapy (Remm et al., 2022). Its complex hydrophobic cell envelope is impermeable to many drugs and is considered as one of the key

features of defense against drug influx (Sarathy et al., 2012). *M. tuberculosis* possesses additional machinery for drug tolerance, which includes multiple efflux pumps that deport antimycobacterial compounds out of the cells, mycobacterial enzymes capable of chemical modification of antibiotics, and alterations in gene expression to adapt to antibiotic-exposed conditions (Briffotaux et al., 2019; Nasiri et al., 2017). Antibiotics also lead to the development of acquired *M. tuberculosis* resistance against it through target mutations (Takiff and Feo, 2015), which is associated with the reduced fitness of the resistant mutants (Andersson and Hughes, 2010). Because of the above-mentioned capabilities of *M. tuberculosis*, illegitimate drug usage by patients frequently causes a high degree of treatment failure leading to disease relapse and emergent drug resistance (Dhar and McKinney, 2010; van den Boogaard et al., 2009) triggering onward transmission and amplification of drug-resistant strain (Barilar and Battaglia, 2024).

Traditional antimycobacterial compounds interfere with the biosynthetic processes, e.g., biogenesis of cell wall, transcription, and protein synthesis, which are necessitated for cell growth (Dhar and McKinney, 2010). A few of these antibiotics like isoniazid, ethambutol, etc. for inhibition of cell wall formation, rifampicin for interference with transcription, and streptomycin for the inhibition of protein synthesis of *M. tuberculosis* are regarded as the frontline anti-TB drugs (Briffotaux et al., 2019). *M. tuberculosis* cells although highly susceptible to death in the presence of these antibiotics *in vitro*, are less affected by the same antimycobacterial agents while grown *in vivo* in mammalian hosts (Dhar and McKinney, 2010; Young et al., 2008; McKinney, 2000). Therefore, chronic TB is more difficult to control through a single antibiotic therapy and calls for second-line regimens. Patient nonadherence to such an extended therapeutical procedure, insufficient health infrastructure, and lack of antibiotics help promote the development of resistant strains of exceedingly slow-growing *M. tuberculosis* (Briffotaux et al., 2019). Hence, multidrug-resistant TB (MDR-TB) and extremely drug-resistant TB (XDR-TB) strains have evolved (Almeida Da Silva and Palomino, 2011; Udwadia et al., 2012) which accentuates the requirement for new strategies to develop novel anti-TB drugs. For that reason, it is essential to comprehensively understand the regulatory networks promoting resistance in *M. tuberculosis* against antibiotics.

Although sRNAs have been identified to be a ubiquitous class of regulators contributing to antibacterial resistance in pathogenic bacteria (Mediati et al., 2021), sRNA-mediated regulation of antibiotic resistance in *M. tuberculosis* has not been investigated yet. Only a handful of sRNAs among a few dozen discovered in *M. tuberculosis* until now have been identified with associated functions given the difficulty of understanding sRNA function *in vivo* in *M. tuberculosis* (Dutta and Srivastava, 2018; Arnvig et al., 2011; Singh et al., 2021). MTS1338 (or ncRv11733) is one among those sRNAs, which exists only in the pathogenic mycobacterial genome (Dutta and Srivastava, 2018; Arnvig et al., 2011; Moores et al., 2017), and is highly accumulated during *M. tuberculosis* infection (Arnvig et al., 2011). Consequently, MTS1338 is highly upregulated in response to stresses associated with infection (Singh et al., 2021; Salina et al., 2019) and configures a stress-resistance signature in *M. tuberculosis* (Martini et al., 2023). Substantial alteration of the transcriptomic profile of *M. tuberculosis* overexpressing MTS1338 suggests its potential role in the global gene regulatory network, which promotes the survival of *M. tuberculosis* in host macrophages through an adaptive mechanism (Martini et al., 2023). Participation of MTS1338 in the regulation of numerous physiological processes firmly indicated that MTS1338 might play an important role in antimycobacterial resistance.

In the current study, we identified that MTS1338 is highly induced while the cells are exposed to antibiotic like rifampicin. Cells with higher intracellular MTS1338 accumulation were ascertained to grow at a higher rate than the cells with basal MTS1338 level. Investigations on how MTS1338 in its higher abundance promotes *M. tuberculosis* growth affirmed that MTS1338 increases the abundance of the mRNA of an efflux protein CydC by binding to its coding region potentially protecting it at the posttranscriptional stage from cellular endoribonucleases. Inhibition of efflux proteins of the cells undergone a prior treatment with rifampicin resulted in a better mycobacterial growth rate for the cells overexpressing MTS1338. A higher abundance of intracellular MTS1338 resulted in a lower accumulation of antibiotics in the cell suggesting a potential role of this sRNA in dealing with mycobacterial adaptation to antibiotics.

2 Materials and methods

2.1 Materials

Middlebrook 7H11 agar, Middlebrook 7H9 broth, and OADC (oleic acid-albumin-dextrose-catalase) were purchased from Difco Laboratories (United States). Tween 80, lysozyme, and antibiotics (rifampicin, tetracycline, kanamycin) were procured from Sigma-Aldrich. RNeasy Mini Kit and UniPro GelEx/clean-up kit were obtained from Qiagen (Germany). Genomic DNA extraction kit, GoTaq green master mix, and nuclease-free water were from Promega. Oligonucleotides were synthesized by Sigma Chemical Co. (United States). SYBR green master mix and iScript™ cDNA synthesis kit were procured from Bio-Rad (Bio-Rad). Restriction enzymes, e.g., BamHI and HindIII were obtained from New England Biolabs. MEGAshortscript™ T7 transcription kit and Max™ Prehyb/hyb buffer solution were purchased from Invitrogen. Hybond-N+ nylon membrane was purchased from GE Healthcare. carbonyl cyanide *m*-chlorophenylhydrazone (CCCP) was purchased from Sigma Chemical Co. (United States). Plasmid pST-Ki was a generous gift from Dr. V. K. Nandicoori of the National Institute of Immunology, India. All other chemicals were of molecular biology grade.

2.2 Bacterial strain and growth conditions

The *M. tuberculosis* avirulent strain H37Ra was used as a model strain. The frozen glycerol stock was streaked on a Middlebrook 7H11 solid agar plate and stored at 37°C for 4–5 weeks. In a culture tube, one colony from the growing plate was inoculated with Middlebrook 7H9 broth (Difco Laboratories) supplemented with 10% OADC (oleic acid-albumin-dextrose-catalase; Difco Laboratories) and 0.05% (v/v) polysorbate 80 (Sigma-Aldrich). Subsequently, the cells were incubated at 37°C under shaking at 200 rpm. Cell growth while attaining OD_{600} 0.6–0.9, was regarded as the exponential growth phase of *M. tuberculosis*.

2.3 Antibiotic treatment

M. tuberculosis H37Ra cells were grown at 37°C in an orbital shaker incubator at 200 rpm until OD_{600} of the culture reached 0.9. The cells were then harvested at room temperature. After that, the cells

were again suspended in 7H9 media and treated with rifampicin (2 μg/mL) for 30 min. Cells cultured under identical conditions without the addition of antibiotics were taken as control.

2.4 RNA isolation and RT-qPCR

Cell pellets with or without prior antibiotic treatment were re-suspended in 4 mL of PBS containing lysozyme (4 mg/mL). Lysozyme treatment was continued for 2 h at 37°C in a water bath with circulation. After that, cells were sonicated for 90 s (with alternate 10 s on or off pulse) using a Branson sonicator at 4°C. Total RNA was extracted using RNeasy Mini Kit (Qiagen). RNA concentration was measured using a JENWAY Genova Nanodrop spectrophotometer and RNA quality was assessed in a 1% agarose gel.

Total RNA (1 μg) from treated/untreated cells was used to synthesize cDNA using iScript™ cDNA synthesis kit (Bio-Rad), along with random hexamer (Bio-Rad C1000, United States) as a primer. Complementary DNAs were diluted 100 times with nuclease-free water and 1 μL of diluted cDNA was employed in a quantitative real-time PCR reaction using SYBR green utilizing a CFX96 Touch™ Real-Time PCR detection system (Bio-Rad). A representative qPCR reaction of 20 μL contains 20 ng of cDNA, 1 μM of forward and reverse primers (P1 & P2 for MTS1338, P5 & P6 for 5S RNA, P7 & P8 for *cydC* mRNA in Supplementary Table S1), 10 μL of SYBR green master mix, and 8 μL of nuclease-free water mix. 5S RNA gene of *M. tuberculosis* was taken as an internal control. The $2^{-\Delta\Delta Ct}$ technique was used to calculate relative gene expression. Every experiment was carried out in compliance with the manufacturer's guidelines.

2.5 Northern blot

Total RNA (15 μg), isolated from untreated or treated *M. tuberculosis* cells, were separated on 2% agarose-formaldehyde gel using 1X MOPS [3-(N-morpholino) propane sulfonic acid] buffer, which was then washed with deionized water. RNA was transferred from agarose gel to Hybond-N+ nylon membrane (GE Healthcare) by downward capillary transfer in 10X SSC buffer at room temperature overnight and UV crosslinked to the membrane by UV crosslinker (Herolab, Germany). A 5′-Cy5 labeled DNA probe (P11 for MTS1338 and P12 for 5S RNA in Supplementary Table S1) was used to detect MTS1338. Hybridization (Shake 'n' Stack™ Hybridization Chamber, Thermo Fisher Scientific, United States) of Cy5-labeled probe to crosslinked RNA on the membrane was promoted by incubating them in Northern Max™ Prehyb/hyb buffer solution (Invitrogen) overnight. The membrane was subsequently washed with pre-warmed SSC buffer three times and the bands were visualized by high-resolution gel imaging for the fluorescence system (G:Box Chemi-XX9, SYNGENE). Bands were quantitated by ImageJ.

2.6 Cloning and overexpression of MTS1338

The genomic DNA of *M. tuberculosis* H37Ra cells was extracted using the Genomic DNA Extraction Kit (Promega Co., United States). The gene encoding MTS1338 was amplified from genomic DNA in a PCR reaction using KOD hot start polymerase (Invitrogen) with primers P3 and P4 listed in Supplementary Table S1. The amplicon was purified by gel extraction (Qiagen). Both the PCR products and the shuttle vector pST-Ki were digested with BamHI and HindIII for 2 h at 37°C. Digested products were purified through phenol: chloroform: isoamyl alcohol (25, 24:1) extraction and were ligated by T4 DNA ligase (New Eng Biolab). The resulting recombinant plasmids (pMTS1338) were transformed into *Escherichia coli* DH5α cells, which were grown on an LB (Kan+) plate overnight at 37°C. Cloning of gene encoding MTS1338 under the control of tetracycline promoter was confirmed by DNA sequencing. Recombinant pMTS1338 from *E. coli* cells was electroporated into *M. tuberculosis* H37Ra cells and subsequent MTS1338 overexpression was monitored upon the addition of tetracycline (1 μg/mL) for 72 h.

2.7 Growth analysis

The 7H9 medium supplemented with 10% OADC and 0.05% Tween 80 was used to grow the mycobacterial bacilli. Carbonyl cyanide 3-chlorophenylhydrazone (4 μg/mL) was added to the cells 5 days after the cells (OD_{600}-0.9) were treated with rifampicin (2 μg/mL). The cells were continued to grow for 16 days under shaking (200 rpm) at 37°C. Growth was monitored by measuring the optical density of the culture at 600 nm every 24 h with a UV spectrophotometer (JASCO).

2.8 RNA decay

Overnight cultures were diluted 1:100 into fresh 7H9 medium supplemented with 10% OADC and 0.05% Tween 80 and grown to exponential phase (OD_{600}-0.9) followed by treatment with 500 μg/mL rifampicin (Chen et al., 2019). Equal volumes of cells were removed for the zero-time sample after 1 min of rifampicin addition to allow complete inhibition of new transcription and immediately mixed with ice-cold stop solution (95% ethanol, 5% phenol). Additional samples were removed at indicated time points in the figure legends. Changes in *cydC* mRNA accumulation were determined by RT-qPCR analysis.

2.9 *In vitro* transcription

Genomic DNA of *M. tuberculosis* H37Ra cells was used as a template for the synthesis of genes of CydC and MTS1338 by PCR amplification using primers (P8 & P14 for *cydC*, P2 & P13 for MTS1338 and P10 & P11 for *katG* mRNA) listed in Supplementary Table S1. The forward primer was fused with a promoter sequence of T7 RNA polymerase. Templates were gel extracted using a QIAquick® gel extraction kit. Each template of 100 nM was added in an *in vitro* transcription reaction using a MEGAshortscript™ T7 transcription kit. Transcripts were extracted with phenol: chloroform: isoamyl alcohol (25: 24: 1) and precipitation overnight with ethanol at-20°C. The concentration of RNA was estimated spectrophotometrically by NanoDrop® spectrophotometer (Maestrogen, Taiwan) and RNA quality was checked on 6% polyacrylamide, 7.5 M urea gel.

2.10 Electrophoretic mobility shift assay

Transcripts of MTS1338 and *cydC* mRNA fragment (916–1,030 residues) were denatured at 80°C for 10 min and then cooled on ice. Binding reactions (10 µL) were conducted by incubating cydC mRNA (10 nM) with increasing amounts of MTS1338 (0–8 µM) at 37°C for 30 min in 1X binding buffer [100 mM Tris acetate pH 7.6, 500 mM NaOAc, and 25 mM Mg $(OAc)_2$]. Aliquots of each binding reaction were separated in an agarose gel (2%) using 1X MOPS buffer at 4°C. Gel was stained with 1X SYBR™ Gold Nucleic Acid Gel Stain (Invitrogen) and bands were visualized by high-resolution gel imaging for the fluorescence system (G: Box Chemi-XX9, SYNGENE).

2.11 EtBr accumulation assay

H37Ra cells harboring empty pST-Ki or recombinant pMTS1338 plasmid were grown in 7H9 medium supplemented with 10% OADC until the mid-exponential phase (OD_{600}-0.9). Cells were then treated with tetracycline (1 µg/mL) for 72 h for the extrachromosomal induction of MTS1338 followed by the addition of EtBr (1 µg/mL). After 10 min of EtBr exposure at 37°C, cells were treated with an efflux pump inhibitor CCCP with a final concentration of 6.25 µM. Cells were then pelleted down by centrifugation at 3500 g for 5 min and then resuspended in 1 mL of Phosphate buffer saline with/without CCCP. Intracellular accumulation of EtBr was measured *in situ* by fluorimetry with excitation at 520 nm and emission at 590 ± 20 nm. Fluorescence was monitored every 20 min, and the measurements were continued for 60 min.

2.12 Statistical analysis

Data obtained from experimental studies were presented as mean ± standard deviation. One-way analysis of variance was conducted, and a difference of $p < 0.05$ was considered statistically significant.

3 Results

3.1 MTS1338 is upregulated following rifampicin treatment

H37Ra cells were used as a model strain for our experiments as both strains of *M. tuberculosis*, H37Ra, and H37Rv exhibit equivalent minimum inhibitory concentrations to most antituberculosis drugs (Heinrichs et al., 2018). Given the induction of MTS1338 in response to multiple infection-associated stresses and its regulation to remodel the global gene expression of *M. tuberculosis*, it insinuated that MTS1338 might play some role in mycobacterial adaptation to antibiotic treatment. To address that hypothesis *M. tuberculosis* H37Ra cells were grown in Middlebrook 7H9 broth supplemented with 10% OADC and 0.05% (v/v) polysorbate 80, until OD_{600} reached 0.9 and then treated with rifampicin (2 mg/mL), a frontline antimycobacterial drug, for 30 min at 37°C under shaking condition. The concentration of rifampicin was used in a similar experiment as described (Lake et al., 2023). Another *M. tuberculosis* culture identically treated except for rifampicin was considered as a control. MTS1338 abundance in the total RNA isolated from rifampicin-treated and untreated cells was measured by RT-qPCR analysis. Figure 1A clearly shows that cells accumulate as much as ~5-fold more MTS1338 in 30 min following rifampicin treatment. In addition, northern blotting for MTS1338 in the total RNA isolated from rifampicin-treated or control cells revealed a 4-fold more accumulation of MTS1338 in rifampicin-treated cells (Figures 1B,C) than in the control untreated cells. These observations lead to the conclusion that MTS1338 is a rifampicin-induced sRNA that is potentially involved in adaptation to rifampicin-treated conditions.

3.2 Enhanced intracellular MTS1338 abundance increases the growth rate in the presence of rifampicin

As MTS1338 accumulates to a higher degree following antibiotic treatment on *M. tuberculosis* cells, it was of immense interest to investigate whether overexpression of MTS1338 ameliorates the growth rate of the cells. To address that question, the gene encoding MTS1338 was cloned in the pST-Ki shuttle vector under the control of P_{tet} promoter, and the recombinant plasmid thus obtained (pMTS1338) was electroporated in *M. tuberculosis* H37Ra cells. Overexpression of MTS1338 was monitored by adding tetracycline (1 µg/mL) to the culture media for 72 h. Estimation of intracellular MTS1338 abundance upon addition of tetracycline resulted in ~3.5-fold more accumulation of MTS1338 when compared to the control cells analyzed by RT-qPCR (Figure 2A). Northern blot analysis (Figure 2B) of MTS1338 in the total RNA isolated from the cells with/without MTS1338 overexpression also substantiated ~4-fold more accumulation of MTS1338 in the cells harboring pMTS1338 plasmid (Figure 2C).

To examine whether higher MTS1338 abundance affects cell growth or not, we monitored the growth of cells with/without extrachromosomal MTS1338 overexpression and found that overexpression of MTS1338 in H37Ra cells under normal conditions did not show any alteration of growth rate (Figure 2D). This fact indicated that a higher accumulation of MTS1338 is not detrimental to cell viability. However, growth analysis in the presence of rifampicin revealed a significant difference in the growth rate of the cells with or without MTS1338 overexpression (Figure 2E). H37Ra cells overexpressing MTS1338 appeared to grow at a higher rate with a generation time of 6 days than the cells containing empty vector (generation time 9 days). This firmly established that MTS1338 promotes cell growth in the presence of first-line antibiotic rifampicin.

3.3 Elevated MTS1338 induces the gene encoding efflux protein CydC

MTS1338-driven increased cellular robustness in opposition to rifampicin apprised us to investigate how MTS1338 acts to relieve the antagonistic effect created by rifampicin. To address that question, we aimed to examine the expression of genes encoding ABC transporters since it is one of the most predominant intrinsic mechanisms by which *M. tuberculosis* can ride out antibiotic treatment is drug efflux (Remm et al., 2022). The mycobacterial *cydC* gene, transcribed from the *cydABDC* gene cluster, encodes an efflux protein. The absence of CydC in *M. tuberculosis* alleviates its ability to survive the transition from acute to chronic infection. Expression of *cydABDC*

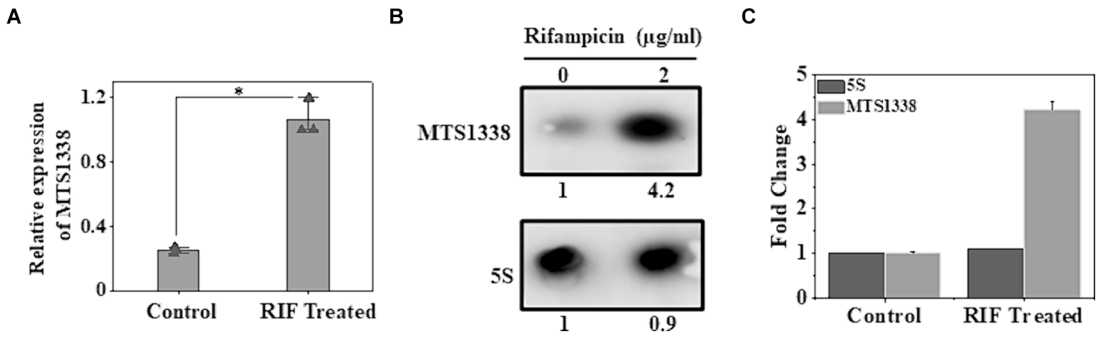

FIGURE 1
Effect of rifampicin **(A)** treatment on the intracellular abundance of MTS1338 in *Mycobacterium tuberculosis* cells. Mid-exponentially grown cells (OD_{600} −0.9) were exposed to rifampicin (2 µg/mL) and then were harvested. Total RNA was isolated and MTS1338 abundance was estimated by RT-qPCR analysis. 5S gene was taken as an internal control. The relative amounts of the transcripts are presented as the average ± standard deviation (SD) from three separate experiments and normalized to the level of the untreated sample. One-way ANOVA was conducted and a difference of $*p < 0.05$ was considered statistically significant. **(B)** Total RNA (15 µg) isolated from the cells treated with/without rifampicin (2 µg/mL) were separated in a 2% agarose formaldehyde gel and analyzed by northern blot. The number under each lane represents the relative amount of MTS1338 when compared to untreated sample, which was set as 1. 5S rRNA gene was taken as a loading control. Northern blots were carried out three times and one representative blot is presented. **(C)** Northern blot experiments were carried out three times with 5′-Cy5 labeled DNA oligonucleotide probes for RNAs. Bands were quantitated by ImageJ. The amount of MTS1338 and 5S RNA in the untreated cell was set at 1.

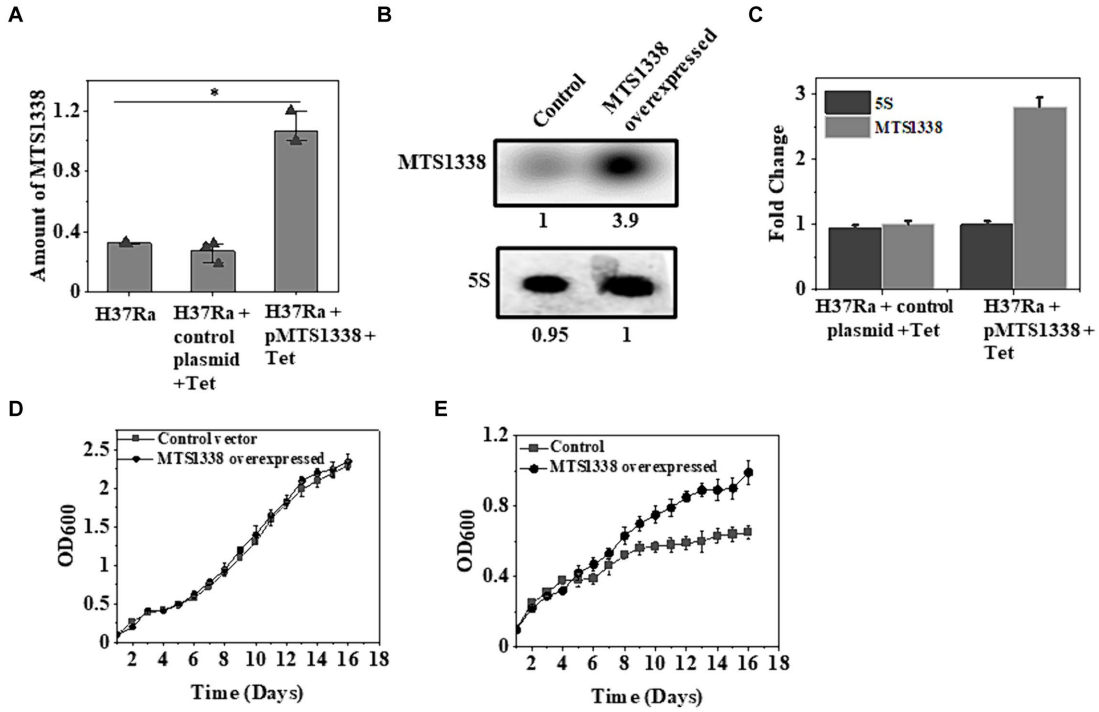

FIGURE 2
A higher MTS1338 abundance increases the growth rate in the presence of rifampicin. **(A)** Tetracycline (1 µg/mL) was added to the exponentially grown *M. tuberculosis* cells (OD_{600} = 0.9) harboring empty or recombinant pMTS1338 plasmids. Cells continued to grow for 72 h and the total RNA was extracted from each sample. MTS1338 abundance was estimated by RT-qPCR analysis. 5S gene was taken as an internal control. The relative amounts of the transcripts are presented as the average ± SD from three separate experiments and normalized to the level of the untreated sample. One-way ANOVA was conducted and a difference of $*p < 0.05$ was considered statistically significant. **(B)** Northern blot was carried out using 15 µg of total RNA isolated from the cells with/without overexpressing MTS1338. 5S RNA gene was taken as loading control. Northern blot experiments were carried out three times and identical results were obtained. A representative of Northern blots was presented. The number under overexpressed lane represents the relative amount of RNA when compared with control lane, which was set 1.0. **(C)** Bands of three independent northern blots were quantitated by ImageJ. Data were presented as the average ± SD. The amount of MTS1338 and 5S RNA in the untreated cell was set at 1. **(D)** H37Ra cells harboring recombinant pMTS1338 plasmid or empty vector were grown at 37°C. OD_{600} was monitored in regular interval and was plotted against time. The data presented was the average ± S.D. of three independent experiments. Growth experiments were also carried out in presence of rifampicin (5 µg/mL) added at the day 1 **(E)**.

has also been shown to be induced by hypoxia and NO stress (Shi et al., 2005). We selected *cydC* gene for our investigation of whether MTS1338 exerts any effect on *cydDC* expression as in many instances *cydDC* transporters are recognized to help persist *M. tuberculosis* against drugs like isoniazid (8). To settle that hypothesis, we compared the expression of *cydC* gene in H37Ra cells harboring either pMTS1338 or empty pST-Ki vectors and found >3-fold induction of *cydC* in MTS1338 overexpressing cells (Figure 3A). Northern blot analysis (Figure 3B) for the determination of *cydC* accumulation revealed that the cells with higher MTS1338 abundance upregulated *cydC* transcripts by >3-fold (Figure 3C), which reinforced RT-qPCR data. These experiments pointed to the involvement of MTS1338 in inducing the *cydC* gene.

Upregulation of *cydC* in response to higher intracellular MTS1338 abundance and enhanced accumulation of MTS1338 following antibiotic treatment instigated us to investigate whether *cydC* is also upregulated in response to antibiotic treatment. To examine that objective, we compared the intracellular *cydC* levels in the cells treated with/without rifampicin by RT-qPCR and northern blot analysis. It is conspicuous from Figure 4A that *cydC* accumulation analyzed through RT-qPCR was induced by ~4-fold following rifampicin treatment. An analogous result of rifampicin-driven *cydC* induction was obtained through northern blot analysis (Figures 4B,C). Investigation of the expression of *cydD*, which encodes a different efflux protein, revealed that rifampicin treatment did not show any significant effect on its intracellular abundance in *M. tuberculosis* (Singh and Dutta, unpublished observation). These experiments firmly established that MTS1338 has a profound effect in maintaining intracellular *cydC* levels against antibiotic treatment.

3.4 MTS1338 directly interacts with the coding region of *cydC* mRNA

MTS1338-mediated upregulation of *cydC* mRNA brought up the question of whether MTS1338 regulates *cydC* abundance by directly interacting with it. To address that question, both *cydC* mRNA and MTS1338 sequences were used in the IntaRNA (Mann et al., 2017) to identify if any complementary region(s) exists between them. A region of 15-nt on *cydC* mRNA (966–980 residues) was found to be completely complementary to an intermediate portion (56–70 residues) of MTS1338 (Figure 5A). To confirm that hypothesis, both MTS1338 RNA and *cydC* mRNA fragments surrounding residues 916 to 1,030 that possesses region complementary to MTS1338 were transcribed and purified *in vitro*. Incubation of MTS1338 with *cydC* fragment resulted in the formation of *cydC*-MTS1338 binary complex, which was observed as a high molecular weight band generated in the gel-shift assay (Figure 5B). Addition of increasing amounts of MTS1338 to a constant amount of *cydC* mRNA gave rise to a concomitant increase in the population of *cydC*-MTS1338 binary complex. This experiment confirmed that MTS1338 directly interacts with the coding region of *cydC* mRNA potentially stabilizing it at the posttranscriptional level. A control experiment with *katG* mRNA did not show any interaction with MTS1338 (Figure 5C).

3.5 MTS1338 overabundance increases the stability of *cydC* mRNA

Direct interaction of MTS1338 to the coding region of *cydC* mRNA raised the question of whether MTS1338 binding to *cydC* mRNA increased its stability *in vivo*. To help answer this question, we first overexpressed MTS1338 in exponentially growing cells (OD_{600}–0.9) and subsequently rifampicin (500 μg/mL) was added to it. The use of this high concentration of rifampicin completely inhibits new transcription. The amount of *cydC* mRNA in the cells with/without overexpressing MTS1338 was measured at different time points after rifampicin addition by RT-qPCR analysis. As can be seen in Figure 6, overexpression of MTS1338 led to dramatic stabilization of the *cydC* message, increasing its half-life from ~4 min

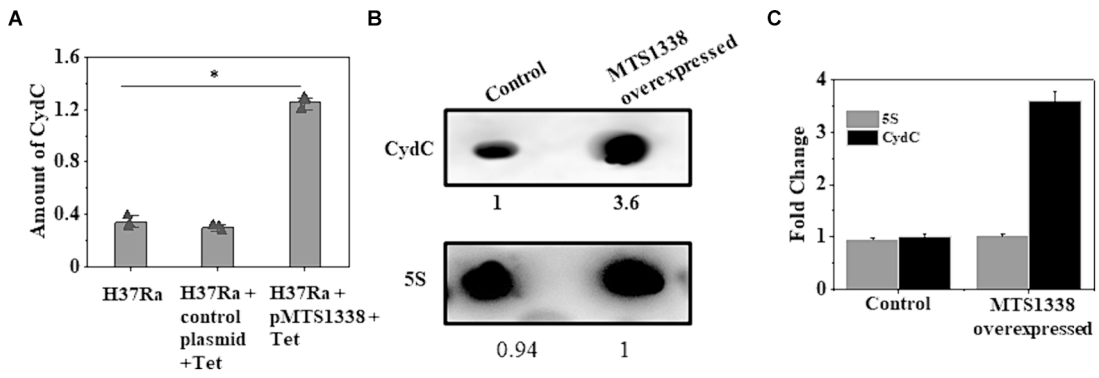

FIGURE 3
(A) Relative expression of *cydC* mRNA was estimated by RT-qPCR analysis in the exponentially grown *M. tuberculosis* cells (OD_{600} = 0.9) harboring control or recombinant pMTS1338 vectors. 5S gene was taken as an internal control. The relative amounts of *cydC* mRNA are presented as the average ± standard deviation from three separate experiments and normalized to the level of the untreated sample. One-way ANOVA was conducted and a difference of $*p < 0.05$ was considered statistically significant. **(B)** Northern blot was carried out using 5′-Cy5-labeled DNA probe to detect *cydC* mRNA present in the total RNA isolated from the cells with/without overexpressing MTS1338. 5S was taken as a loading control. A representative of three independent northern blots with identical results was presented. The number under each lane represents the relative amount of *cydC* when compared with control. **(C)** Bands of three independent northern blots were quantitated by ImageJ. Data were presented as the average ± SD. The amount of *cydC* and 5S RNA in the control cell was set at 1.

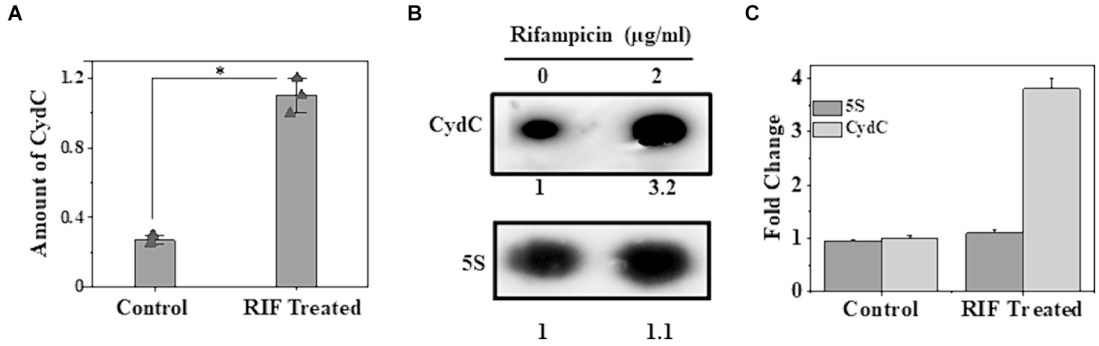

FIGURE 4
Accumulation of *cydC* in *M. tuberculosis* while treated with rifampicin (2 µg/mL). **(A)** Mid-log phase H37Ra cells (OD_{600} = 0.9) were exposed to antibiotics for 30 min at 37°C. Relative amount of *cydC* in the total RNA was measured by RT-qPCR analysis. 5S gene was taken as an internal control. The relative amounts of *cydC* mRNA are presented as the average ± standard deviation from three separate experiments and normalized to the level of the untreated sample. One-way ANOVA was conducted and a difference of $*p < 0.05$ was considered statistically significant. **(B)** Total RNA (15 µg) from rifampicin treated and untreated samples were separated in in a 2% agarose formaldehyde gel and analyzed by northern blot. The number under each lane represents the relative amount of *cydC* when compared to untreated sample, which was set as 1. 5S RNA gene was taken as a loading control. Northern blots were carried out three times and one representative blot is presented. **(C)** Northern blot experiments were carried out three times with 5′-Cy5 labeled DNA oligonucleotide probes for RNAs. Bands were quantitated by ImageJ. The amount of MTS1338 and 5S RNA in the untreated cell was set at 1.

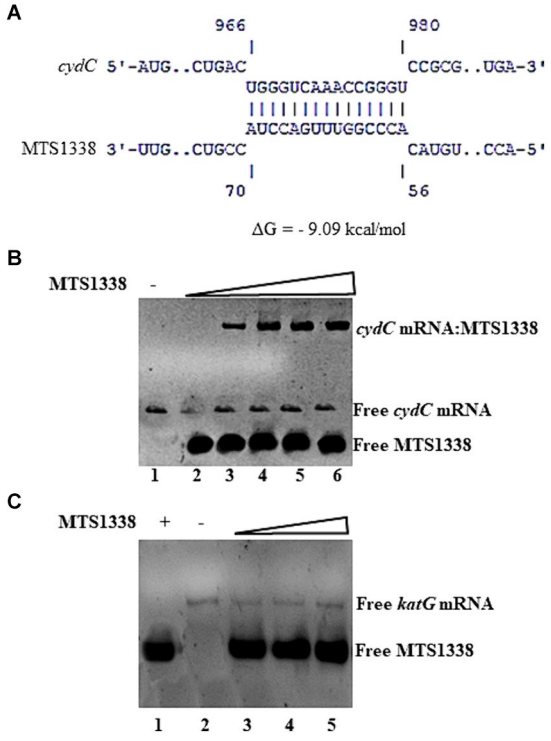

FIGURE 5
(A) Base pairing region between MTS1338 and *cydC* mRNA fragment as predicted by IntaRNA program. The numbering of nucleotides on MTS1338 and *cydC* mRNA is relative to the transcription start site of each RNA. **(B,C)** Interaction between MTS1338 and *cydC* mRNA **(B)** and *katG* **(C)**. Fragment of *cydC* and *katG* mRNA (10 pmol) was incubated with 10, 20 and 30 pmol of MTS1338 (lanes 4, 5, and 6 respectively) in a 20 µL reaction. Numbers at the bottom of the gels represent the lanes **(C)**.

to ~15 min. This firmly indicated that the binding of MTS1338 to *cydC* mRNA protected from intracellular degradation possibly by ribonucleases.

3.6 A higher accumulation of MTS1338 increases rifampicin efflux from axenically grown *Mycobacterium tuberculosis*

We measured intrabacterial ethidium bromide (EtBr) accumulation as a substitute for rifampicin efflux as EtBr has been considered as an artificial efflux pump substrate (Lake et al., 2023). The fluorescence of EtBr increases by ~20-fold when intercalated with DNA (Jernaes and Steen, 1994). Thus, occluding EtBr efflux from *M. tuberculosis* cells by efflux pump inhibitor renders it more fluorescent, which can be measured by spectrofluorimetry. To examine the effect of a higher accumulation of MTS1338 on rifampicin efflux, *M. tuberculosis* cells with/without overexpressing MTS1338 were exposed to EtBr for 10 min at 37°C and the efflux pump inhibitor CCCP was subsequently added to the cells. Cells were then centrifuged and resuspended in PBS and CCCP was added to the resuspended cells. Figure 7A shows the accumulation of EtBr in *M. tuberculosis* with/without overexpressing MTS1338 treated with CCCP. It is evident in Figure 7A that cells with a higher intracellular MTS1338 abundance accumulated as much as 50% less EtBr than what was obtained in the cells with a low abundance of MTS1338. This experiment firmly suggested that a higher abundance of MTS1338 promoted a lower accumulation of EtBr potentially deporting it from the cells.

In a similar line, to investigate the rate of EtBr efflux in cells with empty/recombinant pMTS1338 plasmids, EtBr-containing cells were treated with CCCP and then resuspended in PBS to substantially diminish the inhibitory effect of CCCP on efflux proteins. After that intracellular EtBr accumulation was measured by spectrofluorimetry every 20 min up to 60 min. Figure 7B shows that the decrease in the inhibitory effect of CCCP resulted in the outflow of EtBr from the cells, which was reflected by the concomitant decrease in EtBr fluorescence with increasing time. Interestingly, a nearly 75% decrease in EtBr fluorescence was observed for the cells with higher MTS1338 abundance, whereas for the cells with low intracellular MTS1338 population, only a ~ 20% decrease in EtBr fluorescence was measured after 60 min. This experiment established that MTS1338 facilitates the deportation of EtBr, a surrogate of rifampicin, from the cells.

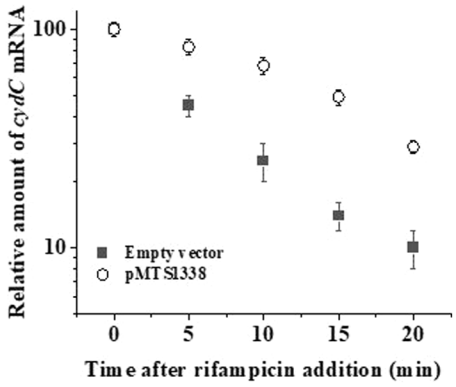

FIGURE 6
Stability of *cydC* mRNA with/without MTS1338 overexpression. Cells harboring either empty or pMTS1338 plasmids were grown to exponential phase (OD_{600}–0.9) and then tetracycline (1 μg/mL) was added to cells. Cells were further grown for 72 h and were treated with 500 mg/liter rifampicin. Samples were withdrawn at the indicated time points and the amount of cydC mRNA was determined by RT-qPCR analysis.

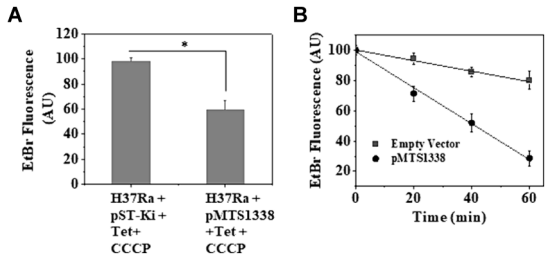

FIGURE 7
(A) Accumulation of EtBr in *M. tuberculosis* cells with/without MTS1338 overexpression. Cells (OD_{600} = 0.9) containing empty or recombinant pMTS1338 plasmids were allowed to grow in presence of tetracycline (1 μg/mL) for 72 h followed by the addition of EtBr (1 μg/mL). After 10 min CCCP (6.25 μM) was added to the culture. Cells were then pelleted down and resuspended in PBS containing CCCP. Intracellular EtBr fluorescence was measured by fluorimetry. Data was presented as the average ± SD from three separate experiments. One-way ANOVA was conducted and a difference of $*p < 0.05$ was considered statistically significant. **(B)** After the treatment with EtBr and CCCP, cells were resuspended in PBS and intracellular accumulation of EtBr was measured by fluorimetry at indicated time points. Data was presented as the average ± SD from three separate experiments.

4 Discussion

Although *M. tuberculosis* possesses an array of eccentric mechanisms to withstand antibiotic action, sRNA-mediated drug tolerance of mycobacteria has not been reported earlier. In the current study, we systematically analyzed the remodeling of an intracellular regulatory circuit of *M. tuberculosis* in response to antibiotic treatment. MTS1338, a distinctive sRNA exists only in pathogenic mycobacterial strains (Arnvig et al., 2011) and can confer pathogenic properties to nonpathogenic mycobacteria while expressed in a heterologous manner (Bychenko et al., 2021). Treatment of first-line antitubercular drug rifampicin on *M. tuberculosis* upregulated MTS1338, which in turn was found to ameliorate its survival in the presence of the drug. The treatment of a second-line drug kanamycin on *M. tuberculosis* also showed an identical effect on MTS1338. Examination of how MTS1338 promotes *M. tuberculosis* survival under rifampicin-exposed conditions revealed that a higher MTS1338 abundance induced an efflux protein CydC that minimizes drug concentration in the cell.

The global emergence of pathogens resistant to antimicrobial agents accounts for the increasing health crisis of people. Multifaceted approaches for the mitigation of disease prevalence by promoting antibiotic stewardship are required to control antimicrobial resistance and tolerance. Understanding how pathogens remodel their gene regulatory pathways against the existing antibiotic arsenal is a critical step for the development of new antimicrobial drugs or improving the self-life of current antibiotics (Mediati et al., 2021). Although multiple mechanisms have been elucidated for mycobacterial resistance against antibiotics, a small RNA regulator contributing to antimycobacterial resistance has never been reported before this study. However, the instances of sRNAs exist in pathogens other than mycobacteria acting as regulatory hubs for antibacterial resistance. A highly conserved sRNA SprX in *Staphylococcus aureus* causing bacteraemia, infective endocarditis, and osteomyelitis in humans alters antibiotic sensitivity by negatively regulating transcription factor SpoVG (Mediati et al., 2021; Eyraud et al., 2014; Liu et al., 2016). Two sRNAs, Sr0161 and ErsA, in multidrug-resistant *Pseudomonas aeruginosa* negatively regulate a major outer-membrane porin OprD, which is responsible for the uptake of carbapenem antibiotic. Thus, sRNA-mediated downregulation of OprD leads to bacterial resistance against carbapenem (Ochs et al., 1999; Zhang et al., 2017). Numerous sRNA in *E. coli*, e.g., MicF, GcvB, RyhB, etc. have been shown to modulate antibiotic sensitivity leading to resistance (Dersch et al., 2017). Many other pathogens like *Salmonella* sp. (Acuña et al., 2016), *Vibrio* sp. (Peschek et al., 2020), etc. exploit sRNAs to develop resistance against antibiotics. MTS1338-mediated growth advantage of *M. tuberculosis* under antibiotic-treated conditions confirms the sRNA orchestration of *cydC* upregulation for mycobacterial adaptation to antibiotic treatment.

Efflux of drugs through membrane transporters or efflux pump proteins is one of the paramount strategies of *M. tuberculosis* for acquiring antibiotic resistance (10). Efflux pumps are membrane-spanning proteins primarily controlled by regulatory systems that have evolved to counter antibiotics (Smith et al., 2013). In the current context, MTS1338 after being induced by rifampicin acts as a pivot that upregulates a higher intracellular abundance of efflux proteins CydC thereby promoting the deportation of drugs leading to the improvement of cellular fitness (Andersson and Hughes, 2010). Thus, CydC activity in *M. tuberculosis* is coupled to MTS1338 regulation and is conceivable to be involved during mycobacterial infection owing to MTS1338's role under that condition. *M. tuberculosis* possesses at least 18 different transporters related to antibiotic susceptibility (Viveiros et al., 2012). Thus, it would not be surprising if MTS1338 controls multiple transporters in response to antibiotic treatment. An example lies in *M. tuberculosis*, as a transcription regulator Lsr2 in this bacterium being upregulated by isoniazid and ethambutol negatively controlled the expression of two transporters IniBAC and EpfA, which led to obtaining resistance against antibiotics (Colangeli et al., 2007). CydC also can be controlled by multiple regulators as it happens in *E. coli* where three regulatory systems for antibiotics controlled a single transporter protein AcrB, a major determinant for multidrug

resistance (Alekshun and Levy, 1997). Additional studies are required to unfold the MTS1338-driven regulatory processes how MTS1338 facilitates the outflow of antibiotics through CydC.

Given the multidimensional role of MTS1338, it would not be surprising if MTS1338 is accountable for turning on other pathways leading to antimycobacterial resistance. As MTS1338 is induced in response to both front-line and second-line drugs, it is conceivable that MTS1338 might promote antibacterial resistance against a broad range of antibiotics. Several sigma factors and WhiB protein transcription factors have been identified to be responsible for antibiotic susceptibility (Miotto et al., 2022). The key among the WhiB proteins that promote antibacterial drug resistance is WhiB7 (Burian et al., 2013; Reeves et al. 2013; Pisu et al., 2017). WhiB7 is upregulated by several 100-folds upon exposure to front-line drugs like rifampicin and is barely controlled by MTS1338 as increased intracellular abundance does not significantly alter the intracellular accumulation of *whiB7* transcript (Singh and Dutta, unpublished observation). Likewise, SigE in *M. tuberculosis* was reported to be one of the leading among 13 Sigma factors gaining resistance against antibiotics (Pisu et al., 2017). *M. tuberculosis* also exploits many other transcription factors like GntR, XRE, etc. to obtain resistance (Miotto et al., 2022). Additional work is required to establish whether MTS1338 is involved in all the abovementioned mechanisms.

The current study depicted a novel antimycobacterial resistance mechanism regulated by a distinctive sRNA MTS1338 in *M. tuberculosis*. This adds substantially to our knowledge of how *M. tuberculosis* triggers a regulatory cascade for acquiring resistance against antimycobacterial drugs controlled by a sRNA, which was never unveiled before.

Data availability statement

The original contributions presented in the study are included in the article/Supplementary material, further inquiries can be directed to the corresponding author.

Author contributions

SS: Data curation, Formal analysis, Investigation, Methodology, Validation, Visualization, Writing – review & editing. TD: Conceptualization, Funding acquisition, Investigation, Project administration, Supervision, Writing – original draft, Writing – review & editing.

Funding

The author(s) declare that financial support was received for the research, authorship, and/or publication of this article. This work was supported by the Indian Council for Medical Research, Govt. of India for funding research grants (no-52/18/2022-BMS and 52/07/2019-BMS) to TD. TD also thanks IIT Delhi for funding the FIRP grant (MI02367G) to initiate this research work.

Acknowledgments

SS acknowledges the Indian Council for Medical Research, Govt. of India for providing her Research Associateship.

Conflict of interest

The authors declare that the research was conducted in the absence of any commercial or financial relationships that could be construed as a potential conflict of interest.

Publisher's note

Supplementary material

The Supplementary material for this article can be found online at: https://www.frontiersin.org/articles/10.3389/fmicb.2024.1469280/full#supplementary-material

References

Acuña, L. G., Barros, M. J., Peñaloza, D., Rodas, P. I., Paredes-Sabja, D., Fuentes, J. A., et al. (2016). A feed-forward loop between SroC and MgrR small RNAs modulates the expression of eptB and susceptibility of polymyxin B in *Salmonella Typhimurium*. *Microbiology* 162, 1996–2004. doi: 10.1099/mic.0.000365

Alekshun, M. N., and Levy, S. B. (1997). Regulation of chromosomally mediated multiple antibiotic resistance: the mar regulon. *Antimicrob. Agents Chemother.* 41, 2067–2075. doi: 10.1128/AAC.41.10.2067

Almeida Da Silva, P. E., and Palomino, J. C. (2011). Molecular basis and mechanisms of drug resistance in *Mycobacterium tuberculosis*: classical and new drugs. *J. Antimicrob. Chemother.* 66, 1417–1430. doi: 10.1093/jac/dkr173

Andersson, D. I., and Hughes, D. (2010). Antibiotic resistance and its cost: is it possible to reverse resistance? *Nat. Rev. Microbiol.* 8, 260–271. doi: 10.1038/nrmicro2319

Arnvig, K. B., Comas, I., Thomson, N. R., Houghton, J., Boshoff, H. I., Croucher, N. J., et al. (2011). Sequence-based analysis uncovers an abundance of noncoding RNA in the total transcriptome of *Mycobacterium tuberculosis*. *PLoS Pathog.* 7:e1002342. doi: 10.1371/journal.ppat.1002342

Arnvig, K. B., and Young, D. B. (2012). Noncoding RNA and its potential role in *Mycobacterium tuberculosis* pathogenesis. *RNA Biol.* 9, 427–436. doi: 10.4161/rna.20105

Barilar, I., and Battaglia, S. (2024). Quantitative measurement of antibiotic resistance in *Mycobacterium tuberculosis* reveals genetic determinants of resistance and susceptibility in a target gene approach. *Nat. Commun.* 15:488. doi: 10.1038/s41467-023-03651-4

Briffotaux, J., Liu, S., and Gicquel, B. (2019). Genome-wide transcriptional responses of *Mycobacterium* to antibiotics. *Front. Microbiol.* 10:249. doi: 10.3389/fmicb.2019.00249

Burian, J., Yim, G., Hsing, M., Axerio-Cilies, P., Cherkasov, A., Spiegelman, G. B., et al. (2013). The mycobacterial antibiotic resistance determinant WhiB7 acts as a transcriptional activator by binding the primary sigma factor SigA (RpoV). *Nucleic Acids Res.* 41, 10062–10076. doi: 10.1093/nar/gkt751

Bychenko, O., Skvortsova, Y., Ziganshin, R., Grigorov, A., Aseev, L., Ostrik, A., et al. (2021). *Mycobacterium tuberculosis* small RNA MTS1338 confers pathogenic properties

to nonpathogenic *Mycobacterium smegmatis*. *Microorganisms* 9:414. doi: 10.3390/microorganisms9020414

Chen, H., Previero, A., and Deutscher, M. P. (2019). A novel mechanism of ribonuclease regulation: GcvB and Hfq stabilize the mRNA that encodes RNase BN/Z during exponential phase. *J. Biol. Chem.* 294, 19997–20008. doi: 10.1074/jbc.RA119.011367

Colangeli, R., Helb, D., Vilchèze, C., Hazbón, M. H., Lee, C. G., Safi, H., et al. (2007). Transcriptional regulation of multi-drug tolerance and antibiotic-induced responses by the histone-like protein Lsr2 in *M. tuberculosis*. *PLoS Pathog.* 3:e87. doi: 10.1371/journal.ppat.0030087

Dersch, P., Khan, M. A., Mühlen, S., and Görke, B. (2017). Roles of regulatory RNAs for antibiotic resistance in bacteria and their potential value as novel drug targets. *Front. Microbiol.* 8:803. doi: 10.3389/fmicb.2017.00803

Dhar, N., and McKinney, J. D. (2010). *Mycobacterium tuberculosis* persistence mutants identified by screening in isoniazid-treated mice. *Proc. Natl. Acad. Sci. USA* 107, 12275–12280. doi: 10.1073/pnas.1003219107

Dutta, T., and Srivastava, S. (2018). Small RNA mediated regulation in bacteria: a growing palette of diverse mechanisms. *Gene* 658, 105–112. doi: 10.1016/j.gene.2018.03.021

Eyraud, A., Tattevin, P., Chabelskaya, S., and Felden, B. (2014). A small RNA controls a protein regulator involved in antibiotic resistance in *Staphylococcus aureus*. *Nucleic Acids Res.* 42, 4892–4905. doi: 10.1093/nar/gku149

Ginsberg, A. M., and Spigelman, M. (2007). Challenges in tuberculosis drug research and development. *Nat. Med.* 13, 290–294. doi: 10.1038/nm0307-290

Heinrichs, M. T., May, R. J., Heider, F., Reimers, T., Peloquin, C. A., and Derendorf, H. (2018). *Mycobacterium tuberculosis* strains H37Ra and H37Rv have equivalent minimum inhibitory concentrations to most antituberculosis drugs. *Int. J. Mycobacteriol.* 7, 156–161. doi: 10.4103/ijmy.ijmy_33_18

Jernaes, M. W., and Steen, H. B. (1994). Staining of *Escherichia coli* for flow cytometry: influx and efflux of ethidium bromide. *Cytometry* 17, 302–309. doi: 10.1002/cyto.990170405

Lake, M. A., Adams, K. N., Nie, F., Fowler, E., Verma, A. K., Dei, S., et al. (2023). The human proton pump inhibitors inhibit *Mycobacterium tuberculosis* rifampicin efflux and macrophage-induced rifampicin tolerance. *Proc. Natl. Acad. Sci. USA* 120, 1–10. doi: 10.1073/pnas.2215512120

Liu, X., Zhang, S., and Sun, B. (2016). SpoVG regulates cell wall metabolism and oxacillin resistance in methicillin-resistant *Staphylococcus aureus* strain N315. *Antimicrob. Agents Chemother.* 60, 3455–3461. doi: 10.1128/AAC.00026-16

Mann, M., Wright, P. R., and Backofen, R. (2017). IntaRNA2.0: enhanced and customizable prediction of RNA–RNA interactions. *Nucleic Acids Res.* 45, W435–W439. doi: 10.1093/nar/gkx279

Martini, B. A., Grigorov, A. S., Skvortsova, Y. V., Bychenko, O. S., Salina, E. G., and Azhikina, T. L. (2023). Small RNA MTS1338 configures a stress resistance signature in *Mycobacterium tuberculosis*. *Int. J. Mol. Sci.* 24:7928. doi: 10.3390/ijms24097928

McKinney, J. D. (2000). In vivo veritas: the search for TB drug targets goes live. *Nat. Med.* 6, 1330–1333. doi: 10.1038/82142

Mediati, D., Wu, S., and Wu, W. (2021). Networks of resistance: small RNA control of antibiotic resistance. *Trends Genet.* 37, 35–45. doi: 10.1016/j.tig.2020.08.016

Miotto, P., Sorrentino, R., de Giorgi, S., Provvedi, R., Cirillo, D. M., and Manganelli, R. (2022). Transcriptional regulation and drug resistance in *Mycobacterium tuberculosis*. *Front. Cell. Infect. Microbiol.* 12:990312. doi: 10.3389/fcimb.2022.990312

Moores, A., Riesco, A. B., Schwenk, S., and Arnvig, K. B. (2017). Expression, maturation and turnover of DrrS, an unusually stable, DosR regulated small RNA in *Mycobacterium tuberculosis*. *PLoS One* 12:e0174079. doi: 10.1371/journal.pone.0174079

Nasiri, M. J., Haeili, M., Ghazi, M., Goudarzi, H., Pormohammad, A., Imani Fooladi, A. A., et al. (2017). New insights into the intrinsic and acquired drug resistance mechanisms in mycobacteria. *Front. Microbiol.* 8:681. doi: 10.3389/fmicb.2017.00681

Ochs, M. M., McCusker, M. P., Bains, M., and Hancock, R. E. W. (1999). Negative regulation of the *Pseudomonas aeruginosa* outer membrane porin OprD selective for imipenem and basic amino acids. *Antimicrob. Agents Chemother.* 43, 1085–1090. doi: 10.1128/AAC.43.5.1085

Peschek, N., Herzog, R., Singh, P. K., Sprenger, M., Meyer, F., Fröhlich, K. S., et al. (2020). RNA-mediated control of cell shape modulates antibiotic resistance in *Vibrio cholerae*. *Nat. Commun.* 11:6067. doi: 10.1038/s41467-020-19890-8

Petchiappan, A., and Chatterji, D. (2017). Antibiotic resistance: current perspectives. *ACS Omega* 2, 7400–7409. doi: 10.1021/acsomega.7b01368

Pisu, D., Provvedi, R., and Espinosa, D. M. (2017). The alternative sigma factors SigE and SigB are involved in tolerance and persistence to antitubercular drugs. *Antimicrob. Agents Chemother.* 61, e01596–e01516. doi: 10.1128/AAC.01596-16

Reeves, A. Z., Campbell, P. J., Sultana, R., Malik, S., Murray, M., Plikaytis, B. B., et al. (2013). Aminoglycoside cross-resistance in *Mycobacterium tuberculosis* due to mutations in the 5′ untranslated region of whiB7. *Antimicrob. Agents Chemother.* 57, 1857–1865. doi: 10.1128/AAC.02191-12

Remm, S., Earp, J. C., Dick, T., Dartois, V., and Seeger, M. A. (2022). Critical discussion on drug efflux in *Mycobacterium tuberculosis*. *FEMS Microbiol. Rev.* 46, 1–15. doi: 10.1093/femsre/fuab042

Salina, E. G., Grigorov, A., Skvortsova, Y., Majorov, K., Bychenko, O., Ostrik, A., et al. (2019). MTS1338, a small *Mycobacterium tuberculosis* RNA, regulates transcriptional shifts consistent with bacterial adaptation for entering into dormancy and survival within host macrophages. *Front. Cell. Infect. Microbiol.* 9:405. doi: 10.3389/fcimb.2019.00405

Sarathy, J. P., Dartois, V., and Lee, E. J. D. (2012). The role of transport mechanisms in *Mycobacterium tuberculosis* drug resistance and tolerance. *Pharmaceuticals* 5, 1210–1235. doi: 10.3390/ph5111210

Shi, L., Sohaskey, C. D., Kana, B. D., Dawes, S., North, R. J., Mizrahi, V., et al. (2005). Change in energy metabolism of *Mycobacterium tuberculosis* in mouse lung and under in vitro conditions affecting aerobic respiration. *Proc. Natl. Acad. Sci. USA* 102, 15629–15634. doi: 10.1073/pnas.0507850102

Singh, S., Nirban, R., and Dutta, T. (2021). MTS1338 in *Mycobacterium tuberculosis* promotes detoxification of reactive oxygen species under oxidative stress. *Tuberculosis* 131:102142. doi: 10.1016/j.tube.2021.102142

Smith, T., Wolff, K. A., and Nguyen, L. (2013). Molecular biology of drug resistance in *Mycobacterium tuberculosis*. *Curr. Top. Microbiol. Immunol.* 358, 53–80. doi: 10.1007/82_2012_303

Takiff, H. E., and Feo, O. (2015). Clinical value of whole-genome sequencing of *Mycobacterium tuberculosis*. *Lancet Infect. Dis.* 15, 1077–1090. doi: 10.1016/S1473-3099(15)00071-7

Taneja, S., and Dutta, T. (2019). On a stake out: mycobacterial small RNA identification and regulation. *Non-coding RNA Res.* 4, 86–95. doi: 10.1016/j.ncrna.2019.05.001

Udwadia, Z. F., Amale, R. A., Ajbani, K. K., and Rodrigues, C. (2012). Totally drug resistant tuberculosis in India. *Clin. Infect. Dis.* 54, 579–581. doi: 10.1093/cid/cir889

van den Boogaard, J., Lyimo, R., Irongo, C. F., Boeree, M. J., Schaalma, H., Aarnoutse, R. E., et al. (2009). Community vs. facility-based directly observed treatment for tuberculosis in Tanzania's Kilimanjaro region. *Int. J. Tuberc. Lung Dis.* 13, 1524–1529. doi: 10.5588/ijtld.09.0032

Viveiros, M., Martins, M., Rodrigues, L., Machado, D., Couto, I., Ainsa, J., et al. (2012). Inhibitors of mycobacterial efflux pumps as potential boosters for TB drugs. *Expert Rev. Anti-Infect. Ther.* 10, 983–998. doi: 10.1586/eri.12.89

Young, D. B., Perkins, M. D., Duncan, K., and Barry, C. E. III. (2008). Confronting the scientific obstacles to global control of tuberculosis. *J. Clin. Invest.* 118, 1255–1265. doi: 10.1172/JCI34614

Zhang, Y. F., Han, K., Chandler, C. E., Tjaden, B., Ernst, R. K., and Lory, S. (2017). Probing the sRNA regulatory landscape of *Pseudomonas aeruginosa*: post-transcriptional control of determinants of pathogenicity and antibiotic susceptibility. *Mol. Microbiol.* 106, 919–937. doi: 10.1111/mmi.13857

frontiers | Frontiers in Microbiology

TYPE Mini Review
PUBLISHED 11 October 2024
DOI 10.3389/fmicb.2024.1409085

OPEN ACCESS

EDITED BY
Lisheng Liao,
South China Agricultural University, China

REVIEWED BY
Eugene A. Rogozhin,
Institute of Bioorganic Chemistry (RAS), Russia
Hiroji Chibana,
Chiba University, Japan

*CORRESPONDENCE
Vinay Kumar Bari
✉ vinay.bari@cup.edu.in;
✉ vinayimt@gmail.com

RECEIVED 29 March 2024
ACCEPTED 26 September 2024
PUBLISHED 11 October 2024

CITATION
Tanwar S, Kalra S and Bari VK (2024) Insights into the role of sterol metabolism in antifungal drug resistance: a mini-review. *Front. Microbiol.* 15:1409085. doi: 10.3389/fmicb.2024.1409085

Insights into the role of sterol metabolism in antifungal drug resistance: a mini-review

Sunita Tanwar, Sapna Kalra and Vinay Kumar Bari*

Department of Biochemistry, School of Basic Sciences, Central University of Punjab, Bathinda, India

Sterols are essential for eukaryotic cells and are crucial in cellular membranes' structure, function, fluidity, permeability, adaptability to environmental stressors, and host-pathogen interactions. Fungal sterol, such as ergosterol metabolism, involves several organelles, including the mitochondria, lipid droplets, endoplasmic reticulum, and peroxisomes that can be regulated mainly by feedback mechanisms and transcriptionally. The majority of sterol transport in yeast occurs via non-vesicular transport pathways mediated by lipid transfer proteins, which determine the quantity of sterol present in the cell membrane. Pathogenic fungi *Candida*, *Aspergillus*, and *Cryptococcus* species can cause a range of superficial to potentially fatal systemic and invasive infections that are more common in immunocompromised patients. There is a significant risk of morbidity and mortality from these infections, which are very difficult to cure. Several antifungal drugs with different modes of action have received clinical approval to treat fungal infections. Antifungal drugs targeting the ergosterol biosynthesis pathway are well-known for their antifungal activity; however, an imbalance in the regulation and transport of ergosterol could lead to resistance to antifungal therapy. This study summarizes how fungal sterol metabolism and regulation can modulate sterol-targeting antifungal drug resistance.

KEYWORDS

ergosterol metabolism, oxysterol binding proteins, sterol transfer proteins, sterol regulation, pathogenic fungi

1 Introduction

Invasive fungal infections increased considerably in immunocompromised or critically ill patients, such as HIV-positive patients, cancer patients undergoing chemotherapy, and organ transplant recipients, which poses a significant global threat to human health (Pfaller and Diekema, 2007; Low and Rotstein, 2011; Garnacho-Montero et al., 2024). Worldwide, 150 million immunocompromised individuals suffer from fungal diseases, which claim the lives of about 1.7 million of them annually (Bongomin et al., 2017; Kainz et al., 2020). Usually, *Candida*, *Aspergillus*, and *Cryptococcus* spp., infections account for more than 90% of nosocomial fungal infections, primarily affecting immunocompromised individuals (Brown et al., 2012). Numerous species of *Candida* can cause invasive candidiasis, a severe infection that can affect the heart, brain, eyes, bones, blood, and other body parts of patients (Pfaller and Diekema, 2007; McCarty and Pappas, 2016; Lass-Flörl et al., 2024). The prevalence of *Candida albicans* and non-albicans species has grown, particularly in the last two decades (Deorukhkar et al., 2014; Pfaller et al., 2014). This is attributable to a rise in immune-related disorders, the overuse of immunosuppressive medicines, and the prolonged use of medical equipment. The *C. albicans* mainly cause candidiasis, however, several non-albicans species such as *C. parapsilosis, C. glabrata, C. krusei, C. tropicalis, C. dubliniensis, C. lusitaniae* also

reported from clinical samples of candidiasis patients (Deorukhkar et al., 2014; Hani et al., 2015; Makanjuola et al., 2018).

Several classes of antifungal drugs with different modes of action have been approved for use in clinical settings to treat fungal infections (Fuentefria et al., 2018). These antifungal drugs include azoles, allylamines, morpholines, polyenes, nucleoside analogs, and echinocandins. Azoles (e.g., fluconazole, voriconazole, and isavuconazole) mainly inhibit the ergosterol biosynthesis pathway enzyme lanosterol-14α-demethylase encoded by *ERG11* and interrupt the ergosterol biosynthesis (Chen and Sobel, 2005; Allen et al., 2015; Lee et al., 2023). Allylamines (e.g., terbinafine and naftifine) inhibit the squalene epoxidase encoded by *ERG1*, and morpholine (e.g., amorolfine, fenpropimorph, and tridemorph) inhibits the biosynthesis of sterol by blocking two successive enzymes (a) C-14 sterol reductase (*ERG24*) and (b) C-8 sterol isomerase (*ERG2*) (Debieu et al., 2000). Polyene (e.g., amphotericin B, nystatin, and natamycin) interacts with ergosterol in the cell membrane, creating pores and causing cell lysis, while echinocandin (e.g., caspofungin and micafungin) mainly inhibits the enzyme *β*-1,3-D-glucan synthase encoded by *FKS1* (Perlin, 2015; Ahmady et al., 2024). Nucleoside analogs, such as 5′-flucytosine (5-FC), are taken up by cytosine permease, a membrane transporter of fungal cells. Cytosine deaminase then transforms the 5-FC into 5-fluorouracil (5-FU), which is its active form. 5-fluorouracil is metabolized to produce 5-fluorouridine monophosphate (5-FUMP) and 5-fluorodeoxyuridine monophosphate (5-FdUMP), which, respectively, blocks RNA and DNA synthesis (Bhattacharya et al., 2020; Sigera and Denning, 2023). The chemical structure of antifungal drugs that selectively target the ergosterol production pathway of *S. cerevisiae* is shown in Figures 1A,B.

The existence of intrinsic, acquired, or clinical resistance poses a significant challenge that limits the potential for the development of novel therapeutics against *Candida* species (Sanguinetti et al., 2015; Chowdhary et al., 2017; Spivak and Hanson, 2018). The rise in clinical isolates of fungal pathogens that are highly virulent and resistant to drugs poses a severe threat to human health (Taei et al., 2019; McDermott, 2022). Public health worldwide is seriously threatened by the emergence of pan-resistant *C. auris* clinical isolates (Lockhart, 2019). Therefore, a fundamental comprehension of the molecular pathways that an appropriate drug can target aids in preventing the development of fungal drug resistance.

Ergosterol, a key sterol in fungal membranes, primarily regulates membrane fluidity, membrane-bound enzyme activity, growth, and other cellular processes, which makes them a potentially valuable target for drug development (Iwaki et al., 2008; Rodrigues, 2018). After being produced in the endoplasmic reticulum (ER), ergosterol is transferred to the plasma membrane (PM), which contains an enormous amount of the cell's free ergosterol pool (Mesmin et al., 2013). Newly produced ergosterol equilibrates with the PM localized sterol pool, with roughly 10^5 ergosterol molecules entering and exiting the PM per second (Hu et al., 2017). Sterols are insoluble in water, hence equilibration of free/available sterols between organelles needs lipid transfer proteins between membranes. Soluble lipid transfer proteins take a lipid from a donor membrane and deposit it to an acceptor membrane (Wong et al., 2019). Oxysterol-binding protein (OSBP) and OSBP-related proteins (ORPs) are key candidates of the eukaryotic gene family, including ORP in humans and oxysterol-binding homologous (Osh) proteins in yeast that transfer and regulate sterols and phospholipids between organelle membranes (Weber-Boyvat et al., 2013). Although ergosterol production and transport are well understood in model yeast, little is known about how they contribute to antifungal drugs. This study describes the key steps in ergosterol production and transport pathways that lead to antifungal drug resistance.

2 Ergosterol biosynthesis pathway

Ergosterol is mainly synthesized in the ER and transferred to various organelles such as mitochondria, Golgi body, and PM through vesicular and non-vesicular transport mechanisms (Lv et al., 2016; Jordá and Puig, 2020; Zheng Koh and Saheki, 2021). Sterol concentrations are low in the ER but raised in secretory organelles, with the maximum concentration in the PM (Zinser et al., 1993; Hannich et al., 2011). Ergosterol comprises four rings, an acyl side chain, and a hydrophilic hydroxyl group that makes it easy to introduce into membranes. Ergosterol's structure varies from cholesterol by two additional double bonds (at position C7 and C8) and an extra methyl group (at position C22 and C23) in the side chain (Vanegas et al., 2012).

Sterol biosynthesis in the model yeast *Saccharomyces cerevisiae* begins with the condensing two acetyl-CoA molecules to produce acetoacetyl-CoA, catalyzed by Erg10p (Liu et al., 2019). Erg13p catalyzes the conversion of a third acetyl-CoA to acetoacetyl-CoA, resulting in 3-hydroxy-3-methylglutarylCoA (HMG-CoA) (Miziorko, 2011). HMG-CoA is then reduced to mevalonate by HMG-CoA reductase encoded by Hmg1p and Hmg2p (Basson et al., 1986). Sterol intermediates block these reductases, making this a critical metabolic checkpoint. Erg12p phosphorylates mevalonate during the subsequent process (Oulmouden and Karst, 1991). Erg8p, a phosphomevalonate kinase, further phosphorylates to produce mevalonate-5-pyrophosphate (Tsay and Robinson, 1991). Next, Erg19p, a mevalonate pyrophosphate decarboxylase, decarboxylates isopentenyl pyrophosphate (IPP) (Berges et al., 1997). *IDI1* encodes the IPP isomerase, which converts IPP to dimethylallyl pyrophosphate (DPP). DPP then condenses with another IPP molecule to produce geranyl pyrophosphate, a further addition of IPP results in the formation of farnesyl pyrophosphate (FPP). The geranyl/FPP synthase, Erg20p, catalyzes both processes (Anderson et al., 1989).

Next, squalene synthase (Farnesyl-diphosphate farnesyl transferase) enzyme Erg9 uses two farnesyl-pyrophosphate (farnesyl-PP) molecules to form squalene. The enzymes squalene epoxidase *ERG1* and lanosterol synthase *ERG7* work in tandem to convert squalene to lanosterol. Lanosterol is converted into 4,4-dimethyl-cholesta 8,14, 24-trienol by lanosterol 14α-demethylase encoded by *ERG11* which is further converted into 4,4-dimethyl-zymosterol which is catalyzed by C14 sterol reductase (*ERG24*). 4,4-dimethyl-zymosterol is further converted into zymosterol by involving enzymes such as *ERG25*, *ERG26*, and *ERG27*. Finally, the enzyme C24-methyltransferase (Erg6p) converts the zymosterol into fecosterol. In the next step, fecosterol is converted into episterol, a reaction catalyzed by the C8 isomerase enzyme *ERG2*, and in the last step, episterol is transformed into ergosterol through a complex process involving C5-sterol desaturase (*ERG3*), C22-sterol desaturase (*ERG5*) and C24-sterol reductase (*ERG4*) reactions (Shakoury-Elizeh et al., 2010; Kathiravan et al., 2012; Joshua and Höfken, 2017; Ward et al., 2018; Liu et al., 2019; Vil et al., 2019). The sterol-desaturase

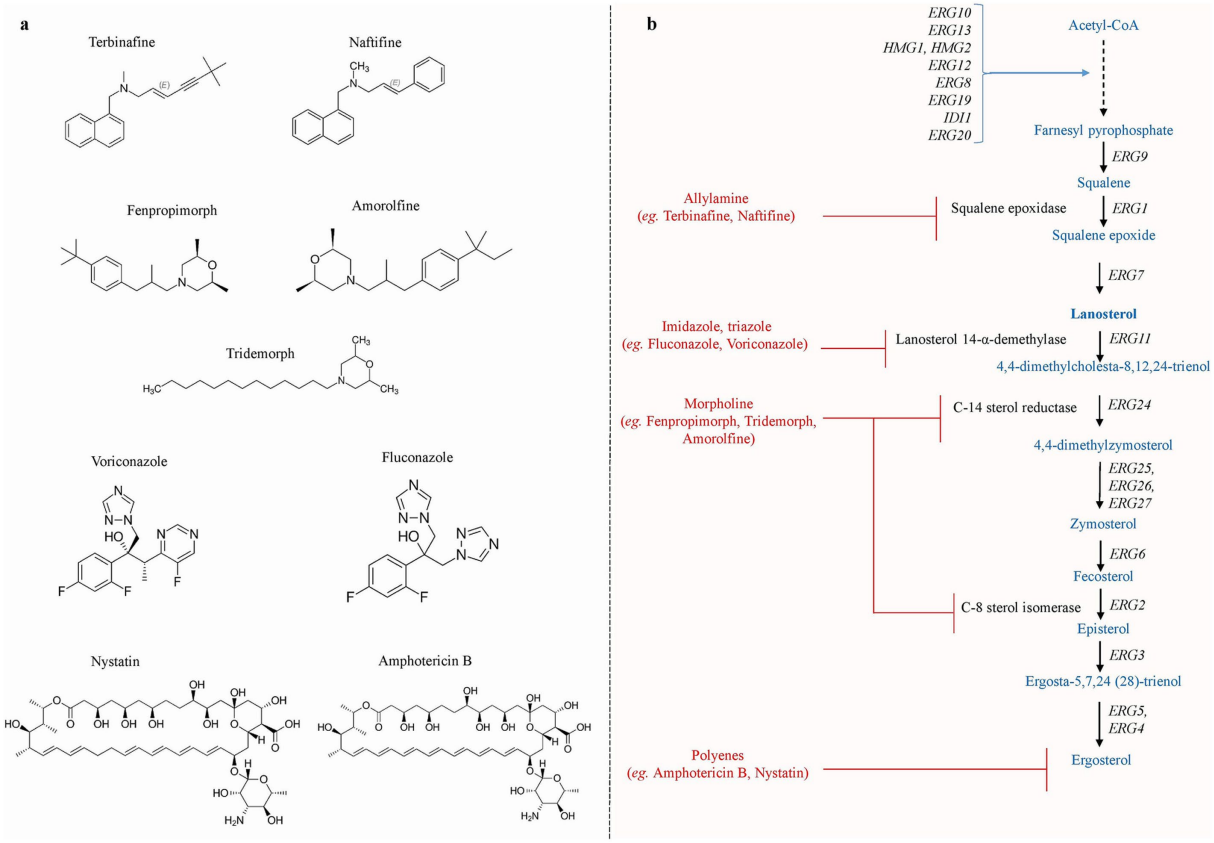

FIGURE 1
(a) The chemical structures of various antifungal drug that specifically targets the ergosterol biosynthesis pathway. **(b)** Schematic representation of ergosterol biosynthesis pathway reported in *S. cerevisiae*. The production of ergosterol molecules begins with the condensation of acetyl-Co and takes place mainly in the ER, whereas farnesyl-PP biosynthesis occurs in the vacuole. Allylamine inhibitors inhibit squalene epoxidase, which is encoded by *ERG1*. Azole inhibitors primarily target *ERG11*, resulting in the generation of hazardous sterols. Morpholines target step catalyzed by *ERG24* and *ERG2*, inhibiting ergosterol production, whereas polyene targets membranes' ergosterol [Adapted and modified from Onyewu et al., 2003].

enzyme, encoded by *CaERG3*, is known to utilize 14α-methyl-fecosterol in *C. albicans*. This enzyme catalyzes the conversion of 14α-methyl-fecosterol to 14α-methyl-ergosta-8,24(28)-dienol-3,6-diol, a toxic sterol linked to the antifungal activity of triazoles. Ergosterol biosynthesis in yeast depends on oxygen and iron at multiple steps such as enzymatic reactions catalyzed by *ERG1, ERG3, ERG5, ERG11*, and *ERG25* use molecular oxygen and heme as the electron acceptor (Jordá et al., 2022).

3 Ergosterol mediated antifungal drug resistance

3.1 Allylamine resistance

These days, allylamines such as naftifine and terbinafine are a relatively new class of synthetic antifungal medications against filamentous, dimorphic, yeast-like fungi (Hammoudi Halat et al., 2022). Allylamines act as non-competitive inhibitors mainly by interfering with the initial rate-limiting step of ergosterol biosynthesis catalyzed by squalene epoxidase encoded by *ERG1* (Petranyi et al., 1984). *C. albicans*, and *C. parapsilosis* squalene epoxidase, are susceptible to allylamine, while mammalian liver squalene epoxidase is significantly less sensitive to allylamines (Ryder, 1987; Ryder and Dupont, 1985). Naftifine is a topical fungicidal that is efficient against dermatophytes and is used to treat cutaneous candidiasis. Terbinafine hypersusceptibility was observed in strains overexpressing *ERG1, ERG9*, and *ERG26*. Erg9p converts FPP to produce squalene, a substrate for Erg1p. The overexpression of Erg9p or Erg1p may cause FPP or squalene pools to be diverted toward ergosterol biosynthesis rather than other cellular functions, leading to susceptibility in these strains (Bhattacharya et al., 2018). The *C. albicans erg2Δ/Δ* and *erg24Δ/Δ* mutants are also susceptible to terbinafine, due to the enhanced fluidity and permeability of their PMs (Luna-Tapia et al., 2015). Low terbinafine susceptibility was observed in oropharyngeal *C. albicans* isolates from HIV-positive individuals in a prior investigation (Odds, 2009). Another study also revealed that, except for *C. lusitaniae*, *C. parapsilosis*, and *C. krusei*, other *Candida* spp., isolates were resistant to terbinafine (MIC >32 mg/L) (Tøndervik et al., 2014).

3.2 Azole resistance

The azole-antifungal is the most extensive and frequently utilized class of antifungal drugs (Jangir et al., 2023). Azole targets the

ergosterol biosynthesis leading to the formation of unusual sterols disrupting the fungal cell membrane. Azoles inhibit the enzyme called lanosterol 14α-demethylase, encoded by *ERG11* (*CYP51*), which is a fungal cytochrome P450-(CYP50) family-dependent enzyme that converts lanosterol into 14α-dimethyl-lanosterol in the ergosterol biosynthesis pathway. The inhibition of this enzyme increases lanosterol and 14α-methyl sterol levels while ergosterol levels decrease. This causes the fungal cell membrane's typical permeability and fluidity to change, which inhibits the growth of fungal cells (Peyton et al., 2015; Zhang et al., 2019). *ERG2* deletion or *HMG1* overexpression strains showed increased susceptibility when treated with azoles due to lower ergosterol contents (Donald et al., 1997; Bhattacharya et al., 2018). In *S. cerevisiae* and *C. albicans Δerg3* and *Δerg6* deletion strains are resistant to fluconazole due to their inability to manufacture toxic dienol, which accumulates in the wild-type cell after azole treatment (Kodedová and Sychrová, 2015). Fluconazole resistance is also observed in *ERG3* deletion/missense mutant strains of *Cryptococcus neoformans*, *C. glabrata*, *C. parapsilosis*, and *C. albicans* (Branco et al., 2017; Sanglard et al., 2003). Mutation in *ERG25* leads to sterol intermediate accumulation and decreases fluconazole's binding affinity (Kodedová and Sychrová, 2015; Cavassin et al., 2021). Overexpression of *ERG11* in *C. albicans*, *C. glabrata*, *C. krusei*, and multidrug resistance *C. auris* showed higher resistance to azoles (He et al., 2015; Feng et al., 2017; Bhattacharya et al., 2019).

3.3 Morpholine resistance

The ergosterol production pathway enzymes, mainly C14-sterol reductase (*ERG24*), and C8-sterol isomerase (*ERG2*) are targeted by the morpholine class of antifungals e.g., amorolfine, fenpropimorph (FEN) and tridemorph, which leads to the accumulation of abnormal sterols ignosterol (ergosta-8,14 dieno) (Polak, 1988; Lorenz and Parks, 1992; Parks and Casey, 1995). The observation of FEN resistance in strains overexpressing *ERG24* supports that Erg24p is the principal morpholine drug target (Henry et al., 2000). In addition, FEN resistance was observed in disruption mutants of *ERG4*. FEN hypersusceptibility was detected in the strains that overexpressed *NCP1*, *ERG1*, and *HMG1* or in *Δerg3* and *Δerg6* deletion strains (Bhattacharya et al., 2018). It was discovered that *C. albicans* sensitivity to the morpholines can be decreased by overexpressing the *ERG2* or *ERG24* genes (Luna-Tapia et al., 2015). The *erg2Δ* deletion mutant of *C. albicans* was sensitive to FEN, whereas the *erg24Δ* deletion mutant was hypersensitive to amorolfine, FEN, and tridemorph. Mutation in the open reading frame of gene *FEN2* from *S. cerevisiae* that encodes a PM H^+-pantothenate symporter was shown to be FEN resistance (Stolz and Sauer, 1999). These findings support the theory that the morpholine's antifungal action depends on the simultaneous inhibition of Erg2p and Erg24p.

3.4 Polyene resistance

Polyene class includes amphotericin B (AmB), nystatin, natamycin, and filipins that target PM ergosterol and create a pore in the membrane (Madaan and Bari, 2023). Changes in ergosterol content or the substitution of sterol intermediates are the causes of polyene resistance (Ahmady et al., 2024). Previous research concluded that *C. lusitaniae* may become resistant to AmB due to mutations in or changes in the expression of ergosterol biosynthesis genes (Young et al., 2003). Elevated *ERG6* transcript levels and decreased ergosterol content were observed in *C. lusitaniae* resistant to AmB, indicating mutations or dysregulation in the ergosterol biosynthesis pathway (Bhattacharya et al., 2018). In clinical isolates of *C. glabrata, ERG6*, and *ERG2* are important targets associated with reduced susceptibility to AmB (Ahmad et al., 2019). AmB-resistant isolates also showed lower expression of the *ERG3* gene, which codes for C5 sterol desaturase, suggesting a possible involvement of *ERG3* in the clinical emergence of AmB resistance (Young et al., 2003). *C. neoformans* strains with sterol compositions corresponding to *ERG2* deletion mutant of *S. cerevisiae* are resistant to AmB (Kelly et al., 1994). A previous study in *S. cerevisiae* reported that, as compared to the parental strain, the mutant lacking *ERG4* was slightly more sensitive to nystatin; moreover, the deletion of *ERG2, ERG6,* and, to a lesser extent, *ERG3*, also conferred resistance to this polyene, most likely because of the decreased drug binding affinity for the accumulated fecosterol, zymosterol, and episterol in these mutants (Kodedová and Sychrová, 2015). Natamycin and nystatin-induced loss of inhibition was demonstrated by the loss of double bonds in the B-ring of ergosterol produced by deletions of *ERG3* (5,6 position) and particularly *ERG2* (7,8 position) (te Welscher et al., 2010).

mRNA expression levels of *ERG3* and *ERG6* were decreased but increased for *ERG11* in AmB-resistant isolates of *C. parapsilosis* (Lotfali et al., 2017). The loss of function of *ERG5* (C22 sterol desaturase) or substitution in *ERG11* has been associated with AmB resistance in *C. albicans* (Martel et al., 2010; Vincent et al., 2013). Inactivation of *ERG2* (C8 sterol isomerase) and *ERG6* (C24 sterol methyl-transferase) was reported to have a similar impact on *C. glabrata* (Ahmad et al., 2019). One of the only mechanisms of AmB resistance in *C. neoformans* that has been described involves a mutation that renders *ERG2* inactivated (Kelly et al., 1994). Altered sterol profile due to mutations in several ergosterol biosynthetic pathways genes *ERG11*, *ERG3*, *ERG2*, and *ERG6* also cause AmB resistance in *Candida* species (Vandeputte et al., 2008; Vincent et al., 2013; Carolus et al., 2021; Rybak et al., 2022). Table 1 lists the genes related to ergosterol metabolism and transport pathways that are implicated in resistance to antifungal drugs.

4 Ergosterol biosynthesis regulation

Ergosterol biosynthesis and degradation must be balanced and regulated to prevent the buildup of free sterols, which can be harmful to cells. Yeast cells have evolved distinct regulatory systems that carefully control the ergosterol composition of lipids. Feedback regulation of ergosterol biosynthesis at the biosynthetic level and transcriptional regulation is responsible for regulating the amount of ergosterol (Jordá and Puig, 2020). Furthermore, the ergosterol pathway enzymes exhibit differential localization. For example, *ERG1* localizes exclusively to the ER to enhance ergosterol synthesis; *ERG6* localizes to the ER, mitochondria, and cytoplasm; however, *ERG1* and *ERG6* also localize in a lipid particle (Leber et al., 1998; Shakoury-Elizeh et al., 2010).

Several enzymes involved in the process of ergosterol biosynthesis work together to control the level of ergosterol produced. Squalene, epoxy squalene, and polyepoxyl squalene, for instance, increase when *ERG27* is inhibited, but not lanosterol, which is identical to that in the

TABLE 1 A list of ergosterol metabolic and transport pathways genes involved in antifungal drug resistance.

Antifungal drugs	Name of the genes involved in ergosterol biosynthesis	Fungal species	Type of genetic approach (Resistance or Sensitive)	References
Amphotericin B	*ERG2, ERG3, ERG5, ERG6, ERG1*	*C. albicans, C. neoformans,C. lusitaniae, S. cerevisiae, C. haemulonii*	Deletion (R)	Ahmad et al. (2019), Lotfali et al. (2017), Martel et al. (2010), and Young et al. (2003)
	ERG26, ERG6	*S. cerevisiae*	Overexpression (S)	Bhattacharya et al. (2018)
	LAM1, LAM2, LAM3	*S. cerevisiae, C. neoformans*	Deletion (S)	Choy et al. (2003) and Sokolov et al. (2020)
	LAM2, LAM4	*S. cerevisiae*	Deletion (S)	
	ERG2	*C. albicans*	Double deletion	Luna-Tapia et al. (2015)
	OSH2	*S. cerevisiae*	Deletion (R)	Bojsen et al. (2016)
	OSHB, OSHE	*A. nidilans*	Deletion(R)	Bühler et al. (2015)
	OSHC, OSHD	*A. nidulans*	Deletion(S)	
Azoles	*ERG11*	*C. glabrata, C. albicans, S. cerevisiae*	Overexpression (R)	Bhattacharya et al., 2018, Kodedová and Sychrová (2015), Lotfali et al. (2017), and Young et al. (2003)
	HMG1, ERG6, ERG3	*C. lusitaniae, C. albicans, S. cerevisiae*	Deletion (R)	
	ERG2	*C. neoformatus*	Deletion(S)	
	ERG24	*C. glabrata*	Deletion (R)	
	HMG1	*S. cerevisiae*	Overexpression (S)	Bhattacharya et al. (2018)
	OSH1, ERG3, ERG6, ERG28	*S. cerevisiae*	Deletion (R)	Anderson et al. (2003)
	LAM2, LAM4	*S. cerevisiae*	Deletion (R)	Sokolov et al. (2020)
Fenpropimorph	*ERG2, ERG24*	*C. albicans*	Deletion (S)	Luna-Tapia et al. (2015)
	HMG1, ERG1	*S. cerevisiae*	Overexpression (S)	Bhattacharya et al. (2018) and Young et al. (2003)
	ERG6, ERG3	*C. lusitaniae, S. cerevisiae*	Deletion (S)	
	ERG24	*S. cerevisiae*	Overexpression (R)	
Tridemorph	*ERG2*	*S. cerevisiae*	Deletion (R)	Valachovic et al. (2001)
Terbinafine	*ERG24, ERG2*	*C. albicans*	Deletion (S)	Onyewu et al. (2003) and Luna-Tapia et al. (2015)
	ERG6	*C. lusitaniae*	Deletion (S)	Young et al. (2003)
	ERG9, ERG1, ERG26	*S. cerevisiae*	Overexpression (S)	Bhattacharya et al. (2018)

*erg7*Δ mutant and suggests that *ERG7* and *ERG27* interact genetically (Teske et al., 2008). Subsequent research demonstrated that *ERG27* can interact with *ERG7* and facilitate a relationship between *ERG7* and lipid particles to inhibit *ERG7* degradation; additionally, *ERG27* regulates *ERG7* activity in lipid particles (Layer et al., 2013). Similarly, double deletion mutants of *ERG24* and *ERG4* cannot grow in either nutrient-rich medium YEPD or a synthetic complete medium in the presence of calcium. This phenomenon is also observed when *ERG24* is altered with three additional genes, namely *ERG3*, *ERG5*, and *ERG6* (Luna-Tapia et al., 2015). Furthermore, the expression of ergosterol synthesis is also regulated by the intracellular transportation of ergosterol.

Two endoplasmic reticulum-localized acyl-coenzyme A: sterol acyltransferases, *ARE1* and *ARE2*, which are significantly implicated in sterol esterification, are encoded by *S. cerevisiae* (Yang et al., 1996). Under normal growth conditions, Are2p esterifies the final product, while Are1p primarily esterifies intermediates in sterol biosynthesis (Valachovic et al., 2001). In *S. cerevisiae*, neutral lipids are generated by four enzymes: Are1p and Are2p, which generate stearyl esters; and Lro1p and Dga1p, which generate triacylglycerol and are stored as lipid droplets (Jacquier et al., 2011). *ARE* genes are differently regulated in response to variations in sterol metabolism. The major isoform of the enzyme in a wild-type cell developing aerobically is Are2p. The accumulation of ergosterol pathway intermediates or heme deficiency causes the *ARE1* gene to be up-regulated, while *ARE2* is repressed under heme deficiency. This suggests that the controlled removal of intermediates in the biosynthesis process before they become toxic or contribute to accumulation in the final product is a novel form of sterol homeostasis (Jensen-Pergakes et al., 2001). Despite altered sterol composition, in an ARE1, ARE2 double mutant, stearyl esters (SE) biosynthesis is blocked without any growth defects (Ploier et al., 2015). The double mutant exhibits an increase in free sterols and a decrease in total sterol biosynthesis, suggesting that the formation of SE can also regulate sterol biosynthesis (Ploier et al., 2015). Optimizing culture conditions and metabolic pathway engineering are the two primary techniques for increasing ergosterol productivity since ergosterol biosynthesis is controlled by genes that regulate the biosynthesis and environmental factors (Náhlík et al., 2017). For example, ergosterol biosynthesis can be markedly increased by overexpressing sterol biosynthesis genes (e.g., *ERG1*, *ERG4*, *EGR9*, and *ERG11*) or *ARE2*. Thus, ergosterol biosynthesis regulation is a complicated process influenced by various factors.

Another important metabolic checkpoint for the biosynthesis of ergosterol is the synthesis of HMG-CoA, which is catalyzed by HMG-CoA reductase (HMGR) (Burg and Espenshade, 2011). Excessive sterols in *S. cerevisiae* can cause HMGR (Hmg2) to be degraded via the ER-related degradation (ERAD) pathway, which lowers mevalonate synthesis and down-regulates sterol production (Espenshade and Hughes, 2007). The ERAD process primarily initiates HMGR degradation with the help of membrane-spanning ubiquitin-protein ligase Hrd1, ubiquitin-conjugating enzyme Ubc7, and the chaperone proteins *NSG1* and *NSG2* (Hampton and Bhakta, 1997; Burg and Espenshade, 2011; Theesfeld and Hampton, 2013; Figure 2A). *ERG1* is also degraded by the ERAD pathway via ubiquitin ligase Doa10 when lanosterol concentration increases to prevent the accumulation of toxic sterol intermediates (Foresti et al., 2013; Huang and Chen, 2023). As a result, ERAD is crucial for preserving cellular sterol homeostasis.

Most fungi including fission yeast *Schizosaccharomyces pombe* and opportunistic pathogen *C. neoformans* contain a homolog of the mammalian sterol regulatory element binding protein (SREBP) known as Sre1, while in *Aspergillus fumigatus* called SrbA (Brown and Goldstein, 1997; Willger et al., 2008; Chang et al., 2009). SREBP-like proteins are activated upon cleavage by SREBP activating protein (SCAP) known as Scp1, that is absent in *A. fumigatus* (Willger et al., 2008). Sre1 localizes to the ER and regulates sterol-specific gene expression (Gómez et al., 2020). Under low sterol conditions, Sre1 gets cleaved and enters the nucleus, binds to sterol regulatory elements (SREs), and increases the expression of sterol-synthesizing genes (Hughes et al., 2005). In addition, hypoxic conditions also induce cleavage of Sre1 and lead to the expression of oxygen-dependent enzymes in the ergosterol biosynthesis pathway including Erg3 and Erg25 (Bien and Espenshade, 2010; Tong et al., 2018). Nevertheless, ergosterol production and absorption are regulated differently depending on the kind of yeast. Fission yeast without Sre1 and Scp1 cannot grow in anaerobic conditions as they cannot manufacture ergosterol at low oxygen levels (Hughes et al., 2005; Stewart et al., 2011; Chong and Espenshade, 2013). Similarly, budding yeast does not take up exogenous sterol, under aerobic or normal growth conditions. But in hypoxic/anaerobic environments, budding yeast does take up exogenous sterol; in fact, sterol absorption is critical to the survivability of budding yeast during anaerobic growth when sterol production is restricted by low oxygen supply (da Costa et al., 2018). Under aerobic circumstances or in the presence of azoles, *C. glabrata* can also absorb cholesterol (Nakayama et al., 2007; Nagi et al., 2013). Moreover, *C. glabrata* can import cholesterol and use it instead of ergosterol when vital genes *ERG1*, *ERG7*, or *ERG11* are knocked down, but this is not the case when *ERG25* and *ERG26* are knocked down (Okamoto et al., 2022).

While budding yeast lacks SREBP homologs, it does have a unique sterol regulatory mechanism that controls ergosterol production. This mechanism involves Upc2 and its paralog Ecm22, both are transcription factors specific to the fungal family able to bind with sterol regulatory elements (SRE) through their amino-terminal Zn_2Cys_6 DNA binding domain (Vik and Rine, 2001; Yang et al., 2015). Lethality results from the deletion of Ecm22 and Upc2, indicating that both proteins are crucial for controlling sterol metabolism in budding yeast (Shianna et al., 2001). Upc2 has a hydrophobic pocket in its C-terminal domain that binds to sterol and controls the protein's transition between the cytosol and nucleus (Vik and Rine, 2001; Marie et al., 2008). Under normal conditions, ergosterol binds with the *UPC2* carboxy-terminal domain causing repression of the *UPC2* transcription factor (Shianna et al., 2001). Under ergosterol depletion or hypoxic conditions, ergosterol ligand dissociation causes conformational changes and the Upc2 transcription factor translocated to the nucleus and activates SRE-containing genes including ergosterol biosynthesis genes, sterol uptake genes (*AVS1*, *PDR11*), and *DAN1/TIR* mannoprotein genes during the anaerobic remodeling of the cell wall (Abramova et al., 2001; Figure 2A).

Dimerization of *UPC2* essential for regulatory function, gain of function mutation in *UPC2* leads to azole resistance while deletion of *UPC2* in *C. albicans* sensitizes them toward azoles (Whaley et al., 2014; Yang et al., 2015). According to previous research, the transcription factors *ECM22* and *UPC2*, the SRE region of the sterol biosynthesis genes enhance their expression under hypoxic conditions (Davies and Rine, 2006; Woods and Höfken, 2016). *AUS1* and *PDR11*, two ATP-binding transporters, can also be expressed in response to *UPC2*, which promotes yeast to absorb sterols from its surroundings. Ergosterol production is further impacted by additional environmental variables such as oxidation, ethanol stimulation, and iron availability (Barchiesi et al., 2005).

5 Ergosterol transport pathways

Sterol transport between organelles and release into the medium rely on vesicular or nonvesicular transport pathway (Jacquier and Schneiter, 2012). Under aerobic conditions, yeast does not incorporate exogenous sterols, however, under hypoxia/anaerobic conditions ability to synthesize sterol is decreased which is compensated by the import of sterol from the medium through nonvesicular intracellular trafficking (Lev, 2010). Newly produced lipids are transported non-selectively from the ER to the PM via secretory vesicle flux (Wong et al., 2019). Lipid transfer proteins and sterol binding proteins are two evolutionarily conserved families of proteins that mediate intracellular sterol distribution (Lin et al., 2023). All eukaryotes have the evolutionarily conserved lipid transport proteins (LTPs) known as Oxysterol-binding protein Homology [Osh] in yeast, and Oxysterol-binding Protein [OSBP] and OSBP-Related Protein [ORP] in mammals (Schulz and Prinz, 2007; Lev, 2010; Ngo et al., 2010). The primary biological functions of OSBP and ORP include signaling, vesicular trafficking, lipid metabolism, and non-vesicular transport (Raychaudhuri and Prinz, 2010; Jackson et al., 2016). It has been demonstrated that these proteins can bind and transport different lipids, such as phosphoinositides (PIPs), and sterols (Ngo et al., 2010; Delfosse et al., 2020; Lin et al., 2023; Nakatsu and Kawasaki, 2021).

There is evidence supporting the function of a cytoplasmic nonvesicular protein sterol transporter, and the structure of an oxysterol-binding protein homolog (OSH) in yeast (Osh4p/Kes1p) has been solved, without a ligand and in complexes with many oxysterols, cholesterol, and ergosterol, identifying it as a sterol-binding protein (Schulz and Prinz, 2007). A seven-member oxysterol-binding protein family (*Osh1-7*) in *S. cerevisiae* performs redundant, overlapping roles in sterol metabolism collectively necessary for maintaining intracellular sterol distribution and homeostasis. All seven proteins are demonstrated to have the highest homology within the restricted region of 150–200 amino acid residues that make up OSBP-related domains (ORD) involved in oxysterol binding and intracellular sterol distribution is significantly changed in mutants lacking any of these proteins, which is consistent with an involvement of Osh proteins in

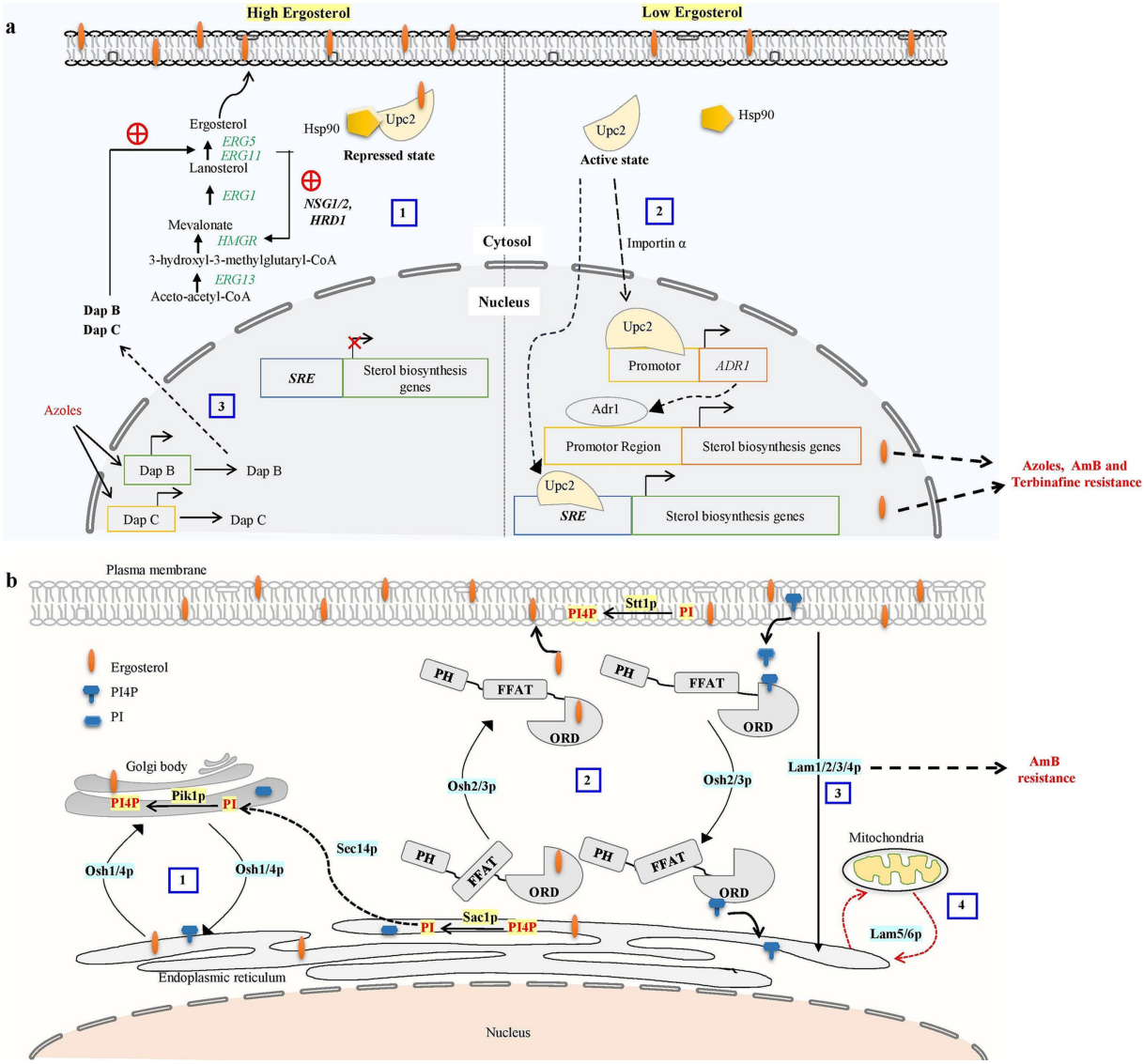

FIGURE 2
(a) Ergosterol biosynthetic pathway regulatory mechanism contributes to antifungal drug resistance. Overabundance of ergosterols may cause HMG-CoA reductase (HMGR) to be degraded via the proteasome, reducing mevalonate synthesis and down-regulating ergosterol biosynthesis. The ER-related degradation (ERAD) pathway mediates the proteasome recognition process of HMGR. The ERAD process primarily initiates HMGR breakdown by *HRD1* and the chaperone proteins *NSG1* and *NSG2* recognizing sterols (Omelchuk et al., 2018). **(1)** In excessive sterol conditions, the ergosterol pathway, specifically transcription factor *UPC2*, binds with ergosterol and Hsp90 and stays in the cytosol as a repressed state. **(2)** Under low ergosterol, dissociation of ergosterol leads to the relocalization of Upc2 from cytosol to the nucleus by nuclear transport proteins such as importins α. transcription factors *UPC2* can bind to the SRE of the sterol biosynthesis genes to promote their expression or Activated Upc2 also triggers the expression of the Adr1 transcription factor, which further serves to direct the expression of ergosterol biosynthesis genes. Activation of Upc2 or Adr1-enhanced azole, AmB, and terbinafine resistance in *Candida* (Shrivastava et al., 2023). **(3)** Three members of the heme-binding damage resistance proteins (Dap) family—*DapA, DapB,* and *DapC* in *A. fumigatus* modulate cytochrome P450 enzymes Erg5 and Erg11 in a coordinated manner and influence azole susceptibility (Song et al., 2016). **(b)** Overview of oxysterol binding protein-mediated sterol transport in *S. cerevisiae*. **(1)** Osh1 and Osh4p acts as a sterol-PI4P exchanger where it acquires the sterol from the donor membrane (ER) and exchange it for a PI4P at the acceptor membrane (trans-Golgi) and then carries the PI4P back to the donor membrane, completing the exchange cycle (Mochizuki et al., 2022). Sec14 protein is involved in the transport of PI from ER to Golgi. PI4P is converted into PI at the ER by Sac1p, and PI is phosphorylated into PI4P at the trans-Golgi by Pik1p (De Saint-Jean et al., 2011). **(2)** *OSH2* and *OSH3* contain the pleckstrin homology (PH) domain in the N-terminal region, the OSBP-related ligand binding domain (ORD) in the C-terminal region, and the (FFAT) motif. These play a part in the counter-transport of ergosterol and PI4P from the ER to the PM and from the PM to the ER, respectively. PI is phosphorylated into PI4P at the PM by Stt1. **(3)** Lam1p, Lam2p, Lam3p, and Lam4p is involved in retrograde transport of sterol. **(4)** *LAM5* and *LAM6* are involved in retrograde transport from ER to mitochondria (Elbaz-Alon et al., 2015; Gatta et al., 2015).

intracellular sterol transport (Beh et al., 2001; Beh and Rine, 2004; Schulz and Prinz, 2007).

All these proteins may have a hydrophobic binding tunnel that is important for interaction with sterol. PH domain located at N- the terminal of Osh1p, Osh2p, and Osh3p proteins may control protein targeting to membranes and function as membrane adaptors by interacting with phospholipids (Powis et al., 2023). Osh1p demonstrated a remarkable dual localization at the Golgi and

nucleus-vacuole (NV) junction (Levine and Munro, 2001). According to the deletion mapping of Osh1p, the PH domain is shown to be targeting the Golgi while the ankyrin repeat targets the NV junction (Kvam and Goldfarb, 2004). Osh2p is present in the PM, primarily found in the budding region of G1 phase cells around the mother-daughter bud neck of S-phase cells and in the scattered cytoplasmic pool (Levine and Munro, 2001). Osh3p is distributed throughout the cytoplasm and Osh4p is localized into the Golgi membrane (Li et al., 2002). Osh4p binds to phosphatidyl inositol 4-phosphate (PI4P) and its conserved OSBP domain is crucial for Osh4p localization to the Golgi membrane (Kyte and Doolittle, 1982; Rogaski et al., 2010). Osh5 protein is involved in the regulation of ergosterol biosynthesis and facilitates the transfer of phosphatidylserine (PtdSer) to autophagosome membranes (Muramoto et al., 2024), while Osh6p and Osh7p, located in the membrane contact site between the ER and PM, preferentially transporting PtdSer from the ER to PM (Maeda et al., 2013).

Primarily all Osh proteins contain a conserved OSBP-related domain (ORD) made up of an N-terminal lid and a β-barrel core, which transports lipids including sterol and phospholipids between membranes. Budding yeast mutants that lack all seven Osh (Osh1-7) proteins are not viable; nevertheless, they can become viable again if they express one of the Osh proteins. Moreover, abrupt Osh protein depletion causes a growth arrest and a massive buildup of sterol in cells (Beh and Rine, 2004). This suggests that Osh proteins perform roles in maintaining cell viability, probably by supporting the distribution of sterol throughout the cell.

Specific Osh proteins mediate the directional transport of sterol between two distinct membrane compartments by exchanging PI4P with sterol. Osh4 and other Osh proteins, including Osh3 and Osh5, mediated sterol transport from the PM to the ER. Osh4 localizes to the Golgi and is involved in controlling the amount of PI4P present in this organelle. Osh4 mutually exclusively binds Sterol and PI4P, and Osh4 counter-transports sterol between artificial membranes *in vitro* in return for PI4P (Rogaski et al., 2010). Previously, it was demonstrated that Osh4p plays a crucial role in maintaining the proper distribution of PI4P in yeast, a function that requires the cooperation of the oxysterol-binding proteins Osh1–Osh7 (LeBlanc and McMaster, 2010; Ling et al., 2014; Figure 2B). Two main PI 4-kinases in budding yeast oversee PI4P production at Golgi and PM. While Stt4 operates at the PM, Pik1 is a lipid kinase in the Golgi apparatus (Audhya et al., 2000). *C. albicans* contains four Osh proteins (Osh2-4 and Osh7), with Osh4 and Osh7 sharing approximately 60% similarity with their *S. cerevisiae* counterparts.

A novel evolutionarily conserved family of LTPs, known as Lam proteins belonging to the steroidogenic acute regulatory protein-related lipid transfer (StART) family was discovered in yeast (Gatta et al., 2015). These StART family proteins contain one or two StART-like domains that are conserved in eukaryotes and involved in transporting sterol between intracellular membranes. Six yeast proteins Ysp1/Lam1, Ysp2/Lam2, Sip3/Lam3, Lam4, Lam5, and Lam6 make up this family in budding yeast exhibit a C-terminal transmembrane region that attaches them to the membrane, and N-terminal StART-like domains, and other pleckstrin-homology (PH) superfamily domain (Gatta et al., 2015; Murley et al., 2015). The budding yeast that lacks Ysp1, Ysp2, or Sip3 exhibits reduced sterol trafficking from the PM to the ER and increased susceptibility to AmB and is rescued by multicopy expression of sterol-binding StART domains (Gatta et al., 2015). This suggests a persistent build-up of PM ergosterol in these yeast mutants. These experiments demonstrate that the Lam proteins help to maintain PM sterol homeostasis in yeast by transporting sterol from the PM to the ER (Figure 2B).

6 Conclusion

Finding inhibitors that target the ergosterol pathways in the fungus and can precisely block them without hurting the host is a significant challenge in the research of antifungals. The extensive use of antifungal drugs to treat fungal disease has led to the emergence of multidrug-resistant clinical isolates. Ergosterol alterations in multidrug resistance isolates can be understood by utilizing high throughput approaches, such as metabolomics of clinical isolate, to analyze changes in metabolic pathways and processes that lead to multi-drug resistance. Despite substantial progress in this area, little is known about the relationship between ergosterol transport control and antifungal drug resistance. Enzymes involved in ergosterol biosynthesis, regulation, and transport are necessary for pathogenic fungi to thrive inside their host species. These enzymes also play a crucial role in the virulence of pathogenic fungi. Thus, the pharmaceutical disruption of the ergosterol biosynthesis and transport would impair their ability to respond appropriately to the environmental stress that host cells experience, restricting the proliferation and pathogenicity of pathogenic fungi. Aspergillosis, candidiasis, and cryptococcosis are severe invasive mycoses that have a high mortality rate in immunocompromised patients. Few antifungal drugs are available to treat such invasive infections, and fungus resistance is increasing quickly. Since fungal ergosterol differs structurally from their mammalian counterparts, the ergosterol biosynthesis and transport pathway provides an opportunity to discover novel antifungal drugs. This review improves our understanding of the synthesis, transport, and regulation of ergosterol, which will aid in creating new inhibitors that specifically target ergosterol metabolism.

Author contributions

ST: Writing – original draft. SK: Formal analysis, Writing – review & editing. VB: Writing – review & editing, Supervision, Project administration.

Funding

The author(s) declare that financial support was received for the research, authorship, and/or publication of this article. This study acknowledges the support from the Science and Engineering Research Board (SERB), New Delhi (Award number SRG/2020/000171/LS) awarded to VKB. The funding agencies had no role in the preparation of the manuscript or in the decision to submit the article for publication.

Conflict of interest

The authors declare that the research was conducted in the absence of any commercial or financial relationships that could be construed as a potential conflict of interest.

Publisher's note

References

Abramova, N. E., Cohen, B. D., Sertil, O., Kapoor, R., Davies, K. J. A., and Lowry, C. V. (2001). Regulatory mechanisms controlling expression of the DAN/TIR mannoprotein genes during anaerobic remodeling of the cell wall in *Saccharomyces cerevisiae*. *Genetics* 157, 1169–1177. doi: 10.1093/genetics/157.3.1169

Ahmad, S., Joseph, L., Parker, J. E., Asadzadeh, M., Kelly, S. L., Meis, J. F., et al. (2019). ERG6 and ERG2 are major targets conferring reduced susceptibility to amphotericin B in clinical *Candida glabrata* isolates in Kuwait. *Antimicrob. Agents Chemother.* 63:18. doi: 10.1128/AAC.01900-18

Ahmady, L., Gothwal, M., Mukkoli, M. M., and Bari, V. K. (2024). Antifungal drug resistance in *Candida*: a special emphasis on amphotericin B. *APMIS* 132, 291–316. doi: 10.1111/apm.13389

Allen, D., Wilson, D., Drew, R., and Perfect, J. (2015). Azole antifungals: 35 years of invasive fungal infection management. *Expert Rev. Anti-Infect. Ther.* 13, 787–798. doi: 10.1586/14787210.2015.1032939

Anderson, M. S., Yarger, J. G., Burck, C. L., and Poulter, C. D. (1989). Farnesyl diphosphate synthetase. Molecular cloning, sequence, and expression of an essential gene from Saccharomyces cerevisiae. *J. Biol. Chem.* 264, 19176–19184. doi: 10.1016/s0021-9258(19)47284-0

Anderson, J. B., Sirjusingh, C., Parsons, A. B., Boone, C., Wickens, C., Cowen, L. E., et al. (2003). Mode of selection and experimental evolution of antifungal drug resistance in Saccharomyces cerevisiae. *Genetics* 163, 1287–98. doi: 10.1093/genetics/163.4.1287

Audhya, A., Foti, M., and Emr, S. D. (2000). Distinct roles for the yeast phosphatidylinositol 4-kinases, Stt4p and Pik1p, in secretion, cell growth, and organelle membrane dynamics. *Mol Bio Cell* 11, 2673–2689. doi: 10.1091/mbc.11.8.2673

Barchiesi, F., Spreghini, E., Tomassetti, S., Arzeni, D., Giannini, D., and Scalise, G. (2005). Comparison of the fungicidal activities of caspofungin and amphotericin B against *Candida glabrata*. *Antimicrob. Agents Chemother.* 49, 4989–4992. doi: 10.1128/AAC.49.12.4989-4992.2005

Basson, M. E., Thorsness, M., and Rine, J. (1986). *Saccharomyces cerevisiae* contains two functional genes encoding 3-hydroxy-3-methylglutaryl-coenzyme a reductase. *Proc. Natl. Acad. Sci. USA* 83, 5563–5567. doi: 10.1073/pnas.83.15.5563

Beh, C. T., Cool, L., Phillips, J., and Rine, J. (2001). Overlapping functions of the yeast oxysterol-binding protein homologues. *Genetics* 157, 1117–1140. doi: 10.1093/genetics/157.3.1117

Beh, C. T., and Rine, J. (2004). A role for yeast oxysterol-binding protein homologs in endocytosis and in the maintenance of intracellular sterol-lipid distribution. *J. Cell Sci.* 117, 2983–2996. doi: 10.1242/jcs.01157

Berges, T., Guyonnet, D., and Karst, F. (1997). The Saccharomyces cerevisiae mevalonate diphosphate decarboxylase is essential for viability, and a single Leu-to-Pro mutation in a conserved sequence leads to thermosensitivity. *J. Bacteriol.* 179, 4664–4670. doi: 10.1128/jb.179.15.4664-4670.1997

Bhattacharya, S., Esquivel, B. D., and White, T. C. (2018). Overexpression or deletion of Ergosterol biosynthesis genes alters doubling time, response to stress agents, and drug susceptibility in *Saccharomyces cerevisiae*. *mBio* 9, e01291–e01218. doi: 10.1128/mBio.01291-18

Bhattacharya, S., Holowka, T., Orner, E. P., and Fries, B. C. (2019). Gene duplication associated with increased fluconazole tolerance in *Candida auris* cells of advanced generational age. *Sci. Rep.* 9:5052. doi: 10.1038/s41598-019-41513-6

Bhattacharya, S., Sae-Tia, S., and Fries, B. C. (2020). Candidiasis and mechanisms of antifungal resistance. *Antibiotics* 9:312. doi: 10.3390/antibiotics9060312

Bien, C. M., and Espenshade, P. J. (2010). Sterol regulatory element binding proteins in fungi: hypoxic transcription factors linked to pathogenesis. *Eukaryot. Cell* 9, 352–359. doi: 10.1128/EC.00358-09

Bojsen, R., Regenberg, B., Gresham, D., and Folkesson, A. (2016). A common mechanism involving the TORC1 pathway can lead to amphotericin B-persistence in biofilm and planktonic Saccharomyces cerevisiae populations. *Sci. Rep.* 21874. doi: 10.1038/srep21874

Bongomin, F., Gago, S., Oladele, R. O., and Denning, D. W. (2017). Global and multi-national prevalence of fungal diseases—estimate precision. *J Fungi (Basel)* 3:57. doi: 10.3390/jof3040057

Branco, J., Fonseca, E., Gomes, N. C., Martins-Cruz, C., Silva, A. P., Silva-Dias, A., et al. (2017). Impact of *ERG3* mutations and expression of ergosterol genes controlled by *UPC2* and *NDT80* in *Candida parapsilosis* azole resistance. *Clin. Microbiol. Infect.* 23, 575.e1–575.e8. doi: 10.1016/j.cmi.2017.02.002

Brown, G. D., Denning, D. W., Gow, N. A., Levitz, S. M., Netea, M. G., and White, T. C. (2012). Hidden killers: human fungal infections. *Sci. Transl. Med.* 4:165rv13. doi: 10.1126/scitranslmed.3004404

Brown, M. S., and Goldstein, J. L. (1997). The SREBP pathway: regulation of cholesterol metabolism by proteolysis of a membrane-bound transcription factor. *Cell* 89, 331–340. doi: 10.1016/S0092-8674(00)80213-5

Bühler, N., Hagiwara, D., and Takeshita, N. (2015). Functional analysis of sterol transporter orthologues in the filamentous fungus *Aspergillus nidulans*. *Eukaryot. Cell* 14, 908–921. doi: 10.1128/EC.00027-15

Burg, J. S., and Espenshade, P. J. (2011). Regulation of HMG-CoA reductase in mammals and yeast. *Prog. Lipid Res.* 50, 403–410. doi: 10.1016/j.plipres.2011.07.002

Carolus, H., Pierson, S., Muñoz, J. F., Subotić, A., Cruz, R. B., Cuomo, C. A., et al. (2021). Genome-wide analysis of experimentally evolved Candida auris reveals multiple novel mechanisms of multidrug resistance. *MBio* 12:333. doi: 10.1128/mBio.03333-20

Cavassin, F. B., Baú-Carneiro, J. L., Vilas-Boas, R. R., and Queiroz-Telles, F. (2021). Sixty years of amphotericin B: an overview of the Main antifungal agent used to treat invasive fungal infections. *Infect. Dis. Ther.* 10, 115–147. doi: 10.1007/s40121-020-00382-7

Chang, Y. C., Ingavale, S. S., Bien, C., Espenshade, P., and Kwon-Chung, K. J. (2009). Conservation of the sterol regulatory element-binding protein pathway and its pathobiological importance in *Cryptococcus neoformans*. *Eukaryot. Cell* 8, 1770–1779. doi: 10.1128/EC.00207-09

Chen, A., and Sobel, J. D. (2005). Emerging azole antifungals. *Expert Opin. Emerg. Drugs* 10, 21–33. doi: 10.1517/14728214.10.1.21

Chong, R., and Espenshade, P. J. (2013). Structural requirements for sterol regulatory element-binding protein (SREBP) cleavage in fission yeast. *J. Biol. Chem.* 288, 20351–20360. doi: 10.1074/jbc.M113.482224

Chowdhary, A., Sharma, C., and Meis, J. F. (2017). *Candida auris*: a rapidly emerging cause of hospital-acquired multidrug-resistant fungal infections globally. *PLoS Pathog.* 13:e1006290. doi: 10.1371/journal.ppat.1006290

Choy, H. L., Gaylord, E. A., and Doering, T. L. (2003). Ergosterol distribution controls surface structure formation and fungal pathogenicity. *mBio* 14:e0135323. doi: 10.1128/mbio.01353-23

da Costa, B. L. V., Basso, T. O., Raghavendran, V., and Gombert, A. K. (2018). Anaerobiosis revisited: growth of *Saccharomyces cerevisiae* under extremely low oxygen availability. *Appl. Microbiol. Biotechnol.* 102, 2101–2116. doi: 10.1007/s00253-017-8732-4

Davies, B. S. J., and Rine, J. (2006). A role for sterol levels in oxygen sensing in *Saccharomyces cerevisiae*. *Genetics* 174, 191–201. doi: 10.1534/genetics.106.059964

De Saint-Jean, M., Delfosse, V., Douguet, D., Chicanne, G., Payrastre, B., Bourguet, W., et al. (2011). Osh4p exchanges sterols for phosphatidylinositol 4-phosphate between lipid bilayers. *J. Cell Biol.* 195, 965–978. doi: 10.1083/jcb.201104062

Debieu, D., Bach, J., Arnold, A., Brousset, S., Gredt, M., Taton, M., et al. (2000). Inhibition of ergosterol biosynthesis by morpholine, piperidine, and spiroketalamine fungicides in *Microdochium nivale*: effect on sterol composition and sterol $\Delta 8 \rightarrow \Delta 7$ isomerase activity. *Pestic. Biochem. Physiol.* 67, 85–94. doi: 10.1006/pest.2000.2485

Delfosse, V., Bourguet, W., and Drin, G. (2020). Structural and functional specialization of OSBP-related proteins. *Contact* 3:251525642094662. doi: 10.1177/2515256420946627

Deorukhkar, S. C., Saini, S., and Mathew, S. (2014). Non-albicans *Candida* infection: an emerging threat. *Interdiscip Perspect Infect Dis* 2014:7. doi: 10.1155/2014/615958

Donald, K. A., Hampton, R. Y., and Fritz, I. B. (1997). Effects of overproduction of the catalytic domain of 3-hydroxy-3-methylglutaryl coenzyme a reductase on squalene synthesis in *Saccharomyces cerevisiae*. *Appl. Environ. Microbiol.* 63, 3341–3344. doi: 10.1128/aem.63.9.3341-3344.1997

Elbaz-Alon, Y., Eisenberg-Bord, M., Shinder, V., Stiller, S. B., Shimoni, E., Wiedemann, N., et al. (2015). Lam6 regulates the extent of contacts between organelles. *Cell Rep.* 12, 7–14. doi: 10.1016/j.celrep.2015.06.022

Espenshade, P. J., and Hughes, A. L. (2007). Regulation of sterol synthesis in eukaryotes. *Annu. Rev. Genet.* 41, 401–427. doi: 10.1146/annurev.genet.41.110306.130315

Feng, W., Yang, J., Xi, Z., Qiao, Z., Lv, Y., Wang, Y., et al. (2017). Mutations and/or Overexpressions of ERG4 and ERG11 genes in clinical azoles-resistant isolates of *Candida albicans*. *Microb. Drug Resist.* 23, 563–570. doi: 10.1089/mdr.2016.0095

Foresti, O., Ruggiano, A., Hannibal-Bach, H. K., Ejsing, C. S., and Carvalho, P. (2013). Sterol homeostasis requires regulated degradation of squalene monooxygenase by the ubiquitin ligase Doa10/Teb4. *eLife* 2:e00953. doi: 10.7554/eLife.00953

Fuentefria, A. M., Pippi, B., Dalla Lana, D. F., Donato, K. K., and de Andrade, S. F. (2018). Antifungals discovery: an insight into new strategies to combat antifungal resistance. *Lett. Appl. Microbiol.* 66, 2–13. doi: 10.1111/lam.12820

Garnacho-Montero, J., Barrero-García, I., and León-Moya, C. (2024). Fungal infections in immunocompromised critically ill patients. *J. Intensive Med.* 4, 299–306. doi: 10.1016/j.jointm.2024.01.005

Gatta, A. T., Wong, L. H., Sere, Y. Y., Calderón-Noreña, D. M., Cockcroft, S., Menon, A. K., et al. (2015). A new family of StART domain proteins at membrane contact sites has a role in ER-PM sterol transport. *eLife* 4:e07253. doi: 10.7554/eLife.07253

Gómez, M., Campusano, S., Gutiérrez, M. S., Sepúlveda, D., Barahona, S., Baeza, M., et al. (2020). Sterol regulatory element-binding protein Sre1 regulates carotenogenesis in the red yeast *Xanthophyllomyces dendrorhous*. *J. Lipid Res.* 61, 1658–1674. doi: 10.1194/jlr.RA120000975

Hammoudi Halat, D., Younes, S., Mourad, N., and Rahal, M. (2022). Allylamines, Benzylamines, and fungal cell permeability: a review of mechanistic effects and usefulness against fungal pathogens. *Membranes* 12:1171. doi: 10.3390/membranes12121171

Hampton, R. Y., and Bhakta, H. (1997). Ubiquitin-mediated regulation of 3-hydroxy-3-methylglutaryl-CoA reductase. *Proc. Natl. Acad. Sci. USA* 94, 12944–12948. doi: 10.1073/pnas.94.24.12944

Hani, U., Shivakumar, H. G., Vaghela, R., Osmani, R. A. M., and Shrivastava, A. (2015). Candidiasis: a fungal infection- current challenges and Progress in prevention and treatment. *Infect. Disord. Drug Targets* 15, 42–52. doi: 10.217 4/1871526515666150320162036

Hannich, J. T., Umebayashi, K., and Riezman, H. (2011). Distribution and functions of sterols and sphingolipids. *Cold Spring Harb. Perspect. Biol.* 3:a004762. doi: 10.1101/cshperspect.a004762

He, X., Zhao, M., Chen, J., Wu, R., Zhang, J., Cui, R., et al. (2015). Overexpression of both ERG11 and ABC2 genes might be responsible for itraconazole resistance in clinical isolates of *Candida krusei*. *PLoS One* 10:e0136185. doi: 10.1371/journal.pone.0136185

Henry, K. W., Nickels, J. T., and Edlind, T. D. (2000). Upregulation of ERG genes in *Candida* species by azoles and other sterol biosynthesis inhibitors. *Antimicrob. Agents Chemother.* 44, 2693–2700. doi: 10.1128/AAC.44.10.2693-2700.2000

Hu, Z., He, B., Ma, L., Sun, Y., Niu, Y., and Zeng, B. (2017). Recent advances in Ergosterol biosynthesis and regulation mechanisms in *Saccharomyces cerevisiae*. *Indian J. Microbiol.* 57, 270–277. doi: 10.1007/s12088-017-0657-1

Huang, L. J., and Chen, R. H. (2023). Lipid saturation induces degradation of squalene epoxidase for sterol homeostasis and cell survival. *Life Sci. Alliance* 6:e202201612. doi: 10.26508/lsa.202201612

Hughes, A. L., Todd, B. L., and Espenshade, P. J. (2005). SREBP pathway responds to sterols and functions as an oxygen sensor in fission yeast. *Cell* 120, 831–842. doi: 10.1016/j.cell.2005.01.012

Iwaki, T., Iefuji, H., Hiraga, Y., Hosomi, A., Morita, T., Giga-Hama, Y., et al. (2008). Multiple functions of ergosterol in the fission yeast *Schizosaccharomyces pombe*. *Microbiol* 154, 830–841. doi: 10.1099/mic.0.2007/011155-0

Jackson, C. L., Walch, L., and Verbavatz, J. M. (2016). Lipids and their trafficking: an integral part of cellular organization. *Dev. Cell* 39, 139–153. doi: 10.1016/j.devcel.2016.09.030

Jacquier, N., Choudhary, V., Mari, M., Toulmay, A., Reggiori, F., and Schneiter, R. (2011). Lipid droplets are functionally connected to the endoplasmic reticulum in *Saccharomyces cerevisiae*. *J. Cell Sci.* 124, 2424–2437. doi: 10.1242/jcs.076836

Jacquier, N., and Schneiter, R. (2012). Mechanisms of sterol uptake and transport in yeast. *J. Steroid Biochem. Mol. Biol.* 129, 70–78. doi: 10.1016/j.jsbmb.2010.11.014

Jangir, P., Kalra, S., Tanwar, S., and Bari, V. K. (2023). Azole resistance in *Candida auris*: mechanisms and combinatorial therapy. *APMIS* 131, 442–462. doi: 10.1111/apm.13336

Jensen-Pergakes, K., Guo, Z., Giattina, M., Sturley, S. L., and Bard, M. (2001). Transcriptional regulation of the two sterol esterification genes in the yeast *Saccharomyces cerevisiae*. *J. Bacteriol.* 183, 4950–4957. doi: 10.1128/JB.183.17.4950-4957.2001

Jordá, T., Barba-Aliaga, M., Rozès, N., Alepuz, P., Martínez-Pastor, M. T., and Puig, S. (2022). Transcriptional regulation of ergosterol biosynthesis genes in response to iron deficiency. *Environ. Microbiol.* 24, 5248–5260. doi: 10.1111/1462-2920.16157

Jordá, T., and Puig, S. (2020). Regulation of Ergosterol biosynthesis in *Saccharomyces cerevisiae*. *Genes* 11:795. doi: 10.3390/genes11070795

Joshua, I., and Höfken, T. (2017). From lipid homeostasis to differentiation: old and new functions of the zinc cluster proteins Ecm22, Upc2, Sut1 and Sut2. *Int. J. Mol. Sci.* 18:772. doi: 10.3390/ijms18040772

Kainz, K., Bauer, M. A., Madeo, F., and Carmona-Gutierrez, D. (2020). Fungal infections in humans: the silent crisis. *Microb Cell* 7, 143–145. doi: 10.15698/mic2020.06.718

Kathiravan, M. K., Salake, A. B., Chothe, A. S., Dudhe, P. B., Watode, R. P., Mukta, M. S., et al. (2012). The biology and chemistry of antifungal agents: a review. *Bioorg. Med. Chem.* 20, 5678–5698. doi: 10.1016/j.bmc.2012.04.045

Kelly, S. L., Lamb, D. C., Taylor, M., Corran, A. J., Baldwin, B. C., and Powderly, W. G. (1994). Resistance to amphotericin B associated with defective sterol Δ8→7 isomerase in a *Cryptococcus neoformans* strain from an AIDS patient. *FEMS Microbiol. Lett.* 122, 39–42. doi: 10.1111/j.1574-6968.1994.tb07140.x

Kodedová, M., and Sychrová, H. (2015). Changes in the sterol composition of the plasma membrane affect membrane potential, salt tolerance and the activity of multidrug resistance pumps in *Saccharomyces cerevisiae*. *PLoS One* 10:e0139306. doi: 10.1371/journal.pone.0139306

Kvam, E., and Goldfarb, D. S. (2004). Nvj1p is the outer-nuclear-membrane receptor for oxysterol-binding protein homolog Osh1p in *Saccharomyces cerevisiae*. *J. Cell Sci.* 117, 4959–4968. doi: 10.1242/jcs.01372

Kyte, J., and Doolittle, R. F. (1982). A simple method for displaying the hydropathic character of a protein. *J. Mol. Biol.* 157, 105–132. doi: 10.1016/0022-2836(82)90515-0

Lass-Flörl, C., Kanj, S. S., Govender, N. P., Thompson, G. R. III, Ostrosky- Zeichner, L., and Govrins, M. A. (2024). Invasive candidiasis. *Nat. Rev. Dis. Primers* 10, 1–18. doi: 10.1038/s41572-024-00503-3

Layer, J. V., Barnes, B. M., Yamasaki, Y., Barbuch, R., Li, L., Taramino, S., et al. (2013). Characterization of a mutation that results in independence of oxidosqualene cyclase (Erg7) activity from the downstream 3-ketoreductase (Erg27) in the yeast ergosterol biosynthetic pathway. *Biochim. Biophys. Acta Mol. Cell Biol. Lipids* 1831, 361–369. doi: 10.1016/j.bbalip.2012.09.012

Leber, R., Landl, K., Zinser, E., Ahorn, H., Spök, A., Kohlwein, S. D., et al. (1998). Dual localization of squalene epoxidase, Erg1p, in yeast reflects a relationship between the endoplasmic reticulum and lipid particles. *Mol. Biol. Cell* 9, 375–386. doi: 10.1091/mbc.9.2.375

LeBlanc, M. A., and McMaster, C. R. (2010). Lipid binding requirements for oxysterol-binding protein Kes1 inhibition of autophagy and endosome-trans-Golgi trafficking pathways. *J. Biol. Chem.* 285, 33875–33884. doi: 10.1074/jbc.M110.147264

Lee, Y., Robbins, N., and Cowen, L. E. (2023). Molecular mechanisms governing antifungal drug resistance. *Antimicrob Resist* 1:5. doi: 10.1038/s44259-023-00007-2

Lev, S. (2010). Non-vesicular lipid transport by lipid-transfer proteins and beyond. *Nat. Rev. Mol. Cell Biol.* 11, 739–750. doi: 10.1038/nrm2971

Levine, T. P., and Munro, S. (2001). Dual targeting of Osh1p, a yeast homologue of oxysterol-binding protein, to both the Golgi and the nucleus-vacuole junction. *Mol. Biol. Cell* 12, 1633–1644. doi: 10.1091/mbc.12.6.1633

Li, X., Rivas, M. P., Fang, M., Marchena, J., Mehrotra, B., Chaudhary, A., et al. (2002). Analysis of oxysterol binding protein homologue Kes1p function in regulation of Sec14p-dependent protein transport from the yeast Golgi complex. *J. Cell Biol.* 157, 63–78. doi: 10.1083/jcb.200201037

Lin, Y., Ran, L., Du, X., Yang, H., and Wu, Y. (2023). Oxysterol-binding protein: new insights into lipid transport functions and human diseases. *Biochim. Biophys. Acta Mol. Cell Biol. Lipids* 1868:159365. doi: 10.1016/j.bbalip.2023.159365

Ling, Y., Hayano, S., and Novick, P. (2014). Osh4p is needed to reduce the level of phosphatidylinositol-4-phosphate on secretory vesicles as they mature. *Mol. Biol. Cell* 25, 3389–3400. doi: 10.1091/mbc.e14-06-1087

Liu, J. F., Xia, J. J., Nie, K. L., Wang, F., and Deng, L. (2019). Outline of the biosynthesis and regulation of ergosterol in yeast. *World J. Microbiol. Biotechnol.* 35:98. doi: 10.1007/s11274-019-2673-2

Lockhart, S. R. (2019). *Candida auris* and multidrug resistance: defining the new normal. *Fungal Genet. Biol.* 131:103243. doi: 10.1016/j.fgb.2019.103243

Lorenz, R. T., and Parks, L. W. (1992). Cloning, sequencing, and disruption of the gene encoding sterol C-14 reductase in *Saccharomyces cerevisiae*. *DNA Cell Biol.* 11, 685–692. doi: 10.1089/dna.1992.11.685

Lotfali, E., Ghajari, A., Kordbacheh, P., Zaini, F., Mirhendi, H., Mohammadi, R., et al. (2017). Regulation of ERG3, ERG6, and ERG11 genes in antifungal-resistant isolates of *Candida parapsilosis*. *Iran. Biomed. J.* 21, 275–281. doi: 10.18869/acadpub.ibj.21.4.275

Low, C. Y., and Rotstein, C. (2011). Emerging fungal infections in immunocompromised patients. *F1000 Med. Rep.* 3:14. doi: 10.3410/M3-14

Luna-Tapia, A., Peters, B. M., Eberle, K. E., Kerns, M. E., Foster, T. P., Marrero, L., et al. (2015). *ERG2* and *ERG24* are required for Normal vacuolar physiology as well as *Candida albicans* pathogenicity in a murine model of disseminated but not vaginal candidiasis. *Eukaryot. Cell* 14, 1006–1016. doi: 10.1128/EC.00116-15

Lv, Q. Z., Yan, L., and Jiang, Y. Y. (2016). The synthesis, regulation, and functions of sterols in *Candida albicans:* well-known but still lots to learn. *Virulence* 7, 649–659. doi: 10.1080/21505594.2016.1188236

Madaan, K., and Bari, V. K. (2023). Emerging role of sphingolipids in amphotericin B drug resistance. *Microb. Drug Resist.* 29, 319–332. doi: 10.1089/mdr.2022.0353

Maeda, K., Anand, K., Chiapparino, A., Kumar, A., Poletto, M., Kaksonen, M., et al. (2013). Interactome map uncovers phosphatidylserine transport by oxysterol-binding proteins. *Nature* 501, 257–261. doi: 10.1038/nature12430

Makanjuola, O., Bongomin, F., and Fayemiwo, S. A. (2018). An update on the roles of non-albicans Candida species in Vulvovaginitis. *J. Fungi* 4:121. doi: 10.3390/jof4040121

Marie, C., Leyde, S., and White, T. C. (2008). Cytoplasmic localization of sterol transcription factors Upc2p and Ecm22p in *S. cerevisiae*. *Fungal Genet. Biol.* 45, 1430–1438. doi: 10.1016/j.fgb.2008.07.004

Martel, C. M., Parker, J. E., Bader, O., Weig, M., Gross, U., Warrilow, A. G. S., et al. (2010). A clinical isolate of *Candida albicans* with mutations in ERG11 (encoding sterol 14α-demethylase) and ERG5 (encoding C22 desaturase) is cross resistant to azoles and

amphotericin B. *Antimicrob. Agents Chemother.* 54, 3578–3583. doi: 10.1128/AAC.00303-10

McCarty, T. P., and Pappas, P. G. (2016). Invasive Candidiasis. *Infect. Dis. Clin. N. Am.* 30, 103–124. doi: 10.1016/j.idc.2015.10.013

McDermott, A. (2022). Drug-resistant fungi on the rise. *Proc. Natl. Acad. Sci. USA* 119:e2217948119. doi: 10.1073/pnas.2217948119

Mesmin, B., Antonny, B., and Drin, G. (2013). Insights into the mechanisms of sterol transport between organelles. *Cell. Mol. Life Sci.* 70, 3405–3421. doi: 10.1007/s00018-012-1247-3

Miziorko, H. M. (2011). Enzymes of the mevalonate pathway of isoprenoid biosynthesis. *Arch. Biochem. Biophys.* 505, 131–143. doi: 10.1016/j.abb.2010.09.028

Mochizuki, S., Miki, H., Zhou, R., and Noda, Y. (2022). The involvement of oxysterol-binding protein-related protein (ORP) 6 in the counter-transport of phosphatidylinositol-4-phosphate (PI4P) and phosphatidylserine (PS) in neurons. *Biochem Biophys Rep* 30:101257. doi: 10.1016/j.bbrep.2022.101257

Muramoto, M., Mineoka, N., Fukuda, K., Kuriyama, S., Masatani, T., and Fujita, A. (2024). Coordinated regulation of phosphatidylinositol 4-phosphate and phosphatidylserine levels by Osh4p and Osh5p is an essential regulatory mechanism in autophagy. *Biochim. Biophys. Acta Biomembr.* 1866:184308. doi: 10.1016/j.bbamem.2024.184308

Murley, A., Sarsam, R. D., Toulmay, A., Yamada, J., Prinz, W. A., and Nunnari, J. (2015). Ltc1 is an ER-localized sterol transporter and a component of ER-mitochondria and ER-vacuole contacts. *J. Cell. Biol.* 209, 539–548. doi: 10.1083/jcb.201502033

Nagi, M., Tanabe, K., Ueno, K., Nakayama, H., Aoyama, T., Chibana, H., et al. (2013). The *Candida glabrata* sterol scavenging mechanism, mediated by the ATP-binding cassette transporter Aus1p, is regulated by iron limitation. *Mol. Microbiol.* 88, 371–381. doi: 10.1111/mmi.12189

Náhlík, J., Hrnčiřík, P., Mareš, J., Rychtera, M., and Kent, C. A. (2017). Towards the design of an optimal strategy for the production of ergosterol from *Saccharomyces cerevisiae* yeasts. *Biotechnol. Prog.* 33, 838–848. doi: 10.1002/btpr.2436

Nakatsu, F., and Kawasaki, A. (2021). Functions of oxysterol-binding proteins at membrane contact sites and their control by phosphoinositide metabolism. *Front. Cell Dev. Biol.* 9:664788. doi: 10.3389/fcell.2021.664788

Nakayama, H., Tanabe, K., Bard, M., Hodgson, W., Wu, S., Takemori, D., et al. (2007). The *Candida glabrata* putative sterol transporter gene CgAUS1 protects cells against azoles in the presence of serum. *J. Antimicrob. Chemother.* 60, 1264–1272. doi: 10.1093/jac/dkm321

Ngo, M. H., Colbourne, T. R., and Ridgway, N. D. (2010). Functional implications of sterol transport by the oxysterol-binding protein gene family. *Biochem. J.* 429, 13–24. doi: 10.1042/BJ20100263

Odds, F. C. (2009). In *Candida albicans*, resistance to flucytosine and terbinafine is linked to MAT locus homozygosity and multilocus sequence typing clade 1. *FEMS Yeast Res.* 9, 1091–1101. doi: 10.1111/j.1567-1364.2009.00577.x

Okamoto, M., Takahashi-Nakaguchi, A., Tejima, K., Sasamoto, K., Yamaguchi, M., Aoyama, T., et al. (2022). Erg25 controls host-cholesterol uptake mediated by Aus1p-associated sterol-rich membrane domains in *Candida glabrata*. *Front. Cell Dev. Biol.* 10:820675. doi: 10.3389/fcell.2022.820675

Omelchuk, O. A., Tevyashova, A. N., and Shchekotikhin, A. E. (2018). Recent advances in antifungal drug discovery based on polyene macrolide antibiotics. *Rus Chem Rev* 87, 1206–1225. doi: 10.1070/RCR4841

Onyewu, C., Blankenship, J. R., Del Poeta, M., and Heitman, J. (2003). Ergosterol biosynthesis inhibitors become fungicidal when combined with calcineurin inhibitors against *Candida albicans, Candida glabrata,* and *Candida krusei*. *Antimicrob. Agents Chemother.* 47, 956–964. doi: 10.1128/AAC.47.3.956-964.2003

Oulmouden, A., and Karst, F. (1991). Nucleotide sequence of the *ERG12* gene of *Saccharomyces cerevisiae* encoding mevalonate kinase. *Curr. Genet.* 19, 9–14. doi: 10.1007/BF00362081

Parks, L. W., and Casey, W. M. (1995). Physiological implications of sterol biosynthesis in yeast. *Ann. Rev. Microbiol.* 49, 95–116. doi: 10.1146/annurev.mi.49.100195.000523

Perlin, D. S. (2015). Mechanisms of echinocandin antifungal drug resistance. *Ann. N. Y. Acad. Sci.* 1354, 1–11. doi: 10.1111/nyas.12831

Petranyi, G., Ryder, N. S., and Stütz, A. (1984). Allylamine derivatives: new class of synthetic antifungal agents inhibiting fungal squalene epoxidase. *Science* 224, 1239–1241. doi: 10.1126/science.6547247

Peyton, L. R., Gallagher, S., and Hashemzadeh, M. (2015). Triazole antifungals: a review. *Drugs Today* 51, 705–718. doi: 10.1358/dot.2015.51.12.2421058

Pfaller, M. A., Andes, D. R., Diekema, D. J., Horn, D. L., Reboli, A. C., Rotstein, C., et al. (2014). Epidemiology and outcomes of invasive candidiasis due to non-albicans species of Candida in 2,496 patients: data from the prospective antifungal therapy (PATH) registry 2004-2008. *PLoS One* 9:e101510. doi: 10.1371/journal.pone.0101510

Pfaller, M. A., and Diekema, D. J. (2007). Epidemiology of invasive candidiasis: a persistent public health problem. *Clin. Microbiol. Rev.* 20, 133–163. doi: 10.1128/CMR.00029-06

Ploier, B., Korber, M., Schmidt, C., Koch, B., Leitner, E., and Daum, G. (2015). Regulatory link between steryl ester formation and hydrolysis in the yeast *Saccharomyces cerevisiae*. *Biochim Biophys Acta-Mol Cell Bio Lipids* 1851, 977–986. doi: 10.1016/j.bbalip.2015.02.011

Polak, A. (1988). Mode of action of Morpholine derivatives. *Ann. N. Y. Acad. Sci.* 544, 221–228. doi: 10.1111/j.1749-6632.1988.tb40406.x

Powis, G., Meuillet, E. J., Indarte, M., Booher, G., and Kirkpatrick, L. (2023). Pleckstrin homology [PH] domain, structure, mechanism, and contribution to human disease. *Biomed. Pharmacother.* 165:115024. doi: 10.1016/j.biopha.2023.115024

Raychaudhuri, S., and Prinz, W. A. (2010). The diverse functions of oxysterol-binding proteins. *Ann Rev Cell Dev Biol* 26, 157–177. doi: 10.1146/annurev.cellbio.042308.113334

Rodrigues, M. L. (2018). The multifunctional fungal Ergosterol. *MBio* 9, e01755–e01718. doi: 10.1128/mBio.01755-18

Rogaski, B., Lim, J. B., and Klauda, J. B. (2010). Sterol binding and membrane lipid attachment to the Osh4 protein of yeast. *J. Phys. Chem. B* 114, 13562–13573. doi: 10.1021/jp106890e

Rybak, J. M., Barker, K. S., Muñoz, J. F., Parker, J. E., Ahmad, S., Mokaddas, E., et al. (2022). In vivo, emergence of high-level resistance during treatment reveals the first identified mechanism of amphotericin B resistance in *Candida auris*. *Clin. Microbiol. Infect.* 28, 838–843. doi: 10.1016/j.cmi.2021.11.024

Ryder, N. S. (1987). Squalene epoxidase as the target of antifungal allylamines. *Pest Sci* 21, 281–288. doi: 10.1002/ps.2780210405

Ryder, N. S., and Dupont, M. C. (1985). Inhibition of squalene epoxidase by allylamine antimycotic compounds. A comparative study of the fungal and mammalian enzymes. *Biochem. J.* 230, 765–770. doi: 10.1042/bj2300765

Sanglard, D., Ischer, F., Parkinson, T., Falconer, D., and Bille, J. (2003). *Candida albicans* mutations in the Ergosterol biosynthetic pathway and resistance to several antifungal agents. *Antimicrob. Agents Chemother.* 47, 2404–2412. doi: 10.1128/AAC.47.8.2404-2412.2003

Sanguinetti, M., Posteraro, B., and Lass-Flörl, C. (2015). Antifungal drug resistance among Candida species: mechanisms and clinical impact. *Mycoses* 58, 2–13. doi: 10.1111/myc.12330

Schulz, T. A., and Prinz, W. A. (2007). Sterol transport in yeast and the oxysterol binding protein homologue (OSH) family. *Biochim. Biophys. Acta Mol. Cell Biol. Lipids* 1771, 769–780. doi: 10.1016/j.bbalip.2007.03.003

Shakoury-Elizeh, M., Protchenko, O., Berger, A., Cox, J., Gable, K., Dunn, T. M., et al. (2010). Metabolic response to Iron deficiency in *Saccharomyces cerevisiae*. *J. Biol. Chem.* 285, 14823–14833. doi: 10.1074/jbc.M109.091710

Shianna, K. V., Dotson, W. D., Tove, S., and Parks, L. W. (2001). Identification of a UPC2 homolog in *Saccharomyces cerevisiae* and its involvement in aerobic sterol uptake. *J. Bacteriol.* 183, 830–834. doi: 10.1128/JB.183.3.830-834.2001

Shrivastava, M., Kouyoumdjian, G. S., Kirbizakis, E., Ruiz, D., Henry, M., Vincent, A. T., et al. (2023). The Adr1 transcription factor directs regulation of the ergosterol pathway and azole resistance in *Candida albicans*. *MBio* 14, e01807–e01823. doi: 10.1128/mbio.01807-23

Sigera, L. S. M., and Denning, D. W. (2023). Flucytosine and its clinical usage. *Ther Adv Infect Dis.* 10:20499361231161387. doi: 10.1177/20499361231161387

Sokolov, S. S., Vorobeva, M. A., Smirnova, A. I., Smirnova, E. A., Trushina, N. I., Galkina, K. V., et al. (2020). LAM genes contribute to environmental stress tolerance but sensibilize yeast cells to azoles. *Front. Microbiol.* 11:38. doi: 10.3389/fmicb.2020.00038

Song, J., Zhai, P., Zhang, Y., Zhang, C., Sang, H., Han, G., et al. (2016). The *Aspergillus fumigatus* damage resistance protein family coordinately regulates Ergosterol biosynthesis and azole susceptibility. *MBio* 7:e01919. doi: 10.1128/mBio.01919-15

Spivak, E. S., and Hanson, K. E. (2018). *Candida auris:* an emerging fungal pathogen. *J. Clin. Microbiol.* 56, e01588–e01517. doi: 10.1128/JCM.01588-17

Stewart, E. V., Nwosu, C. C., Tong, Z., Roguev, A., Cummins, T. D., Kim, D. U., et al. (2011). Yeast SREBP cleavage activation requires the Golgi Dsc E3 ligase complex. *Mol. Cell.* 42, 160–171. doi: 10.1016/j.molcel.2011.02.035

Stolz, J., and Sauer, N. (1999). The fenpropimorph resistance gene FEN2 from *Saccharomyces cerevisiae* encodes a plasma membrane H+-pantothenate symporter. *J. Biol. Chem.* 274, 18747–18752. doi: 10.1074/jbc.274.26.18747

Taei, M., Chadeganipour, M., and Mohammadi, R. (2019). An alarming rise of non-albicans *Candida* species and uncommon yeasts in the clinical samples; a combination of various molecular techniques for identification of etiologic agents. *BMC. Res. Notes* 12:779. doi: 10.1186/s13104-019-4811-1

te Welscher, Y. M., Jones, L., van Leeuwen, M. R., Dijksterhuis, J., de Kruijff, B., Eitzen, G., et al. (2010). Natamycin inhibits vacuole fusion at the priming phase via a specific interaction with ergosterol. *Antimicrob. Agents Chemother.* 54, 2618–2625. doi: 10.1128/AAC.01794-09

Teske, B., Taramino, S., Bhuiyan, M. S. A., Kumaraswami, N. S., Randall, S. K., Barbuch, R., et al. (2008). Genetic analyses involving interactions between the ergosterol biosynthetic enzymes, lanosterol synthase (Erg7p) and 3-ketoreductase (Erg27p), in the yeast *Saccharomyces cerevisiae*. *Biochim. Biophys. Acta Mol. Cell Biol. Lipids* 1781, 359–366. doi: 10.1016/j.bbalip.2008.04.017

Theesfeld, C. L., and Hampton, R. Y. (2013). Insulin-induced gene protein (INSIG)-dependent sterol regulation of Hmg2 endoplasmic reticulum-associated degradation (ERAD) in yeast. *J. Biol. Chem.* 288, 8519–8530. doi: 10.1074/jbc.M112.404517

Tøndervik, A., Sletta, H., Klinkenberg, G., Emanuel, C., Powell, L. C., Pritchard, M. F., et al. (2014). Alginate oligosaccharides inhibit fungal cell growth and potentiate the activity of antifungals against Candida and *Aspergillus spp*. *PLoS One* 9:e112518. doi: 10.1371/journal.pone.0112518

Tong, J., Manik, M. K., and Im, Y. J. (2018). Structural basis of sterol recognition and nonvesicular transport by lipid transfer proteins anchored at membrane contact sites. *Proc. Natl. Acad. Sci. USA* 115, E856–E865. doi: 10.1073/pnas.1719709115

Tsay, Y. H., and Robinson, G. W. (1991). Cloning and characterization of *ERG8* an essential gene of *Saccharomyces cerevisiae* that encodes phosphomevalonate kinase. *Mol. Cell. Biol.* 11, 620–631. doi: 10.1128/mcb.11.2.620-631.1991

Valachovic, M., Hronská, L., and Hapala, I. (2001). Anaerobiosis induces complex changes in sterol esterification pattern in the yeast *Saccharomyces cerevisiae*. *FEMS Microbiol. Lett.* 197, 41–45. doi: 10.1111/j.1574-6968.2001.tb10580.x

Vandeputte, P., Tronchin, G., Larcher, G., Ernoult, E., Bergès, T., Chabasse, D., et al. (2008). A nonsense mutation in the ERG6 gene leads to reduced susceptibility to polyenes in a clinical isolate of *Candida glabrata*. *Antimicrob. Agents Chemother.* 52, 3701–3709. doi: 10.1128/AAC.00423-08

Vanegas, J. M., Contreras, M. F., Faller, R., and Longo, M. L. (2012). Role of unsaturated lipid and ergosterol in ethanol tolerance of model yeast biomembranes. *Biophys. J.* 102, 507–516. doi: 10.1016/j.bpj.2011.12.038

Vik, Å., and Rine, J. (2001). Upc2p and Ecm22p, dual regulators of sterol biosynthesis in *Saccharomyces cerevisiae*. *Mol. Cell. Biol.* 21, 6395–6405. doi: 10.1128/mcb.21.19.6395-6405.2001

Vil, V., Gloriozova, T. A., Poroikov, V. V., Terentev, A. O., Savidov, N., and Dembitsky, V. M. (2019). Naturally occurring of α, β-diepoxy-containing compounds: origin, structures, and biological activities. *Appl. Microbiol. Biotechnol.* 103, 3249–3264. doi: 10.1007/s00253-019-09711-4

Vincent, B. M., Lancaster, A. K., Scherz-Shouval, R., Whitesell, L., and Lindquist, S. (2013). Fitness trade-offs restrict the evolution of resistance to amphotericin B. *PLoS Biol.* 11:e1001692. doi: 10.1371/journal.pbio.1001692

Ward, D. M., Chen, O. S., Li, L., Kaplan, J., Bhuiyan, S. A., Natarajan, S. K., et al. (2018). Altered sterol metabolism in budding yeast affects mitochondrial iron–sulfur (Fe-S) cluster synthesis. *J. Biol. Chem.* 293, 10782–10795. doi: 10.1074/jbc.RA118.001781

Weber-Boyvat, M., Zhong, W., Yan, D., and Olkkonen, V. M. (2013). Oxysterol-binding proteins: functions in cell regulation beyond lipid metabolism. *Biochem. Pharmacol.* 86, 89–95. doi: 10.1016/j.bcp.2013.02.016

Whaley, S. G., Caudle, K. E., Vermitsky, J. P., Chadwick, S. G., Toner, G., Barker, K. S., et al. (2014). UPC2A is required for high-level azole antifungal resistance in *Candida glabrata*. *Antimicrob. Agents Chemother.* 58, 4543–4554. doi: 10.1128/AAC.02217-13

Willger, S. D., Puttikamonkul, S., Kim, K. H., Burritt, J. B., Grahl, N., Metzler, L. J., et al. (2008). A sterol-regulatory element binding protein is required for cell polarity, hypoxia adaptation, azole drug resistance, and virulence in *Aspergillus fumigatus*. *PLoS Pathog.* 4:e1000200. doi: 10.1371/journal.ppat.1000200

Wong, L. H., Gatta, A. T., and Levine, T. P. (2019). Lipid transfer proteins: the lipid commute via shuttles, bridges and tubes. *Nat. Rev. Mol. Cell Biol.* 20, 85–101. doi: 10.1038/s41580-018-0071-5

Woods, K., and Höfken, T. (2016). The zinc cluster proteins Upc2 and Ecm22 promote filamentation in *Saccharomyces cerevisiae* by sterol biosynthesis-dependent and -independent pathways. *Mol. Microbiol.* 99, 512–527. doi: 10.1111/mmi.13244

Yang, H., Bard, M., Bruner, D. A., Gleeson, A., Deckelbaum, R. J., Aljinovic, G., et al. (1996). Sterol esterification in yeast: a two-gene process. *Science* 272, 1353–1356. doi: 10.1126/science.272.5266.1353

Yang, H., Tong, J., Lee, C. W., Ha, S., Eom, S. H., and Im, Y. J. (2015). Structural mechanism of ergosterol regulation by fungal sterol transcription factor Upc2. *Nat. Commun.* 6:6129. doi: 10.1038/ncomms7129

Young, L. Y., Hull, C. M., and Heitman, J. (2003). Disruption of Ergosterol biosynthesis confers resistance to amphotericin B in *Candida lusitaniae*. *Antimicrob. Agents Chemother.* 47, 2717–2724. doi: 10.1128/AAC.47.9.2717-2724.2003

Zhang, J., Li, L., Lv, Q., Yan, L., Wang, Y., and Jiang, Y. (2019). The fungal CYP51s: their functions, structures, related drug resistance, and inhibitors. *Front. Microbiol.* 10:691. doi: 10.3389/fmicb.2019.00691

Zheng Koh, D. H., and Saheki, Y. (2021). Regulation of plasma membrane sterol homeostasis by nonvesicular lipid transport. *Contact* 4:251525642110424. doi: 10.1177/25152564211042451

Zinser, E., Paltauf, F., and Daum, G. (1993). Sterol composition of yeast organelle membranes and subcellular distribution of enzymes involved in sterol metabolism. *J. Bacteriol.* 175, 2853–2858. doi: 10.1128/jb.175.10.2853-2858.1993

frontiers | Frontiers in Microbiology

TYPE Original Research
PUBLISHED 18 October 2024
DOI 10.3389/fmicb.2024.1459162

OPEN ACCESS

EDITED BY
Juan A. Ayala,
Autonomous University of Madrid, Spain

REVIEWED BY
Sangita Dixit,
Siksha O Anusandhan University, India
Valentine Usongo,
Health Canada, Canada

*CORRESPONDENCE
Qingcao Li
✉ lqc_lab@163.com
Guangliang Wu
✉ wuguangliang2024@126.com

RECEIVED 03 July 2024
ACCEPTED 09 October 2024
PUBLISHED 18 October 2024

CITATION
Yang Y, Zhang H, Zhao R, Qiu X, Ye J, Lu W, Li Q and Wu G (2024) Distribution diversity and expression regulation of class 1 integron promoters in clinical isolates of *Morganella morganii*.
Front. Microbiol. 15:1459162.
doi: 10.3389/fmicb.2024.1459162

Distribution diversity and expression regulation of class 1 integron promoters in clinical isolates of *Morganella morganii*

Ye Yang[1], Hui Zhang[2], Rongqing Zhao[1], Xuedan Qiu[1], Jinglu Ye[1], Wenjun Lu[3], Qingcao Li[1]* and Guangliang Wu[4]*

[1]Department of Clinical Laboratory, The Affiliated LiHuiLi Hospital of Ningbo University, Ningbo, China, [2]Department of Clinical Laboratory, Ninghai County Chengguan Hospital, Ningbo, China, [3]Department of Intensive Care Units, The Affiliated LiHuiLi Hospital of Ningbo University, Ningbo, China, [4]Department of Clinical Pharmacy, The Affiliated LiHuiLi Hospital, Ningbo University, Ningbo, China

Background: *Morganella morganii* is an emerging nosocomial opportunistic pathogen with increasing multidrug resistance. Antibiotic resistance, driven primarily by the horizontal transfer of resistance genes, has become a global health crisis. Integrons, mobile genetic elements, are now understood to facilitate the transfer of these genes, contributing to the rapid proliferation of resistant strains. Understanding the regulatory role of integrons in drug resistance gene expression is crucial for developing novel strategies to combat this pressing public health issue.

Objective: To investigate the distribution of promoter types in the variable regions of class 1 integrons isolated from clinical isolates of *M. morganii* and their regulatory role in the expression of downstream drug resistance gene cassettes.

Methods: Ninety seven clinical isolates of *M. morganii* were screened for the presence of class 1 integrons (*intI1*) using polymerase chain reaction (PCR). Gene cassettes within the variable regions of positive isolates were characterized, and the gene cassette promoter Pc variants and downstream auxiliary promoter P2 were identified. Enterobacterial repetitive intergenic consensus (ERIC)-PCR was employed for homology analysis. Recombinant plasmids containing different variable region promoters and gene cassettes were constructed to evaluate drug resistance genes and integrase (*intI1*) expression levels using reverse transcription-quantitative PCR (RT-qPCR) and antimicrobial susceptibility testing.

Results: Of the clinical isolates, 28.9% ($n = 28/97$) were positive for class 1 integrons. 24.7% ($n = 24/97$) of these isolates carried gene cassettes encoding resistance to aminoglycosides and trimethoprim. Three Pc promoter types (PcH1, PcS, and PcW) were identified, while all P2 promoters were inactive with a 14-base pair spacing between the −35 and −10 regions. ERIC-PCR analysis classified the integron-positive strains into 6 genotypes, with high consistency in promoter types and gene cassettes within each genotype. RT-qPCR and antimicrobial susceptibility testing demonstrated that strong promoters significantly enhanced the expression of downstream drug resistance gene cassettes compared to weak promoters. Additionally, RT-qPCR revealed a negative correlation between *intI1* expression and Pc promoter strength.

Conclusion: Class 1 integrons are prevalent in *M. morganii*. The promoter types within these integrons are diverse, and promoter strength is closely linked to downstream gene cassette expression. Integron-positive strains exhibit high homology, suggesting horizontal gene transfer and dissemination in clinical settings.

KEYWORDS

***Morganella morganii*, integron, promoter, expression regulation, homology**

1 Introduction

Morganella morganii, a member of the *Enterobacteriaceae* family, has historically been detected infrequently in clinical settings (Agrawal et al., 2021). While traditionally associated with urinary tract infections, wound infections, and bloodstream infections (Laupland et al., 2022; Shi et al., 2022; Gameiro et al., 2023; Kvopka et al., 2023; Li et al., 2023; Yeşil et al., 2023; Alsaadi et al., 2024), its clinical isolation rate has been rapidly increasing in recent years, leading to severe invasive infections (Zaric et al., 2021; Alelyani et al., 2022; Behera et al., 2023a; Elmi et al., 2024). Due to its high mortality rates in specific patient populations, the World Health Organization has designated *M. morganii* as a globally prioritized pathogen (Behera et al., 2023b). Some clinically isolated strains of *M. morganii* have acquired resistance to multiple antibiotics through the carriage of various drug resistance genes, posing serious challenges for clinical infection control (Liu et al., 2016). Horizontal transfer of drug resistance genes, facilitated by mobile genetic elements such as integrons, is a common mechanism for acquiring resistance in bacteria (Leverstein-van Hall et al., 2002; von Wintersdorff et al., 2016; Coluzzi et al., 2023). However, the role of integrons in *M. morganii* resistance has been largely understudied.

Current evidence suggests that integrons, typically consisting of three main components: a 5′ conserved region, a variable region containing various drug resistance gene cassettes, and a 3′ conserved region that varies with integron type, play a pivotal role in the horizontal transfer of drug resistance genes among bacteria (Hall and Stokes, 1993). They are natural cloning and expression vectors, capturing and disseminating gene cassettes through site-specific recombination (Hall and Collis, 2006). One of the most extensively studied integron types is class 1 integrons, which include the Pc promoter in the 5′ conserved region. As most gene cassettes lack promoters, the Pc promoter plays a crucial role in regulating the expression of downstream gene cassettes within integrons (Hanau-Berçot et al., 2002; Tseng et al., 2014). In some cases, the Pc promoter complements the auxiliary promoter P2, forming a Pc-P2 dual promoter configuration that further influences gene regulation (Stokes et al., 1997). The strength of the promoter, determined by transcriptional dominance, varies among different Pc variants defined by their −35 and −10 hexamer sequences. The most common Pc promoters in clinical and natural settings are Pc strong (PcS), Pc weak (PcW), Pc Hybrid 1 (PcH1), and Pc Hybrid 2 (PcH2) (Fonseca and Vicente, 2022). The transcription level of genes within integrons largely depends on the regulatory role of these promoters (Novačić et al., 2022), influenced by factors such as promoter strength and proximity to the gene cassette (Jacquier et al., 2009). Integron-positive *M. morganii* can express resistance to relevant drug resistance genes within the integron, and the expression of these genes is primarily dependent on the regulation of the variable region Pc promoter. The horizontal transmission of drug resistance genes between different bacterial strains, facilitated by integron-carrying *M. morganii*, poses a significant challenge in clinical settings. To investigate the relationship between variable region promoters of class 1 integrons in *M. morganii* and the regulation of drug resistance gene expression, this study analyzed antibiotic resistance data from non-duplicated clinical isolates collected from November 2015 to August 2021 at the Affiliated LiHuiLi Hospital of Ningbo University. The findings of this study provide valuable insights into the mechanism and expression regulation of drug resistance genes in integron-positive *M. morganii*, which has significant clinical implications for the prevention and treatment of this rare pathogen.

2 Materials and methods

2.1 Strains and plasmids

Ninety seven non-duplicated clinical isolates of *M. morganii* were collected from urine, bile, and other specimen types at the Affiliated LiHuiLi Hospital of Ningbo University between November 2015 and August 2021. Strains lacking complete clinical data were excluded. This study was approved by the Medical Ethics Committee of the Affiliated LiHuiLi Hospital of Ningbo University. *Escherichia coli* DH5α served as the integron-negative control strain, *Proteus mirabilis* 47437 as the class 1 integron-positive control strain, *E. coli* JM109 as the competent strain, and *E. coli* ATCC25922 as the control strain for antimicrobial susceptibility testing. Plasmid pACYC184 was used as the cloning and expression vector. All strains and plasmids were maintained in our laboratory.

2.2 Detection of integron-positive strains and variable gene cassettes

DNA templates were extracted from experimental strains using the boiling method. PCR amplification was performed using *intI1* screening primers (intF & P2R, Table 1) at an annealing temperature of 55°C. PCR products were analyzed by agarose gel electrophoresis to identify positive bands. Sequencing analysis was conducted to confirm the presence of class 1 integrons in the positive strains. Gene cassettes within the variable regions of class 1 integron-positive strains were amplified using specific primers (5CS & 3CS, Table 1) at an annealing temperature of 55°C. Positive bands were visualized by agarose gel electrophoresis, and sequencing of the PCR products was followed by comparison with the BLAST database to determine the composition of variable gene cassettes in these strains.

TABLE 1 Oligonucleotide primers used in this study.

Primer	Sequence (5′ → 3′)	Target gene	References
intF	CCAAGCTCTCGGGTAACATC	*intI1*	Lu et al. (2022)
P2R	GCCCAGCTTCTGTATGGAAC		Lu et al. (2022)
5CS	GGCATCCAAGCAGCAAG	Variable region	Lu et al. (2022)
3CS	AAGCAGACTTGACCTGA		Lu et al. (2022)
ERIC2	AAGTAAGTGACTGGGGTGAGCG	ERIC-PCR	Lu et al. (2022)
dfrA17R	GGATATCAGGACCACTACCGATTAC	Pc, P2	This study
aac(6′)R	GAAGCCAACCCATCAGACAG		This study
dfrA12R	GATAAATGCGTACTGATTCCGAGTTC		This study
aadBR	CAATGTGACCTGCGTTGTGTC		This study
dfrA32R	GGAATATCAGGACCACTACCGATTAC		This study
aadA1R	CTACCTCTGATAGTTGAGTCGATACTTC		This study
aacA4R	CAACGTGTTTTGAAGGCCTTC		This study
dfrA7R	GAGTAACTGCTCACCTTTTGCTG		This study
dfrA15R	CTGCCATTAGTGATAGTTTCACGATAC		This study
aadA2R	GCTTAGCACCTCTGATAGTTGGTTC		This study
aadF2	CGATGAGCGAAATGTAGTG	*aadA2*	Wei (2010)
aadR2	AAGACGGGCTGATACTGG		Wei (2010)
QCMF	GGAGTGAATACCACGACG	*cat*	Wei (2010)
QCMR	GGATTGGCTGAGACGAA		Wei (2010)

2.3 The distribution of promoters and their relationship with resistance in class 1 integron-positive strains

To identify Pc and P2 promoters in class 1 integron-positive strains, reverse primers were designed based on the sequences of the first gene cassettes at the 5′-conserved sequence (5CS) end, in conjunction with the forward primer intF (Table 1). PCR was conducted with annealing temperatures ranging from 52°C to 56°C for 35 cycles. Amplified products were visualized by agarose gel electrophoresis, and positive bands were sequenced to determine the promoter types. Clinical isolates were categorized according to their integron promoter types. A retrospective analysis of antibiotic resistance data was performed for each group of isolates, followed by a comparative analysis to evaluate differences in antibiotic resistance profiles among the various integron promoter-based groups.

2.4 ERIC-PCR detection of integron-positive strains

Enterobacterial repetitive intergenic consensus (ERIC) sequences are non-coding and highly conserved regions originally discovered in Enterobacteriaceae. Enterobacterial repetitive intergenic consensus-polymerase chain reaction (ERIC-PCR) involves the design of primers based on the conserved ERIC region for PCR amplification. The number and size of ERIC bands in the bacterial genome are then determined, and the degree of bacterial relatedness is calculated for typing purposes. Compared to other typing methods, ERIC-PCR is a popular choice due to its lower cost and faster operation (Meacham et al., 2003; Banoub et al., 2022). In the present study, integron-positive strains were subjected to ERIC-PCR analysis (using primer ERIC2, Table 1, annealing temperature 40°C, 40 cycles) to assess homology. Positive bands and their positions on agarose gel electrophoresis of PCR products were recorded, photographed, and compiled into a matrix table. NTsys 2.10e software was used to generate a clustering dendrogram. Additionally, integron-positive strains were genotyped, and homology analysis was conducted in conjunction with Pc promoter and drug resistance gene cassettes in the variable region.

2.5 Constructing strains containing recombinant plasmids

Two sets of recombinant plasmids were constructed based on different promoter types and gene cassettes within the variable region. The first set employed various variable region promoters while maintaining the same gene cassette, while the second set utilized the same variable region promoter and gene cassette but varied the distance from the Pc promoter. The pACYC184 plasmid, which confers chloramphenicol resistance, served as the vector. HindIII and AseI restriction enzymes were chosen to digest the plasmid, replacing the *tet* promoter to avoid interference with the integron promoters in the recombinant gene fragment (Figure 1). The larger fragment of the digested plasmid was then purified. A synthetic gene fragment, encompassing the integrase *intI1* to 3CS region (including the variable region promoter), was ligated to this purified plasmid fragment. The resulting recombinant plasmids were confirmed through sequencing and subsequently transformed into competent *E. coli* JM109 cells.

2.6 RT-qPCR and antimicrobial susceptibility testing of constructed strains

Total RNA was extracted from the logarithmic growth phase of the constructed strains. The extracted RNA was purified and subjected to reverse transcription (RT) to obtain cDNA templates, which were then diluted to appropriate concentrations for subsequent quantitative PCR (qPCR) detection. qPCR was performed using specific primers targeting the genes of interest in the constructed strains. The pACYC184 plasmid-encoded *cat* gene was used as an internal reference gene. Relative expression levels of genes were calculated using the $2^{-\Delta\Delta Ct}$ method. The expression levels of the target gene and the integrase gene *intI1* were analyzed to compare transcriptional differences among the various constructed strains.

Antimicrobial susceptibility testing and interpretation of experimental results was conducted following Clinical and Laboratory Standards Institute (CLSI) guidelines (M-100, Ed 2022) (CLSI, 2022). The broth microdilution method was used to determine the minimum inhibitory concentrations (MICs) of antibiotics mediated by drug resistance gene cassettes in the variable region. Chloramphenicol (mediated by the internal reference gene *cat*) and tetracycline (mediated by gene *tet*) were also tested in each constructed strain. *E. coli* ATCC25922 served as the quality control strain for susceptibility testing, and *E. coli* JM109 was used as the negative control strain. The Kirby-Bauer (K-B) disk diffusion method was employed to validate the results obtained from MIC determination, allowing for a comparison of resistance differences among the constructed strains.

2.7 Statistical analysis

In this study, the comparison of drug resistance rates between different groups was analyzed using Fisher's exact test (two-sided) with SPSS 25.0 software, considering a significance level of $p < 0.05$. Gene relative expression levels in qPCR were analyzed using one-way ANOVA for multiple comparisons among strains with GraphPad Prism 8.0 software, using a significance level of $p < 0.05$.

3 Results

3.1 Detection of class 1 integrons and gene cassettes of variable regions

We identified 28 out of 97 clinical isolates of *M. morganii* as positive for *intI1*, resulting in a positivity rate of 28.9% (Supplementary material: Sequence of *intI1*). Among these *intI1*-positive isolates, 10 different types of gene cassettes were amplified, while 4 isolates did not amplify any gene cassettes (Supplementary material: Sequence of variable region). The amplified gene cassettes primarily conferred resistance to aminoglycosides and trimethoprim, as shown in Table 2.

3.2 Distribution of promoters and their relationship with antibiotic resistance in *Morganella morganii*

Among the 28 strains positive for class 1 integrons, three types of Pc promoters were detected: PcH1 ($n = 19$), PcS ($n = 5$), and PcW ($n = 4$). PcS exhibited stronger promoter activity, PcW showed weaker activity, and PcH1 demonstrated intermediate strength. All downstream P2 promoters were inactive types, spaced 14 base pairs apart from the −35 to −10 regions (Supplementary material: Sequence of promoter). Based on the different types of variable region promoters in the integrons, the positive strains were categorized into three groups. Retrospective analysis of drug resistance data was conducted among strains containing different types of variable region promoters. Although there were no significant differences in resistance rates to cotrimoxazole, gentamicin, or tobramycin among the groups ($p > 0.05$), strains in the PcS group exhibited higher resistance rates to all antibiotics compared to the PcH1 and PcW groups, while the PcW group demonstrated the lowest resistance rates among the three groups (Figure 2).

3.3 ERIC-PCR typing results

ERIC-PCR fingerprinting of the 28 class 1 integron-positive strains was encoded and organized into a matrix table (Supplementary Figure S1; ERIC-PCR electrophoretogram). NTsys 2.10e software was used to generate a dendrogram with a reference line set at 75% similarity (Bakhshi et al., 2018). Based on this analysis, the positive strains were classified into 6 distinct genotypes (A, B, C, D, E, F). Genotype A was the most prevalent, with 11 strains, followed by genotype C with 7 strains. The predominant type of variable region promoter Pc was PcH1. Gene cassette dfrA was the dominant gene in the variable region of type A isolates, which exhibited high resistance to trimethoprim. Type B isolates primarily carried the PcH1/dfrA17-aadA5 combination, associated with resistance to aminoglycosides and trimethoprim. Type C isolates predominantly had the PcS promoter and showed relatively high resistance rates to various antibiotics. The distribution of gene cassettes was concentrated, primarily consisting of aminoglycoside and trimethoprim drug resistance gene cassettes. Specific details are illustrated in Figure 3.

3.4 Construction of strains containing recombinant plasmids

Based on five class 1 integron-positive strains of *M. morganii* (MM-6, MM-26, MM-41, MM-62, MM-86), each containing the *aadA2* gene cassette in the variable region, the Pc promoters were PcH1, PcH1, PcH1, PcW, and PcS, respectively. The P2 sequences were uniformly inactive, spanning 14 base pairs between the −35 and −10 regions. Gene fragments containing integrase, promoters, variable region gene cassettes, and inter-cassette sequences were synthesized according to actual sequencing results (Supplementary material: The gene synthesis of target segment in recombinant plasmids). These gene fragments were used to recombine plasmids, resulting in the creation of five recombinant strains named JM-6, JM-26, JM-41, JM-62, and JM-86, as listed in Table 3.

3.5 Real-time quantitative PCR results of *aadA2* and *intI1* in constructed strains

The five constructed strains were divided into two groups based on their Pc promoter and *aadA2* gene cassette configurations:

10.3389/fmicb.2024.1459162

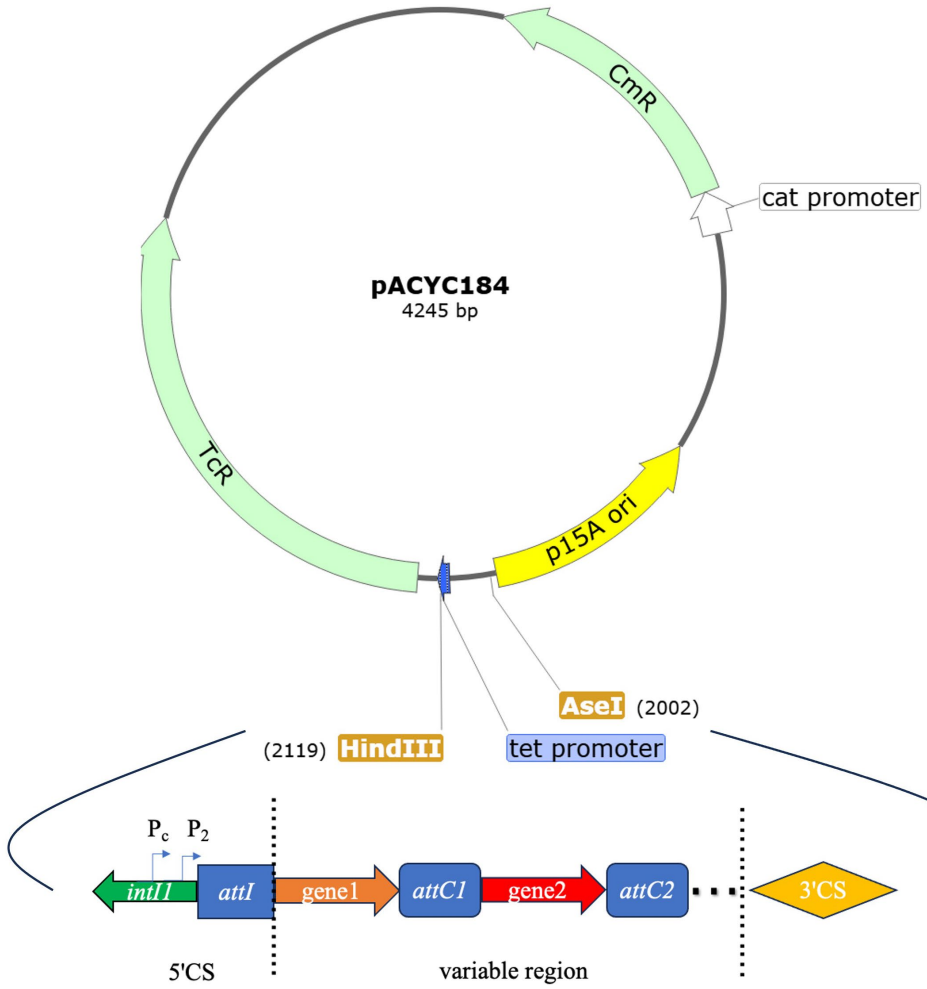

FIGURE 1
pACYC184 plasmid map and the sites of enzyme digestion HindIII and AseI. The pACYC184 plasmid map shows the positions of HindIII and AseI. The *tet* promoter has been disrupted by enzymatic cleavage. The map of the recombinant gene fragment that was integrated into the digested plasmid: the map includes the complete sequence from *intI1* to 3CS. *tet*: tetracycline resistance gene, *cat*: chloramphenicol resistance gene.

TABLE 2 Variable region gene cassette distribution.

Number of strains	Length (bp)	Gene cassette of variable region
9	1,393	*dfrA17-aadA5*
3	474	*dfrA17*
3	792	*aadA2*
2	1,697	*dfrA12-aadA2*
2	474	*dfrA7*
1	1,442	*aacA4-orfD-aadB*
1	474	*dfrA15*
1	2,966	*aadB-aadA2-cmlA6*
1	2,763	*dfrA32-ereA1-aadA2*
1	1,149	*aac(6′)-Ib-cr-arr-3*
4	–	ND

Group 1 comprised strains JM-41, JM-62, and JM-86, which had different Pc promoters but all carried the *aadA2* gene cassette. Group 2 included strains JM-6, JM-26, and JM-41, which had the same Pc promoter but varied in the distance between the *aadA2* gene cassette and the Pc promoter. In the qPCR analysis, strain JM-41 served as the reference strain. Multiple comparisons among the strains revealed that JM-86 exhibited the highest relative expression of the *aadA2* gene compared to the other four strains, with a significant statistical difference ($p < 0.0001$). The relative expression in JM-86 was approximately 100 times higher than that in JM-62, which had the lowest expression. The relative expression of the *intI1* gene followed the order JM-62 > JM-41 > JM-86, with statistically significant differences among the strains ($p < 0.001$). JM-62 showed approximately 50 times higher expression than JM-86, which had the lowest expression level. For further details, please refer to Figure 4.

3.6 Results of antimicrobial susceptibility testing for constructed strains

Antibiotic susceptibility testing was conducted on the five constructed strains carrying aminoglycoside and trimethoprim

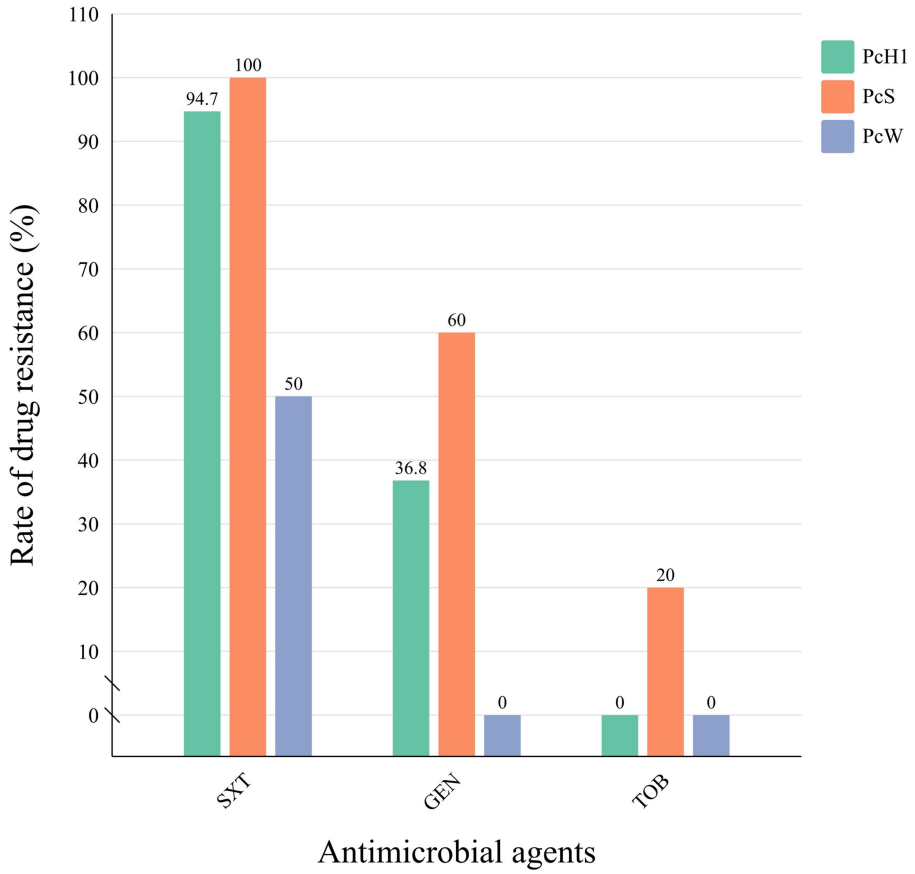

FIGURE 2
The comparison of antibiotic resistance rates among different promoter groups in *Morganella morganii* isolates. STX, cotrimoxazole; GEN, gentamicin; TOB: tobramycin.

resistance gene cassettes using the microbroth dilution method for streptomycin, amikacin, chloramphenicol, and tetracycline. The results revealed streptomycin MIC values obtained by microbroth dilution were in the order JM-86 > JM-41 > JM-26 > JM-6 > JM-62. The K-B assay confirmed this trend, with inhibition zone diameters for streptomycin aligning closely with the microbroth dilution results (JM-86 < JM-41 < JM-26 < JM-6 = JM-62). Amikacin showed no variation in MIC values or inhibition zone diameters among the constructed strains, indicating susceptibility across all strains. All constructed strains exhibited resistance to chloramphenicol. Only JM-86 demonstrated intermediate resistance to tetracycline in both microbroth dilution and K-B assays, while the other strains were sensitive. The antibiotic sensitivity testing results for the quality control strain *E. coli* ATCC25922 and the negative control *E. coli* JM109 fell within the effective range, as shown in Table 4.

4 Discussion

M. morganii, the sole species within the genus *Morganella*, is a widely distributed bacterium that serves as a significant reservoir for the cloning and dissemination of various antibiotic resistance genes. In recent years, antibiotic resistance in *M. morganii* has been rapidly increasing, primarily driven by exogenous genetic elements such as transposons and integrons (Luo et al., 2022). While previous research on *M. morganii* has primarily focused on case analyses for treatment, epidemiology, and broad-spectrum β-lactamase analysis (Shrestha et al., 2020; Marado and Guerra, 2022; Alsaadi et al., 2024), studies investigating the correlation between its resistance mechanisms and the expression regulation of drug resistance gene cassettes within integrons are limited. This study employed clinical isolates of *M. morganii* positive for class 1 integrons collected over the past 6 years from our hospital. We initially screened these strains for drug resistance gene cassettes and promoters in the variable region, then analyzed the correlation between strain resistance and variable region promoters in integrons. Additionally, we constructed strains containing different types of promoters and gene cassettes in the variable region to conduct qPCR and antimicrobial susceptibility tests, thereby analyzing the regulatory role of variable region promoters in class 1 integrons on gene cassette expression.

Studies on class 1 integrons are more prevalent in *Enterobacteriaceae* bacteria such as *E. coli*, *Klebsiella pneumoniae*, and non-fermenting bacteria like *Pseudomonas aeruginosa* and *Acinetobacter baumannii* (Han et al., 2008; Wei et al., 2013; Bocharova et al., 2020; Farajzadeh Sheikh et al., 2024). In contrast, few studies have focused on *M. morganii* and class 1 integrons. Among the 97 non-duplicated clinical isolates of *M. morganii* in this study, the prevalence of class 1 integron-positive

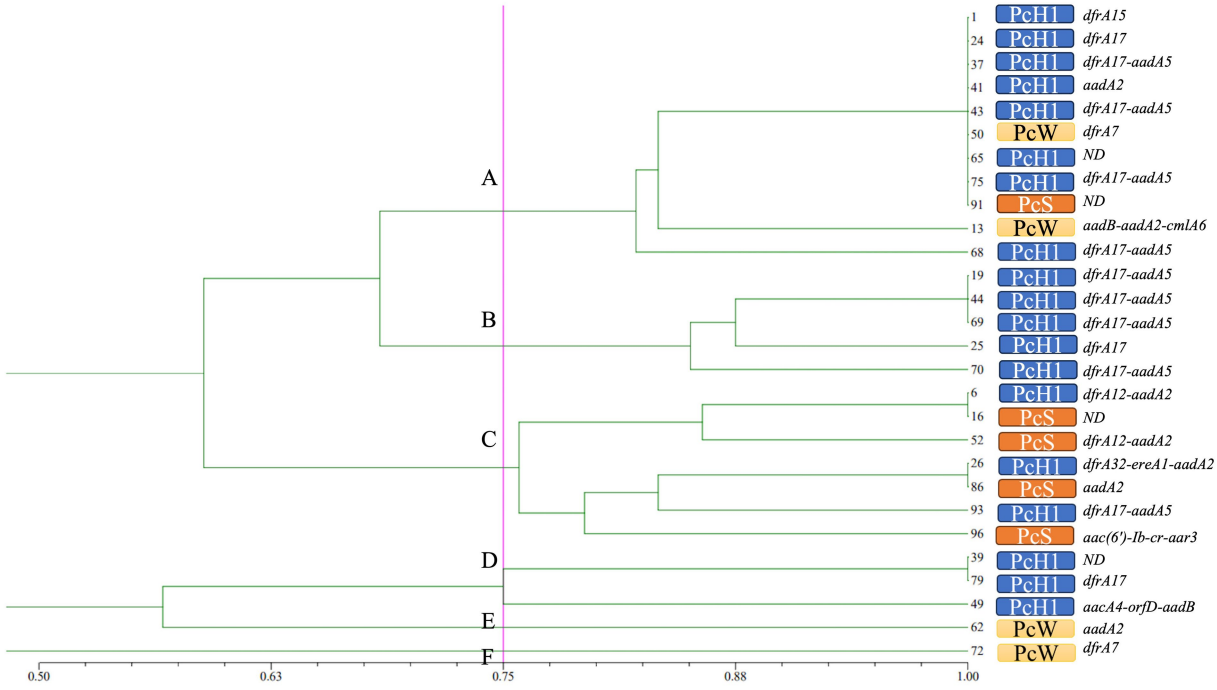

FIGURE 3
The dendrogram of ERIC-PCR. The solid magenta line represents the 75% homologous gene typing reference line. On the right side of the dendrogram are serial numbers of strains, variable region promoter Pc and gene cassettes of integrons successively.

TABLE 3 Distribution of variable region promoters and gene cassettes of 5 isolates and 5 constructed strains.

Strains	Pc		Pc	The activity of P2	Variable region gene
	−35 region	−10 region			
MM-6	TGGACA	TAAACT	PcH1	Inactive	*dfrA12-aadA2*
MM-26	TGGACA	TAAACT	PcH1	Inactive	*dfrA32-ereA1-aadA2*
MM-41	TGGACA	TAAACT	PcH1	Inactive	*aadA2*
MM-62	TGGACA	TAAGCT	PcW	Inactive	*aadA2*
MM-86	TTGACA	TAAACT	PcS	Inactive	*aadA2*
JM-6	TGGACA	TAAACT	PcH1	Inactive	*dfrA12-aadA2*
JM-26	TGGACA	TAAACT	PcH1	Inactive	*dfrA32-ereA1-aadA2*
JM-41	TGGACA	TAAACT	PcH1	Inactive	*aadA2*
JM-62	TGGACA	TAAGCT	PcW	Inactive	*aadA2*
JM-86	TTGACA	TAAACT	PcS	Inactive	*aadA2*

aadA2: gene of adenosine transferase for aminoglycosides.

strains was 28.9%, lower than that observed in common *Enterobacteriaceae* bacteria. This lower prevalence might be attributed to the relatively lower detection rate of *M. morganii* in clinical settings. Wei et al. reported a detection rate of class 1 integrons in clinical isolates of *E. coli* as 72% (Wei et al., 2013), and in another study of *K. pneumoniae*, the positivity rate of class 1 integrons was 31.5% (Farajzadeh Sheikh et al., 2024). The host bacteria in these studies exhibited relatively higher levels of antibiotic resistance compared to the M. morganii isolates in the current study. The detected variable region gene cassettes in class 1 integron-positive strains primarily included aminoglycoside resistance genes (*aadA*, *aacA4*, *aadB*) and the trimethoprim resistance gene (*dfrA*), consistent with findings from other genera with class 1 integron-positive strains (Xiao et al., 2019; Li et al., 2022). In this study, some integron-positive strains failed to amplify gene cassettes, possibly due to atypical gene cassettes in the variable region. This could be attributed to gene recombination or insertion mutations in transposons, leading to the absence of the 3′ conserved segment or an excessive number of gene cassettes in the variable region. The latter may have exceeded the capability of conventional PCR amplification, resulting in amplification failure. Further validation using inverse PCR (Green and Sambrook, 2019; Figueroa-Bossi et al., 2024) techniques is necessary to address this issue (Odetoyin et al., 2017).

Extensive research has confirmed that promoters are crucial in regulating gene expression (Carrier et al., 2018; Brandis et al.,

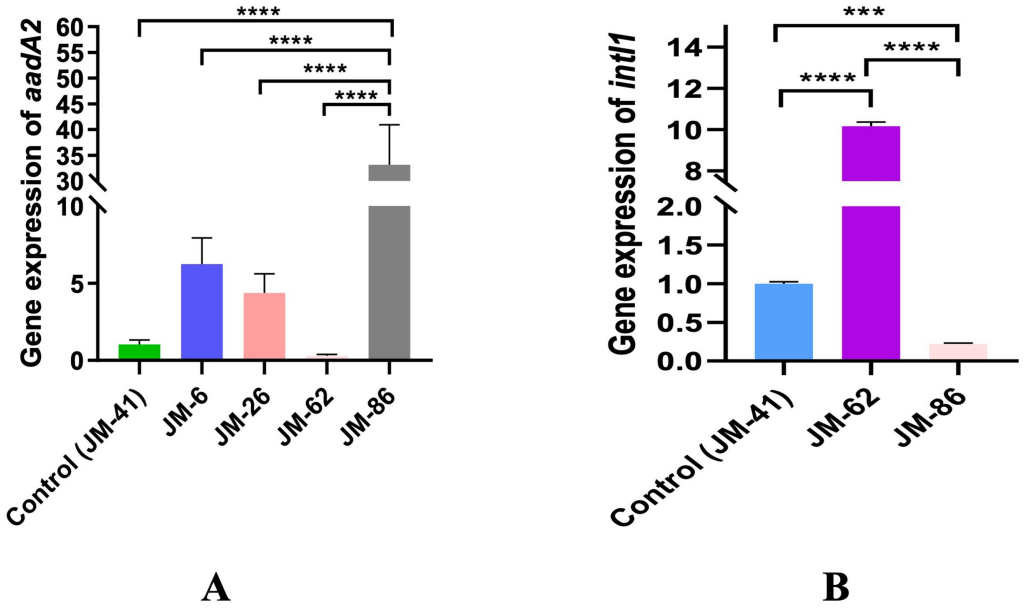

FIGURE 4
(A) The relative expression of *aadA2* in different constructed strains; **(B)** The relative expression of *intI1* in different constructed strains, ****$p < 0.0001$, ***$p < 0.001$.

TABLE 4 The antimicrobial sensitivity test results of constructed strains to each antibiotic.

Strains\ antibiotics	MIC (μg/ml)				K-B (mm)			
	STR	AK	CHL	TE	STR	AK	CHL	TE
JM-6	8	0.25	32	1	13	22	6	25
JM-26	16	0.25	32	1	11	23	6	26
JM-41	32	0.25	32	4	10	22	6	20
JM-62	4	0.25	32	4	13	21	6	23
JM-86	128	0.25	32	8	6	22	6	14
25922	4	0.5	2	1	20	23	27	23
JM109	1	0.25	4	2	15	21	25	26

STR, streptomycin; AK, amikacin; CHL, chloramphenicol; TE, tetracycline.

2021). Consequently, the expression of gene cassettes within integrons is significantly influenced by the variable region promoters. In this study, the predominant Pc promoter type in class 1 integron-positive strains was PcH1, a relatively weak promoter. The detection rates of PcS and PcW were lower than that of PcH1. The detection rate of PcH1 was also relatively high in other class 1 integron-positive Enterobacteriaceae. For instance, a study of class 1 integron-positive isolates of Proteus revealed a detection rate of PcH1 as high as 51%, making it the most common type (Xiao et al., 2019). Another study on the molecular characterization of class 1 integrons in carbapenem-resistant Enterobacteriaceae showed that PcH1 was also the predominant Pc (Wang et al., 2023). All downstream P2 promoters, containing 14 bases between the −35 and −10 regions, were inactive. Retrospective analysis of antibiotic resistance data in class 1 integron-positive strains did not reveal significant statistical differences in resistance rates to aminoglycosides or trimethoprim among strains with different Pc strengths. However, strains with stronger Pc promoters exhibited numerically higher resistance rates to these antibiotics than those with weaker Pc promoters. This observation reflects the fact that integrons contribute only partially to the host bacterium's drug resistance genes. Furthermore, the expression and level of drug resistance genes may be influenced by various internal and external factors. Most integrons are located on plasmids or transposons (Liebert et al., 1999), which can potentially impact the resistance of the host bacterium, though not necessarily dominantly. To minimize interference and further explore the effect of variable region promoters within integrons on downstream gene expression, we used the low-copy plasmid pACYC184 as the vector. Recombinant plasmids were constructed to include variable region promoters and gene cassettes from class 1 integrons. Gene segments were synthesized based on actual sequencing results from experimental strains, preserving the natural configuration of integrons in these strains to a great extent. Additionally, HindIII and AseI were selected as the sites of enzyme digestion to replace the original *tet* promoter on the plasmid, positioning them away from the internal *cat* reference gene. This design allows the inserted gene segments to maximize the expression of drug resistance genes.

The strength of promoters and their distance from gene cassettes are primary factors influencing the transcription of downstream gene cassettes (Fonseca and Vicente, 2022). This project found significant differences in the expression efficiency of the antibiotic resistance gene cassette *aadA2* mediated by promoters of different strengths. qPCR results confirmed that stronger Pc promoters in integrons corresponded to higher transcription levels of downstream gene cassettes. In antimicrobial susceptibility tests, only strain JM-86, carrying a strong promoter, exhibited intermediate resistance to tetracycline in both microbroth dilution and K-B methods, whereas other strains remained sensitive. This suggests that the Pc promoter within the recombinant plasmid may regulate the downstream *tet* gene to some extent, highlighting the substantial impact of promoter strength on regulating gene expression. Interestingly, contrary to expectations based on other studies (Jacquier et al., 2009; Souque et al., 2021), the distance of Pc to downstream gene cassettes did not similarly affect gene expression in our experiment. Under the condition of identical Pc types, strains JM-6 and JM-26, located farther from Pc, exhibited higher relative expression levels of *aadA2* compared to the closer strain JM-41. Previous research in class 2 integrons has suggested that functional promoters of gene cassettes, like *ereA* located at the second position in the array, may enhance the expression of adjacent gene cassettes (Fonseca and Vicente, 2022), potentially explaining the increased expression of *aadA2* in strain JM-26 at a distance. Additionally, the copy number of plasmids within engineered bacteria also influences gene cassette expression levels (Stokes and Hall, 1989). Furthermore, the gene segments used in this study were derived from clinical strains containing unknown functional sequences within integrons that might also regulate the expression of gene cassettes in the variable region, warranting further investigation. Notably, the expression levels of *intI1* in strains with different Pc strengths exhibited an inverse relationship with *aadA2* expression: stronger Pc promoters correlated with higher expression levels of antibiotic resistance genes in the variable region but lower expression levels of *intI1*. This suggests that the integrase's ability for integration and excision may decrease, maintaining bacterial stability internally, consistent with the literature (Wei et al., 2011). Differences in streptomycin MICs observed among engineered strains using microbroth dilution indicate varied regulatory effects of different promoter expressions, whereas no differences were observed for other aminoglycoside antibiotics like amikacin. This discrepancy likely stems from the product of *aadA2* being an aminoglycoside adenylyl transferase, which confers resistance to streptomycin and spectinomycin but not necessarily to other aminoglycosides (Bito and Susani, 1994; Walker et al., 2001).

The horizontal transfer of drug resistance genes is the fastest and most common way to spread clinical resistant strains (Warnes et al., 2012; Mathers et al., 2015), making homogeneity analysis of integron-positive strains particularly important. Herein, ERIC-PCR was used to analyze the homogeneity of 28 non-repetitive clinical isolates of *M. morganii* positive for class 1 integrons, using a similarity cutoff of 0.75. The results revealed three main genotypes: A, B, and C, comprising 11, 5, and 7 isolates, respectively. The distribution of promoter types and gene cassettes in the variable region was relatively concentrated within these genotypes. Furthermore, analysis of the strain data indicated that integron-positive *M. morganii* strains were predominantly found in the ICU and urology departments. This distribution is likely associated with the working environment of these departments. Factors such as surgical procedures in the ICU, critically ill patients, a high frequency of medical devices, and frequent operations increase the risk of cross-infection. Similarly, urological procedures involving catheterization and intravenous administration are invasive, contributing further to this risk. Therefore, it is crucial to enhance disinfection and sterilization of departmental environments and surgical instruments, as well as to standardize medical procedures such as intravenous administration and catheterization to minimize or prevent cross-infection. These measures aim to reduce the potential for clonal spread of integrons within hospitals.

Mobile genetic elements play a role in the horizontal transfer of drug resistance genes. Under antibiotic stress, class 1 integrons can capture gene cassette-like structures from DNA fragments ingested by bacteria and integrate them into attI1 sites through upregulation of integrase expression. Attempted transcription and translation of reading frames present in gene cassettes occur through variable region promoters and the mechanisms of translation termination-reinitiation coupling. Regardless of whether the reading frame in the gene cassette has a promoter or ribosomal binding site, if the expression product of the reading frame can confer resistance to the antibacterial agent, the strain can survive. The captured drug resistance gene cassettes can be disseminated through the proliferation and horizontal transfer of strains, leading to the emergence and dissemination of bacterial resistance (Guerin et al., 2009).

5 Conclusion

In summary, integron promoters exhibit a diverse distribution, predominantly carrying drug resistance gene cassettes for aminoglycosides and trimethoprim. The strength of the class 1 integron variable region promoters significantly correlates with the expression levels of downstream gene cassettes. It is likely that the clonal spread of class 1 integron-positive *M. morganii* occurs within our local healthcare setting. This study aimed to investigate the promoter distribution characteristics of class 1 integrons and their regulatory effects on drug resistance genes in *M. morganii* isolates, providing a theoretical basis for the prevention and treatment of infections with *M. morganii* in clinical practice. Additionally, this study may offer new insights for addressing other rare clinical bacteria with increasing drug resistance in the future. The effect of antibiotic factors on integrons will be studied in our future work.

Data availability statement

The datasets presented in this study can be found in online repositories. The names of the repository/repositories and accession number(s) can be found in the article/Supplementary material.

Author contributions

YY: Data curation, Formal analysis, Investigation, Methodology, Writing – original draft. HZ: Investigation, Supervision, Writing – original draft. RZ: Data curation, Methodology, Writing – review & editing. XQ: Investigation, Project administration, Resources, Supervision, Writing – original draft. JY: Investigation, Supervision, Writing – original draft. WL: Data curation, Investigation, Writing

– original draft. QL: Funding acquisition, Methodology, Supervision, Writing – review & editing. GW: Methodology, Supervision, Writing – review & editing.

Funding

The author(s) declare that financial support was received for the research, authorship, and/or publication of this article. This study was supported by grants from the Medical and Health Research Project of Zhejiang Province (Grant No. 2024KY288), the Key Cultivation Disciplines Foundation of Ningbo Medical Centre Lihuili Hospital (Grant No. 2022-P07), and was partly supported by the Traditional Chinese Medicine Research Project of Zhejiang Province (Grant No. 2024ZL940), and Ningbo Health Science and Technology Plan Project (Grant No. 2022Y03).

Acknowledgments

We thank Home for Researchers editorial team (www.home-for-researchers.com) for language editing service.

Conflict of interest

The authors declare that the research was conducted in the absence of any commercial or financial relationships that could be construed as a potential conflict of interest.

Publisher's note

Supplementary material

The Supplementary material for this article can be found online at: https://www.frontiersin.org/articles/10.3389/fmicb.2024.1459162/full#supplementary-material

References

Agrawal, K. U., Limaye Joshi, K., and Gad, M. (2021). A rare case of fulminant acute postoperative *Morganella morganii* Endophthalmitis. *Ocul. Immunol. Inflamm.* 31, 123–126. doi: 10.1080/09273948.2021.1993269

Alelyani, F. M., Almutawif, Y. A., Ali, H. M., Aljohani, R. Z., Almutairi, A. Z., and Murshid, W. R. (2022). A pituitary abscess caused by *Morganella morganii*: a case report. *Am. J. Case Rep.* 23:e936743. doi: 10.12659/ajcr.936743

Alsaadi, A., Alghamdi, A. A., Akkielah, L., Alanazi, M., Alghamdi, S., Abanamy, H., et al. (2024). Epidemiology and clinical characteristics of *Morganella morganii* infections: a multicenter retrospective study. *J. Infect. Public Health* 17, 430–434. doi: 10.1016/j.jiph.2023.12.013

Bakhshi, B., Afshari, N., and Fallah, F. (2018). Enterobacterial repetitive intergenic consensus (ERIC)-PCR analysis as a reliable evidence for suspected *Shigella* spp. outbreaks. *Braz. J. Microbiol.* 49, 529–533. doi: 10.1016/j.bjm.2017.01.014

Banoub, J., Kundu, J., Kansal, S., Rathore, S., Kaundal, M., Angrup, A., et al. (2022). Evaluation of ERIC-PCR and MALDI-TOF as typing tools for multidrug resistant *Klebsiella pneumoniae* clinical isolates from a tertiary care center in India. *PLoS One* 17:e0271652. doi: 10.1371/journal.pone.0271652

Behera, D. U., Dixit, S., Gaur, M., Mishra, R., Sahoo, R. K., Sahoo, M., et al. (2023a). Sequencing and characterization of *M. morganii* strain UM869: a comprehensive comparative genomic analysis of virulence, antibiotic resistance, and functional pathways. *Genes* 14:1279. doi: 10.3390/genes14061279

Behera, D. U., Ratnajothy, K., Dey, S., Gaur, M., Sahoo, R. K., Sahoo, S., et al. (2023b). *In vitro* synergistic interaction of colistin and other antimicrobials against intrinsic colistin-resistant *Morganella morganii* isolates. *3 Biotech* 13:127. doi: 10.1007/s13205-023-03551-w

Bito, A., and Susani, M. (1994). Revised analysis of aadA2 gene of plasmid pSa. *Antimicrob. Agents Chemother.* 38, 1172–1175. doi: 10.1128/aac.38.5.1172

Bocharova, Y., Savinova, T., Lazareva, A., Polikarpova, S., Gordinskaya, N., Mayanskiy, N., et al. (2020). Genotypes, carbapenemase carriage, integron diversity and oprD alterations among carbapenem-resistant *Pseudomonas aeruginosa* from Russia. *Int. J. Antimicrob. Agents* 55:105899. doi: 10.1016/j.ijantimicag.2020.105899

Brandis, G., Gockel, J., Garoff, L., Guy, L., and Hughes, D. (2021). Expression of the qepA1 gene is induced under antibiotic exposure. *J. Antimicrob. Chemother.* 76, 1433–1440. doi: 10.1093/jac/dkab045

Carrier, M.-C., Lalaouna, D., and Massé, E. (2018). Broadening the definition of bacterial small RNAs: characteristics and mechanisms of action. *Ann. Rev. Microbiol.* 72, 141–161. doi: 10.1146/annurev-micro-090817-062607

CLSI (2022). Performance standards for antimicrobial susceptibility testing. *32nd* Edn CLSI supplement M100. Wayne, PA: Clinical and Laboratory Standards Institute.

Coluzzi, C., Guillemet, M., Mazzamurro, F., Touchon, M., Godfroid, M., Achaz, G., et al. (2023). Chance favors the prepared Genomes_ horizontal transfer shapes the emergence of antibiotic resistance mutations in Core genes. *Mol. Biol. Evol.* 40:msad217. doi: 10.1093/molbev/msad217

Elmi, S. M., Obame, F. L. O., Dokponou, Y. C. H., Yassin, M. R., Attari, S. E., El Asri, A. C. C., et al. (2024). Brain abscess caused by *Morganella morganii*: a case report and review of the literature. *Surg. Neurol. Int.* 15:7. doi: 10.25259/sni_759_2023

Farajzadeh Sheikh, A., Abdi, M., and Farshadzadeh, Z. (2024). Molecular detection of class 1, 2, and 3 integrons in hypervirulent and classic *Klebsiella pneumoniae* isolates: a cross-sectional study. *Health Sci. Rep.* 7:e1962. doi: 10.1002/hsr2.1962

Figueroa-Bossi, N., Balbontín, R., and Bossi, L. (2024). Mapping transposon insertion sites by inverse polymerase chain reaction and sanger sequencing. *Cold Spring Harb. Protoc.* 2024:108197. doi: 10.1101/pdb.prot108197

Fonseca, É. L., and Vicente, A. C. (2022). Integron functionality and genome innovation: an update on the subtle and smart strategy of integrase and gene cassette expression regulation. *Microorganisms* 10:224. doi: 10.3390/microorganisms10020224

Gameiro, I., Botelho, T., Martins, A. I., Henriques, R., and Lapa, P. (2023). *Morganella morganii*: a rare cause of early-onset neonatal Sepsis. *Cureus* 15:e45600. doi: 10.7759/cureus.45600

Green, M. R., and Sambrook, J. (2019). Inverse polymerase chain reaction (PCR). *Cold Spring Harbor Protoc.* 2019, 170–174. doi: 10.1101/pdb.prot095166

Guerin, E., Cambray, G., Sanchez-Alberola, N., Campoy, S., Erill, I., Da Re, S., et al. (2009). The SOS response controls integron recombination. *Science* 324:1034. doi: 10.1126/science.1172914

Hall, R. M., and Collis, C. M. (2006). Mobile gene cassettes and integrons: capture and spread of genes by site-specific recombination. *Mol. Microbiol.* 15, 593–600. doi: 10.1111/j.1365-2958.1995.tb02368.x

Hall, R. M., and Stokes, H. W. (1993). Integrons:novel DNA elements which capture genes by site-specific recombination. *Genetica* 90, 115–132. doi: 10.1007/BF01435034

Han, H. L., Jang, S. J., Park, G., Kook, J. K., Shin, J. H., Shin, S. H., et al. (2008). Identification of an atypical integron carrying an IS26-disrupted aadA1 gene cassette in *Acinetobacter baumannii*. *Int. J. Antimicrob. Agents* 32, 165–169. doi: 10.1016/j.ijantimicag.2008.03.009

Hanau-Berçot, B., Podglajen, I., Casin, I., and Collatz, E. (2002). An intrinsic control element for translational initiation in class 1 integrons. *Mol. Microbiol.* 44, 119–130. doi: 10.1046/j.1365-2958.2002.02843.x

Jacquier, H., Zaoui, C., Sanson-Le Pors, M. J., Mazel, D., and Berçot, B. (2009). Translation regulation of integrons gene cassette expression by the attC sites. *Mol. Microbiol.* 72, 1475–1486. doi: 10.1111/j.1365-2958.2009.06736.x

Kvopka, M., Chan, W., Baranage, D., and Sia, D. (2023). Morganella morganii and *Enterococcus faecalis* endophthalmitis following intravitreal injection. *BMC Ophthalmol.* 23:450. doi: 10.1186/s12886-023-03198-4

Laupland, K., Paterson, D., Edwards, F., Stewart, A., and Harris, P. (2022). *Morganella morganii*, an emerging cause of bloodstream infections. *Microbiol. Spectr.* 10:e0056922. doi: 10.1128/spectrum.00569-22

Leverstein-Van Hall, M., Box, A., Blok, H., Paauw, A., Fluit, A., and Verhoef, J. (2002). Evidence of extensive interspecies transfer of integron-mediated antimicrobial resistance genes among multidrug-resistant Enterobacteriaceae in a clinical setting. *J. Infect. Dis.* 186, 49–56. doi: 10.1086/341078

Li, W., Ma, J., Sun, X., Liu, M., and Wang, H. (2022). Antimicrobial resistance and molecular characterization of gene cassettes from class 1 Integrons in *Escherichia coli* strains. *Microb. Drug Resist.* 28, 413–418. doi: 10.1089/mdr.2021.0172

Li, C., Wang, H., Zhang, J., Wang, Z., Wei, Y., and Zhu, Y. (2023). Endocarditis induced by *M. morganii* in an immunocompetent patient without underlying valvular abnormalities. *Heliyon* 9:e17069. doi: 10.1016/j.heliyon.2023.e17069

Liebert, C. A., Hall, R. M., and Summers, A. O. (1999). Transposon Tn 21, flagship of the floating genome. *Microbiol. Mol. Biol. Rev.* 63, 507–522. doi: 10.1128/mmbr.63.3.507-522.1999

Liu, H., Zhu, J., Hu, Q., and Rao, X. (2016). *Morganella morganii*, a non-negligent opportunistic pathogen. *Int. J. Infect. Dis.* 50, 10–17. doi: 10.1016/j.ijid.2016.07.006

Lu, W., Qiu, X., Chen, K., Zhao, R., Li, Q., and Wu, Q. (2022). Distribution and molecular characterization of functional class 2 Integrons in clinical *Proteus mirabilis* isolates. *Infect. Drug Resist.* 15, 465–474. doi: 10.2147/idr.S347119

Luo, X. W., Liu, P. Y., Miao, Q. Q., Han, R. J., Wu, H., Liu, J. H., et al. (2022). Multidrug resistance genes carried by a novel transposon Tn7376 and a Genomic Island named MMGI-4 in a pathogenic *Morganella morganii* isolate. *Microbiol. Spectr.* 10:e0026522. doi: 10.1128/spectrum.00265-22

Marado, D., and Guerra, M. (2022). Fulminans Purpura due to *Morganella morganii*. *Eur. J. Case Rep. Internal Med.* 9:003670. doi: 10.12890/2022_003670

Mathers, A. J., Peirano, G., and Pitout, J. D. D. (2015). The role of epidemic resistance plasmids and international high-risk clones in the spread of multidrug-resistant Enterobacteriaceae. *Clin. Microbiol. Rev.* 28, 565–591. doi: 10.1128/cmr.00116-14

Meacham, K. J., Zhang, L., Foxman, B., Bauer, R. J., and Marrs, C. F. (2003). Evaluation of genotyping large numbers of *Escherichia coli* isolates by Enterobacterial repetitive intergenic consensus-PCR. *J. Clin. Microbiol.* 41, 5224–5226. doi: 10.1128/jcm.41.11.5224-5226.2003

Novačić, A., Menéndez, D., Ljubas, J., Barbarić, S., Stutz, F., Soudet, J., et al. (2022). Antisense non-coding transcription represses the PHO5 model gene at the level of promoter chromatin structure. *PLoS Genet.* 18:e1010432. doi: 10.1371/journal.pgen.1010432

Odetoyin, B. W., Labar, A. S., Lamikanra, A., Aboderin, A. O., and Okeke, I. N. (2017). Classes 1 and 2 integrons in faecal *Escherichia coli* strains isolated from mother-child pairs in Nigeria. *PLoS One* 12:e0183383. doi: 10.1371/journal.pone.0183383

Shi, H., Chen, X., Yao, Y., and Xu, J. (2022). *Morganella morganii*: an unusual analysis of 11 cases of pediatric urinary tract infections. *J. Clin. Lab. Anal.* 36:e24399. doi: 10.1002/jcla.24399

Shrestha, S., Tada, T., Sherchan, J. B., Uchida, H., Hishinuma, T., Oshiro, S., et al. (2020). Highly multidrug-resistant *Morganella morganii* clinical isolates from Nepal co-producing NDM-type metallo-β-lactamases and the 16S rRNA methylase ArmA. *J. Med. Microbiol.* 69, 572–575. doi: 10.1099/jmm.0.001160

Souque, C., Escudero, J. A., and Maclean, R. C. (2021). Integron activity accelerates the evolution of antibiotic resistance. *eLife* 10:e62474. doi: 10.7554/eLife.62474

Stokes, H. W., and Hall, R. M. (1989). A novel family of potentially mobile DNA elements encoding site-specific gene-integration functions: integrons. *Mol. Microbiol.* 3, 1669–1683. doi: 10.1111/j.1365-2958.1989.tb00153.x

Stokes, H. W., O'Gorman, D. B., Recchia, G. D., Parsekhian, M., and Hall, R. M. (1997). Structure and function of 59-base element recombination sites associated with mobile gene cassettes. *Mol. Microbiol.* 26, 731–745. doi: 10.1046/j.1365-2958.1997.6091980.x

Tseng, C.-S., Yen, Y.-C., Chang, C.-C., and Hsu, Y.-M. (2014). Polymorphism of gene cassette promoter variants of class 1 integron harbored in S. Choleraesuis and typhimurium isolated from Taiwan. *Biomedicine* 4:20. doi: 10.7603/s40681-014-0020-3

Von Wintersdorff, C. J. H., Penders, J., Van Niekerk, J. M., Mills, N. D., Majumder, S., Van Alphen, L. B., et al. (2016). Dissemination of antimicrobial resistance in microbial ecosystems through horizontal gene transfer. *Front. Microbiol.* 7:173. doi: 10.3389/fmicb.2016.00173

Wang, T., Zhu, Y., Zhu, W., Cao, M., and Wei, Q. (2023). Molecular characterization of class 1 integrons in carbapenem-resistant Enterobacterales isolates. *Microb. Pathog.* 177:106051. doi: 10.1016/j.micpath.2023.106051

Walker, R. A., Lindsay, E., Woodward, M. J., Ward, L. R., and Threlfall, E. J. (2001). Variation in clonality and antibiotic-resistance genes among multiresistant *Salmonella enterica* serotype typhimurium phage-type U302 (MR U302) from humans, animals, and foods. *Microb. Drug Resist.* 7, 13–21. doi: 10.1089/107662901750152701

Warnes, S. L., Highmore, C. J., and Keevil, C. W. (2012). Horizontal transfer of antibiotic resistance genes on abiotic touch surfaces: implications for public health. *MBio* 3, e00489–e00412. doi: 10.1128/mBio.00489-12

Wei, Q. H. (2010). The research of regulation mechamism for integron capturing and expressing 477 antibiotic resistance gene cassettes in bacteria. Ph.D. Thesis,: Fudan University.

Wei, Q., Jiang, X., Li, M., Chen, X., Li, G., Li, R., et al. (2011). Transcription of integron-harboured gene cassette impacts integration efficiency in class 1 integron. *Mol. Microbiol.* 80, 1326–1336. doi: 10.1111/j.1365-2958.2011.07648.x

Wei, Q., Jiang, X., Li, M., Li, G., Hu, Q., Lu, H., et al. (2013). Diversity of gene cassette promoter variants of class 1 Integrons in Uropathogenic *Escherichia coli*. *Curr. Microbiol.* 67, 543–549. doi: 10.1007/s00284-013-0399-1

Xiao, L., Wang, X., Kong, N., Cao, M., Zhang, L., Wei, Q., et al. (2019). Polymorphisms of gene cassette promoters of the class 1 Integron in clinical Proteus isolates. *Front. Microbiol.* 10:790. doi: 10.3389/fmicb.2019.00790

Yeşil, M., Özcan, Ö., Karasu, N., and Kağan Yılmaz, B. (2023). Atypical compartment syndrome of the forearm due to mixed infection with Proteus mirabilis and *Morganella morganii* after a penetrating injury: a limb-saving approach. *Joint Dis. Relat. Surg.* 34, 752–756. doi: 10.52312/jdrs.2023.1066

Zaric, R. Z., Jankovic, S., Zaric, M., Milosavljevic, M., Stojadinovic, M., and Pejcic, A. (2021). Antimicrobial treatment of *Morganella morganii* invasive infections: systematic review. *Indian J. Med. Microbiol.* 39, 404–412. doi: 10.1016/j.ijmmb.2021.06.005

frontiers | Frontiers in Microbiology

TYPE Original Research
PUBLISHED 05 November 2024
DOI 10.3389/fmicb.2024.1470454

OPEN ACCESS

EDITED BY
Octavio Luiz Franco,
Catholic University of Brasilia (UCB), Brazil

REVIEWED BY
Tanmay Dutta,
Indian Institutes of Technology (IIT), India
Somanon Bhattacharya,
Wuxi Advanced Therapeutics, Inc., United States
Camila Maurmann De Souza,
Universidade Católica Dom Bosco, Brazil

*CORRESPONDENCE
Liangsheng Guo
✉ gls2135@sina.com

†These authors have contributed equally to this work

RECEIVED 25 July 2024
ACCEPTED 14 October 2024
PUBLISHED 05 November 2024

CITATION
Zheng L, Xu Y and Guo L (2024) Unveiling genome plasticity as a mechanism of non-antifungal-induced antifungal resistance in *Cryptococcus neoformans*. *Front. Microbiol.* 15:1470454. doi: 10.3389/fmicb.2024.1470454

Unveiling genome plasticity as a mechanism of non-antifungal-induced antifungal resistance in *Cryptococcus neoformans*

Lijun Zheng[1†], Yi Xu[2†] and Liangsheng Guo[3*]

[1]Department of Ultrasound Medicine, The Second Affiliated Hospital of Soochow University, Suzhou, China, [2]Department of Pharmacy, The 960th Hospital of PLA, Jinan, China, [3]Department of Obstetrics and Gynecology, The Second Affiliated Hospital of Soochow University, Suzhou, China

Cryptococcus neoformans, a critical priority pathogen designated by the World Health Organization, poses significant therapeutic challenges due to the limited availability of treatment options. The emergence of antifungal resistance, coupled with cross-resistance, further hampers treatment efficacy. Aneuploidy, known for its ability to induce diverse traits, including antifungal resistance, remains poorly understood in *C. neoformans*. We investigated the impact of tunicamycin, a well-established ER stress inducer, on aneuploidy formation in *C. neoformans*. Our findings show that both mild and severe ER stress induced by tunicamycin lead to the formation of aneuploid strains in *C. neoformans*. These aneuploid strains exhibit diverse karyotypes, with some conferring resistance or cross-resistance to antifungal drugs fluconazole and 5-flucytosine. Furthermore, these aneuploid strains display instability, spontaneously losing extra chromosomes in the absence of stress. Transcriptome analysis reveals the simultaneous upregulation of multiple drug resistance-associated genes in aneuploid strains. Our study reveals the genome plasticity of *C. neoformans* as a major mechanism contributing to non-antifungal-induced antifungal resistance.

KEYWORDS

***Cryptococcus neoformans*, tunicamycin, aneuploidy, drug resistance, fluconazole**

Introduction

Cryptococcus species are significant contributors to opportunistic fungal infections in individuals infected with HIV worldwide. The incidence and mortality rates associated with these infections are particularly high in sub-Saharan Africa (ref). *C. neoformans* and *C. gattii* are the primary causative agents of cryptococcosis, which typically manifests as meningitis and pneumonia. The global annual estimated death toll from cryptococcal meningitis is approximately 181,100, with the majority of cases occurring in sub-Saharan Africa (Rajasingham et al., 2017). In 2022, the World Health Organization (WHO) released its inaugural list of priority fungal pathogens, categorizing *Cryptococcus neoformans*, *Candida auris*, *Aspergillus fumigatus*, and *Candida albicans* as "critical priority" pathogens (WHO, 2022).

Currently, treatment options for cryptococcosis are limited to three classes of antifungals: azoles, polyenes, and 5-flucytosine (5FC). Unfortunately, there has been a steady increase in antifungal resistance among clinical isolates of *C. neoformans*. For instance, studies of clinical isolates of *C. neoformans* collected from 134 sites across 40 countries indicated that resistance to fluconazole (FLC) increased from 7.3% between 1997 and 2000 to 11.7% between 2005 and

2007 (Pfaller et al., 2010). Today, FLC resistance is relatively common, particularly in relapse cases of cryptococcal meningitis (Bongomin et al., 2018).

Antifungal resistance often arises from genetic mutations that alter drug targets or increase drug efflux (Fisher et al., 2022). Notably, while point mutations in the *ERG11* gene can induce FLC resistance, the primary mechanism of FLC resistance observed *in vitro* and *in vivo* involves increased *ERG11* copy numbers and overexpression, facilitated by the formation of extra copies of Chromosome 1 (Sionov et al., 2010; Zafar et al., 2019; Yang et al., 2021a). Similarly, in over 50% of clinical fluconazole-resistant isolates of *C. albicans*, amplification of the left arm of Chromosome 5, which houses *ERG11* and *TAC1*, has been detected. *TAC1* encodes a transcription factor that regulates efflux pump genes (Selmecki et al., 2006; Selmecki et al., 2008). Thus, aneuploidy, which involves changes in gene copy numbers, is a common strategy used by human pathogens to rapidly adapt to stress (Tsai and Nelliat, 2019). Importantly, aneuploidy is considered as a significant mutation that can drive phenotypic changes by simultaneously altering the copy number and expression of hundreds of genes. This alteration can lead to the emergence of complex traits as a result of a single mutational event (Pavelka et al., 2010; Chen et al., 2012). Recent studies have highlighted the role of aneuploidy in mediating rapid adaptation to antifungal drugs and, in some cases, cross-adaptation to unrelated drugs in species such as *C. albicans* (Yang et al., 2019; Yang et al., 2021b), *C. parapsilosis* (Yang et al., 2021c; Sun et al., 2023a), and *C. neoformans* (Yang et al., 2021a).

The endoplasmic reticulum (ER) is a vital organelle in eukaryotic cells, responsible for protein folding and secretion. When the ER becomes overwhelmed with unfolded proteins, ER stress occurs, leading to a range of cellular responses (Luoma, 2013). Tunicamycin (TUN), a commonly used chemical, induces ER stress by inhibiting protein glycosylation, causing the accumulation of unfolded proteins (Wu et al., 2018). Recent studies have demonstrated that aneuploidy plays a crucial role in adapting to TUN-induced ER stress in yeast species. For example, in *Saccharomyces cerevisiae* and *C. albicans*, exposure to TUN primarily results in the formation of disomy of Chromosome II and trisomy of Chromosome 2, respectively. These aneuploidies are associated with specific genes that confer TUN resistance, including *ALG7*, *PRE7*, and *YBR085C-A* in *S. cerevisiae*, and *ALG7*, *RTA2*, and *RTA3* in *C. albicans* (Beaupere et al., 2018; Yang et al., 2021b). Furthermore, TUN-induced trisomy of Chromosome 2 in *C. albicans* has been shown to confer cross-adaptation to caspofungin and hydroxyurea (Yang et al., 2021b). In contrast, the mechanisms by which *C. neoformans* adapts to ER stress remain poorly understood, including whether this adaptation is accompanied by the acquisition of new traits, such as antifungal resistance.

Reference strains are a crucial component of laboratory research, providing a standardized genotype that facilitates the comparison of scientific observations within a specific species across the research community. *C. neoformans* strain H99 (ATCC 208821) was originally isolated on February 14 1978 by Dr. John Perfect at Duke University Medical Center from a 28-year-old male with Hodgkin's disease (Janbon et al., 2014), and has since established itself as the most commonly utilized reference strain for *C. neoformans* worldwide. While several distinct lineages of H99 have arisen, displaying diverse levels of virulence as a result of storage, passage, and subculturing across various laboratories, thorough sequencing analyses of these strains have uncovered a limited number of unique mutations among them. Overall, the strains exhibit significant similarity in both growth characteristics and antifungal susceptibility (Fernandes et al., 2022). However, although H99 serves as an excellent model for grasping the fundamental biology of *C. neoformans*, conducting comparative analyses of clinical isolates will significantly enhance our understanding (Jackson et al., 2023).

In this study, we exposed the *C. neoformans* laboratory strain H99 to both mild and severe ER stresses induced by TUN to investigate the effects on antifungal resistance. Our findings showed that TUN primarily induced aneuploidy in *C. neoformans*, resulting in diverse karyotypes with recurring amplifications of Chromosomes 4 and 6, either individually or in combination with amplifications of other chromosomes. Notably, specific aneuploid strains exhibited resistance to FLC or 5FC, and some displayed cross-resistance to both drugs. We also observed that these aneuploid strains were unstable, with spontaneous loss of extra chromosomes and reversion to euploidy when grown in the absence of stress. Importantly, exposure to TUN also triggered cross-resistance to FLC in one clinical isolate of *C. neoformans*. Furthermore, our results indicate that cross-adaptation to ER stress and FLC in aneuploid strains was attributed to the simultaneous upregulation of multiple genes across the genome. This study highlights the role of ER stress in inducing aneuploidy formation and underscores the potential of non-antifungal-induced genome plasticity in driving antifungal resistance in *C. neoformans*.

Materials and methods

Strains and growth conditions

The *C. neoformans* laboratory strain H99 served as the wild-type strain in this study. Stock cultures were preserved in a glycerol solution and stored at a temperature of −80°C. Cells were routinely cultured in a nutrient-rich medium called Yeast extract-Peptone-Dextrose (YPD) at a temperature of 30°C in a shaking incubator set to a moderate speed of 150–200 rpm. To solidify the medium, agar was added at a concentration of 2% (w/v). The drugs used in this study were dissolved in a solvent called dimethyl sulfoxide (DMSO) and stored at a temperature of −20°C.

Growth curves of H99 in the presence of tunicamycin

H99 was thawed from the −80°C freezer and streaked onto YPD-agar plates, which were then incubated at 30°C for 72 h. After incubation, cells were resuspended in YPD broth and their densities were adjusted to 2.5×10^3 cells/mL in YPD broth with or without TUN in a 96-well plate. The TUN concentrations were 0.03–0.125 μg/mL. The plate was then incubated at 30°C, and the optical density at 595 nm (OD_{595}) was monitored using a Tecan plate reader (Infinite F200 PRO, Tecan, Switzerland) at 15-min intervals for 72 h. The data are presented as the mean ± standard deviation (SD) of three biological replicates.

Spot assay

Cells were re-suspended in distilled water and adjusted to a concentration of 1×10^7 cells/mL. Following this, 3 μL of 10-fold serial

dilutions were spotted onto YPD agar plates with or without the presence of drugs. The petri dish plates were then incubated at 30°C and photographed after 72 h.

Broth microdilution assay

The broth microdilution method was performed in accordance with the Clinical and Laboratory Standards Institute (CLSI) M27-2017 guidelines (CLSI, 2017) with minor modifications.

Stock solutions of the drugs (TUN and FLC in YPD broth; 5FC in SD broth) were prepared and subjected to a twofold dilution process. A volume of 0.1 mL of each drug at varying concentrations was sequentially dispensed into U-shaped wells of 96-well microdilution plates (Thermo Fisher Scientific), resulting in final drug concentrations ranging from 0.125 to 128 μg/mL (FLC and 5FC) or 0.03–32 μg/mL (TUN).

To prepare the inoculum of test strains, 3–5 colonies were suspended in sterile saline and standardized to a turbidity of 0.5 McFarland using a spectrophotometer (NanoPhotometer® NP80, Implen, Germany). The inoculum was then diluted with either YPD broth (for TUN and FLC) or SD broth (for 5FC). Following this, 0.1 mL of the yeast suspension was added to each well of the 96-well microdilution plates, yielding a final inoculum concentration between 0.5×10^3 and 2.5×10^3 CFU/mL. The plates were subsequently incubated at 35°C. The minimum inhibitory concentration (MIC) was defined as the lowest drug concentration at which complete growth inhibition was observed. Three replicates were conducted for each drug concentration.

Isolating mutants using low dose of tunicamycin

To generate mutants, we inoculated approximately 2.5×10^3 cells/mL of the H99 strain into 1.5 mL of YPD broth containing a low concentration of 0.06 μg/mL of TUN. We performed three biological replicates. After 72 h of incubation with shaking, the cultures were washed and diluted with distilled water. We then spread approximately 300 cells onto YPD plates and incubated them at 30°C for 72 h. From each culture, we randomly selected 120 colonies and tested them for resistance to TUN using a spot assay.

Induction of mutations with high-dose tunicamycin

To generate mutants, we suspended cells in distilled water and adjusted the concentration to 1×10^7 cells/mL. We then spread 100 μL of this suspension onto YPD plates supplemented with a high concentration of 0.25 μg/mL TUN. The plates were incubated at 30°C for 5 days, allowing for the selection of resistant mutants. We randomly selected 30 mutants for further analysis and characterization. These 30 mutants were maintained in a −80°C freezer.

Assay for genome instability

To investigate the genome instability of the aneuploid strain with disomies of Chromosomes 4 and 6, we performed the following steps: First, the strain with Chrs (4,6) x2 was thawed from the-80°C freezer and streaked onto YPD-agar plates, which were then incubated at 30°C for 72 h. From the resulting colonies, we randomly selected one small colony and suspended it in distilled water. We then diluted the cells in distilled water and spread approximately 200 cells onto a YPD plate, which was incubated at 30°C for 72 h. After incubation, we observed small (S), medium (M), and large (L) colonies. We randomly selected four colonies from each size category for further analysis.

Next-generation sequencing

DNA extraction, library construction, and sequencing were performed using previously described methods (Yang et al., 2021d). The data was then visualized using Ymap (Abbey et al., 2014). The raw fastq files were uploaded to Ymap (version 1.0)[1] and plotted as a function of chromosome position using the *C. neoformans* H99 reference genome (NCBI RefSeq assembly no. GCF_000149245.1).

RNA-seq

Comparative analysis of strains: To investigate the transcriptome profiles of the strains, we performed RNA-seq as described previously with minor modifications (Ke et al., 2024). We first streaked the strains onto YPD plates from the −80°C freezer and incubated them at 30°C for 72 h. We then selected colonies with similar sizes, suspended them in a solution with an optical density (OD) of 0.1, and grew them in a shaker at 30°C until they reached an OD of 1.0. The cells were then collected by centrifugation and frozen in liquid nitrogen.

Treatment of H99 with TUN: We grew H99 in YPD broth in a shaker at 30°C from an OD of 0.1 to 1.0, and then divided the culture into two batches. One batch was treated with TUN at a final concentration of 0.25 μg/mL, while the other batch was treated with an equal volume of DMSO. Three hours later, the cells were collected by centrifugation and frozen in liquid nitrogen.

Total RNA extraction, purification, library construction, and sequencing were performed as described previously (Ke et al., 2024). We obtained three biological replicates for each strain and used DESeq2 (Love et al., 2014) to analyze the differential gene expression profiles. We considered genes with a False Discovery Rate (FDR)-adjusted p value <0.05 and expression fold changes of more than 1.5 or less than −1.5 as differentially expressed.

Statistical analysis

Significance analysis of differences between growth curves was performed using Tukey HSD (Honestly Significant Difference) test.

1 http://lovelace.cs.umn.edu/Ymap/

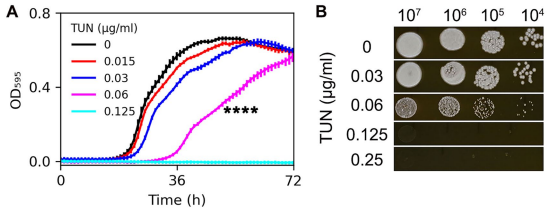

FIGURE 1
Assessment of H99 susceptibility to tunicamycin. Susceptibility was evaluated in both broth and solid medium using twofold increased concentrations of TUN. (A) Cells were cultured in a 96-well plate. Optical density at 595nm (OD_{595}) was monitored every hour for 72h at 30°C using a Tecan plate reader. Data are presented as the mean±SD of three biological replicates. (B) 3μL of 10-fold serial dilutions of cell suspensions were spotted on YPD agar plates supplemented with TUN. The plates were then incubated at 30°C for 3days and subsequently photographed.

Results

Tunicamycin impact on *C. neoformans* H99 growth

The sensitivity of the *C. neoformans* lab strain H99 to TUN was evaluated. In YPD broth, the minimum inhibitory concentration (MIC) of TUN was found to be 0.125 μg/mL. Additionally, TUN at a concentration of 0.06 μg/mL significantly inhibited the growth of H99 ($p < 0.001$, Tukey test), while TUN at a concentration of 0.03 μg/mL did not significantly inhibit growth ($p > 0.05$, Tukey test) (Figure 1A).

On YPD agar plates, H99 was able to grow in the presence of TUN at a concentration of 0.06 μg/mL, although the resulting colonies were smaller than those on the control plate. TUN at concentrations of 0.125 μg/mL and 0.25 μg/mL completely inhibited the growth of H99 (Figure 1B).

Based on these results, TUN at a concentration of 0.06 μg/mL in YPD broth was found to be sub-inhibitory to H99, while TUN at a concentration of 0.125 μg/mL on YPD agar (and in YPD broth) was inhibitory to H99.

Selective pressure of sub-MIC tunicamycin leads to emergence of antifungal resistant mutants

We explored whether sub-MIC concentrations of TUN could select for adaptive mutants in the H99 strain. We cultured the strain in YPD broth supplemented with 0.06 μg/mL TUN, starting with a cell density of approximately 2.5×10^3 cells/mL. After 72 h, we randomly selected 120 colonies from each culture and tested them for TUN susceptibility, with three biological replicates. Among these colonies, we identified five mutants that outperformed the parent strain (Figure 2A). The broth microdilution assay revealed that the parent strain H99 exhibited a MIC of 0.125 μg/mL for TUN, whereas the five mutants displayed MICs ranging from 0.5 to 1 μg/mL. Consequently, the five mutants demonstrated greater resistance to TUN compared to the parent strain.

Sequencing analysis of five selected mutants revealed diverse aneuploid karyotypes: Low-#1 had disomy of Chr12 (Chr12x2), Low-#2 had disomies of Chr9 and Chr12 (Chrs (9,12) x2), Low-#5 had disomies of Chr6 and Chr12 (Chrs (6,12) x2), and Low-#3 and Low-#4 had segmental disomy of the left arm of Chr4 (SegChr4x2) (Figure 2B). Thus, exposure to sub-inhibitory levels of TUN led to the selection of aneuploid TUN-resistant mutants with diverse karyotypes.

Variation analysis revealed few genetic mutations in the mutants (Supplementary Table S1). Low-#1 had a missense mutation in CNAG_06222, encoding the large subunit ribosomal protein L32e, while Low-#3 had a missense mutation in CNAG_00807, whose function is unknown.

We further examined whether the mutants displayed cross-resistance to antifungal drugs. Spot assays demonstrated that mutants with SegChr4x2 were more resistant to FLC than H99, while mutants with Chr12x2 and Chrs (9,12) x2 were more resistant to 5FC than H99 (Figure 2C). The broth microdilution assay indicated that the parent strain H99 had a MIC of 32 μg/mL for FLC, while the two mutants containing SegChr4x2 exhibited MICs greater than 128 μg/mL. For 5FC, H99 displayed an MIC of 0.5 μg/mL, whereas the mutants with Chr12x2 and Chrs (9,12) x2 had MICs of 4 μg/mL.

Thus, depending on the aneuploid chromosome, certain mutants exhibited cross-resistance to antifungals.

Exposure to high concentrations of tunicamycin selects for diverse aneuploid mutants

We plated approximately 1 million H99 cells on YPD plates containing 0.125 μg/mL and 0.25 μg/mL TUN, respectively. After 5 days, we observed lawn growth on the plate with 0.125 μg/mL TUN, while 92 colonies grew on the plate with 0.25 μg/mL TUN. We randomly selected 30 mutants from the latter plate for further analysis. Whole-genome sequencing revealed that 8 mutants had a normal euploid karyotype, while 22 mutants displayed diverse aneuploid karyotypes, consisting of 18 distinct patterns. Notably, 17 out of 22 aneuploids exhibited disomy or trisomy of Chromosomes 4 and 6, either alone or in combination with other chromosomes. Five aneuploids had either Chr4x2 or Chr6x2, but not both, along with disomy of 2–6 other chromosomes (Figure 3). This suggests that amplifications of Chr4 and Chr6, alone or in combination with other chromosomes, were the primary genomic changes among mutants selected under high TUN concentration.

We identified several genetic mutations in the mutants (Supplementary Table S1). For example, mutants high-#8 and high-#12 had the same frameshift mutation in gene CNAG_06130, while mutants high-#15, high-#17, and high-#26 had missense mutations in CNAG_05936, CNAG_01727, and CNAG_05396,

10.3389/fmicb.2024.1470454

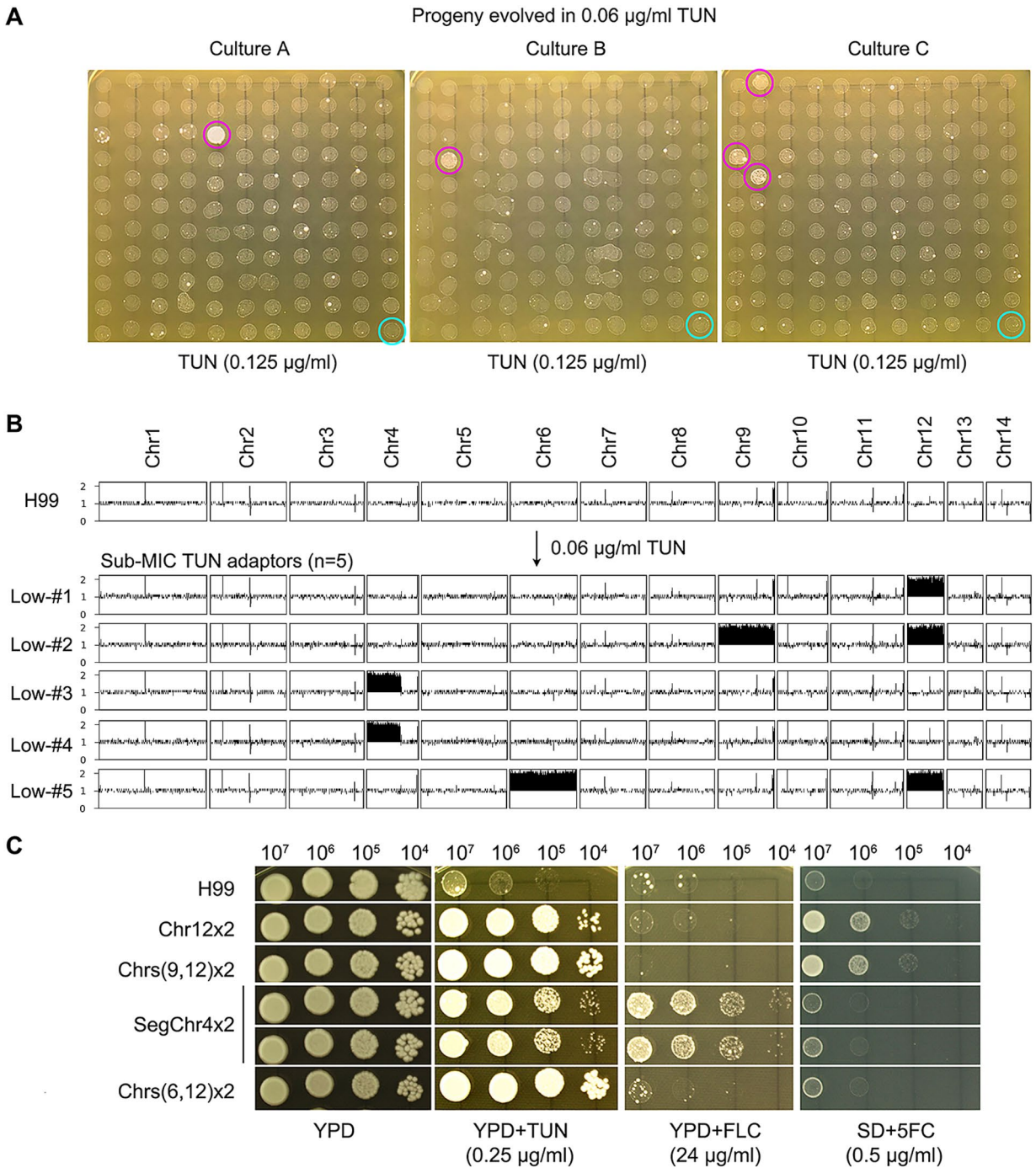

FIGURE 2
Selection of aneuploid mutants with antifungal resistance by low concentrations of tunicamycin. (A) The wild-type strain H99 was cultured in YPD broth supplemented with sub-minimal inhibitory concentration (sub-MIC) of TUN. Three biological replicates were conducted, and 120 colonies from each culture were randomly selected for testing their resistance to TUN (magenta circles) compared to the wild type (cyan circles). The five colonies displaying resistance were subjected to sequencing. (B) The karyotypes of the wild type and the five resistant colonies were visualized using Ymap. The y-axis represents copy number, while the x-axis indicates the location of the sequence reads on the chromosome. (C) The five mutants were subjected to spot assay to evaluate their resistance to TUN, fluconazole (FLC), and 5-flucytosine (5FC). Testing for 5FC was conducted on SD medium, while YPD medium was used for other tests.

respectively. Mutant high-#20 had a missense mutation in CNAG_04310 and a stop-gained mutation in CNAG_06382, while mutant high-#29 had missense mutations in CNAG_03862 and CNAG_03059. However, the functions of proteins encoded by CNAG_06130, CNAG_04310, CNAG_03862, and CNAG_03059 remain unknown.

Some supra-MIC mutants are cross-resistant to fluconazole and/or 5-flucytosine

We found that some mutants that grew in the presence of high concentrations of TUN also showed resistance to other antifungal

10.3389/fmicb.2024.1470454

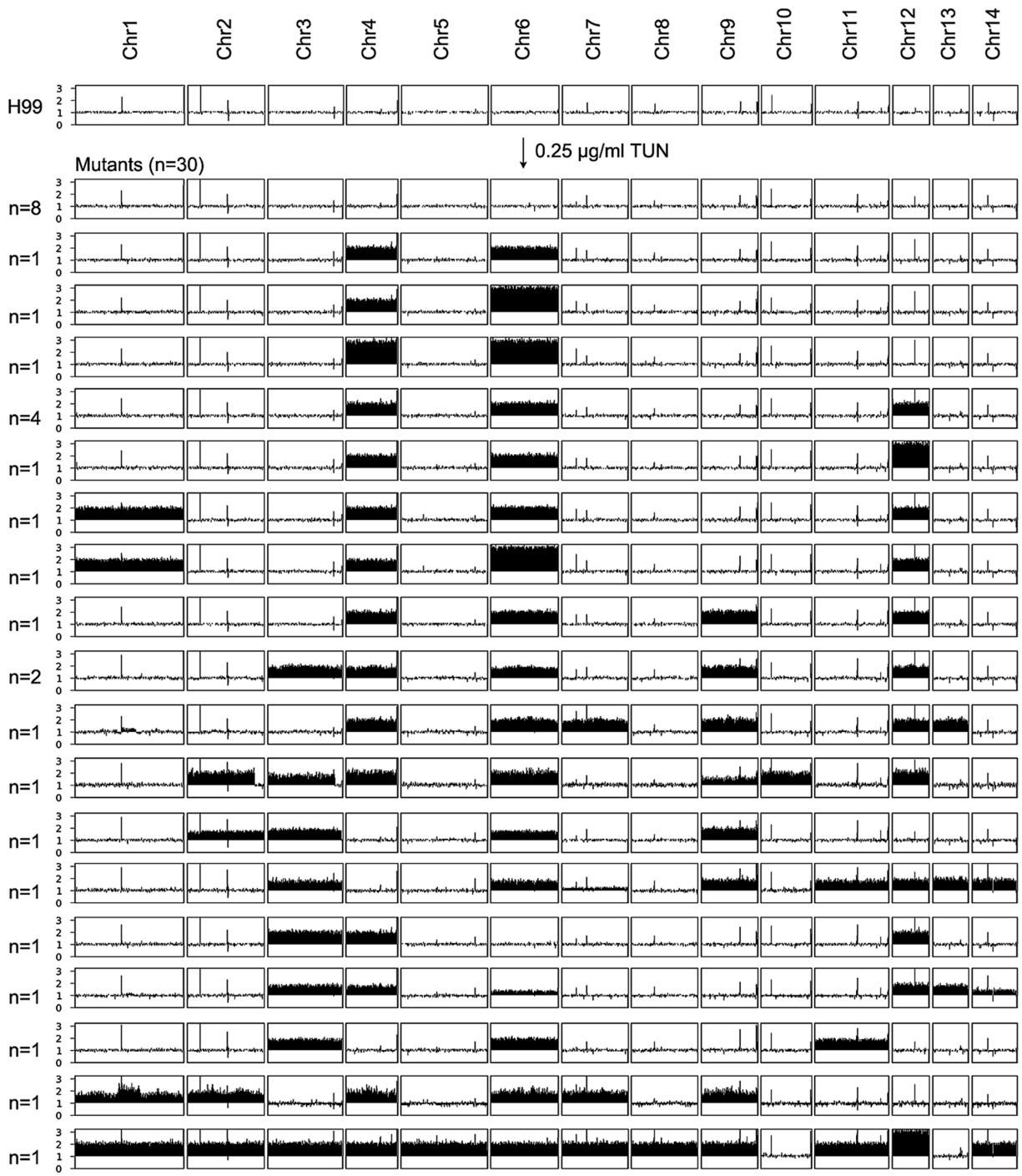

FIGURE 3
Karyotypes of mutants selected by high concentrations of tunicamycin. The wild-type strain H99 was exposed to supra-minimal inhibitory concentration (supra-MIC) of TUN. Thirty mutants were randomly selected for sequencing. The karyotypes of these mutants were visualized using Ymap, and the number of mutants bearing each karyotype is indicated in the figure.

drugs, including FLC and 5FC. To further investigate this, we tested the antifungal resistance of all these mutants using disk diffusion assays. Based on their resistance profiles, we categorized the mutants into four distinct groups (Figure 4).

One group of mutants was resistant to 5FC only and consisted of 8 mutants, which had MICs for 5FC ranging from 1 to 8 μg/mL. Interestingly, three of these mutants had a normal euploid karyotype, while the remaining five had amplifications of at least three chromosomes.

Another group of mutants was resistant to FLC only and consisted of three mutants, each having an MIC of 64 μg/mL for FLC. Each of these mutants had distinct chromosomal changes, including disomy of Chromosomes 4 and 6, disomy of Chromosome 4 and trisomy of Chromosome 6, and disomy of Chromosomes 4, 6, and 12.

10.3389/fmicb.2024.1470454

A third group of mutants showed cross-resistance to both 5FC and FLC, and consisted of only one mutant. The MICs for FLC and 5FC were 128 μg/mL and 8 μg/mL, respectively. This mutant had a complex karyotype, with disomy of Chromosomes 1, 4, 6, and 12.

The final group of mutants did not show obvious resistance to either 5FC or FLC, and consisted of 18 mutants. However, some of these mutants were hypersensitive to FLC, while others were hypersensitive to 5FC.

Aneuploidy is unstable

A mutant with a chromosomal abnormality, Chrs (4,6) x2, was analyzed for its physical characteristics and genetic stability. To do this, around 400 cells of the mutant were grown on a special agar plate (Figure 5A). After two days, differences in the size of the resulting colonies were observed (Figure 5A). The area of each colony was then measured (Figure 5B). Colonies that were smaller than 0.03 cm^2 were classified as small, those between 0.035 cm^2 and 0.04 cm^2 as medium, and those larger than 0.045 cm^2 as large (Figure 5A,B). Four colonies from each size group were randomly selected for further genetic analysis. The results showed that all four small colonies still had the Chrs (4,6) x2 abnormality, while the four medium colonies had a different abnormality, Chr4x2, and the four large colonies had a normal chromosome count (Figure 5C). This suggests that the Chrs (4,6) x2 mutant is unstable and may tend to lose the extra copy of chromosome 6 or all extra chromosomes.

Randomly selected S, M, and L colonies, one from each type, were compared to the H99 strain for resistance to TUN. The spot assay indicated that both S and M colonies exhibited resistance, while the L colony did not (Supplementary Figure S1). Thus, the presence of an additional copy of Chr4 alone was sufficient to confer resistance to TUN, and the loss of all extra copies of aneuploid chromosomes resulted in a loss of TUN resistance.

Aneuploidy causes cross-resistance to tunicamycin and fluconazole via regulating expression of multiple genes across the genome

Our study reveals that disomy of Chrs (4,6), either alone or in combination with disomy of other chromosomes, was the primary genomic alteration among the mutants. Additionally, Chrs (4,6) x2 conferred resistance not only to TUN but also to FLC. To elucidate why Chrs (4,6) x2 led to cross-resistance to both drugs, we compared the transcriptome of one Chrs (4,6) x2 mutant to that of the wild type (Figure 6).

Transcription of 392 genes was detected on Chr4, with 312 genes showing ratios higher than 1.3. Similarly, transcription of 533 genes

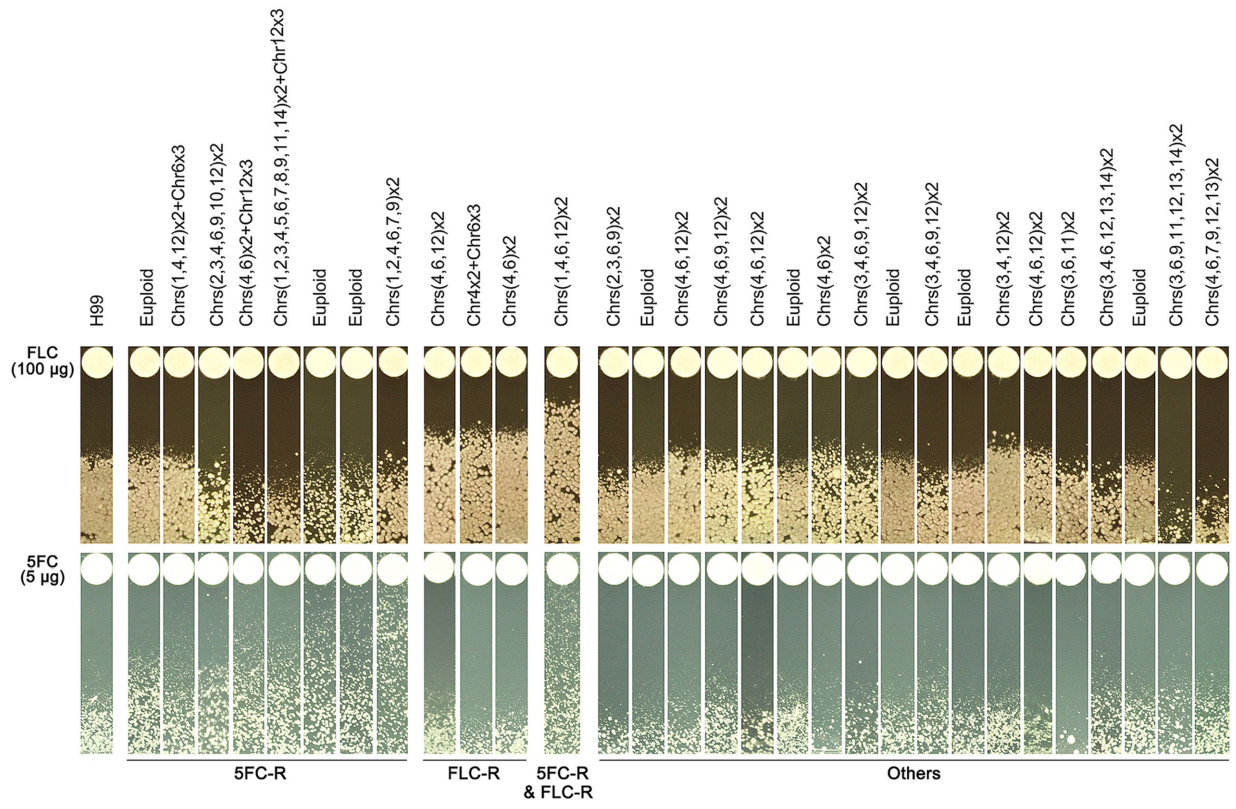

FIGURE 4
Profile of antifungal resistance in mutants induced by supra-MIC tunicamycin. Thirty mutants, induced by supra-minimal inhibitory concentration (supra-MIC) of TUN, were tested using disk diffusion assays. The top panel shows disks containing 200 μg of fluconazole (FLC), while the bottom panel shows disks containing 5 μg of 5-flucytosine (5FC). The diameter of the inhibition zone is inversely proportional to the level of drug resistance. The plates were incubated at 30°C for 3 days and then photographed. YPD plates were used for FLC testing, and SD plates were used for 5FC testing.

10.3389/fmicb.2024.1470454

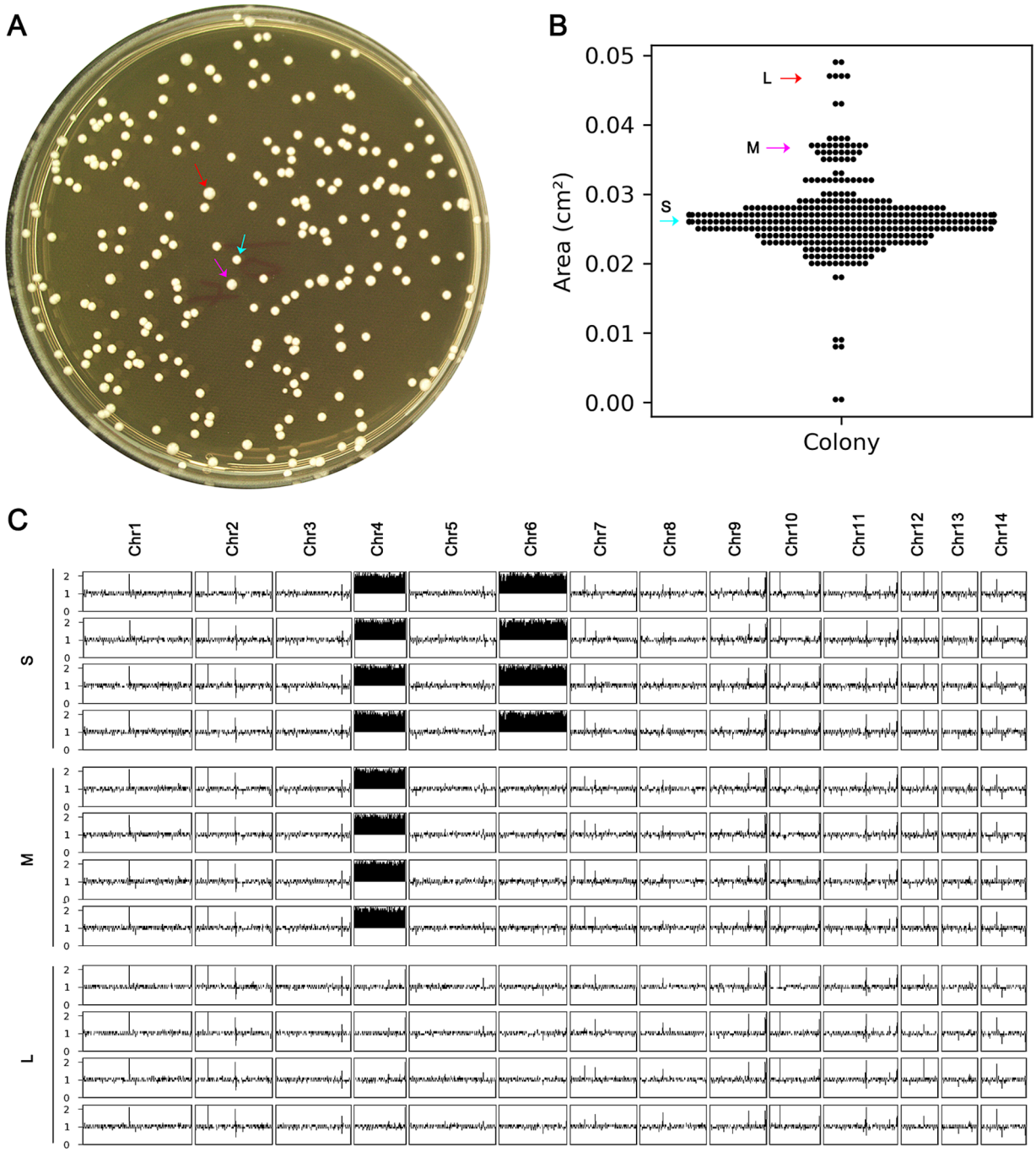

FIGURE 5
Instability of complex aneuploidy. (A) A mutant with disomies of Chr4 and Chr6 was spread on YPD plate. (B) After 48 h of growth, the areas of the colonies were measured. (C) Colonies were classified as small (S), medium (M), or large (L), indicated by cyan, magenta, and red arrows, respectively. Four colonies of each category were randomly selected for sequencing, and the karyotypes were visualized using Ymap.

was detected on Chr6, with 442 genes having ratios higher than 1.3. Consequently, 79.6 and 82.9% of transcribed genes on Chr4 and Chr6, respectively, were up-regulated at least 1.3 times in the Chrs (4,6) x2 strain compared to H99. In contrast, on euploid chromosomes, only 7.5–12.1% of genes were up-regulated to this extent.

Overall, 910 genes were up-regulated across the genome, with 267 and 388 genes on Chr4 and Chr6, respectively. Conversely, 990 genes were down-regulated, with only 8 and 4 on Chr4 and Chr6, respectively. Thus, 72.0% (655 out of 910) of the up-regulated and 1.2% (12 out of 990) of the down-regulated genes were located on aneuploid chromosomes. Consequently, disomy of Chr4 and Chr6 generally led to increased expression of genes on the aneuploid chromosomes and altered expression of genes on euploid chromosomes.

Gene ontology (GO) analysis revealed that 21 genes involved in response to TUN (GOID: 1904576) were significantly enriched among the up-regulated genes, with 14 of them located on Chr4 or Chr6

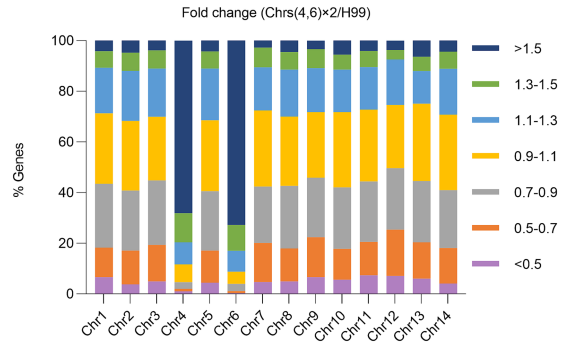

FIGURE 6
Impact of aneuploidy on transcription of genes across the genome. The transcriptome of a mutant with Chrs (4,6) x2 was compared to the haploid wild type H99. Relative expression was determined based on the expression ratio of a target gene in the aneuploid strain versus in H99. The graph displays the proportions of genes on each chromosome falling within specified relative expression ratio ranges.

(Supplementary Table S2). Notably, among the genes encoding efflux pumps, *AFR1*/CNAG_00730, *MDR1*/CNAG_00796, and *PDR16*/CNAG_04984 were up-regulated, with *AFR1* and *MDR1* on Chr1 and *PDR16* on Chr4. Among the *ERG* genes, only *ERG19*/CNAG_05125 and *ERG20*/CNAG_02084 were up-regulated, with *ERG19* on Chr4 and *ERG20* on Chr6. Conversely, *ERG4*/CNAG_02830 was down-regulated (Supplementary Table S2). However, other *ERG* genes, such as *ERG11*/CNAG_00040, *ERG3*/CNAG_00519, or *ERG6*/CNAG_03819, showed no differential expression in Chrs (4,6) x2 compared to H99. Thus, we propose that Chrs (4,6) x2 confers resistance to TUN and FLC by simultaneously up-regulating multiple genes on both euploid and aneuploid chromosomes.

Exposure to tunicamycin leads to cross-resistance to fluconazole in a clinical isolate of *C. neoformans*

We investigated whether TUN also induced antifungal resistance in clinical isolates. Approximately 1 million cells of the clinical isolate GLS#4458 were spread on YPD-agar plates supplemented with TUN. After 5 days, the plate with 0.125 μg/mL TUN showed lawn growth, while the plate with 0.25 μg/mL TUN displayed a few 100 visible colonies (Figure 7A). Sixteen mutants (#1–#16) were randomly selected. Spot assays revealed that all of them were able to grow in the presence of 0.25 μg/mL TUN, whereas growth of the wild-type GLS#4458 was completely inhibited (Figure 7B), indicating that all the mutants developed resistance to TUN. Disk assays were conducted using disks containing 200 μg FLC, and three mutants, #1, #9, and #12, exhibited smaller inhibition zones compared to the parent strain (Figure 7C), suggesting that these three mutants acquired resistance to FLC.

Discussion

ER is a fundamental organelle found in eukaryotic cells. Traditionally, studies investigating ER stress induced by chemical agents have mainly focused on elucidating the associated signaling pathways. However, recent research has uncovered a connection between ER stress and the formation of aneuploidy in yeast species, with subsequent implications for the fortuitous development of antifungal resistance (Beaupere et al., 2018; Yang et al., 2021b). To our knowledge, our study represents the first direct link between ER stress and the emergence of antifungal resistance, including cross-resistance, in *C. neoformans*. It's important to note that while aneuploidy itself generally does not confer resistance to various stresses, including antifungal drugs, it's the specific aneuploidy of particular chromosome (s) that can alter susceptibility to specific stressors.

The mechanisms underlying TUN-induced ER stress and its subsequent role in aneuploidy formation in *C. neoformans* remain elusive. Aneuploidy provides a fitness advantage under stress conditions by directly regulating genes on the aneuploid chromosome or indirectly impacting genes on euploid chromosomes (Pavelka et al., 2010). In species like *S. cerevisiae* and *C. albicans*, TUN-induced amplification of specific chromosomes is attributed to the presence of particular genes, such as *ALG7* (Beaupere et al., 2018; Yang et al., 2021b). However, in the genome of *C. neoformans*, *ALG7*/CNAG_06901 is located on Chr3, and only a minority of mutants exhibit amplification of Chr3. Instead, amplification of Chr4 and Chr6 emerges as the predominant genomic alteration among the mutants. Gene ontology (GO) analysis has identified at least 14 genes on Chr4 and Chr6 associated with resistance to TUN (refer to Supplementary Table S2). Future investigations will focus on determining whether amplification of these genes in the wild type is sufficient to confer resistance to TUN.

In the Chrs (4,6) x2 strain, which exhibited resistance to FLC, several genes encoding efflux pumps, such as *AFR1* and *MDR1* on Chr1, as well as *PDR16* on Chr4, were up-regulated compared to the wild type. However, most of the *ERG* genes, including *ERG11*, showed no differential expression. We propose that Chrs (4,6) x2 induces cross-resistance to TUN and FLC by concurrently up-regulating multiple genes on both aneuploid and euploid chromosomes.

The TUN-selected mutants exhibit diverse genomic alterations, including increases in copy number across various chromosomes and to varying extents, while showing few genetic mutations, suggesting that TUN primarily induces genome instability rather than hypermutation in *C. neoformans*. ER stress and genome damage are interconnected, as ER stress can induce genome instability by impeding the repair of double-strand breaks (DSBs) (Yamamori et al., 2013). DSBs are particularly detrimental to genome integrity (Blackford and Jackson, 2017), and their unrepaired status contributes to genome instability, leading to chromosome missegregation and aneuploidy formation (Srivastava and Raghavan, 2015; Blackford and Jackson, 2017).

Our study illustrates that brief exposure to mild ER stress is adequate to trigger aneuploidy in *C. neoformans*, mirroring the previous findings in *C. albicans* (Yang et al., 2021b). Additionally, besides ER stress, short-term exposure to sub-inhibitory concentrations of FLC also prompts aneuploidy in *C. neoformans* (Yang et al., 2021a) and *C. albicans* (Sun et al., 2023b; Todd et al., 2023; Yang et al., 2023). Thus, we propose that the genome plasticity of fungal pathogens can be readily and swiftly induced by mild stresses.

Our study underscores the genome plasticity of *C. neoformans* as a swift and reversible mechanism for adapting to TUN-induced ER stress, offering fresh insights into the mechanism underlying the emergence of antifungal resistance.

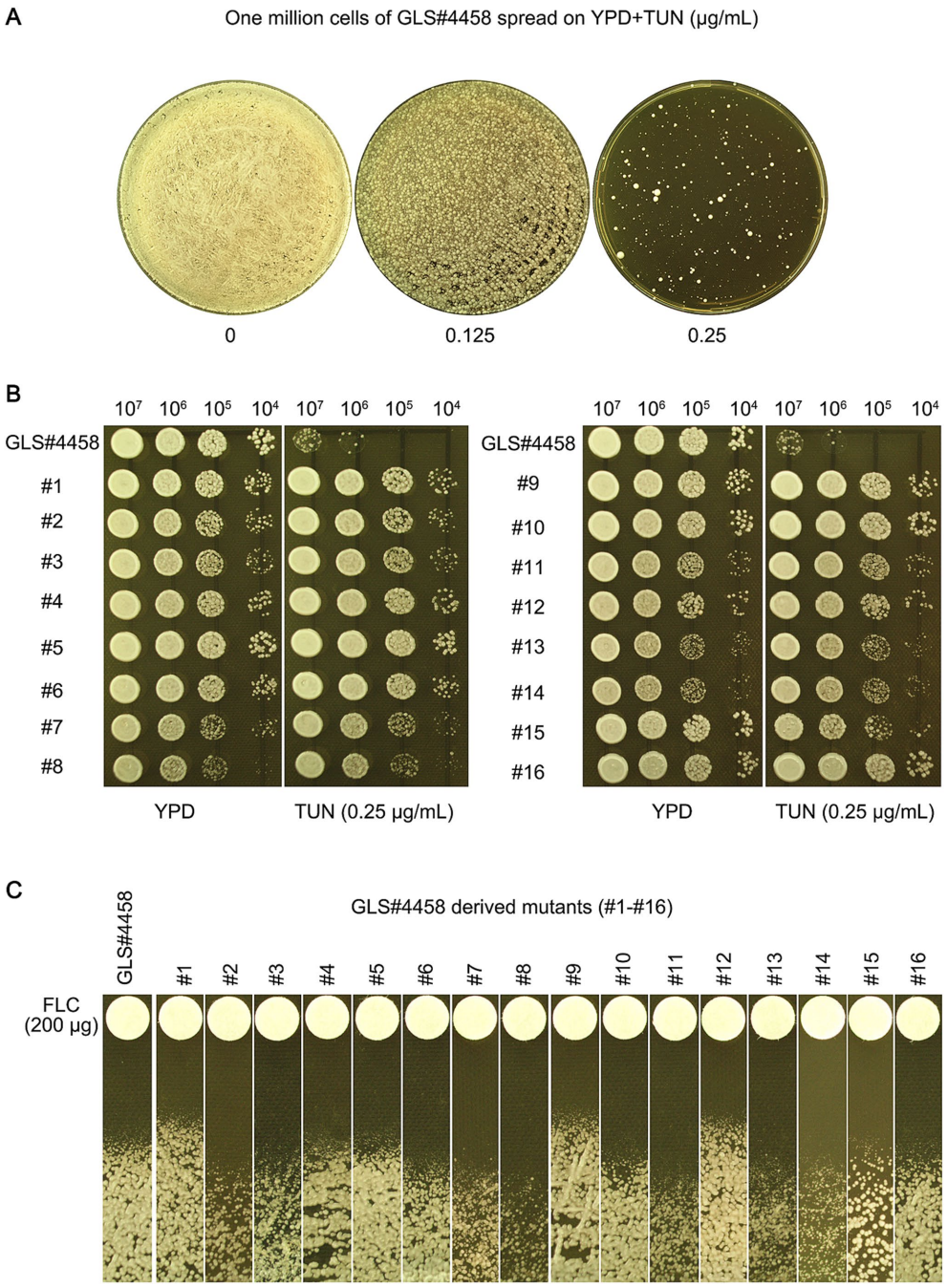

FIGURE 7
Tunicamycin induces fluconazole resistance in clinical isolate of *C. neoformans*. (A) GLS#4458 is a clinical isolate of *C. neoformans*. The cells of GLS#4458 were suspended in distilled water and adjusted to a concentration of 1.0×10^7cells/mL. A volume of 100μL of the cell suspension was spread onto YPD-agar medium supplemented with TUN, with drug concentrations indicated in the figure. The plates were incubated at 30°C for 5days before being photographed. Sixteen colonies (#1–#16) were randomly selected from the plate containing 0.25μg/mL for further analysis. (B) A spot assay was conducted to compare the resistance to TUN between the 16 mutants and the wild type. For each strain, 3μL of 10-fold serial dilutions were spotted on YPD-agar plates with 0.25μg/mL TUN or without TUN (as a control). The plates were then incubated at 30°C for 3days and subsequently photographed. (C) In the disk diffusion assay, disks containing 200μg FLC were used. The plates were incubated at 30°C for 3days before being photographed.

Data availability statement

The datasets presented in this study can be found in online repositories. The names of the repository/repositories and accession number(s) can be found below: https://www.ebi.ac.uk/arrayexpress/, E-MTAB-12268, E-MTAB-12276, EMTAB- 12286 and E-MTAB-12275.

Author contributions

LZ: Data curation, Formal analysis, Investigation, Methodology, Validation, Visualization, Writing – review & editing. YX: Conceptualization, Data curation, Formal analysis, Funding acquisition, Investigation, Methodology, Validation, Visualization,

Writing – review & editing. LG: Conceptualization, Funding acquisition, Project administration, Resources, Supervision, Writing – original draft, Writing – review & editing.

Funding

The author(s) declare that financial support was received for the research, authorship, and/or publication of this article. This study was supported by the Science and Technology Development Plan of Suzhou (SLJ2022018), Scientific Research Project of Suzhou Commission of Health (GSWS2020028) to Liang-sheng Guo, Natural Science Foundation of Shandong Province (ZR2023MH227) and the National Natural Science Foundation of China (81402978) to Yi Xu.

Acknowledgments

We thank Dr. Feng Yang of Shanghai Tenth People's Hospital for assistance in analyzing NGS data and for critical reading of the manuscript.

Conflict of interest

The authors declare that the research was conducted in the absence of any commercial or financial relationships that could be construed as a potential conflict of interest.

Publisher's note

All claims expressed in this article are solely those of the authors and do not necessarily represent those of their affiliated organizations, or those of the publisher, the editors and the reviewers. Any product that may be evaluated in this article, or claim that may be made by its manufacturer, is not guaranteed or endorsed by the publisher.

Supplementary material

The Supplementary material for this article can be found online at: https://www.frontiersin.org/articles/10.3389/fmicb.2024.1470454/full#supplementary-material

References

Abbey, D. A., Funt, J., Lurie-Weinberger, M. N., Thompson, D. A., Regev, A., Myers, C. L., et al. (2014). YMAP: a pipeline for visualization of copy number variation and loss of heterozygosity in eukaryotic pathogens. *Genome Med.* 6:100. doi: 10.1186/s13073-014-0100-8

Beaupere, C., Dinatto, L., Wasko, B. M., Chen, R. B., VanValkenburg, L., Kiflezghi, M. G., et al. (2018). Genetic screen identifies adaptive aneuploidy as a key mediator of ER stress resistance in yeast. *Proc. Natl. Acad. Sci. USA* 115, 9586–9591. doi: 10.1073/pnas.1804264115

Blackford, A. N., and Jackson, S. P. (2017). ATM, ATR, and DNA-PK: the trinity at the heart of the DNA damage response. *Mol. Cell* 66, 801–817. doi: 10.1016/j.molcel.2017.05.015

Bongomin, F., Oladele, R. O., Gago, S., Moore, C. B., and Richardson, M. D. (2018). A systematic review of fluconazole resistance in clinical isolates of cryptococcus species. *Mycoses* 61, 290–297. doi: 10.1111/myc.12747

Chen, G., Rubinstein, B., and Li, R. (2012). Whole chromosome aneuploidy: big mutations drive adaptation by phenotypic leap. *BioEssays* 34, 893–900. doi: 10.1002/bies.201200069

CLSI (Ed.) (2017). Reference method for broth. (Dilution) antifungal susceptibility testing of yeasts. 4th ed. CLSI standard M27. Wayne, PA: Clinical and Laboratory Standards Institute.

Fernandes, K. E., Fraser, J. A., and Carter, D. A. (2022). Lineages derived from *Cryptococcus neoformans* type strain H99 support a link between the capacity to be pleomorphic and virulence. *MBio* 13:e0028322. doi: 10.1128/mbio.00283-22

Fisher, M. C., Alastruey-Izquierdo, A., Berman, J., Bicanic, T., Bignell, E. M., Bowyer, P., et al. (2022). Tackling the emerging threat of antifungal resistance to human health. *Nat. Rev. Microbiol.* 20, 557–571. doi: 10.1038/s41579-022-00720-1

Jackson, K. M., Ding, M., and Nielsen, K. (2023). Importance of clinical isolates in *Cryptococcus neoformans* research. *J Fungi (Basel)* 9:364. doi: 10.3390/jof9030364

Janbon, G., Ormerod, K. L., Paulet, D., Byrnes, E. J. 3rd, Yadav, V., Chatterjee, G., et al. (2014). Analysis of the genome and transcriptome of *Cryptococcus neoformans* var. grubii reveals complex RNA expression and microevolution leading to virulence attenuation. *PLoS Genet.* 10:e1004261. doi: 10.1371/journal.pgen.1004261

Ke, W., Xie, Y., Chen, Y., Ding, H., Ye, L., Qiu, H., et al. (2024). Fungicide-tolerant persister formation during cryptococcal pulmonary infection. *Cell Host Microbe* 32, 276–289.e7. doi: 10.1016/j.chom.2023.12.012

Love, M. I., Huber, W., and Anders, S. (2014). Moderated estimation of fold change and dispersion for RNA-seq data with DESeq2. *Genome Biol.* 15:550. doi: 10.1186/s13059-014-0550-8

Luoma, P. V. (2013). Elimination of endoplasmic reticulum stress and cardiovascular, type 2 diabetic, and other metabolic diseases. *Ann. Med.* 45, 194–202. doi: 10.3109/07853890.2012.700116

Pavelka, N., Rancati, G., Zhu, J., Bradford, W. D., Saraf, A., Florens, L., et al. (2010). Aneuploidy confers quantitative proteome changes and phenotypic variation in budding yeast. *Nature* 468, 321–325. doi: 10.1038/nature09529

Pfaller, M. A., Diekema, D. J., Gibbs, D. L., Newell, V. A., Ellis, D., Tullio, V., et al. (2010). Results from the ARTEMIS DISK global antifungal surveillance study, 1997 to 2007: a 10.5-year analysis of susceptibilities of Candida species to fluconazole and voriconazole as determined by CLSI standardized disk diffusion. *J. Clin. Microbiol.* 48, 1366–1377. doi: 10.1128/JCM.02117-09

Rajasingham, R., Smith, R. M., Park, B. J., Jarvis, J. N., Govender, N. P., Chiller, T. M., et al. (2017). Global burden of disease of HIV-associated cryptococcal meningitis: an updated analysis. *Lancet Infect. Dis.* 17, 873–881. doi: 10.1016/S1473-3099(17)30243-8

Selmecki, A., Forche, A., and Berman, J. (2006). Aneuploidy and isochromosome formation in drug-resistant *Candida albicans*. *Science* 313, 367–370. doi: 10.1126/science.1128242

Selmecki, A., Gerami-Nejad, M., Paulson, C., Forche, A., and Berman, J. (2008). An isochromosome confers drug resistance in vivo by amplification of two genes, ERG11 and TAC1. *Mol. Microbiol.* 68, 624–641. doi: 10.1111/j.1365-2958.2008.06176.x

Sionov, E., Lee, H., Chang, Y. C., and Kwon-Chung, K. J. (2010). *Cryptococcus neoformans* overcomes stress of azole drugs by formation of disomy in specific multiple chromosomes. *PLoS Pathog.* 6:e1000848. doi: 10.1371/journal.ppat.1000848

Srivastava, M., and Raghavan, S. C. (2015). DNA double-strand break repair inhibitors as cancer therapeutics. *Chem. Biol.* 22, 17–29. doi: 10.1016/j.chembiol.2014.11.013

Sun, L. L., Li, H., Yan, T. H., Cao, Y. B., Jiang, Y. Y., and Yang, F. (2023a). Aneuploidy enables cross-tolerance to unrelated antifungal drugs in *Candida parapsilosis*. *Front. Microbiol.* 14:1137083. doi: 10.3389/fmicb.2023.1137083

Sun, L. L., Li, H., Yan, T. H., Fang, T., Wu, H., Cao, Y. B., et al. (2023b). Aneuploidy mediates rapid adaptation to a subinhibitory amount of fluconazole in *Candida albicans*. *Microbiol. Spectr.* 11, e0301622–e0303022. doi: 10.1128/spectrum.03016-22

Todd, R. T., Soisangwan, N., Peters, S., Kemp, B., Crooks, T., Gerstein, A., et al. (2023). Antifungal drug concentration impacts the Spectrum of adaptive mutations in *Candida albicans*. *Mol. Biol. Evol.* 40:msad009. doi: 10.1093/molbev/msad009

Tsai, H. J., and Nelliat, A. (2019). A double-edged sword: aneuploidy is a prevalent strategy in fungal adaptation. *Genes (Basel)* 10:787. doi: 10.3390/genes10100787

WHO (2022). WHO fungal priority pathogens list to guide research, development and public health action. Geneva: World Health Organization.

Wu, J., Chen, S., Liu, H., Zhang, Z., Ni, Z., Chen, J., et al. (2018). Tunicamycin specifically aggravates ER stress and overcomes chemoresistance in multidrug-resistant gastric cancer cells by inhibiting N-glycosylation. *J. Exp. Clin. Cancer Res.* 37:272. doi: 10.1186/s13046-018-0935-8

Yamamori, T., Meike, S., Nagane, M., Yasui, H., and Inanami, O. (2013). ER stress suppresses DNA double-strand break repair and sensitizes tumor cells to ionizing radiation by stimulating proteasomal degradation of Rad51. *FEBS Lett.* 587, 3348–3353. doi: 10.1016/j.febslet.2013.08.030

Yang, F., Gritsenko, V., Lu, H., Zhen, C., Gao, L., Berman, J., et al. (2021a). Adaptation to fluconazole via aneuploidy enables cross-adaptation to amphotericin B and flucytosine in *Cryptococcus neoformans*. *Microbiol. Spectr.* 9:e0072321. doi: 10.1128/Spectrum.00723-21

Yang, F., Gritsenko, V., Slor Futterman, Y., Gao, L., Zhen, C., Lu, H., et al. (2021b). Tunicamycin potentiates antifungal drug tolerance via aneuploidy in *Candida albicans*. *MBio* 12:e0227221. doi: 10.1128/mBio.02272-21

Yang, F., Lu, H., Wu, H., Fang, T., Berman, J., and Jiang, Y. Y. (2021c). Aneuploidy underlies tolerance and cross-tolerance to drugs in *Candida parapsilosis*. *Microbiol. Spectr.* 9:e0050821. doi: 10.1128/Spectrum.00508-21

Yang, F., Scopel, E. F. C., Li, H., Sun, L. L., Kawar, N., Cao, Y. B., et al. (2023). Antifungal tolerance and resistance emerge at distinct drug concentrations and rely upon different aneuploid chromosomes. *MBio* 14:e0022723. doi: 10.1128/mbio.00227-23

Yang, F., Teoh, F., Tan, A. S. M., Cao, Y., Pavelka, N., and Berman, J. (2019). Aneuploidy enables cross-adaptation to unrelated drugs. *Mol. Biol. Evol.* 36, 1768–1782. doi: 10.1093/molbev/msz104

Yang, F., Todd, R. T., Selmecki, A., Jiang, Y. Y., Cao, Y. B., and Berman, J. (2021d). The fitness costs and benefits of trisomy of each *Candida albicans* chromosome. *Genetics* 218:iyab056. doi: 10.1093/genetics/iyab056

Zafar, H., Altamirano, S., Ballou, E. R., and Nielsen, K. (2019). A titanic drug resistance threat in *Cryptococcus neoformans*. *Curr. Opin. Microbiol.* 52, 158–164. doi: 10.1016/j.mib.2019.11.001

frontiers | Frontiers in Microbiology

TYPE Original Research
PUBLISHED 05 February 2025
DOI 10.3389/fmicb.2025.1508941

OPEN ACCESS

EDITED BY
Shicheng Chen,
Northern Illinois University, United States

REVIEWED BY
Okon Okwong Kenneth,
Federal University Wukari, Nigeria
Anima Nanda,
Sathyabama Institute of Science and Technology, India

*CORRESPONDENCE
Mahmuda Yasmin
✉ yasmin@du.ac.bd

RECEIVED 10 October 2024
ACCEPTED 13 January 2025
PUBLISHED 05 February 2025

CITATION
Saha P, Kabir RB, Ahsan CR and Yasmin M (2025) Multidrug resistance of *Pseudomonas aeruginosa*: do virulence properties impact on resistance patterns? *Front. Microbiol.* 16:1508941. doi: 10.3389/fmicb.2025.1508941

Multidrug resistance of *Pseudomonas aeruginosa*: do virulence properties impact on resistance patterns?

Poulomi Saha[1], Rubaiya Binte Kabir[2], Chowdhury Rafiqul Ahsan[1] and Mahmuda Yasmin[1]*

[1]Department of Microbiology, University of Dhaka, Dhaka, Bangladesh, [2]Department of Microbiology, Dhaka Medical College, Dhaka, Bangladesh

Introduction: Patients with nosocomial infections are at risk of multidrug-resistant (MDR) *Pseudomonas aeruginosa* since these bacteria slow down the entire treatment process, increasing the morbidity and mortality of patients staying in hospital. The purpose of the research was to assess the simultaneous presence of multidrug resistance and virulence factors among nosocomial strains of *P. aeruginosa* to evaluate significant association among them.

Methods: One hundred and eight clinical isolates of *P. aeruginosa* were found in a variety of samples taken from patients having nosocomial infection, including wound swabs, pus, sputum, tracheal aspirate, and urine. An antibiogram was performed to investigate the pathogen's antibiotic sensitivity pattern against 14 widely used antibiotics in Bangladesh. Virulence factors were evaluated, and the presence of ten β-lactamase and six virulence genes was analyzed by performing PCR. By using a binary logistic regression test with a 95% confidence interval, the relationship between MDR phenotypes and the virulence attributes was assessed.

Results: The susceptibility rate among the isolates was 70–75% for aminoglycosides (amikacin, gentamicin, netilmicin), 15–20% for cephalosporins (ceftazidime, ceftriaxone), 30–35% for quinolones (ciprofloxacin, levofloxacin), 10–15% for tetracyclines (tigecycline, doxycycline), 15–20% for carbapenem (meropenem), 10–15% for sulfonamide (co-trimoxazole), 5–10% for amoxiclav, and 30–35% for piperacillin/tazobactam. A total of 74.1% of the strains carried metallo-β-lactamase (MBL) genes. Among the isolates, 89% showed hemolytic activity, 80–90% produced different pigments such as fluorescein and pyoverdine, 46% were strong biofilm producers, and all the isolates presented different types of motilities (swimming, swarming, and twitching). The virulence genes (*lasB, exoS, toxA, aprA, algD,* and *plcH*) were detected within a range of 60–80% of the isolates.

Discussion: Only the *toxA* gene and twitching motility showed a significant correlation (p-value = 0.001 and 0.028, respectively) with multidrug resistance in the clinical *P. aeruginosa* isolates which indicates that it can be used as a drug target to combat these organisms. The high prevalence of MDR strains and their association with virulence factors revealed the potential of the pathogen to cause an infection. The current study advocates for immediate epidemiological surveillance of MDR *P. aeruginosa* strains in Bangladesh to impede the rapid dissemination of this opportunistic pathogen.

KEYWORDS

multidrug resistance, virulence properties, *Pseudomonas aeruginosa*, nosocomial infection, β-lactamase

1 Introduction

Pseudomonas aeruginosa is the leading organism responsible for nosocomial infections worldwide. Its capability to produce various potent virulence properties and resistance to various classes of antibiotics has called out the emergence to study the current condition of our country, Bangladesh, regarding the serious issue of multidrug resistance and its dissemination by *P. aeruginosa,* which contributes to in-patient morbidity and mortality (Spagnolo et al., 2021). The ability of multi-drug resistant (MDR) *P. aeruginosa* strains to colonize and grow in settings that other bacterial species cannot, gives them a greater capacity to generate epidemic outbreaks. For an infection to continue and raise patient morbidity in a hospital setting, the bacteria need to be pathogenic and resistant to antibiotics (Martínez and Baquero, 2002). Virulence factors of the pathogen facilitate its persistence and resistance to various environmental stresses including the stringent conditions inside the patients' body during medication. *P. aeruginosa* possesses genes that enable them to better adapt to their surroundings in this way (Beceiro et al., 2012).

Even though *P. aeruginosa* infections are rarely fatal, the bacteria have developed a high resistance to a number of antimicrobial medicines due to the presence of efflux systems, the production of enzymes that break down antibiotics, reduced outer membrane permeability, and target modifications. As a result, multidrug-resistant strains have become more common (Bassetti et al., 2018; Jácome et al., 2012). By means of intrinsic chromosomally encoded or genetically acquired resistance features, *P. aeruginosa* exhibits the majority of these known resistance mechanisms, hindering the main classes of antibiotics, including aminoglycosides, β-lactams, polymyxins, and quinolones (Bassetti et al., 2018). GIM, AIM, SPM, IMP, and VIM are examples of class B metallo-β-lactamases (MBLs), which are also the predominant mechanism of acquired resistance to carbapenems. While varieties of IMP and VIM have been documented globally, GIM, AIM, and SPM have only been observed in a few select geographic areas, such as São Paulo and Germany (Zhao and Hu, 2010). High-risk MDR strains of *P. aeruginosa* are distributed around the world due to a combination of factors including mutation accumulation, horizontally acquired resistance mechanisms, and intrinsic resistance to some antibiotics (del Barrio-Tofiño et al., 2017).

Many virulence factors, including the presence of flagella, pili, and lipopolysaccharides, which are all components of the bacterial structure, along with other factors the bacteria produce and liberate into the adjacent tissue, where the infection expands, such as pigments, proteolytic enzymes, DNases, and toxins, are linked to the pathogenicity of *Pseudomonas* spp. (Pang et al., 2019). Because biofilms are naturally resistant to antimicrobial treatments, biofilm production is another factor contributing to pathogenicity. *P. aeruginosa*'s biofilm exhibits many resistance mechanisms that render it clinically accountable for numerous chronic infections, which are managed by quorum sensing (QS). Moreover, exoenzyme S, exotoxin A, siderophores, quorum sensing system proteins, type III secretory proteins, elastase enzyme, and alginate pigments account for infection initiation and both acute and chronic stages of diseases inside the host.

To lessen the possibility of MDR *P. aeruginosa* strains disseminating, we require information about the isolates' patterns of antimicrobial susceptibility (Sawa et al., 2014). The World Health Organization (WHO) advocates nosocomial surveillance to enhance infection control practices, particularly in the healthcare sector, and to assist doctors in selecting between directed or empirical treatment (Palavutitotai et al., 2018). To address AMR worldwide, it stressed the significance of creating and sustaining reliable surveillance and reporting systems for AMR genetics, mechanics, and epidemiology (World Health Organization, 2020).

Antimicrobial medicines are commonly provided to patients in Bangladesh; nevertheless, hospitals are currently facing a shortage of pharmaceuticals for patients' treatment because MDR *P. aeruginosa* is becoming more common. From 2015 to 2018, the number of MDR isolates increased year over year, and by 2019, the increase had nearly doubled from 2015 (Safain et al., 2020). In accordance with the present situation, it is essential to understand the correlation between pathogenicity and antibiotic resistance before making drug choices to eliminate the pathogen. This study intends to convene more knowledge on virulence genes and their relevance to the MDR phenotype of *P. aeruginosa* strains to help design ample therapeutic and control strategies to combat this pathogen.

2 Materials and methods

2.1 Sample collection and isolation of *Pseudomonas aeruginosa*

The time frame for conducting this study was from February 2023 to December 2023. The inclusion criteria of the patients were being clinically non-responding to antibiotics, and the exclusion criteria were not having nosocomial infections and being outdoor patients or staying at the hospital for less than 7 days. According to patient records, a total of 132 non-duplicate isolates were obtained from distinct samples (wound swab, urine, tracheal aspirate, pus, and sputum) of patients suffering from nosocomial infections (NIs) at Dhaka Medical College Hospital (DMCH), Bangladesh. Information was gathered about the patients' age, sex, and place of origin for the samples. Every isolate was obtained from a separate patient, and the patients were not associated with epidemic outbreaks. To identify pure colonies of *P. aeruginosa*, the isolates were picked from the MacConkey agar plates, onto which the raw samples were cultured, and then streaked onto Cetrimide agar. *Pseudomonas aeruginosa* isolates were determined by their colony characteristics on Cetrimide agar medium followed by a series of biochemical tests (Gram staining, catalase, oxidase, sugar fermentation, nitrate reduction, motility, indole, urea, citrate utilization, methyl red, and Voges-Proskauer) and molecular identification based on 16S rRNA gene sequencing for further study.

2.2 Antimicrobial susceptibility test

The pathogens' antibiogram was assessed using the disk diffusion method onto Mueller–Hinton agar in accordance with the CLSI (Clinical and Laboratory Standards) guidelines. The antimicrobials tested for resistance included ciprofloxacin (5 μg), co-trimoxazole (25 μg), amikacin (30 μg), ceftazidime (30 μg), piperacillin/tazobactam (100/10 μg), levofloxacin (5 μg), amoxicillin/clavulanic acid (20/10 μg), doxycycline (30 μg), aztreonam (30 μg), ceftriaxone (5 μg), meropenem (10 μg), netilmicin (10 μg), gentamicin (10 μg), and tigecycline (30 μg). The strains were classified as

pandrug-resistant (PDR, non-susceptible to all antimicrobial classes), extensively drug-resistant (XDR, non-susceptible to all but two classes), multidrug-resistant (MDR, non-susceptible to ≥3 antimicrobial classes), and low-level drug-resistant (LDR).

2.3 Toxin production

Hemolysin and pigment production were evaluated on blood agar (8%) and cetrimide agar plates, respectively. A clear zone around the colonies elucidated the beta-hemolytic activity of the *P. aeruginosa* strains, and the lack of a clear halo was identified as a negative result. Pigments produced on the cetrimide agar were pyoverdine (green), pyocyanin (blue-green), and fluorescein (yellow).

2.4 Enzyme production

Proteolytic enzyme (gelatinase) production was studied by stabbing in 4% gelatin media containing test tubes. Hydrolysis (partial or total) of gelatin indicated the production of gelatinase enzyme by the isolates, while a lack of hydrolysis indicated a negative result.

2.5 Motility assay

As three types of motility can be detected in *P. aeruginosa* strains, a motility assay was carried out on Luria–Bertani (LB) agar plates using different concentrations of agar to evaluate the following types of motility: twitching (1% agar), swarming (0.5% agar), and swimming (0.3% agar). The media were inoculated with the overnight cultured strains using sterile yellow tips on the surface of the agar to study swarming, by stabbing halfway down the thick agar media for evaluating swimming and for twitching the strains were introduced at the bottom of the agar. All culture plates were kept overnight at a 37°C incubator. To evaluate the twitching motility, the 1% agar plates were flooded with TM developer solution and left for up to 30 min. The colony on the agar surface was scraped away by a sterile loop, and the solution was decanted. The remaining interstitial colony attached to the Petri plate is indicative of the twitching motility of the isolates.

2.6 Biofilm production

P. aeruginosa strains were inoculated in LB broth on a 96-well microtiter plate to quantify biofilm formation. As a negative control, a sterile broth was used to assure sterility. Biofilm producers were differentiated from non-biofilm producers by measuring their OD values. If the value is ≤ (average OD of negative control +3σ), the strain was considered non-biofilm producer, and the isolates having OD value > (ANC + 3σ) were interpreted as biofilm producer strains.

2.7 Identification of virulence and MBL genes

DNA extraction of clinical *P. aeruginosa* isolates was carried out by boiling DNA method. The presence of 6 virulence genes (*plcH, lasB, exoS, algD, toxA,* and *aprA*) and 10 MBL genes ($bla_{\text{VIM-2}}$, bla_{SPM}, bla_{SIM}, bla_{DIM}, bla_{BIC}, $bla_{\text{OXA-48}}$, bla_{GIM}, bla_{SHV}, bla_{DHA}, and bla_{AIM}) was evaluated by amplifying the genes with specific primers listed in Tables 1, 2, respectively. Previously well-characterized strains were used as controls in this study. PCR conditions were maintained as in the reference articles, respectively. Gel electrophoresis was conducted by running the amplified PCR products for 50 min at 100 V using a 1.5% agarose gel using 1X TBE buffer. The sizes of the amplicons were determined by comparing them with the mobility of the 100 bp and 1 kb + DNA ladder (NEB, UK). The amplicons were visualized, and the gels were photographed using the gel documentation system (Axygen, USA) having a UV trans-illuminator.

2.8 Statistical analysis of data

Using binary logistic regression analysis, with a 95% confidence interval at a 5% significance level, the relationship between MDR phenotypes and the virulence factors as well as

TABLE 1 Oligonucleotide primers used in amplifying of virulence genes.

Target gene	Primers	Primer sequence (5` → 3`)	Amplicon size (bp)	References
algD	AlgD-F	ATG CGA ATC AGC ATC TTT GGT	1,310	Lanotte et al. (2004)
	AlgD-R	CTA CCA GCA GAT GCC CTC GGC		
aprA	AprA-F	GTC GAC CAG GCG GCG GAG CAG ATA	993	Schmidtchen et al. (2001)
	AprA-R	GCC GAG GCC GCC GTA GAG GAT GTC		
lasB	LasB-F	GGA ATG AAC GAG GCG TTC TC	300	Lanotte et al. (2004)
	LasB-R	GGT CCA GTA GTA GCG GTT GG		
plcH	PlcH-F	GAA GCC ATG GGC TAC TTC AA	307	Lanotte et al. (2004)
	PlcH-R	AGA GTG ACG AGG AGC GGT AG		
exoS	ExoS-F	CTT GAA GGG ACT CGA CAA GG	504	Lanotte et al. (2004)
	ExoS-R	TTC AGG TCC GCG TAG TGA AT		
toxA	ToxA-F	GGA GCG CAA CTA TCC CAC T	150	Michalska and Wolf (2015)
	ToxA-R	TGG TAG CCG ACG AAC ACA TA		

10.3389/fmicb.2025.1508941

TABLE 2 Oligonucleotide primers used in amplifying MBL genes.

Target Gene	Primers	Primer sequence (5` → 3`)	Amplicon size (bp)	References
bla_{VIM-2}	VIM-2-F	ATTGGTCTATTTGACCGCGTC	801	
	VIM-2-R	TGCTACTCAACGACTGAGCG		
bla_{SPM}	SPM-F	AAAATCTGGGTACGCAAACG	271	Poirel et al. (2011)
	SPM-R	ACATTATCCGCTGGAACAGG		
bla_{AIM}	AIM-F	CTGAAGGTGTACGGAAACAC	322	
	AIM-R	GTTCGGCCACCTCGAATTG		
bla_{SIM}	SIM-F	TACAAGGGATTCGGCATCG	570	
	SIM-R	TAATGGCCTGTTCCCATGTG		
bla_{BIC}	BIC-F	TATGCAGCTCCTTTAAGGGC	537	
	BIC-R	TCATTGCGGTGCCGTACAC		
bla_{GIM}	GIM-F	TCGACACACCTTGGTCTGAA	477	
	GIM-R	AACTTCCAACTTTGCCATGC		
bla_{SHV}	SHV-F	TTTATGGCGTTACCTTTGACC	1,050	Mathlouthi et al. (2016)
	SHV-R	ATTTGTCGCTCTTTACTCGC		
bla_{DHA}	DHA-F	AACTTTCACAGGTGTGCTGGGT	405	Liu and Liu (2016)
	DHA-R	CCGTACGCATACTGGCTTTGC		
bla_{OXA-48}	OXA-48-F	GCGTGGTTAAGGATGAACAC	438	Poirel et al. (2011)
	OXA-48-R	CATCAAGTTCAACCCAACCG		
bla_{DIM}	DIM-F	GCTTGTCTTCGCTTGCTAACG	699	
	DIM-R	CGTTCGGCTGGATTGATTTG		

epidemiological and clinical factors was assessed. The statistical program SPSS version 25 (IBM, New York, USA) was used for the analysis.

3 Results

3.1 Identification of clinical isolates of *Pseudomonas aeruginosa*

Initially collected 132 isolates taken from patients aged 25–68 years were undergone biochemical tests (Supplementary Table S1), and of them, 108 isolates were plausibly identified as *Pseudomonas aeruginosa*. Twenty-five selected isolates out of 108 were further identified as *P. aeruginosa* using molecular techniques based on 16S rRNA gene sequencing (Supplementary Table S2). Among the patients, 46% were male and 54% were female having low fever and UTI.

3.2 Antibiotic resistance profile of *Pseudomonas aeruginosa* isolates

The prevalence rate of antibiotic resistance was found to be extremely high (53.7–98.1%) for all antimicrobial agents tested among the 108 clinical isolates of *P. aeruginosa*. In comparison with the other 13 antibiotics (doxycycline, meropenem, ceftazidime, tigecycline, levofloxacin, aztreonam, amoxiclav, netilmicin, gentamycin, co-trimoxazole, ceftriaxone, ciprofloxacin, and amikacin), *P. aeruginosa* strains exhibited significantly less resistance (53.7%) against piperacillin–tazobactam. Comparing the isolates to the other antibiotics revealed the highest level of resistance to aztreonam (98.1%) which belongs to the class monobactam (Figure 1). Amoxiclav (93.5%), ceftriaxone (94.4%), and doxycycline (95.4%) are the remaining drugs that came next in order of resistance (Figure 1).

Out of 108 isolates, only 1 was found to be resistant to each of the 14 antibiotics across 8 distinct classes. The other 107 strains were found to be resistant to at least one of the antibiotics tested. Of them, one strain was resistant to two antibiotics of different classes, while two isolates were found to be resistant to only one antibiotic. These strains of *P. aeruginosa* (2.7%) fall into the low-level drug-resistant (LDR) category. A total of 27.8% of the isolates were classified as MDR strains because they exhibited resistance to at least three classes of antibiotics. Since 58.3% showed no resistance to at least two classes of antibiotics, they were classified as extensively drug-resistant (XDR). A total of 10.2% of the clinical *P. aeruginosa* strains tested positive for every antibiotic and thus fell under the category of pandrug-resistant (PDR).

3.3 Prevalence of β-lactamase genes in *Pseudomonas aeruginosa* isolates

PCR and gel electrophoresis were performed to detect the presence of beta-lactamase genes in the *P. aeruginosa* isolates (Figure 2). The rates of different classes of beta-lactamase (Ambler classes A, B, C, and D) gene production among the clinical

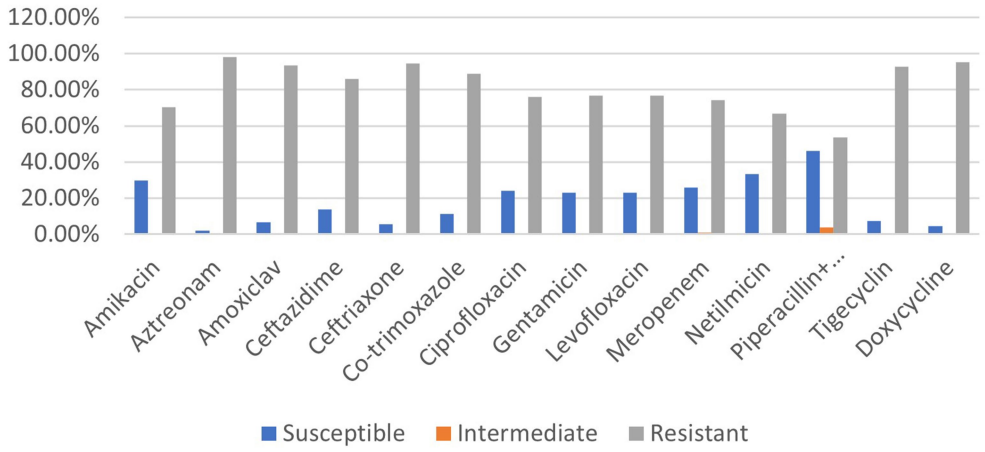

FIGURE 1
Prevalence rate of clinical *P. aeruginosa* strains resistant to different classes of antibiotics.

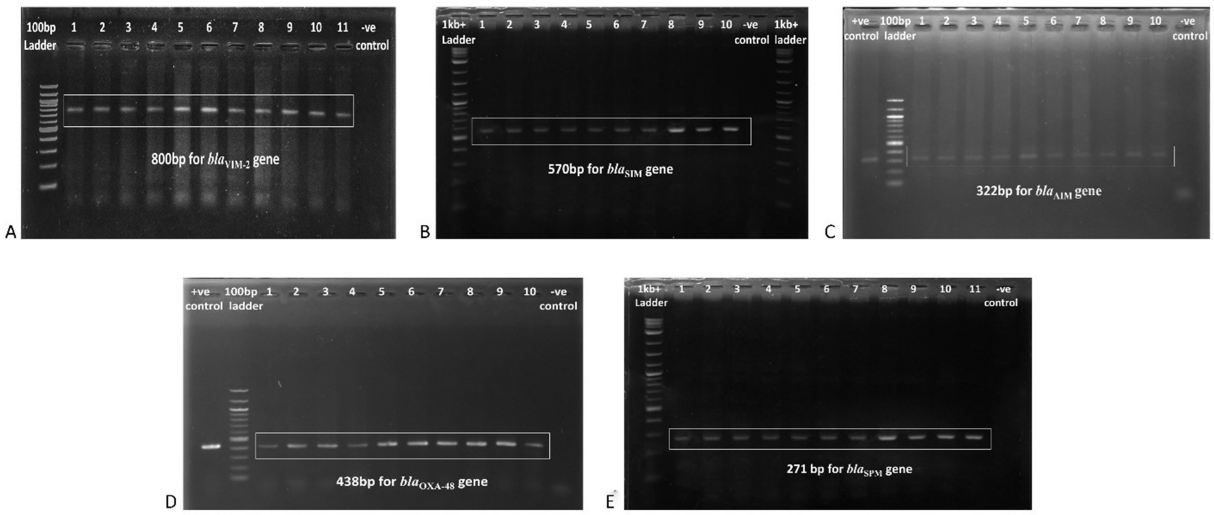

FIGURE 2
Gel electrophoresis (1.5% agarose) of the beta-lactamase genes present in the *P. aeruginosa* isolates, **(A)** bla_{VIM-2} gene at 800 bp, **(B)** bla_{SIM} gene at 570 bp, **(C)** bla_{AIM} gene at 322 bp, **(D)** bla_{OXA-48} gene at 438 bp, and **(E)** bla_{SPM} gene at 271 bp.

Pseudomonas aeruginosa isolates are shown in Figure 3. Among the 10 beta-lactamase genes, 6 are under class B (bla_{VIM-2}, bla_{SPM}, bla_{SIM}, bla_{DIM}, bla_{GIM}, and bla_{AIM}), 2 of them are classified as class A (bla_{BIC} and bla_{SHV}), 1 is from class D (bla_{OXA-48}), and another 1 is from class C (bla_{DHA}). Most of the isolates (74.1%) were detected positive for MBL genes, which are under class B beta-lactamases. Among them, 37.5% harbored the bla_{VIM-2} gene, followed by bla_{SPM} (32.5%), bla_{AIM} (27.5%), and bla_{GIM} (2.5%) genes. Only one isolate was found to be positive for the bla_{DIM} gene, while the bla_{SIM} gene was not identified in any of the isolates. The highest rate of MBL gene production was found in strains isolated from wound swabs (50.1%).

Class D beta-lactamase (bla_{OXA-48}) gene was found in 23.2% of the *P. aeruginosa* isolates, followed by class A beta-lactamase genes ($n = 3$, 2.7%). No isolates were found to harbor the class C beta-lactamase gene.

3.4 Identification of virulence factors in *Pseudomonas aeruginosa* isolates

All but two isolates of *P. aeruginosa* showed different types of motilities, and most of the strains (84.26%) were capable of swimming which requires rotating flagella, followed by twitching (80.56%) which indicates the existence of type IV pili and swarming (59.25%). The second most frequently found virulence factor synthesized by the *P. aeruginosa* isolates was pigment (88.89%). Among the pigment-producing strains, 70.83% produced fluorescein and subsequently pyoverdine (28.12%) and pyocyanin (9.37%). A total of 7.30% of the strains produced both pigments, fluorescein, and pyoverdine. Gelatinase production was marked in 84.26% of the *P. aeruginosa* strains followed by hemolysin (73.15%) and biofilm formation (67.59%) (Figure 4).

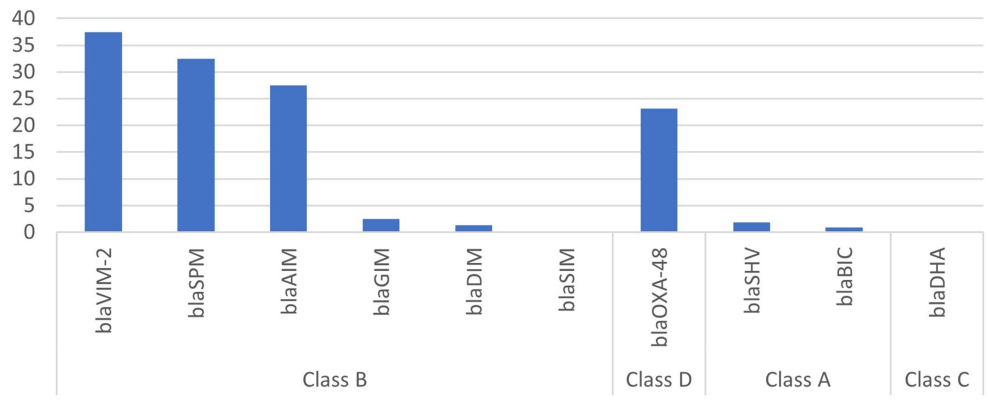

FIGURE 3
Prevalence of different classes of beta-lactamase gene-producing clinical isolates of *Pseudomonas aeruginosa*.

3.5 Identification of virulence genes

Among the six virulence genes, *plcH* and *lasB* were most frequent among the *P. aeruginosa* isolates (92.59 and 94.44%, respectively) (Figure 5). A total of 82.41% of the strains harbored the *toxA* gene, and the prevalence of the *toxA* gene among MDR *P. aeruginosa* strains was 90.27%. A total of 70.37% of the isolates were found to be positive for the *algD* gene. A total of 62.96 and 55.56% of the isolates were found positive for *aprA* and *exoS* genes, respectively. In addition, 18.52% of the strains were positive for all the virulence genes tested. The frequency of the virulence genes among different sample types is depicted in Table 3.

3.6 Correlation of factors with MDR phenotypes

Biofilm formation, gelatinase activity, hemolysin, and pigment production, which are known virulence factors for *P. aeruginosa,* were found to have no statistically significant correlation with the MDR pattern of *P. aeruginosa* isolates. Among the three types of motilities, swimming and swarming had no association while twitching appeared to be significantly associated ($p < 0.05$) with the level of antibiotic resistance. MDR strains were statistically more likely to harbor the *toxA* gene than the other five when analyzing the virulence genes (Figure 6).

In the statistical model developed for determining the virulence factors as the risk factors for the MDR pattern, the strongest predictor of multidrug resistance was the *toxA* gene, recording an odds ratio (OR) of 8.45 (Table 4). This indicated that the *P. aeruginosa* isolates containing the *toxA* gene were 8.45 times more likely to be multidrug-resistant than the isolates lacking the *toxA* gene. In addition, the odds ratio for twitching motility was 3.31, which indicated that the existence of this type of motility, which is acquired by type IV pili, enhanced the risk of the strains to be MDR by 3.31 times, as found in the statistical analysis. Epidemiological clinical factors such as patient's age, sex, and types of samples were analyzed and not found to be statistically related to antibiotic resistance.

4 Discussion

The global dissemination of antibiotic resistance among Gram-negative bacteria is a burning concern for the medical science as the whole world is heading to the pre-antibiotic era. *Pseudomonas aeruginosa* plays a major role in this concern as this opportunistic pathogen causes nosocomial infection in in-patients. The present study demonstrates an alarming state of antibiotic resistance where the *P. aeruginosa* strains have become resistant to almost all antipseudomonal antibiotics. Even carbapenems, which are considered last-line antibiotic drugs, are not able to cure infections sustained by *P. aeruginosa*. In this study, 74.08% of the strains were resistant to carbapenem, and 86.11 to 93.44% of the strains were resistant to third-generation cephalosporins whereas susceptibility of *Pseudomonas* spp. to third-generation cephalosporins ranged from 43.3 to 46.7% in the last decade in Bangladesh (Begum et al., 2013). However, the antibiogram revealed combination drugs as the most effective drug (46.29%) among all antibiotics used against *P. aeruginosa* strains followed by netilmicin (33.33%).

A total of 66.67% of the strains showed resistance to all but two groups of antibiotics used in this study, which are regularly prescribed in Bangladesh for the treatment of nosocomial infections caused by *P. aeruginosa*. These clinical isolates of *P. aeruginosa* are now classified as extensively drug-resistant (XDR) strains rather than multidrug-resistant (MDR). If unchecked use of antibiotics goes on, in the near future all *P. aeruginosa* strains will become pandrug-resistant and patients will die of secondary nosocomial infections rather than of the disease they went to hospital for treatment.

The prevalence of beta-lactamase genes of the four Ambler classes (classes A–D) was evaluated in this study, which showed the highest rampancy for MBL genes (class B). The $bla_{\text{VIM-2}}$ (37.5%), bla_{SPM} (32.5%), and bla_{AIM} (27.5%) are the predominant MBLs among the clinical isolates of *P. aeruginosa,* followed by class D (23.2%) and class A (2.8%) beta-lactamase genes. In a study in 2020, the prevalence rate of the $bla_{\text{VIM-2}}$ gene in clinical *P. aeruginosa* isolates in China was 18.8%, followed by bla_{SIM} (6.0%) and bla_{SPM} (4.0%) (Wang and Wang, 2020), while in this study 32.5% strain was found to harbor the bla_{SPM} gene but no strain was positive for *the* bla_{SIM} gene. The frequency of

10.3389/fmicb.2025.1508941

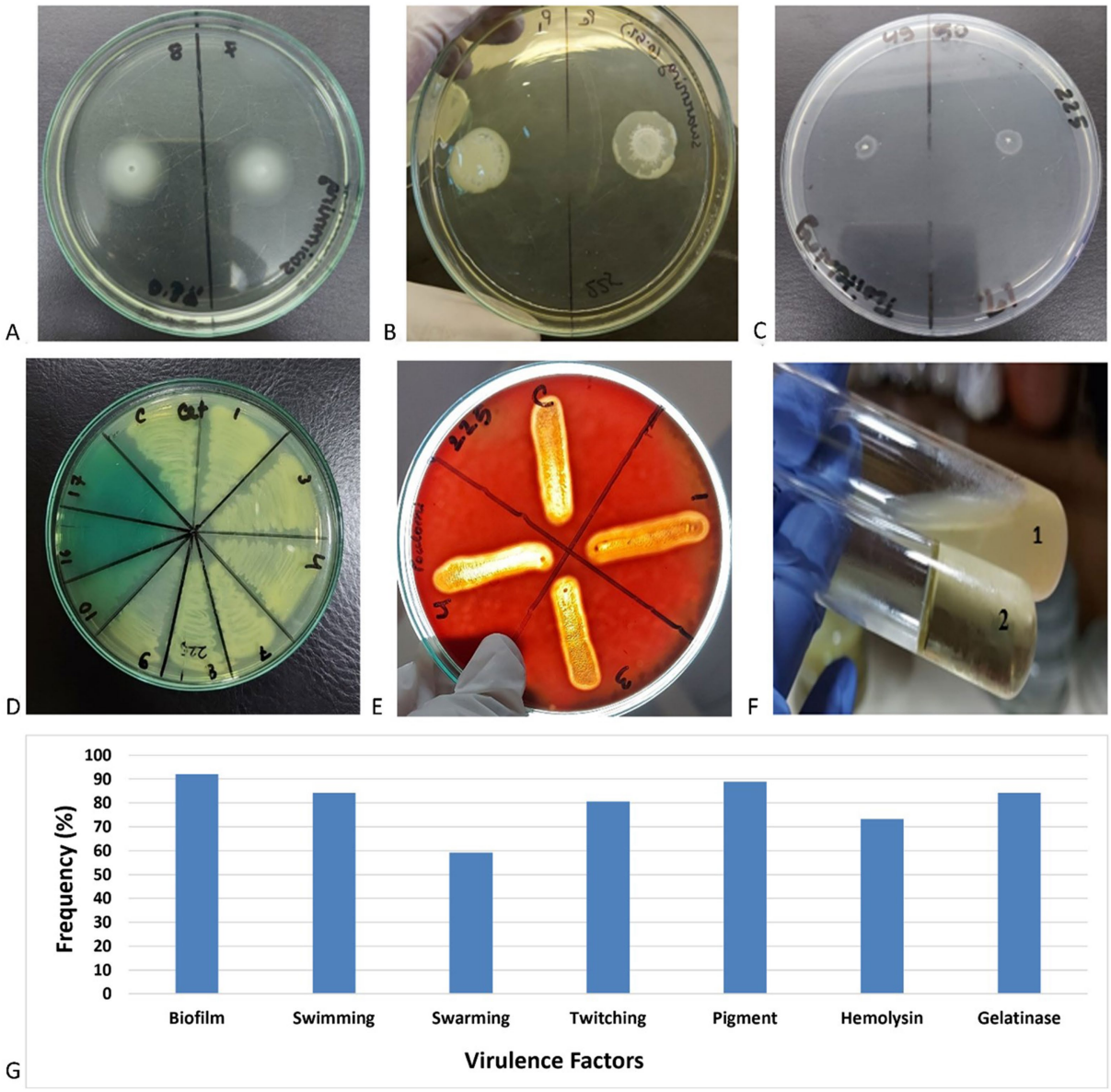

FIGURE 4
Examples of the experiments for the production of **(A)** swimming, **(B)** swarming, **(C)** twitching, **(D)** pigments, **(E)** hemolysins, **(F)** gelatinase (1: gelatinase positive and 2: gelatinase negative), and **(G)** frequency of different virulence factors in clinical *Pseudomonas aeruginosa* isolates.

the bla_{GIM} gene was found to be 2.5%, which is greater than that in China.

In another study in South Africa, the bla_{SHV} gene was found in 69.5% of *P. aeruginosa* strains (Hosu et al., 2021), in contrast to 2.8% of class A beta-lactam producers in our study. In this study, all strains were negative for class C beta-lactamase genes but in a study of Iran 33.0% of *P. aeruginosa* isolates were found to be positive for class C beta-lactamase genes (Sharifi et al., 2019). Our study depicts that in Bangladesh, class B or MBL genes have the highest prevalence followed by class D and class A beta-lactamases.

Virulence factors such as pigment, hemolysin, biofilm, and motility assist the pathogen in developing an infection inside the host body. In the present study, the most frequently found virulence factor was motility, and twitching motility was directly related to MDR. This indicates the presence of type IV pili is a prominent factor for the pathogen to be virulent and antibiotic-resistant at the same time. Type IV pili is used by *P. aeruginosa* not only for surface motility but also as a sensor to modulate virulence and surface-induced gene expression (Persat et al., 2015).

Gelatinase secreted by the pathogen can degrade a broad range of host substrates such as collagen and complement and delay the airway epithelial wound repair by altering the actin cytoskeleton (de Bentzmann et al., 2000). A total of 84.26% of the strains were found to produce gelatinase enzyme.

Pigments such as pyoverdine, pyocyanin, and fluorescein were produced by 88.89% of the strains. Pyocyanin is secreted by T2SS and can decline lung function by its free radical and pro-inflammatory effects (Hall et al., 2016). Pyoverdine is a fluorescent pigment that is a potent iron (III) scavenger and acts as a siderophore satisfying the pathogen's absolute iron

10.3389/fmicb.2025.1508941

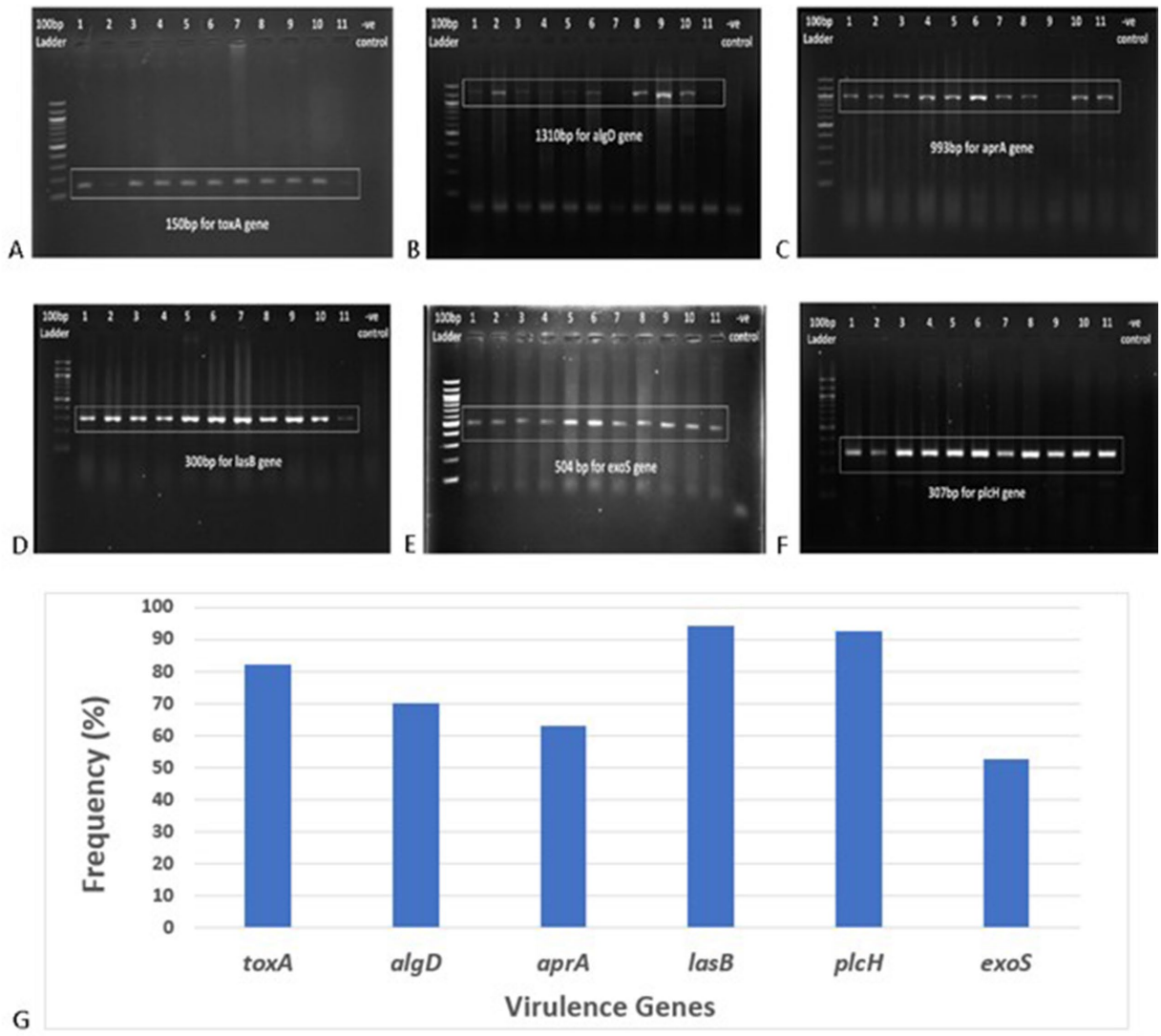

FIGURE 5
Gel electrophoresis (1.5% agarose) of the virulence genes present in *P. aeruginosa* isolates, **(A)** *toxA* gene at 150 bp, **(B)** *algD* gene at 1310 bp, **(C)** *aprA* gene at 993 bp, **(D)** *lasB* gene at 300 bp, **(E)** *exoS* gene at 504 bp, **(F)** *plcH* gene at 307 bp, and **(G)** frequency of different virulence genes in clinical *Pseudomonas aeruginosa* isolates.

TABLE 3 **Prevalence of different virulence genes among clinical samples.**

Clinical sample	*toxA*	*algD*	*aprA*	*lasB*	*plcH*	*exoS*
Pus	33%	67%	67%	67%	100%	100%
Sputum	100%	67%	33%	100%	100%	100%
Tracheal Aspirate	86%	86%	29%	100%	86%	100%
Wound Swab	100%	71%	76%	100%	100%	86%
Urine	100%	89%	56%	100%	100%	89%

requirement (Dauner and Skerra, 2020). Beta-hemolysin production plays a major role in disseminating infection by creating pores in cell membranes and assisting the pathogen to extend the wounds.

Biofilm production provides the pathogen with high resistance to host defense, antibiotics, and disinfectants leading to the establishment of chronic infections in in-patients (Lee and Yoon, 2017). Biofilm formation was seen in 67.59% of the isolates, and 41.1% of them were strong biofilm producers followed by 26.03% moderate and 32.88% weak biofilm-forming strains.

In this study, six virulence genes were evaluated to observe their prevalence in the nosocomial strains of *P. aeruginosa*. Then, association of these genes with the antibiotic resistance profile of the test isolates was measured statistically.

10.3389/fmicb.2025.1508941

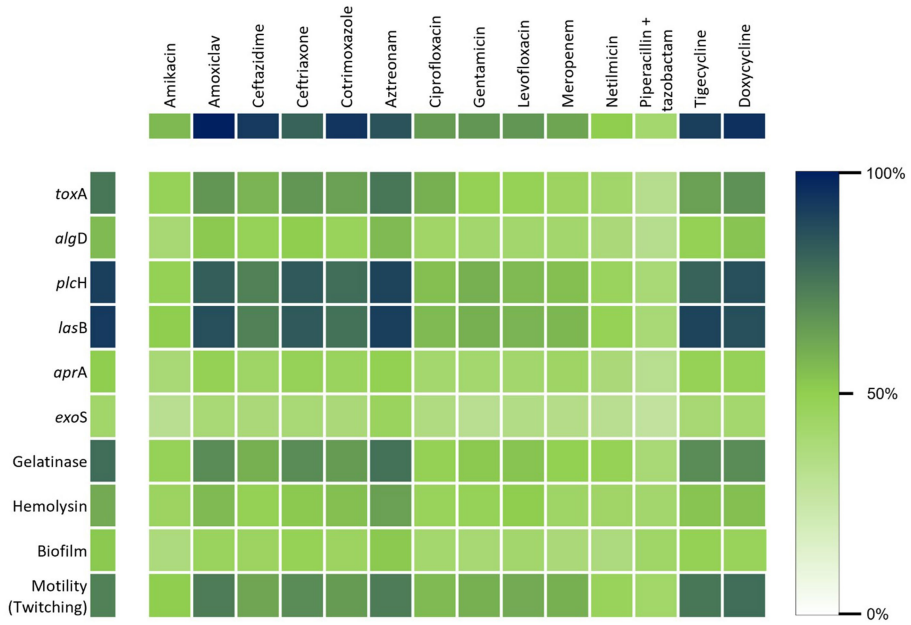

FIGURE 6
Heat map shows the correlation between the virulence properties and the resistance of *P. aeruginosa* against the commonly used antibiotics.

TABLE 4 **Statistical association among different virulence factors and MDR/XDR strains of *Pseudomonas aeruginosa*.**

Virulence factors	XDR/MDR			Total Isolates	p-value	OR	95% CI
		–	+				
Biofilm	–	12	35	47	0.262	1.737	0.6–4.5
	+	21	40	61			
Swimming	–	8	8	16	0.183	2.257	0.6–7.4
	+	29	63	92			
Swarming	–	11	32	43	0.255	0.597	0.2–1.4
	+	24	41	65			
Twitching	–	11	10	21	0.028	3.305	1.1–9.5
	+	25	62	87			
Pigment	–	5	8	13	0.865	1.130	0.2–4.6
	+	30	65	95			
Hemolysin	–	11	18	29	0.654	1.246	0.4–3.2
	+	25	54	79			
Gelatinase	–	8	8	16	0.565	1.468	0.3–5.4
	+	29	63	92			
exoS	–	2	3	5	0.339	0.402	0.2–1.5
	+	37	66	103			
toxA	–	17	10	27	0.001	8.45	2.8–24.8
	+	16	65	81			
plcH	–	2	6	8	0.238	0.302	0.1–2.2
	+	35	65	100			
lasB	–	4	2	6	0.400	2.131	0.3–12.4
	+	33	69	102			
aprA	–	10	28	38	0.352	1.857	0.5–6.8
	+	15	55	70			
algD	–	13	29	42	0.619	1.297	0.4–3.6
	+	22	44	66			

CI: confidence interval; OR: odds ratio.

All the virulence factors and virulence genes were under the null hypothesis that there is no significant correlation between the MDR traits and virulence factors of the clinical *P. aeruginosa* isolates, except the *toxA* gene and twitching motility. This gene was found to be associated with the MDR traits of nosocomial strains of *P. aeruginosa*, assessed statistically with binary regression analysis. As shown in Table 4, biofilm had no significant correlation with the MDR pattern, although it is well-known for the pathogenesis of clinical *P. aeruginosa*.

Multidrug resistance of *P. aeruginosa* is an alarming concern in Bangladesh. Our knowledge to date about their virulence capability is scanty. Our findings reveal that multidrug resistance and virulence factors are mutually complementary while infecting and causing disease in the patient's body. Although we have analyzed various virulence properties among MDR strains, most of them were not associated with the resistance pattern. We found that the *toxA* gene and twitching motility are significantly associated with the MDR pattern. Therefore, they can be utilized as new therapeutic targets to treat nosocomial infections caused by MDR *P. aeruginosa* (Alabdali, 2021).

Data availability statement

The original contributions presented in the study are included in the article/Supplementary material, further inquiries can be directed to the corresponding author.

Ethics statement

The studies involving humans were approved by Ethical Committee of Dhaka Medical College, Dhaka Medical College, Dhaka, Bangladesh. The studies were conducted in accordance with the local legislation and institutional requirements. The participants provided their written informed consent to participate in this study.

Author contributions

PS: Conceptualization, Data curation, Formal analysis, Investigation, Methodology, Software, Validation, Visualization, Writing – original draft. RK: Methodology, Writing – original draft. CA: Formal analysis, Project administration, Supervision, Writing – review & editing. MY: Formal analysis, Project administration, Supervision, Writing – review & editing, Conceptualization, Data curation, Funding acquisition, Investigation, Methodology, Resources, Software, Validation, Visualization.

Funding

The author(s) declare that financial support was received for the research, authorship, and/or publication of this article. The authors express gratitude to the DU Centennial Grant for providing financial support.

Conflict of interest

The authors declare that the research was conducted in the absence of any commercial or financial relationships that could be construed as a potential conflict of interest.

Generative AI statement

The author(s) declare that no Gen AI was used in the creation of this manuscript.

Publisher's note

All claims expressed in this article are solely those of the authors and do not necessarily represent those of their affiliated organizations, or those of the publisher, the editors and the reviewers. Any product that may be evaluated in this article, or claim that may be made by its manufacturer, is not guaranteed or endorsed by the publisher.

Supplementary material

The Supplementary material for this article can be found online at: https://www.frontiersin.org/articles/10.3389/fmicb.2025.1508941/full#supplementary-material

References

Alabdali, Y. A. J. (2021). Detection and association of toxA gene with antibiotics resistance in *Pseudomonas aeruginosa* strains isolated from different sources in Al Muthanna city. *Gene Rep* 25:101358. doi: 10.1016/j.genrep.2021.101358

Bassetti, M., Vena, A., Croxatto, A., Righi, E., and Guery, B. (2018). How to manage *Pseudomonas aeruginosa* infections. *Drugs. Context* 7, 1–18. doi: 10.7573/dic.212527

Beceiro, A., Tomás, M., and Bou, G. (2012). Antimicrobial resistance and virulence: a beneficial relationship for the microbial world? *Enferm. Infecc. Microbiol. Clin.* 30, 492–499. doi: 10.1016/j.eimc.2012.01.011

Begum, S., Salam, M. A., Alam, K. F., Begum, N., Hassan, P., and Haq, J. A. (2013). Detection of extended spectrum β-lactamase in Pseudomonas spp. isolated from two tertiary care hospitals in Bangladesh. *BMC. Res. Notes* 6:7. doi: 10.1186/1756-0500-6-7

Dauner, M., and Skerra, A. (2020). Scavenging bacterial Siderophores with engineered Lipocalin proteins as an alternative antimicrobial strategy. *Chembiochem* 21, 601–606. doi: 10.1002/cbic.201900564

de Bentzmann, S., Polette, M., Zahm, J.-M., Hinnrasky, J., Kileztky, C., Bajolet, O., et al. (2000). *Pseudomonas aeruginosa* virulence factors delay airway epithelial wound repair by altering the actin cytoskeleton and inducing overactivation of epithelial matrix metalloproteinase−2. *Lab. Investig.* 80, 209–219. doi: 10.1038/labinvest.3780024

del Barrio-Tofiño, E., López-Causapé, C., Cabot, G., Rivera, A., Benito, N., Segura, C., et al. (2017). Genomics and susceptibility profiles of extensively drug-resistant *Pseudomonas aeruginosa* isolates from Spain. *Antimicrob. Agents Chemother.* 61:17. doi: 10.1128/AAC.01589-17

Hall, S., McDermott, C., Anoopkumar-Dukie, S., McFarland, A., Forbes, A., Perkins, A., et al. (2016). Cellular effects of Pyocyanin, a secreted virulence factor of *Pseudomonas aeruginosa*. *Toxins* 8:236. doi: 10.3390/toxins8080236

Hosu, M. C., Vasaikar, S. D., Okuthe, G. E., and Apalata, T. (2021). Detection of extended spectrum beta-lactamase genes in *Pseudomonas aeruginosa* isolated from patients in rural eastern Cape Province, South Africa. *Sci. Rep.* 11:570. doi: 10.1038/s41598-021-86570-y

Jácome, P. R., Alves, L. R., Cabral, A. B., Lopes, A. C., and Maciel, M. A. (2012). Phenotypic and molecular characterization of antimicrobial resistance and virulence factors in *Pseudomonas aeruginosa* clinical isolates from Recife, state of Pernambuco, Brazil. *Rev. Soc. Bras. Med. Trop.* 45, 707–712. doi: 10.1590/S0037-86822012000600010

Lanotte, P., Watt, S., Mereghetti, L., Dartiguelongue, N., Rastegar-Lari, A., Goudeau, A., et al. (2004). Genetic features of *Pseudomonas aeruginosa* isolates from cystic fibrosis patients compared with those of isolates from other origins. *J. Med. Microbiol.* 53, 73–81. doi: 10.1099/jmm.0.05324-0

Lee, K., and Yoon, S. S. (2017). *Pseudomonas aeruginosa* biofilm, a programmed bacterial life for fitness. *J. Microbiol. Biotechnol.* 27, 1053–1064. doi: 10.4014/jmb.1611.11056

Liu, X.-Q., and Liu, Y.-R. (2016). Detection and genotype analysis of AmpC β-lactamase in *Klebsiella pneumoniae* from tertiary hospitals. *Exp. Ther. Med.* 12, 480–484. doi: 10.3892/etm.2016.3295

Martínez, J. L., and Baquero, F. (2002). Interactions among strategies associated with bacterial infection: pathogenicity, Epidemicity, and antibiotic resistance. *Clin. Microbiol. Rev.* 15, 647–679. doi: 10.1128/CMR.15.4.647-679.2002

Mathlouthi, N., Al-Bayssari, C., El Salabi, A., Bakour, S., Ben Gwierif, S., Zorgani, A. A., et al. (2016). Carbapenemases and extended-spectrum β-lactamases producing Enterobacteriaceae isolated from Tunisian and Libyan hospitals. *J. Infect. Dev. Countries* 10, 718–727. doi: 10.3855/jidc.7426

Michalska, M., and Wolf, P. (2015). Pseudomonas exotoxin a: optimized by evolution for effective killing. *Front. Microbiol.* 6:963. doi: 10.3389/fmicb.2015.00963

Palavutitotai, N., Jitmuang, A., Tongsai, S., Kiratisin, P., and Angkasekwinai, N. (2018). Epidemiology and risk factors of extensively drug-resistant *Pseudomonas aeruginosa* infections. *PLoS One* 13:e0193431. doi: 10.1371/journal.pone.0193431

Pang, Z., Raudonis, R., Glick, B. R., Lin, T. J., and Cheng, Z. (2019). Antibiotic resistance in *Pseudomonas aeruginosa*: mechanisms and alternative therapeutic strategies. *Biotechnol. Adv.* 37, 177–192. doi: 10.1016/j.biotechadv.2018.11.013

Persat, A., Inclan, Y. F., Engel, J. N., Stone, H. A., and Gitai, Z. (2015). Type IV pili mechanochemically regulate virulence factors in *Pseudomonas aeruginosa*. *Proc. Natl. Acad. Sci.* 112, 7563–7568. doi: 10.1073/pnas.1502025112

Poirel, L., Walsh, T. R., Cuvillier, V., and Nordmann, P. (2011). Multiplex PCR for detection of acquired carbapenemase genes. *Diagn. Microbiol. Infect. Dis.* 70, 119–123. doi: 10.1016/j.diagmicrobio.2010.12.002

Safain, K. S., Bhuyan, G. S., Tasnim, S., Hasib, S. H., Sultana, R., and Islam, M. S. (2020). Situation of antibiotic resistance in Bangladesh and its association with resistance genes for horizontal transfer. *Biorxiv*. doi: 10.1101/2020.04.06.027391

Sawa, T., Shimizu, M., and Moriyama, K. (2014). Association between *Pseudomonas aeruginosa* type III secretion, antibiotic resistance, and clinical outcome: a review. *Crit. Care* 18:668. doi: 10.1186/s13054-014-0668-9

Schmidtchen, A., Wolff, H., and Hansson, C. (2001). Differential proteinase expression by *Pseudomonas aeruginosa* derived from chronic leg ulcers. *Acta Derm. Venereol.* 81, 406–409. doi: 10.1080/000155501317208336

Sharifi, H., Pouladfar, G., Shakibaie, M. R., Pourabbas, B., Mardaneh, J., and Mansouri, S. (2019). Prevalence of β-lactamase genes, class 1 integrons, major virulence factors and clonal relationships of multidrug-resistant *Pseudomonas aeruginosa* isolated from hospitalized patients in southeast of Iran. *Iran. J. Basic Med. Sci.* 22, 806–812. doi: 10.22038/ijbms.2019.35063.8340

Spagnolo, A. M., Sartini, M., and Cristina, M. L. (2021). *Pseudomonas aeruginosa* in the healthcare facility setting. *Rev. Med. Microbiol.* 32, 169–175. doi: 10.1097/MRM.0000000000000271

Wang, W., and Wang, X. (2020). Prevalence of metallo-β-lactamase genes among *Pseudomonas aeruginosa* isolated from various clinical samples in China. *J. Lab. Med.* 44, 197–203. doi: 10.1515/labmed-2019-0162

World Health Organization (2020). Global antimicrobial resistance surveillance system (GLASS) report: Early implementation 2020. Geneva: World Health Organization.

Zhao, W. H., and Hu, Z. Q. (2010). β-Lactamases identified in clinical isolates of *Pseudomonas aeruginosa*. *Crit. Rev. Microbiol.* 36, 245–258. doi: 10.3109/1040841X.2010.481763

frontiers | Frontiers in Microbiology

TYPE Original Research
PUBLISHED 26 February 2025
DOI 10.3389/fmicb.2025.1543509

OPEN ACCESS

EDITED BY
Shicheng Chen,
Northern Illinois University, United States

REVIEWED BY
Mahmuda Yasmin,
University of Dhaka, Bangladesh
Muzafar Ahmad Rather,
University of Minnesota Twin Cities, United States

*CORRESPONDENCE
Yunsong Yu
✉ yvys119@zju.edu.cn
Jianhua Tang
✉ jhtang2002@tju.edu.cn

RECEIVED 11 December 2024
ACCEPTED 13 February 2025
PUBLISHED 26 February 2025

CITATION
Zhao L, Pu J, Liu Y, Cai H, Han M, Yu Y and Tang J (2025) High prevalence of carbapenem-resistant *Pseudomonas aeruginosa* and identification of a novel VIM-type metallo-β-lactamase, VIM-92, in clinical isolates from northern China. *Front. Microbiol.* 16:1543509. doi: 10.3389/fmicb.2025.1543509

High prevalence of carbapenem-resistant *Pseudomonas aeruginosa* and identification of a novel VIM-type metallo-β-lactamase, VIM-92, in clinical isolates from northern China

Linbo Zhao[1], Jiekun Pu[2], Yunning Liu[2], Heng Cai[3], Meijuan Han[4], Yunsong Yu[3]* and Jianhua Tang[5]*

[1]Hebei Key Laboratory of Neuropharmacology, Hebei North University, Zhangjiakou, China, [2]Department of Pharmacy, The First Affiliated Hospital of Hebei North University, Zhangjiakou, China, [3]Department of Infectious Diseases, Sir Run Run Shaw Hospital, Zhejiang University School of Medicine, Hangzhou, China, [4]Department of Pharmacy, Cangzhou Central Hospital, Cangzhou, Hebei, China, [5]Institute of Disaster and Emergency Medicine, Tianjin University, Tianjin, China

Carbapenem-resistant *Pseudomonas aeruginosa* (CRPA) has become a serious global health concern due to the limited treatment options. The primary resistance mechanism in CRPA involves the production of metallo-β-lactamases (MBLs), making MBL-producing *P. aeruginosa* a significant component of CRPA cases. To understand the prevalence of CRPA in hospitals in northern China, we conducted a preliminary screening and identification of CRPA in 143 clinical isolates of *P. aeruginosa* collected from various departments of a tertiary hospital between 2021 and 2023, analyzing CRPA resistance trends in certain regions of northern China during this period. We identified 71 CRPA isolates that exhibited high carbapenem resistance and phylogenetic tree analysis revealed that ST244 CRPA isolates had widely spread across various departments of the same hospital over three consecutive years. We also identified two VIM-producing isolates, PJK40 and PJK43, both of which carried the same novel VIM-type metallo-β-lactamase, VIM-92, encoded by a newly identified gene, bla_{VIM-92}, closely related to bla_{VIM-24}. bla_{VIM-92} was embedded in class 1 integrons within the Tn*1403* transposon. The bla_{VIM-92}-carrying plasmid, pPJK40, was found to resemble the pJB37 megaplasmid. The expression of VIM-92 and VIM-24 in DH5α and PAO1 revealed similar effects of the MICs of β-lactams, except for aztreonam. The high prevalence of CRPA in clinical settings, and the identification of VIM-92, highlights the urgent need for ongoing surveillance of CRPA and emerging MBL variants in *P. aeruginosa*.

KEYWORDS

***Pseudomonas aeruginosa*, epidemiological investigation, metallo-β-lactamase, VIM-92, plasmid**

1 Introduction

Pseudomonas aeruginosa (*P. aeruginosa*) is a Gram-negative, opportunistic pathogen commonly associated with hospital-acquired infections, especially in immunocompromised patients and individuals with cystic fibrosis (Qin et al., 2022). Carbapenem antibiotics are often the first-line treatment for *P. aeruginosa* infections due to their broad antibacterial spectrum, potent activity, and rapid onset (Takahashi et al., 2021). However, the global CRPA increase has become a significant health concern. *P. aeruginosa* can acquire resistance to carbapenem through various mechanisms, producing carbapenemase enzymes encoded by carbapenemase genes as a primary resistance pathway (Tenover et al., 2022). To date, class A, B, and D carbapenemases have been identified in *P. aeruginosa*, with class B metallo-β-lactamase (MBL) enzymes, such as Verona Integron-encoded Metallo-β-lactamase (VIM), imipenemases (IMP), and New Delhi metallo-β-lactamase (NDM), being the most prevalent (Park and Koo, 2022). MBLs can hydrolyze most β-lactams, except monobactams, but remain unaffected by novel β-lactamase inhibitors such as avibactam, vaborbactam, relebactam, and nacubactam (Jean et al., 2019). Consequently, therapeutic options for infections caused by MBL-producing *P. aeruginosa* are substantially limited. In addition, bacterial secretion systems played a significant role in the infection and pathogenesis of CRPA. The virulence of CRPA was closely associated with its encoded secretion systems, including type I to type VI secretion systems (Wood et al., 2015). Among these, the type III secretion system (T3SS) was the most complex and virulent secretion system in CRPA, primarily involving four virulence factors: *exoY*, *exoT*, *exoU*, and *exoS*.

The VIM-type enzyme is the most prevalent MBL in Europe, with over 80 variants identified to date (Botelho et al., 2019). According to relevant literature, the detection rate of CRPA in northern China is significantly higher than in other regions, with VIM-type enzymes being more frequently detected than other types of MBLs (Wu et al., 2024). Among these, $bla_{\text{VIM-2}}$ is the most frequently reported carbapenemase-encoding gene in *P. aeruginosa* spp. In recent years, isolates carrying novel VIM-type alleles have continuously been identified. According to recent literature, $bla_{\text{VIM-84}}$, a novel VIM-type MBLs, was first reported in the IncP-2 megaplasmid of *P. aeruginosa* (Wang et al., 2023). This indicates the potential for the transfer and spread of $bla_{\text{VIM-84}}$ in *Pseudomonas* species. In another study, researchers characterized a *Pseudomonas monteilii* (*P. monteilii*) isolate carrying $bla_{\text{VIM-84}}$ for the first time, which conferring resistance to β-lactams (Tu et al., 2024). Genome analysis revealed that $bla_{\text{VIM-84}}$ was located within a class I integron, with Tn*3* surrounding. This structure suggested potential for dissemination. MBL-encoding genes are typically integrated within class I integrons and are transmitted via mobile genetic elements, which commonly embed bla_{VIM} genes into genetic cassettes, facilitating their widespread dissemination (Zhang et al., 2023).

Zhangjiakou, in China, the location of this study, occupies a unique geographic position at the intersection of Beijing, Tianjin, Hebei, and Inner Mongolia, which can contribute to different sources of infection and epidemiological patterns. The First Affiliated Hospital of Hebei North University, a tertiary hospital in Zhangjiakou, serves as a central healthcare facility, providing critical data to understand antimicrobial resistance trends in northern China. These data support regional and interregional public health collaborations and comparative studies on *P. aeruginosa* resistance. For this study, we collected 143 *P. aeruginosa* isolates from clinical specimens submitted by various departments at our hospital between January 1, 2021, and December 31, 2023. Following culture, identification, and antimicrobial susceptibility testing, we analyzed the transmission dynamics within the hospital and resistance patterns of CRPA. After excluding duplicate isolates from the same patient and sample size, we identified 71 CRPA isolates. Among these, two were VIM-producing *P. aeruginosa*, PJK40 and PJK43. Whole-genome sequencing revealed that the genetic sequences of these two isolates were identical, and both of them carried a new variant of VIM-2, VIM-92, with the difference of isolation sources. Therefore, to avoid redundancy, we selected PJK40, strained from lavage fluid, further analyzed the genetic characterization of this isolate, and evaluated the effect of VIM-92 on antibiotic resistance.

2 Materials and methods

2.1 Collection and identification of bacteria isolates

Clinical isolates of *P. aeruginosa* were obtained from patient samples at the First Affiliated Hospital of Hebei North University using selective *Pseudomonas* Isolation Agar plates. And then identification was confirmed using matrix-assisted laser desorption ionization-time of flight mass spectrometry (Bruker Daltonik GmbH, Bremen, Germany). Data on 143 *P. aeruginosa* isolates, including the year of detection, department, and source of the isolates, were retrieved from the hospital's electronic medical records.

2.2 Antimicrobial susceptibility determination

The minimum inhibitory concentrations (MICs) of antibiotics were determined using the broth microdilution method. The antibiotics tested included Meropenem (Hanhui Pharmaceutical Co., Ltd., China), Imipenem (Merck Sharp & Dohme Corp., USA), Cefepime (Jiangsu Hengrui Pharmaceutical Co., Ltd., China), Piperacillin (Suzhou Erye Pharmaceutical Co., Ltd., China), Ceftazidime (Guangdong Jincheng Jinsu Pharmaceutical Co., Ltd., China), Tazobactam (Meilunbio, China), Avibactam (MedChemExpress, USA), Aztreonam (Sigma-Aldrich, USA), Ciprofloxacin (Fluka Analytical, USA), Amikacin (Meilunbio, China), and Colistin (Sigma-Aldrich, USA). *P. aeruginosa* isolate ATCC 27853 and *Klebsiella pneumoniae* ATCC 700603 were used as quality control isolates. The diluted cultures were incubated overnight at 37°C, and results were interpreted according to the CLSI performance standards (30th Edition) (Clinical and Laboratory Standards Institute, 2020). According to the CLSI standards, CRPA were defined as *P. aeruginosa* exhibiting resistance to any carbapenem, including imipenem and meropenem. In this study, isolates with a MIC ≥128 were classified as highly resistant isolates (Park and Koo, 2022). The VIM alleles were identified by PCR amplification of the full ORF, using primer pairs VIM-F (5′-tgccgtagaagaacagcaag-3′) and VIM-R (5′-gcaacttcatgttatgccgc-3′). The PCR products were sequenced using Sanger sequencing.

2.3 Whole-genome sequencing and bioinformatics analysis

All 71 CRPA isolates were subjected to second-generation sequencing on the Illumina HiSeq platform. Genomic DNA was extracted using the QIAamp DNA Mini Kit (Qiagen, Hilden, Germany) following the manufacturer's instructions. Sequencing was performed on the Illumina HiSeq platform, and raw reads were assembled using Shovill 0.9.0.[1] Additionally, two VIM-producing isolates were selected for third-generation sequencing. For these isolates, hybrid assembly that combined Illumina and Nanopore reads was conducted with Unicycler v.0.4.8 (Wick et al., 2017). Multilocus sequence typing (MLST) was determined through PubMLST,[2] and gene annotation was performed with Prokka v.1.14.6 (Seemann, 2014). ABRicate v.1.0.0[3] was used for the identification of resistance genes and virulence factors, while sequence alignment against the plasmid was performed using BWA-MEM (Li, 2014). Genetic sequence comparisons and visualizations were generated using Easyfig 2.2.5 and BRIG-0.95 (Alikhan et al., 2011; Sullivan et al., 2011). Based on the annotation results from Prokka, the genomic data of 71 CRPA isolates were selected for pan-genome analysis using Roary v.3.13.0 (Page et al., 2015). Phylogenetic tree construction was conducted with FastTree v.2.1.11 (Price et al., 2009) using default parameters, and the tree was visualized and annotated with features using ChiPlot (Xie et al., 2023).

2.4 Conjugation of plasmids

Conjugation experiments were conducted using clinical isolates as donors and a rifampin-resistant derivative of *P. aeruginosa* PAO1 as the recipient. The selection was performed with rifampicin (300 μg/mL) and ceftazidime-avibactam (16 μg/mL). The donor and recipient bacterial colonies were cultured in 2 mL of Luria-Bertani (LB) medium and shaken at 37°C for 4 h. The isolates were mixed in LB medium in a 1:1 ratio (100 μL each). A 20 μL aliquot of the mixture was placed on a sterile 0.22-μm pore-size Millipore filter of 0.22-m size on a Mueller-Hinton (MH) agar plate and cocultured at 37°C overnight. The bacterial lawn formed on the filter was harvested, resuspended in 200 μL of LB broth, and seeded on agar containing selective antibiotics. After overnight incubation at 37°C, colonies that grew in the selective plates were confirmed by PCR amplification.

2.5 Cloning procedures

Plasmid pGK1900 was designed to express MBL genes. In brief, the oriT and traJ region from plasmid pCasPA (Chen et al., 2018), and the GmR region from plasmid pEX18Gm (Hoang et al., 1998), were amplified and recombined into the broad-host-range plasmid pACRISPR (Chen et al., 2018), which carries the pRO1600 oriV and T7 promoter. The final plasmid, pGK1900, was constructed.

The bla_{VIM-92} gene, along with its upstream predicted promoter (identified using Softberry),[4] was amplified from the clinical isolate PJK40 and cloned into pGK1900 using the Hieff Clone Plus One Step Cloning Kit (Li et al., 2022). The resulting VIM-expressing plasmids were introduced into *Escherichia coli* DH5α via chemical transformation and into *P. aeruginosa* PAO1 by electroporation.

2.6 Data analysis

SPSS 20.0 and WHONET v5.6 software (WHO Collaborating Centre for Surveillance of Antimicrobial Resistance, Boston, MA, USA) were used to analyze the data. The counting data were expressed as the number of cases (n) and rate (%).

3 Results

3.1 Collection and distribution of CRPA

Between 2021 and 2023, 143 *P. aeruginosa* isolates were detected, of which 71 were identified as CRPA, excluding duplicate isolates from the same patient, resulting in a CRPA detection rate of 49.65%. Statistical analysis indicated a significant downward trend in the CRPA detection rate over the 3 years ($Z = 1.850$, $p = 0.0174$) (Supplementary Table S1). These 71 CRPA isolates were distributed between various departments, with the highest proportion of other departments (20 isolates, 28.17%), followed by the Respiratory Department (18 isolates, 25.35%) and the International Medical Department (14 isolates, 19.72%) (Supplementary Table S2). And the primary source of CRPA specimens was sputum, accounting for 55 isolates (77.46%), followed by lavage fluid and other sources, each with five isolates (7.04%) (Supplementary Table S3).

3.2 MIC for CRPA

The CRPA isolates exhibited high resistance rates to carbapenems, with imipenem (98.59%) and meropenem (78.87%). Resistance to most cephalosporins (ceftazidime, cefepime), β-lactams (aztreonam), enzyme inhibitor complexes (piperacillin/tazobactam, ceftazidime/avibactam) and quinolones (ciprofloxacin, levofloxacin) exceeded 49%, indicating a multidrug-resistant profile. In contrast, the isolates remained relatively susceptible to amikacin and polymyxins, with resistance rates below 34%, suggesting that these agents may still be effective treatment options. During the 3-year period, the resistance rate to piperacillin-tazobactam initially declined but then increased ($p < 0.05$), while resistance to ceftazidime-avibactam, aztreonam, imipenem, ciprofloxacin, levofloxacin, and amikacin showed a decreasing trend ($p < 0.05$). No statistically significant differences were observed in resistance rates to ceftazidime, cefepime, meropenem, and colistin (Table 1). MICs for 71 CRPA isolates are provided in Supplementary Table S4.

1 https://github.com/tseemann/shovill
2 https://pubmlst.org/organisms/pseudomonas-aeruginosa
3 https://github.com/tseemann/abricate
4 http://www.softberry.com

10.3389/fmicb.2025.1543509

TABLE 1 Changes in drug resistance rates of CRPA isolates to commonly used antibiotics from 2021 to 2023.

Department	2021 (*n* = 24)		2022 (*n* = 25)		2023 (*n* = 22)		Total (*n* = 71)		X^2	*p*
	Isolate count	Proportion (%)	Isolate count	Proportion (%)	Isolate count	Proportion (%)	Isolate count	Proportion (%)		
PTZ	14	58.33	9	36	16	72.73	39	54.93	6.546	0.038
CAZ	16	66.67	11	44	15	68.18	42	59.15	3.679	0.159
CZA	16	66.67	7	28	13	59.09	36	50.7	8.221	0.016
FEP	17	70.83	10	40	16	72.73	43	60.56	2.259	0.323
AZT	17	70.83	14	56	15	68.18	46	64.79	8.442	0.015
IMI	24	100	25	100	21	95.45	70	98.59	6.849	0.033
MEM	22	91.67	15	60	19	86.36	56	78.87	1.342	0.511
CIP	18	75	5	20	12	54.55	35	49.3	15.171	<0.001
LEV	20	83.33	7	28	13	59.09	40	56.34	15.340	<0.001
AK	15	62.5	2	8	7	31.82	24	33.8	16.310	<0.001
COL	1	4.17	2	8	1	4.55	4	5.63	0.409	0.815

PTZ, piperacillin-tazobactam; CAZ, ceftazidime; CZA, ceftazidime-avibactam; FEP, cefepime; AZT, aztreonam; IMI, imipenem; MEM, meropenem; CIP, ciprofloxacin; LEV, levofloxacin; AK, amikacin; COL, colistin.

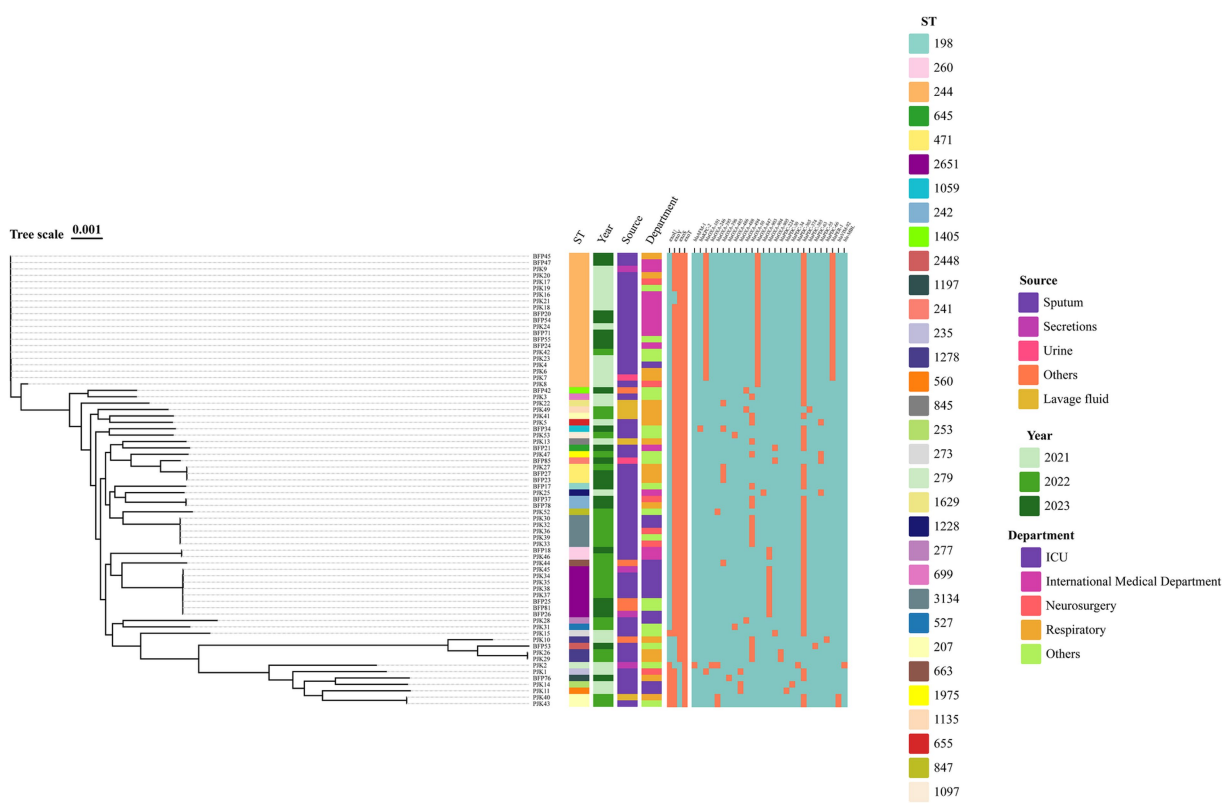

FIGURE 1
The phylogenetic tree based on the concatenated set of core genes displays the evolutionary relationships among the 71 CRPA isolates. The primary features of CRPA isolates are indicated in various colors, and the presence of T3SS virulence factors and resistance genes is represented by orange.

3.3 Genomic features of the 71 CRPA isolates

To further understand the relationships between the 71 CRPA isolates, we constructed a phylogenetic tree based on the nucleotide composition of core genes (Figure 1). MLST is a an unambiguous, portable and nucleotide-based technique for typing bacteria using the sequences of internal fragments of (usually) seven house-keeping genes (Maiden et al., 1998; Spratt, 1999; Urwin and Maiden, 2003). Among the 71 CRPA isolates, 32 sequence types (STs) were identified, with the predominant types being ST244, ST2651, and ST3134, accounting for 29.6% (21/71), 11.3% (8/71), and 7.0%

(5/71), respectively. The analysis of STs among the 71 CRPA isolates over 3 years (2021–2023) revealed distinct trends. In 2021, ST244 was the predominant type, accounting for the majority of isolates (24 isolates). In 2022, both ST3134 and ST2651 were the most prevalent types, each represented by 5 isolates. By 2023, ST244 re-emerged as the dominant type, once again constituting the largest proportion of isolates. Notably, ST1278 was prevalent in the first 2 years but disappeared in 2023. Meanwhile, ST60, ST471, and ST2651 began to emerge as significant types starting from 2022. Combined analysis of the ST types, departmental distribution, and isolation years of the 71 CRPA isolates revealed that ST244 CRPA was consistently detected across different departments of the same hospital over a three-year period. In addition, T3SS virulence factor analysis showed that the virulence factor *exoT* had the highest carriage rate at 100% (71/71), followed by *exoS* and *exoY*, both at 90.1% (64/71), while *exoU* had the lowest carriage rate at 11.3% (8/71). Notably, isolate PJK15 carried all four T3SS virulence factors, which may contribute to its high virulence potential (Supplementary Figure S2).

We predicted resistance genes in the 71 CRPA isolates and identified a total of 54 resistance genes. Among these, four carbapenemase-producing isolates, PJK2, BFP34, PJK40, and PJK43, were detected, carrying the resistance genes bla_{AFM}, bla_{KPC}, and bla_{VIM}. Isolate PJK2 carried the highest number of resistance genes, with a total of 23. The distribution of shared and unique resistance genes is shown in the Supplementary Figure S1.

3.4 Identification of VIM-carrying isolates

Bioinformatic analysis of the 71 CRPA isolates revealed mutations in the VIM alleles in two isolates. These two VIM-producing *P. aeruginosa* isolates were identified as PJK40 and PJK43. Sequence analysis revealed that the VIM gene sequences of the two isolates were identical, with the difference of isolation sources. Therefore, PJK40 was selected for further analysis to avoid redundancy. PJK40, carried a novel VIM allele and was isolated from a patient's bronchoalveolar lavage fluid. Genome sequencing classified PJK40 as sequence type (ST) 207. PCR and sequencing revealed this isolate harbors a novel allele, bla_{VIM-92} (GenBank accession: PQ563311). In the amino acid sequence, VIM-24 has an arginine-to-leucine substitution at residue 205 (GenBank accession: HM855205.1), while VIM-92 shows a valine-to-isoleucine substitution at residue 236 (Supplementary Figure S3).

3.5 Effects of VIM-24 and VIM-92 on the MICs of β-lactams

To better understand the role bla_{VIM-92} in conferring β-lactam resistance, bla_{VIM-92} was cloned in the plasmid pGK1900 and transformed into *E. coli* DH5α and *P. aeruginosa* PAO1. The effects VIM-92 on β-lactam resistance to β-lactam differed between DH5α and PAO1 (Table 2).

In DH5α, VIM-92 increased the MICs of meropenem, imipenem, piperacillin, cefepime, ceftazidime, piperacillin-tazobactam, and ceftazidime-avibactam by more than 8 times. In PAO1, the MICs of all β-lactams, except for aztreonam, increased by more than 16-fold due to the presence of VIM-92. This is expected, as VIM-92 is an MBL that does not hydrolyze aztreonam. We subsequently cloned bla_{VIM-24} using the same method. Antimicrobial susceptibility testing revealed minimal differences in antibiotic resistance effects between VIM-24 and VIM-92.

3.6 The characteristics of VIM-carrying plasmids

Whole-genome sequencing of PJK40 revealed multiple acquired resistance genes, with bla_{VIM-92} embedded in the plasmid pPJK40. The pPJK40 plasmid showed query coverage of 82, 81, and 79% with pJB37 (GenBank accession: KY494864.1), pWTJH36 (GenBank accession: CP104591.1), and pPUV-16 (GenBank accession: MT732194.1), respectively (Figure 2). The backbones of these homologous plasmids were similar to those of the IncP-2 plasmid pOZ176, suggesting that they belong to the same megaplasmid family (Zhang et al., 2021). The complete sequence of pPJK40 is 467,425 bp, contains 583 ORFs, and exhibits a GC content of 57%. This plasmid contains a few resistance genes organized into a gene cluster, approximately 144 to 159 kbp, which includes the bla_{VIM-92} gene. The differences between pPJK40, pJB37, pWTJH36, and pPUV-16 are mainly due to the presence of insertion sequences (ISs) or integrase-encoding genes, indicating that these plasmids have evolved through multiple insertions and recombination events.

Among the homologous plasmids identified in the NCBI database, pPJK40 shows the highest similarity to pJB37, the first bla_{VIM-2}-carrying megaplasmid described in *P. aeruginosa* (Botelho et al., 2017). pPJK40 shares 81% query coverage and 99.97% sequence identity with pJB37, according to the BLAST analysis (Figure 3). Several conserved regions were observed between the two

TABLE 2 MICs of β-lactam antibiotics for the bla_{VIM-24} and bla_{VIM-92} transformants.

Isolates	MICs of antibiotics (mg/L)							
	MEM	IMI	PIP	AZT	FEP	CAZ	PTZ	CZA
DH5α (pGK1900)	<0.06	0.5	4	0.25	<0.06	1	2	1
DH5α (pGK1900-VIM2 4)	128	16	>128	0.125	1	16	>128	64
DH5α (pGK1900-VIM92)	8	4	128	<0.06	0.5	32	128	16
PAO1 (pGK1900)	2	2	4	4	4	2	8	2
PAO1 (pGK1900-VIM24)	>128	128	>128	8	>128	>128	>128	>128
PAO1 (pGK1900-VIM92)	128	32	128	8	64	>128	128	128

MEM, meropenem; IMI: imipenem; PIP, piperacillin; AZT, aztreonam; FEP, cefepime; CAZ, ceftazidime; PTZ, piperacillin-tazobactam; CZA, ceftazidime-avibactam.

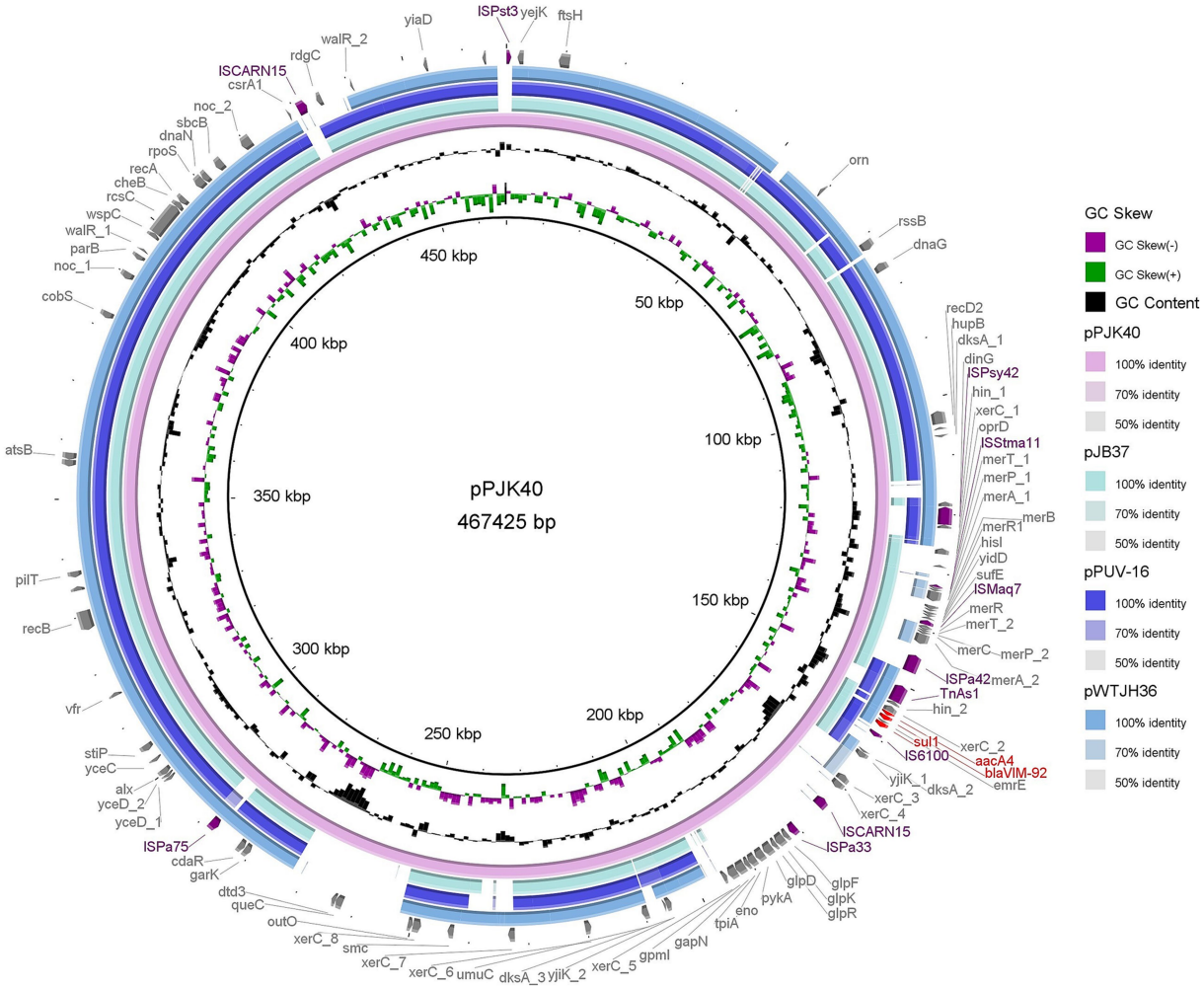

FIGURE 2
Comparison of pPJK40 with other plasmids. The rings represent the alignment of sequence reads from pJB37, pPUV-16, and pWTJH36 against pPJK40. Both pJB37 and pPUV-16 contain bla_{VIM-2}, while pWTJH36 contains bla_{VIM-85}.

plasmids, reflecting a high degree of sequence similarity. The resistance gene cluster in pPJK40 spans 11,365 bp and contains multiple genetic elements and resistance genes, including bla_{VIM-92}. The strong sequence similarity between this region and the corresponding cluster on pJB37 suggests that these plasmids share similar structural features that support the preservation and transmission of resistance genes. In particular, the insertion sequence downstream of bla_{VIM-92} may enhance its mobility, facilitating the spread of resistance genes across bacterial species (Figure 3).

Conjugation assays were conducted to assess the transferability of pPJK40. All three experiments were unsuccessful, suggesting that this plasmid is non-conjugative.

3.7 Genetic contexts of bla_{VIM} alleles in *Pseudomonas aeruginosa*

Numerous VIM alleles have been reported in *P. aeruginosa* (Pournaras et al., 2003; Siarkou et al., 2009). In a previous report, sequencing revealed that both bla_{VIM-84} (GenBank accession: ON688661.1) and bla_{VIM-85} (GenBank accession: ON688662.1) had a length of 801 bp and they were highly similar to bla_{VIM-24} (GenBank accession: HM855205), with nucleotide identities of 99.88 and 99.75%, respectively (Wang et al., 2023). In this study, according to BLASTn search, bla_{VIM-92} was highly similar to bla_{VIM-84} and bla_{VIM-85}, with a nucleotide identity of 99.63 and 99.5%, respectively. Therefore, we selected the plasmids pWTJH2 (GenBank accession: CP104585.1), pWTJH6 (GenBank accession: CP104587.1), and pPJK40 to compare the genetic backgrounds of the VIM alleles in *P. aeruginosa* (Figure 4).

In plasmids pWTJH2 and pWTJH6, the bla_{VIM-84} and bla_{VIM-85} genes are embedded within class 1 integrons. Similarly, in the plasmid pPJK40, the bla_{VIM-92} gene is also embedded in a class 1 integron. The bla_{VIM-84} gene is the second cassette in a class 1 integron, with the fosE gene located upstream. The downstream cassettes include aac(6′)-Ib4, $bla_{OXA-101}$, and ant1 within an integron that originally carried bla_{VIM-24}. In this integron, the qacEΔ1 and sul1 genes in the 3′ conserved segment (3’-CS) were replaced by an IS26 element.

For the bla_{VIM-85} genetic environment, the 3’-CS is interrupted by a gene encoding GNAT family N-acetyltransferase, clipped by

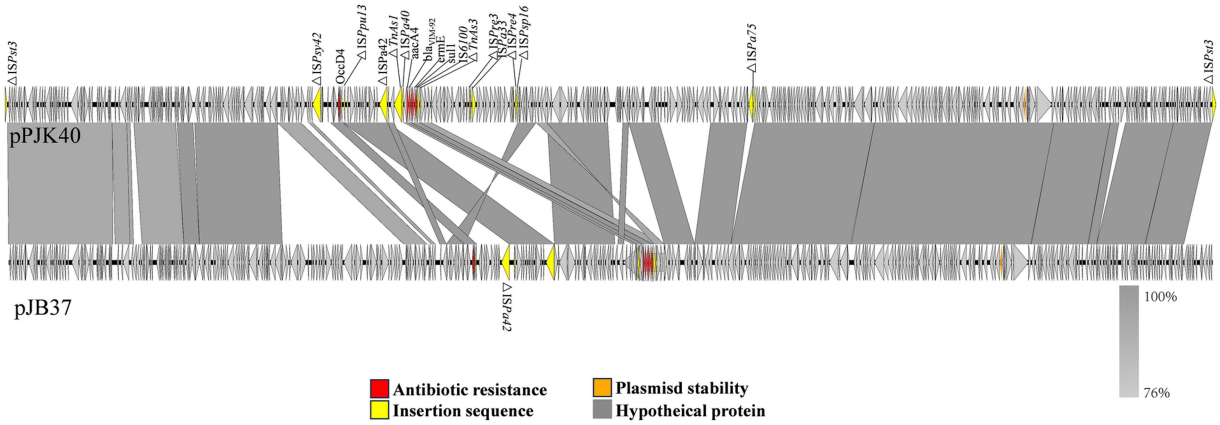

FIGURE 3
Comparison of pPJK40 and pJB37. The arrow direction indicates the transcription direction of each ORF. The dark yellow arrows represent mobile elements, the red arrows represent resistance genes, and the gray and blue arrows represent predicted ORFs.

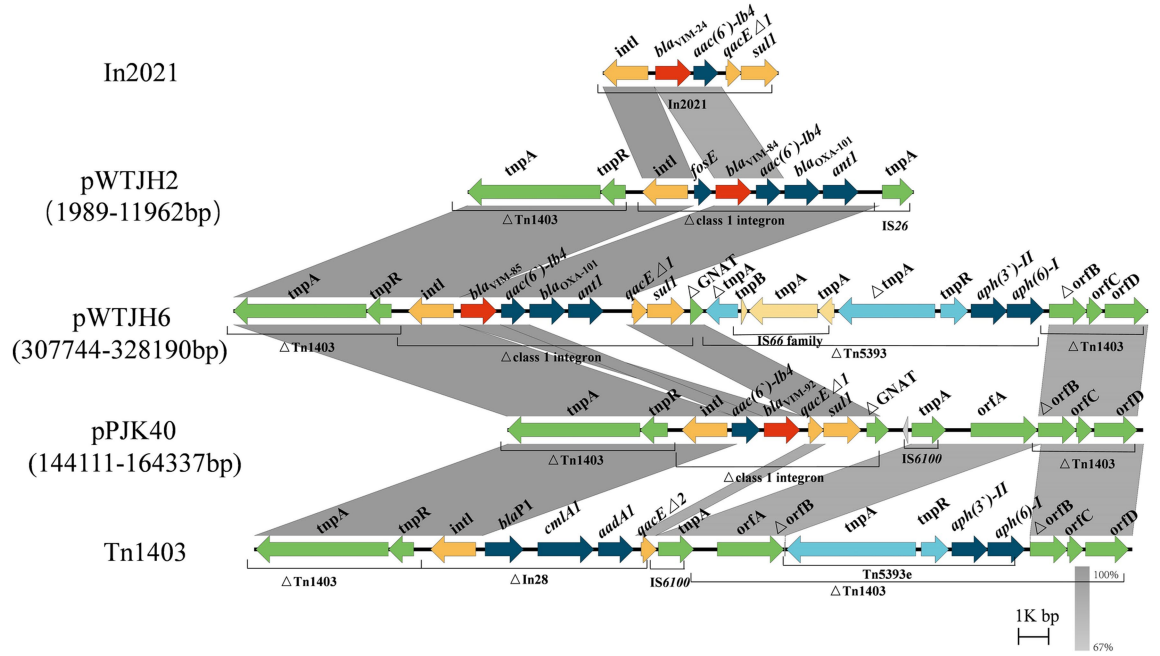

FIGURE 4
Comparison of the genetic environments of *bla*$_{VIM}$. Shaded regions indicate nucleotide identity (67–100%). Red arrows represent *bla*$_{VIM}$ and other antibiotic resistance genes, shown in dark blue. The yellow, green, and light blue arrows represent structures of mobile elements.

the insertion of transposon Tn*5393*. A similar genetic structure was observed in *bla*$_{VIM-92}$, characterized by the arrangement intI-aac(6′)-Ib4-*bla*$_{VIM-92}$-qacEΔ1-sul1. In this configuration, *bla*$_{VIM-92}$ is embedded within the second gene cassette of a class 1 integron, with the aac(6′)-Ib4 resistance gene positioned upstream. In particular, the downstream *bla*$_{OXA-101}$ and ant1 genes are absent. The integron harboring *bla*$_{VIM-92}$ was inserted into transposon Tn*1403* (GenBank accession: AF313472.2), which contains a backbone with the genes tnpA, tnpR, and orfABCD, along with a class 1 integron and Tn*5393*. In Tn*5393*, the tnpA gene is interrupted by an IS66 family insertion (Stokes et al., 2007).

4 Discussion

Pseudomonas aeruginosa is capable of quickly evolving and developing resistance to adapt to environmental conditions, especially in hospital settings. For example, studies have shown that after prolonged exposure in different hospital environments, *P. aeruginosa* adapts to the host environment, modulating the expression of numerous virulence factors and acquiring or developing mechanisms for antibiotic resistance, including resistance to carbapenems (Cameron et al., 2022). This adaptability is a major factor contributing to the frequent occurrence of hospital-acquired infections. In China, surveillance data

from 2021 reported that *P. aeruginosa* accounted for 7.96% of hospital-acquired infections, highlighting its significant role in clinical settings (Yan et al., 2022). Among these, CRPA has become increasingly prevalent due to the widespread use of antibiotics. CRPA poses a major threat to public health, with its rising detection rates associated with increased morbidity and mortality (Litwin et al., 2020). Furthermore, CRPA exhibits resistance not only to carbapenems but also to multiple classes of antibiotics, severely limiting treatment options (Ning and Yang, 2022). The extensive dissemination of CRPA and its ability to transfer resistance genes to other bacteria underscore the need for effective surveillance and control measures to curb its spread and impact.

In this study, the average annual CRPA detection rate in the First Affiliated Hospital of Hebei North University from 2021 to 2023 was 16.55%, derived by averaging the overall detection rate of 46.95% over 3 years, which was comparable to the national detection rate reported for 2022 (16.6%), but slightly lower than the rate for Hebei Province in the same year (17.4%) (Yu et al., 2022). With the widespread use of antibiotics, the detection rate of *P. aeruginosa* resistant to multiple antibiotics is increasing yearly (Litwin et al., 2020). Due to the high mortality rate, propensity for cross-infection, and difficulty in treatment, the emergence of CRPA had made infection control in hospitals increasingly difficult. Although the detection rate of CRPA may differ across regions, its higher detection rate in specific areas, especially within local hospital environments, emphasizes the critical need for focused surveillance and control strategies (Huang et al., 2023). This difference in detection rates may be related to factors such as the hospital classification level, patient demographics, regional conditions, and the impact of the COVID-19 pandemic. In the present work, 71 CRPA isolates mainly came from four key departments: respiratory, the others, international medical department and the ICU. Notably, the department distribution of CRPA is largely consistent with previous reports (Li et al., 2021). Patients in these departments are often critically ill, require prolonged hospital stays, frequently undergo invasive procedures (e.g., tracheal intubation and tracheostomy), leading to Device-associated Hospital-acquired Infections (DA-HAIs) in some patients, and have multiple underlying conditions. Related studies suggested that the incidence of infections in ICU patients might have varied across different geographical regions, hospitals, and even among different ICUs within the same hospital. The types of infections, the profiles of pathogens causing these infections, and their antimicrobial susceptibility patterns also varied depending on the location (Alfouzan et al., 2021). These factors collectively facilitated the spread of CRPA. Long-term use of antibiotics and immunosuppressants compromises immune function, increasing susceptibility to CRPA infection (Rossi et al., 2021; Pettigrew et al., 2019). Many studies showed that inappropriate and irrational use of antibiotics to treat infections led to the emergence of multidrug-resistant (MDR) isolates of common bacterial isolates (Rizzo et al., 2019). This results in prolonged hospital stays, significantly increased morbidity and mortality, and contributes to the spread of CRPA. These findings demonstrate the importance of judicious use of antibiotics following antimicrobial guidelines. When performing invasive procedures on CRPA patients, strict aseptic protocols, improved surface disinfection, timely equipment replacement, and early tube removal are crucial to prevent infection. Subsequently, statistical analysis was conducted on the types of specimens, and it was found that most CRPA isolates were detected in sputum specimens, accounting for 77.46%, which is consistent with reports that CRPA is mainly strained from sputum (Gill et al., 2022). However, as *P. aeruginosa* is part of normal respiratory flora, it can quickly colonize the respiratory tract as an opportunistic pathogen. Thus, interpreting the results of respiratory cultures requires careful assessment to confirm infection. Previous research (Yan et al., 2022) has linked CRPA strained from sputum to higher long-term mortality, indicating that it may be a potential source of hospital-acquired infections that warrant attention.

In recent years, the detection rate of MBLs has increased significantly, with a broad distribution across bacterial species and geographic regions, making them a focal point of clinical concern (Safavi et al., 2020). MBL genes can reside on integrons, transposons, plasmids, chromosomes, or other genetic elements, and their plasmid-mediated mobility improves transferability, contributing to bacterial resistance. Clinically, carbapenems such as imipenem, meropenem, ertapenem, and doripenem are ineffective against MBLs, except for monobactams (Bush, 2001). Therefore, the presence of MBLs is likely to increase the risk of treatment failure in carbapenem-resistant *P. aeruginosa* infections. The increasing prevalence of MBLs highlights their growing significance in hospital-acquired infections, further emphasizing the urgent need for effective surveillance and control strategies to mitigate their public health impact. Among acquired MBL genotypes, blaVIM is the most prevalent, with multiple variants differentiated by gene and translated amino acid sequences. In this study, VIM-producing isolates accounted for 1.40% (2/143) of all isolates, with VIM-92-producing isolates belonging to the sequence type ST207. Although the global prevalence of ST207 may be lower than classic sequence types such as ST235 and ST111, it has been reported in some regions as an MDR isolate carrying carbapenemase genes, such as blaVIM or blaNDM (Gondal et al., 2024). ST244 CRPA was consistently detected in the same hospital over three consecutive years. This observation suggested the dissemination of ST244 isolates producing OXA-101 and PER-1 enzymes within the hospital. In the analysis of T3SS virulence factors, we identified an isolate, PJK15, which carried four virulence factors. Previous studies had generally suggested that *exoU* and *exoS* were mutually exclusive due to occupying the same chromosomal locus (Freschi et al., 2019). However, recent studies have revealed that high-risk clones co-carrying the T3SS effector genes *exoS* and *exoU* are capable of causing community-acquired infections (CAIs) in non-immunocompromised young individuals, likely due to the enhanced virulence profiles of these isolates (Song et al., 2023). In our study, we hypothesized that the coexistence of these virulence factors in PJK15 was induced by mutations triggered by environmental pressures on the isolate. The simultaneous presence of both virulence factors could potentially influence the severity of the infection and the response to treatment, highlighting the urgent need for further investigation.

We identified two *P. aeruginosa* isolates, PJK40 and PJK43, carrying the $bla_{\text{VIM-92}}$ gene and selected PJK40 for further study in this research. This isolate exhibited elevated MICs for β-lactams, cephalosporins, and β-lactam combination agents, attributed to acquiring the resistant plasmid pPJK40. The $bla_{\text{VIM-92}}$ gene is located on a pJB37-like megaplasmid of the IncP-2 family. Typically, plasmids acquire resistance genes through mobile elements, allowing their spread within and between bacterial species (Hall et al., 2022). However, the results of our conjugation experiments indicated that pPJK40 was not conjugative, likely due to its specific structural configuration, which includes the $bla_{\text{VIM-92}}$ resistance gene. Antimicrobial susceptibility testing comparing PAO1 MICs expressing $bla_{\text{VIM-92}}$ and $bla_{\text{VIM-24}}$ indicated that $bla_{\text{VIM-92}}$ confers similar or, in some cases, higher resistance to most antibiotics, except for aztreonam. This suggests that VIM-92 may be equally or more effective than VIM-24 in mediating antibiotic resistance.

In conclusion, with its unique geographic location, our study in Zhangjiakou identified 71 CRPA isolates and analyzed CRPA resistance

trends in certain regions of northern China from 2021 to 2023. Among the CRPA isolates, two produced the novel metallo-β-lactamase, VIM-92. bla_{VIM-92} was in a pJB37-like plasmid within a distinct genetic context compared to other VIM alleles in *P. aeruginosa*. We also identified an isolate carrying four T3SS virulence factors simultaneously. With the continuous emergence of carbapenemase-producing *P. aeruginosa*, these findings highlight the importance of ongoing surveillance and comparative studies to inform effective antimicrobial stewardship and public health interventions in the northern region.

Data availability statement

The datasets presented in this study can be found in online repositories. The names of the repository/repositories and accession number(s) can be found at: https://www.ncbi.nlm.nih.gov/genbank/, PQ563311; https://www.ncbi.nlm.nih.gov/genbank/, ON688661.1; https://www.ncbi.nlm.nih.gov/genbank/, HM855205; https://www.ncbi.nlm.nih.gov/genbank/, CP104585.1; https://www.ncbi.nlm.nih.gov/genbank/, CP104587.1; https://www.ncbi.nlm.nih.gov/genbank/, AF313472.2; https://www.ncbi.nlm.nih.gov/genbank/, KY494864.1; https://www.ncbi.nlm.nih.gov/genbank/, CP104591.1; https://www.ncbi.nlm.nih.gov/genbank/, MT732194.1; https://www.ncbi.nlm.nih.gov/genbank/, ON688662.1.

Ethics statement

This study was approved for exemption from ethical review by the Ethics Committee of the First Affiliated Hospital of Hebei North University (Approval Number: K2024334). It involves a retrospective analysis of anonymized clinical data and was conducted in accordance with the ethical standards of the institution. The data were collected from clinical isolates of *Pseudomonas aeruginosa* without any direct interaction with human participants. As the study utilized only anonymized data and did not involve any identifiable personal information, ethical approval was not required. All data were handled in compliance with local legislation and institutional requirements to ensure the protection of patient privacy.

Author contributions

LZ: Conceptualization, Data curation, Investigation, Methodology, Software, Visualization, Writing – original draft. JP: Conceptualization, Data curation, Methodology, Validation, Writing – review & editing. YL: Data curation, Investigation, Methodology, Validation, Writing – review & editing. HC: Methodology, Software, Validation, Writing – review & editing. MH: Data curation, Investigation, Writing – review & editing. YY: Conceptualization, Data curation, Methodology, Resources, Validation, Writing – original draft, Writing – review & editing. JT: Conceptualization, Data curation, Funding acquisition, Investigation, Methodology, Writing – review & editing.

Funding

The author(s) declare financial support was received for the research, authorship, and/or publication of this article. This work was financially supported by the research project "Optimization of Anti-Infective Therapy for Carbapenem-Resistant Pseudomonas aeruginosa Based on PK/PD Models and *In Vitro* Susceptibility Testing" (Grant No. ZF2025275), led by Jianhua Tang from the Department of Pharmacy, The First Hospital of Hebei North University.

Acknowledgments

We thank the staff from the Department of Infectious Diseases, Sir Run Run Shaw Hospital, for their participation in this study.

Conflict of interest

The authors declare that the research was conducted in the absence of any commercial or financial relationships that could be construed as a potential conflict of interest.

Generative AI statement

The authors declare that no Gen AI was used in the creation of this manuscript.

Publisher's note

Supplementary material

The Supplementary material for this article can be found online at: https://www.frontiersin.org/articles/10.3389/fmicb.2025.1543509/full#supplementary-material

References

Alfouzan, W., Dhar, R., Abdo, N. M., Alali, W. Q., and Rabaan, A. A. (2021). Epidemiology and microbiological profile of common healthcare associated infections among patients in the intensive care unit of a general Hospital in Kuwait: a retrospective observational study. *J Epidemiol Glob Health* 11, 302–309. doi: 10.2991/jegh.k.210524.001

Alikhan, N.-F., Petty, N. K., Ben Zakour, N. L., and Beatson, S. A. (2011). BLAST ring image generator (BRIG): simple prokaryote genome comparisons. *BMC Genomics* 12:402. doi: 10.1186/1471-2164-12-402

Botelho, J., Grosso, F., and Peixe, L. (2019). Antibiotic resistance in *Pseudomonas aeruginosa* - mechanisms, epidemiology and evolution. *Drug Resist. Updat.* 44:100640. doi: 10.1016/j.drup.2019.07.002

Botelho, J., Grosso, F., Quinteira, S., Mabrouk, A., and Peixe, L. (2017). The complete nucleotide sequence of an IncP-2 megaplasmid unveils a mosaic architecture comprising a putative novel blaVIM-2-harbouring transposon in *Pseudomonas aeruginosa*. *J. Antimicrob. Chemother.* 72, 2225–2229. doi: 10.1093/jac/dkx143

Bush, K. (2001). New beta-lactamases in gram-negative bacteria: diversity and impact on the selection of antimicrobial therapy. *Clin. Infect. Dis.* 32, 1085–1089. doi: 10.1086/319610

Cameron, D. R., Pitton, M., Oberhaensli, S., Schlegel, K., Prod'hom, G., Blanc, D. S., et al. (2022). Parallel evolution of *Pseudomonas aeruginosa* during a prolonged ICU-infection outbreak. *Microbiol Spectr* 10:e0274322. doi: 10.1128/spectrum.02743-22

Chen, W., Zhang, Y., Zhang, Y., Pi, Y., Gu, T., Song, L., et al. (2018). CRISPR/Cas9-based genome editing in Pseudomonas aeruginosa and cytidine deaminase-Mediated Base editing in Pseudomonas species. *iScience* 6, 222–231. doi: 10.1016/j.isci.2018.07.024

Clinical and Laboratory Standards Institute (2020). Performance standards for antimicrobial susceptibility testing. Available at: https://d.wanfangdata.com.cn/standard/CLSI%20M100-2022 (Accessed February 19, 2025).

Freschi, L., Vincent, A. T., Jeukens, J., Emond-Rheault, J.-G., Kukavica-Ibrulj, I., Dupont, M.-J., et al. (2019). The *Pseudomonas aeruginosa* Pan-genome provides new insights on its population structure, horizontal gene transfer, and pathogenicity. *Genome Biol. Evol.* 11, 109–120. doi: 10.1093/gbe/evy259

Gill, C. M., and Nicolau, D. P.ERACE-PA Global Study Group (2022). Carbapenem-resistant *Pseudomonas aeruginosa*: an assessment of frequency of isolation from ICU versus non-ICU, phenotypic and genotypic profiles in a multinational population of hospitalized patients. *Antimicrob. Resist. Infect. Control* 11:146. doi: 10.1186/s13756-022-01187-8

Gondal, A. J., Choudhry, N., Niaz, A., and Yasmin, N. (2024). Molecular analysis of Carbapenem and aminoglycoside resistance genes in Carbapenem-resistant *Pseudomonas aeruginosa* clinical strains: a challenge for tertiary care hospitals. *Antibiotics* 13:191. doi: 10.3390/antibiotics13020191

Hall, J. P. J., Botelho, J., Cazares, A., and Baltrus, D. A. (2022). What makes a megaplasmid? *Philos. Trans. R. Soc. B* 377:20200472. doi: 10.1098/rstb.2020.0472

Hoang, T. T., Karkhoff-Schweizer, R. R., Kutchma, A. J., and Schweizer, H. P. (1998). A broad-host-range Flp-FRT recombination system for site-specific excision of chromosomally-located DNA sequences: application for isolation of unmarked *Pseudomonas aeruginosa* mutants. *Gene* 212, 77–86. doi: 10.1016/s0378-1119(98)00130-9

Huang, W., Wei, X., Xu, G., Zhang, X., and Wang, X. (2023). Carbapenem-resistant *Pseudomonas aeruginosa* infections in critically ill children: prevalence, risk factors, and impact on outcome in a large tertiary pediatric hospital of China. *Front. Public Health* 11:1088262. doi: 10.3389/fpubh.2023.1088262

Jean, S. S., Gould, I. M., Lee, W. S., and Hsueh, P. R.International Society of Antimicrobial Chemotherapy (ISAC) (2019). New drugs for multidrug-resistant gram-negative organisms: time for stewardship. *Drugs* 79, 705–714. doi: 10.1007/s40265-019-01112-1

Li, H. (2014). Aligning sequence reads, clone sequences and assembly con*gs with BWA-MEM. *arXiv: Genomics*. doi: 10.6084/M9.FIGSHARE.963153.V1

Li, Z.-J., Wang, K.-W., Liu, B., Zang, F., Zhang, Y., Zhang, W.-H., et al. (2021). The distribution and source of MRDOs infection: a retrospective study in 8 ICUs, 2013-2019. *Infect Drug Resist* 14, 4983–4991. doi: 10.2147/IDR.S332196

Li, Y., Zhu, Y., Zhou, W., Chen, Z., Moran, R. A., Ke, H., et al. (2022). *Alcaligenes faecalis* metallo-β-lactamase in extensively drug-resistant *Pseudomonas aeruginosa* isolates. *Clin. Microbiol. Infect.* 28, 880.e1–880.e8. doi: 10.1016/j.cmi.2021.11.012

Litwin, A., Fedorowicz, O., and Duszynska, W. (2020). Characteristics of microbial factors of healthcare-associated infections including multidrug-resistant pathogens and antibiotic consumption at the university intensive care unit in Poland in the years 2011-2018. *Int. J. Environ. Res. Public Health* 17:6943. doi: 10.3390/ijerph17196943

Maiden, M. C., Bygraves, J. A., Feil, E., Morelli, G., Russell, J. E., Urwin, R., et al. (1998). Multilocus sequence typing: a portable approach to the identification of clones within populations of pathogenic microorganisms. *Proc. Natl. Acad. Sci. USA* 95, 3140–3145. doi: 10.1073/pnas.95.6.3140

Ning, W., and Yang, J. (2022). Research hotspots and trends of *Pseudomonas aeruginosa* drug resistance: a study based on CiteSpace. *Microbiol. China* 49, 4942–4956. doi: 10.13344/j.microbiol.china.220336

Page, A. J., Cummins, C. A., Hunt, M., Wong, V. K., Reuter, S., Holden, M. T. G., et al. (2015). Roary: rapid large-scale prokaryote pan genome analysis. *Bioinformatics* 31, 3691–3693. doi: 10.1093/bioinformatics/btv421

Park, Y., and Koo, S. H. (2022). Epidemiology, molecular characteristics, and virulence factors of Carbapenem-resistant *Pseudomonas aeruginosa* isolated from patients with urinary tract infections. *Infect Drug Resist* 15, 141–151. doi: 10.2147/IDR.S346313

Pettigrew, M. M., Gent, J. F., Kong, Y., Halpin, A. L., Pineles, L., Harris, A. D., et al. (2019). Gastrointestinal microbiota disruption and risk of colonization with Carbapenem-resistant *Pseudomonas aeruginosa* in intensive care unit patients. *Clin. Infect. Dis.* 69, 604–613. doi: 10.1093/cid/ciy936

Pournaras, S., Maniati, M., Petinaki, E., Tzouvelekis, L. S., Tsakris, A., Legakis, N. J., et al. (2003). Hospital outbreak of multiple clones of *Pseudomonas aeruginosa* carrying the unrelated metallo-beta-lactamase gene variants blaVIM-2 and blaVIM-4. *J. Antimicrob. Chemother.* 51, 1409–1414. doi: 10.1093/jac/dkg239

Price, M. N., Dehal, P. S., and Arkin, A. P. (2009). FastTree: computing large minimum evolution trees with profiles instead of a distance matrix. *Mol. Biol. Evol.* 26, 1641–1650. doi: 10.1093/molbev/msp077

Qin, S., Xiao, W., Zhou, C., Pu, Q., Deng, X., Lan, L., et al. (2022). *Pseudomonas aeruginosa*: pathogenesis, virulence factors, antibiotic resistance, interaction with host, technology advances and emerging therapeutics. *Signal Transduct. Target. Ther.* 7:199. doi: 10.1038/s41392-022-01056-1

Rizzo, K., Horwich-Scholefield, S., and Epson, E. (2019). Carbapenem and cephalosporin resistance among Enterobacteriaceae in healthcare-associated infections, California, USA1. *Emerg. Infect. Dis.* 25, 1389–1393. doi: 10.3201/eid2507.181938

Rossi, E., la, R., Bartell, J. A., Marvig, R. L., Haagensen, J. A. J., Sommer, L. M., et al. (2021). *Pseudomonas aeruginosa* adaptation and evolution in patients with cystic fibrosis. *Nat. Rev. Microbiol.* 19, 331–342. doi: 10.1038/s41579-020-00477-5

Safavi, M., Bostanshirin, N., Hajikhani, B., Yaslianifard, S., van Belkum, A., Goudarzi, M., et al. (2020). Global genotype distribution of human clinical isolates of New Delhi metallo-β-lactamase-producing *Klebsiella pneumoniae*; a systematic review. *J Glob Antimicrob Resist* 23, 420–429. doi: 10.1016/j.jgar.2020.10.016

Seemann, T. (2014). Prokka: rapid prokaryotic genome annotation. *Bioinformatics* 30, 2068–2069. doi: 10.1093/bioinformatics/btu153

Siarkou, V. I., Vitti, D., Protonotariou, E., Ikonomidis, A., and Sofianou, D. (2009). Molecular epidemiology of outbreak-related *pseudomonas aeruginosa* strains carrying the novel variant blaVIM-17 metallo-beta-lactamase gene. *Antimicrob. Agents Chemother.* 53, 1325–1330. doi: 10.1128/aac.01230-08

Song, Y., Mu, Y., Wong, N.-K., Yue, Z., Li, J., Yuan, M., et al. (2023). Emergence of hypervirulent *Pseudomonas aeruginosa* pathotypically armed with co-expressed T3SS effectors ExoS and ExoU. *hLife* 1, 44–56. doi: 10.1016/j.hlife.2023.02.001

Spratt, B. G. (1999). Multilocus sequence typing: molecular typing of bacterial pathogens in an era of rapid DNA sequencing and the internet. *Curr. Opin. Microbiol.* 2, 312–316. doi: 10.1016/S1369-5274(99)80054-X

Stokes, H. W., Elbourne, L. D. H., and Hall, R. M. (2007). Tn1403, a multiple-antibiotic resistance transposon made up of three distinct transposons. *Antimicrob. Agents Chemother.* 51, 1827–1829. doi: 10.1128/AAC.01279-06

Sullivan, M. J., Petty, N. K., and Beatson, S. A. (2011). Easyfig: a genome comparison visualizer. *Bioinformatics* 27, 1009–1010. doi: 10.1093/bioinformatics/btr039

Takahashi, T., Tada, T., Shrestha, S., Hishinuma, T., Sherchan, J. B., Tohya, M., et al. (2021). Molecular characterisation of carbapenem-resistant *Pseudomonas aeruginosa* clinical isolates in Nepal. *J Glob Antimicrob Resist* 26, 279–284. doi: 10.1016/j.jgar.2021.07.003

Tenover, F. C., Nicolau, D. P., and Gill, C. M. (2022). Carbapenemase-producing -an emerging challenge. *Emerging Microbes Infections* 11, 811–814. doi: 10.1080/22221751.2022.2048972

Tu, J., Liu, Y., Xu, W., Dong, X., Zhang, L., Qian, J., et al. (2024). Genome characteristics of an MDR *Pseudomonas monteilii* carrying a novel VIM-type β-lactamase, blaVIM-84. *J Glob Antimicrob Resist* 39, 199–201. doi: 10.1016/j.jgar.2024.09.007

Urwin, R., and Maiden, M. C. J. (2003). Multi-locus sequence typing: a tool for global epidemiology. *Trends Microbiol.* 11, 479–487. doi: 10.1016/j.tim.2003.08.006

Wang, N., Lei, T., Zhu, Y., Li, Y., Cai, H., Zhang, P., et al. (2023). Characterization of two novel VIM-type metallo-β-lactamases, VIM-84 and VIM-85, associated with the spread of IncP-2 megaplasmids in *Pseudomonas aeruginosa*. *Microbiol Spectr* 11:e0154423. doi: 10.1128/spectrum.01544-23

Wick, R. R., Judd, L. M., Gorrie, C. L., and Holt, K. E. (2017). Unicycler: resolving bacterial genome assemblies from short and long sequencing reads. *PLoS Comput. Biol.* 13:e1005595. doi: 10.1371/journal.pcbi.1005595

Wood, S. J., Goldufsky, J. W., Bello, D., Masood, S., and Shafikhani, S. H. (2015). *Pseudomonas aeruginosa* ExoT induces mitochondrial apoptosis in target host cells in a manner that depends on its GTPase-activating protein (GAP) domain activity*. *J. Biol. Chem.* 290, 29063–29073. doi: 10.1074/jbc.M115.689950

Wu, Y., Chen, J., Zhang, G., Li, J., Wang, T., Kang, W., et al. (2024). In-vitro activities of essential antimicrobial agents including aztreonam/avibactam, eravacycline, colistin and other comparators against carbapenem-resistant bacteria with different carbapenemase genes: a multi-Centre study in China, 2021. *Int. J. Antimicrob. Agents* 64:107341. doi: 10.1016/j.ijantimicag.2024.107341

Xie, J., Chen, Y., Cai, G., Cai, R., Hu, Z., and Wang, H. (2023). Tree visualization by one Table (tvBOT): a web application for visualizing, modifying and annotating phylogenetic trees. *Nucleic Acids Res.* 51, W587–W592. doi: 10.1093/nar/gkad359

Yan, M., Zheng, B., Li, Y., and Lv, Y. (2022). Antimicrobial susceptibility trends among gram-negative Bacilli causing bloodstream infections: results from the China antimicrobial resistance surveillance trial (CARST) program, 2011-2020. *Infect Drug Resist* 15, 2325–2337. doi: 10.2147/IDR.S358788

Yu, Y., Shao, C., Gong, X., Quan, H., Liu, D., Chen, Q., et al. (2022). Antimicrobial resistance surveillance of Tigecycline-resistant strains isolated from herbivores in Northwest China. *Microorganisms* 10:2432. doi: 10.3390/microorganisms10122432

Zhang, X., Wang, L., Li, D., Li, P., Yuan, L., Yang, F., et al. (2021). An IncP-2 plasmid sublineage associated with dissemination of blaIMP-45 among carbapenem-resistant *Pseudomonas aeruginosa*. *Emerg Microbes Infect* 10, 442–449. doi: 10.1080/22221751.2021.1894903

Zhang, X., Zhu, Y., Gao, Y., Li, W., Wang, Y., and Li, Y. (2023). Evaluation and analysis of multidrug resistance- and hypervirulence-associated genes in carbapenem-resistant *Pseudomonas aeruginosa* strains among children in an area of China for five consecutive years. *Front. Microbiol.* 14:1280012. doi: 10.3389/fmicb.2023.1280012

Frontiers in Microbiology

Explores the habitable world and the potential of microbial life

The largest and most cited microbiology journal which advances our understanding of the role microbes play in addressing global challenges such as healthcare, food security, and climate change.

Discover the latest Research Topics

See more →

Frontiers

Avenue du Tribunal-Fédéral 34
1005 Lausanne, Switzerland
frontiersin.org

Contact us

+41 (0)21 510 17 00
frontiersin.org/about/contact